



The
University
Of
Sheffield.

Assessing the Excitability Changes of DRG Neurons in Models of Diabetic Neuropathy

Katerina Kaloyanova Kaloyanova

A thesis submitted in partial fulfilment of the requirements for the degree
of Doctor of Philosophy

The University of Sheffield Faculty of Science

Department of Biomedical Science

April / 2021

ACKNOWLEDGEMENTS

I wish to express my deepest gratitude to my supervisor Dr. Mohammed Nassar. From the day we met, he has shown unwavering belief in me and my potential. He always prioritised my health and mental wellbeing and made me believe in myself, even during my most difficult times of self-doubt. Since day one, he has treated me as an equal colleague and listened and considered my ideas and questions. Despite his extremely busy schedule, he always found time to help with any difficulties I had, both personal and professional. Because of his never-ending patience and support, I never felt alone in my challenges throughout the last four years. Dr. Nassar's extensive scientific knowledge and professionalism made this work what it is, but his kindness, enthusiasm and profound belief in my abilities made me the scientist I am today. I feel truly lucky and blessed to have had the best supervisor one could have asked for. Thank you! You made me a better scientist and person and for that I will be eternally grateful.

I am extremely grateful to my advisors Dr. Liz Seward and Prof. Walter Marcotti for their encouragement as well as expert guidance and constructive remarks, which helped refine and advance this research. I would also like to extend my sincerest thanks to Zainab Mohammed for training and helping me in the first months of this degree and trusting me with continuing some of her own work. I would also like to thank Nadya and Jiahao, whose contribution to the data analysis for Chapter 5 was instrumental to the results presented here.

During this degree, I was fortunate to meet some exceptional people: Eve, Judit and Mohamed, who were always around to lend a listening ear, for a laugh or just a chat. With you around, this experience was enjoyable despite the difficulties. My special thanks are extended to Mohamed – thank you for checking on me and keeping me company during the long hours of calcium imaging experiments, for your endless encouraging and comforting words and for supporting me through my worries – big or small. I wish to also thank my closest friends Elisabetta, Beth and Ainhua who have been by my side since we all started our first science degrees together. Thank you all for your understanding and positive vibes. Ainhua, we went through this hand in hand and you understood my struggles better than anyone. Thank you for the numerous coffees, chats, advice and your sincere friendship.

My sincere appreciation goes to Patrick Wood, for all his love and continuing support. Thank you for encouraging me to be ambitious and embark on this journey. Thank you for helping me practice all my talks and presentations, for listening to my venting, for making me laugh so hard I cry and for always taking care of me when I could not do it myself. You are my home and family here.

Finally, I would like to extend my deepest gratitude to my loving family in Bulgaria. Thank you for encouraging your only child to begin her education in a country so far away from you 8 years ago. Thank you for all your sacrifices, all your phone calls, all the postcards and parcels you have sent. Thank you for reminding me of how far I have come in times when I felt that I could not continue. Your tremendous belief and trust empower me to achieve things I never believed I could. This work is fully dedicated to you – my parents. I love you both.

ABSTRACT

Diabetic neuropathy (DN) is the most common type of neuropathy, with 25-50% of patients experiencing pain at any stage of its progression. However, the understanding of the pathophysiology of DN is still incomplete. No disease-modifying treatments have yet been developed and pain is only treated symptomatically with drugs targeting the central nervous system (CNS). These have limited efficacy and can produce serious side effects. Research into novel analgesics is turning away from the CNS and now focusing on the peripheral nervous system (PNS) and more specifically the pain-sensing neurons (nociceptors) to produce better-targeted and safer treatments. However, to this end, a suitable medium-to-high throughput screening tool is needed, able to discriminate nociceptors from non-nociceptors in a heterogeneous cell population, such as the dorsal root ganglia (DRG). Previously, our lab showed a link between the veratridine (VTD)-induced oscillatory (OS) and slow decay (SD) calcium response profiles with nociceptors and non-nociceptors, respectively. Here, we validated the VTD-response profiles as broad functional markers of these DRG subpopulations using mice with genetically ablated nociceptors (1.8-DTA). Then, by using voltage-gated sodium channel (VGSC) blockers with different specificities, we demonstrated that the VTD- Ca^{2+} imaging assay can be used as a drug screening platform for drugs, individually or in novel combinations. The VTD- Ca^{2+} imaging assay was then applied in combination with nociceptive agonists to investigate the excitability changes in distinct neuronal subpopulations during DN. In *db/db* mice, during the early metabolic phase, small- to medium-diameter nociceptors showed 1.4 -fold increased sensitivity to CAP and 1.2-fold increased VGSC excitability. In the late, NEU phase, small-diameter nociceptors showed increased sensitivity to CAP (1.6-fold) and increased VGSC excitability (1.4-fold), whereas medium nociceptors show decreased sensitivity to AITC (1.8-fold) . This is the first study to characterise phase- and subpopulation-specific excitability changes in the well-established *db/db* mouse model. Collectively, these results point to specific subpopulations of DRG neurons affected during the early and late stages of DN. These findings could aid in the better targeting of novel therapies for the treatment of DN and pain. Furthermore, we have demonstrated that the VTD- Ca^{2+} imaging assay can be applied as a tool for the characterisation of excitability changes in distinct DRG subpopulations during neuropathological conditions such as DN.

DECLARATION

I declare that the work presented in this thesis is my own original research and has been composed entirely by myself. All supporting literature, resources, and collaborative contributions have been acknowledged clearly.

Part of this work has been published prior to submission of this thesis under the title:

“An unbiased and efficient assessment of excitability of sensory neurons for analgesic drug discovery”

PAIN, 2020

Signature:

Katerina Kaloyanova Kaloyanova,

April 2021

LIST OF ABBREVIATIONS

| | |
|-------------------------|--|
| •OH | Superhydroxyl |
| AGE | Advanced glycation end products |
| AITC | Allyl isothiocyanate |
| AMH | A δ -mechano-heat |
| AP | Action potential |
| AR | Aldose reductase |
| ATP | Adenosine 5'-triphosphate |
| AUC | Area under curve |
| CAP | Capsaicin |
| CGRP | Calcitonin gene-related peptide |
| CIP | Channelopathy-associated insensitivity to pain |
| CNS | Central nervous system |
| DAG | Diacylglycerol |
| DN | Diabetic neuropathy |
| DoA | Days of age |
| DRG | Dorsal root ganglia |
| eGFP | Enhanced green fluorescent protein |
| FADH₂ | Flavin dinucleotide + hydrogen |
| FEPS | Familial episodic pain syndrome |
| FFAs | Free fatty acids |

| | |
|-----------------------------------|---|
| GECI | Genetically encoded calcium indicator |
| GlcNac | 5-diphosphate-N-acetylglucosamine |
| GLUT | Glucose transporter |
| GoF | Gain of function |
| GP | Glutathione peroxidase |
| H₂O₂ | Hydrogen peroxide |
| HFD | High fat diet |
| IB4 | Isolectin B4 |
| ID | Intermediate decay |
| IEM | Inherited erythromelalgia |
| IENF | Intraepidermal nerve fibre |
| iPSC | Induced pluripotent stem cell |
| IR | Insulin resistance |
| KO | Knock-out |
| LDL | Low density lipoproteins |
| LoF | Loss of function |
| LOX1 | Oxidized-LDL-receptor 1 |
| LTMR | Low-threshold mechanoreceptors |
| NADH | Nicotinamide dinucleotide + hydrogen |
| NADPH | Reduced nicotinamide adenine dinucleotide phosphate |
| NCV | Nerve conduction velocity |

| | |
|------------------|---|
| NF200 | Neurofilament 200 |
| NOD | Non-obese diabetic |
| OS | Oscillatory |
| P2X3 | P2X purinoceptor 3 |
| PARP | Poly(ADP-ribose) polymerase |
| PC12 | Pheochromocytoma cells |
| PDN | Painful diabetic neuropathy |
| PKA | Protein kinase A |
| PKC | Protein kinase C |
| PNS | Peripheral nervous system |
| RAGE | Receptor for advanced glycation end products |
| RD | Rapid decay |
| RMP | Resting membrane potential |
| ROS | Reactive oxygen species |
| SC | Schwann cell |
| scRNA-seq | Single-cell PCR and RNA sequencing |
| SD | Slow decay |
| SNRI | Serotonin and noradrenaline reuptake inhibitors |
| STZ | Streptozotocin |
| T1D | Type 1 diabetes |
| T1DN | Type 1 diabetic neuropathy |

| | |
|--------------|--|
| T2D | Type 2 diabetes |
| T2DN | Type 2 diabetic neuropathy |
| TCA | Tricyclic antidepressants |
| TH | Tyrosine hydroxylase |
| TLR4 | Toll-like receptor 4 |
| TRP | Transient receptor potential-activated |
| TTX | Tetrodotoxin |
| TTX-R | Tetrodotoxin resistant |
| TTX-S | Tetrodotoxin sensitive |
| VGCC | Voltage-gated calcium channels |
| VGKC | Voltage-gated potassium channels |
| VGSC | Voltage-gated sodium channel |
| VTD | Veratridine |
| WoA | Weeks of age |

TABLE OF CONTENTS

| | |
|--|------------|
| ACKNOWLEDGEMENTS | II |
| ABSTRACT | III |
| DECLARATION | IV |
| LIST OF ABBREVIATIONS | V |
| CHAPTER 1: INTRODUCTION | 1 |
| 1.1. THE NERVOUS SYSTEM AND DORSAL ROOT GANGLIA (DRG) NEURONS | 2 |
| 1.1.1. DRG NEURONS: HETEROGENEITY AND CLASSIFICATION | 3 |
| 1.1.2. DRG NEURONS EXCITABILITY | 6 |
| 1.2. PAIN: THE GOOD AND THE BAD | 8 |
| 1.2.1. THE PAIN SIGNALLING PATHWAY | 8 |
| 1.2.2. PAIN AS A DISEASE | 9 |
| 1.2.3. DRG-EXPRESSED CHANNELS AND RECEPTORS INVOLVED IN PAIN | 10 |
| 1.2.3.1. Voltage-gated sodium channels | 11 |
| 1.2.3.2. Transient receptor potential cation channels: TRPV1 and TRPA1 | 17 |
| 1.2.3.3. Purinoceptors: P ₂ X purinoceptor 3 (P ₂ X ₃) | 21 |
| 1.3. DIABETIC NEUROPATHY AND PAIN | 22 |
| 1.3.1. DIABETES | 23 |
| 1.3.1.1. Type 1 Diabetes – an autoimmune response | 24 |
| 1.3.1.2. Type 2 Diabetes – a lifestyle problem | 25 |
| 1.3.2. DIABETIC NEUROPATHY | 27 |
| 1.3.2.3. T1D and T2D inconsistencies | 28 |
| 1.3.3. MECHANISMS IMPLICATED IN (PAINFUL) DIABETIC NEUROPATHY | 29 |
| 1.3.2.1. Damage to the microvasculature supplying the neurons | 30 |
| 1.3.2.2. Metabolic pathways | 30 |
| 1.3.2.3. Ion channel alterations | 37 |
| 1.3.4. CURRENT DIABETIC NEUROPATHY TREATMENTS | 38 |
| 1.3.3.1. Diabetic neuropathy management | 39 |

| | |
|--|-----------|
| 1.3.3.2. Management of painful diabetic neuropathy (PDN) | 40 |
| 1.3.3.3. Why are there no disease-modifying therapies for diabetic neuropathy? | 46 |
| 1.4. MODELLING DIABETIC NEUROPATHY | 47 |
| 1.4.1. MODELLING DIABETIC NEUROPATHY <i>IN VITRO</i> | 47 |
| 1.4.2. EXPERIMENTAL ANIMAL MODELS OF DIABETIC NEUROPATHY | 49 |
| 1.4.2.1. Genetically induced models of diabetic neuropathy | 50 |
| 1.4.2.2. Chemically induced models of diabetic neuropathy | 51 |
| 1.4.2.3. Diet-induced models of diabetic neuropathy | 52 |
| 1.4.2.4. Considerations when selecting a model | 52 |
| 1.5. VERATRIDINE-BASED CALCIUM IMAGING ASSAY FOR NEURONAL EXCITABILITY ASSESSMENT | 53 |
| 1.5.1. CALCIUM IMAGING TECHNIQUE | 54 |
| 1.5.1.1. Calcium indicators | 54 |
| 1.5.2. ACTIVATING NEURONS | 56 |
| 1.5.2.1. The constellation pharmacology approach | 56 |
| 1.5.2.2. Veratridine | 57 |
| 1.5.3. VERATRIDINE-INDUCED CALCIUM RESPONSE PROFILES AS FUNCTIONAL INDICATORS OF DRG NEURONAL SUBPOPULATIONS | 59 |
| 1.6. AIMS | 62 |
| | |
| CHAPTER 2: MATERIALS & METHODS | 64 |
| | |
| 2.1 MATERIALS | 64 |
| 2.1.1. ANIMALS: | 64 |
| 2.1.2 CELL CULTURE REAGENTS | 64 |
| 2.1.3 PHARMACOLOGICAL COMPOUNDS | 65 |
| 2.1.4. REAGENTS, CHEMICALS AND SOLVENTS | 65 |
| 2.1.5. TOOLS, EQUIPMENT AND LABWARE | 66 |
| 2.1.6. SOLUTION AND MEDIUM RECIPES | 67 |
| 2.2. METHODS | 67 |
| 2.2.1. PREPARATION OF MOUSE DORSAL ROOT GANGLIA NEURONAL CULTURE | 67 |
| 2.2.1.1 Isolation of DRG | 67 |
| 2.2.1.2 DRG digestion | 68 |
| 2.2.1.3 Dissociation of neurons and seeding | 68 |
| 2.2.1.4. Adjustments to glucose concentration in culture for in vitro hyperglycaemia experiments | 68 |
| 2.2.2. CALCIUM IMAGING OF DRG NEURONS | 69 |

| | |
|---|----|
| 2.2.2.1. DRG cells loading with Fura-2AM | 69 |
| 2.2.2.2. Experimental set up | 69 |
| 2.2.2.3. Recording of calcium responses | 70 |
| 2.2.3. DATA PROCESSING AND STATISTICAL ANALYSIS OF CALCIUM IMAGING DATA | 70 |
| 2.2.3.1. Analysis of recorded calcium imaging responses | 70 |
| 2.2.3.2. Neuronal cell size analysis | 71 |
| 2.2.3.3. Statistical tests | 71 |

CHAPTER 3: VALIDATION OF THE DISTINCT VERATRIDINE CALCIUM RESPONSE PROFILES AS FUNCTIONAL MARKERS FOR NOCICEPTORS AND NON-NOCICEPTORS **73**

CHAPTER 4: ASSESSING EXCITABILITY CHANGES IN DRG NEURONS UNDER IN VITRO HYPERGLYCEMIC CONDITIONS **85**

| | |
|---|-----------|
| 4.1. INTRODUCTION | 85 |
| 4.2. AIMS | 86 |
| 4.3. METHOD | 86 |
| 4.3.1. GLUCOSE CONCENTRATION AND EXPOSURE TIME IN <i>IN VITRO</i> -INDUCED HYPERGLYCAEMIA | 86 |
| 4.3.2. CALCIUM IMAGING | 88 |
| 4.4. RESULTS | 88 |
| 4.4.1. THE NUMBER OF AVAILABLE NEURONS FOR IMAGING EXPERIMENTS DECLINES WITH TIME IN CULTURE | 88 |
| 4.4.2. TIME IN CULTURE, BUT NOT <i>IN VITRO</i> -INDUCED HYPERGLYCAEMIA, AFFECTS RESPONSES TO NOCICEPTIVE AGONISTS | 89 |
| 4.4.3. TIME IN CULTURE LEADS TO SUBTLE CHANGES IN VGSC ACTIVITY, AFFECTED BY <i>IN VITRO</i> INDUCED HYPERGLYCAEMIA | 92 |
| 4.5. DISCUSSION | 96 |

CHAPTER 5: ASSESSING THE EXCITABILITY CHANGES IN DRG NEURONS FROM DIABETIC *DB/DB* MICE **101**

| | |
|--|------------|
| 5.1. INTRODUCTION | 101 |
| 5.2. AIMS | 105 |
| 5.3. METHODS | 105 |
| 5.3.1. DRG NEURON CULTURE FROM <i>DB/DB</i> MICE | 105 |
| 5.3.2. CALCIUM IMAGING | 105 |

| | |
|--|----------------|
| 5.4. RESULTS | 105 |
| 5.4.1. THE NUMBER OF DRG NEURONS DERIVED FROM <i>DB/DB</i> MICE FOR EACH PHASE AND CONDITION | 105 |
| 5.4.2. THE OVERALL CELL SIZE DISTRIBUTION IS SHIFTED TOWARDS SMALLER CELLS IN DRG FROM <i>DB/DB</i> MICE | 106 |
| 5.4.3. PERSISTENT INCREASE IN THE SENSITIVITY TO CAPSAICIN IN SMALL DRG NEURONS FROM <i>DB/DB</i> MICE | 109 |
| 5.4.4. VGSC ACTIVITY IN SMALL DRG NOCICEPTORS FROM <i>DB/DB</i> MICE IS INCREASED DURING THE COURSE OF DIABETIC NEUROPATHY | 113 |
| 5.5. DISCUSSION | 116 |
| 5.5.1. CELL SIZE DISTRIBUTION IN <i>DB/DB</i> MICE DRG THROUGH THE COURSE OF DIABETIC NEUROPATHY | 117 |
| 5.5.2. DIABETIC NEUROPATHY LEADS TO INCREASING SENSITIVITY TO CAPSAICIN IN <i>DB/DB</i> MOUSE DRG NEURONS | 118 |
| 5.5.3. DIABETIC NEUROPATHY LEADS TO A DECREASE IN THE SENSITIVITY TO AITC IN THE <i>DB/DB</i> MOUSE DRG NEURONS | 121 |
| 5.5.4. DRG NEURONS FROM <i>DB/DB</i> MICE HAVE INCREASED VGSC ACTIVITY IN CELLS WITH THE OS VTD-RESPONSE PROFILE | 123 |
| 5.5.5. DIABETIC NEUROPATHY LEADS TO EXCITABILITY CHANGES IN SPECIFIC NEURONAL SUBPOPULATIONS | 125 |
| CHAPTER 6: LIMITATIONS & FUTURE DIRECTIONS | 129 |
| 6.1. VERATRIDINE AND Ca^{2+} IMAGING AS A TOOL WITH MULTIPLE APPLICATIONS | 130 |
| 6.1.2. ADVANTAGES | 130 |
| 6.1.3. LIMITATIONS & RECOMMENDATIONS | 131 |
| 6.1.4. APPLICATIONS | 133 |
| 6.2. MODELLING DIABETIC NEUROPATHY IN A DISH – A REALISTIC GOAL OR AN UNFEASIBLE CHALLENGE? | 134 |
| 6.3. STUDYING EXCITABILITY OF DRG NEURONS DERIVED FROM DIABETIC ANIMALS | 137 |
| 6.4. CONCLUSION | 141 |
| BIBLIOGRAPHY | 143 |

LIST OF FIGURES

CHAPTER 1

| | |
|--|----|
| Figure 1.1. Cross section of a spinal cord illustrating the relative position of the dorsal root ganglion containing the cell bodies of sensory neurons _____ | 2 |
| Figure 1.2. A simplified visualisation of the action potential generation in neurons and phases of depolarisation and repolarisation and thresholds _____ | 7 |
| Figure 1.3. The ion channels involved in the pain signalling pathway _____ | 9 |
| Figure 1.4. Diagram depicting the thermal sensitivity spectrum of thermoTRP channels. _____ | 17 |
| Figure 1.5. Normal physiology of glucose metabolism. _____ | 22 |
| Figure 1.6. Insulin production compared between healthy, type 1 diabetes and type 2 diabetes setting. _____ | 25 |
| Figure 1.7. Metabolic mechanisms of diabetic neuropathy. _____ | 30 |
| Figure 1.8. Currently established treatment strategy for painful diabetic neuropathy. _____ | 40 |
| Figure 1.9. Structure and properties of chemical and genetically encoded calcium indicators. _____ | 54 |
| Figure 1.10. Veratridine (VTD) action on voltage-gated sodium channels (VGSCs). _____ | 57 |
| Figure 1.11. Veratridine (VTD) applied to mouse DRG neurons produces four distinct VTD-response profiles that could be indicative of specific neuronal subpopulations. _____ | 59 |

CHAPTER 3

| | |
|--|----|
| Figure 1. Assessments of the excitability of nociceptors and non-nociceptors based on veratridine-response profiles. _____ | 74 |
| Figure 2. The OS population is reduced in mice lacking most nociceptors. _____ | 75 |
| Figure 3. Reference veratridine-response patterns for “safe” and “unsafe” analgesic drugs. _____ | 76 |
| Figure 4. Evaluating the effect of PF-04856246 and A-803467 on nociceptors and non-nociceptors. _____ | 78 |

Figure 5. The additive effects of a combination of PF-04856264 and A-803467 on nociceptors. _____ 79

Figure 6. Applications of the veratridine-based calcium assay. _____ 80

CHAPTER 4

Figure 4.1. A schematic of the experimental protocol used in the current experiments. _____ 87

Figure 4.2. The availability of neurons for Ca²⁺ imaging declines the longer the culture is maintained. _____ 88

Figure 4.3. Responses of DRG neurons under control and hyperglycaemic conditions to nociceptive agonists. _____ 89

Figure 4.4. Responses to VTD by DRG neurons cultured for 1 to 5 days in high glucose or standard conditions. _____ 91

Figure 4.5. Analysis of the effect time in culture and hyperglycaemic conditions have on VTD-response parameters. _____ 93

CHAPTER 5

Figure 5.1. An excerpt from a paper by Guest and Rahmoune (2018) characterising the diabetic phenotype of a 10 week old db/db mouse and comparing parameters to a wild type mouse. _____ 100

Figure 5.2. A comprehensive summary of the available molecular, physiological, behavioural and transcriptomic research on the db/db mouse model with observations categorised according to diabetic neuropathy phases. _____ 101

Figure 5.3. Frequency distribution of neuronal diameter sizes from control (lean) and diabetic (db/db) mice for each phase of diabetic neuropathy: early, metabolic and late, neuronal. _____ 105

Figure 5.4. Distribution of neuronal soma diameter in three size groups _____ 106

Figure 5.5. The percentage of lean and db/db-derived neurons responsive to nociceptive agonists in each phase of diabetic neuropathy. _____ 108

Figure 5.6. Size distribution of CAP(+) neurons from control (lean) and diabetic (db/db) mice for each phase of diabetic neuropathy: early, metabolic and late, neuronal. _____ 109

| | |
|--|-----|
| Figure 5.7. Distribution of neurons responsive to specific all nociceptive agonists in the MET phase or AITC-only in the NEU phase in three size groups. _____ | 110 |
| Figure 5.8. Responses to VTD by DRG neurons derived from lean or db/db mice during the metabolic or neuronal phase of diabetic neuropathy. _____ | 111 |
| Figure 5.9. Size distribution of neurons with the OS VTD-response profile from control (lean) and diabetic (db/db) mice for each phase of diabetic neuropathy. ____ | 112 |
| Figure 5.10. The percentage of OS neurons from lean and db/db responsive to nociceptive agonists – alone or in combinations, in each phase of diabetic neuropathy. _____ | 113 |
| Figure 5.11. Graphic summary of the affected subpopulations of DRG neurons and their known properties in db/db mice in the metabolic (MET) and neuronal (NEU) phases of diabetic neuropathy. _____ | 125 |

LIST OF TABLES

CHAPTER 1

| | |
|---|----|
| Table 1.1. Table summarising the relationship between neuronal properties and features. CV, conduction velocity. _____ | 4 |
| Table 1.2. Summary of the most commonly used markers for neuronal subpopulations. _____ | 6 |
| Table 1.3. Voltage-gated sodium channel isoforms discovered to date with respective gene, tissue distribution and sensitivity to tetrodotoxin. _____ | 10 |
| Table 1.4. Summary of the main characteristics for diabetes type 1 and 2. _____ | 23 |
| Table 1.5. Current FDA-approved treatments for painful diabetic neuropathy with their therapeutic targets, most common side effects and serious adverse effects summarised. _____ | 41 |
| Table 1.6. A range of novel drugs in development for the treatment of painful diabetic neuropathy. _____ | 43 |

CHAPTER 2

| | |
|--|----|
| Table 2.1. Cell culture reagents. _____ | 63 |
| Table 2.2. Pharmacological compounds. _____ | 64 |
| Table 2.3. Reagents, chemicals and solvents. _____ | 64 |
| Table 2.4. Tools, equipment and labware. _____ | 65 |

CHAPTER 4

| | |
|--|----|
| Table 4.1. Studies that used varying concentrations and exposure times of glucose in in vitro DRG cultures and the main conclusions reached. _____ | 86 |
| Table 4.2. The total number of neurons decreases the longer the culture is maintained. _____ | 88 |

CHAPTER 5

| | |
|---|-----|
| Table 5.1 Number of neurons for each mouse (N) of each phase (MET or NEU) for each condition (CTRL or <i>db/db</i>). _____ | 104 |
|---|-----|

| | |
|---|-----|
| Table 5.2. Summary table of the identified properties of the DRG neuronal subpopulations affected in <i>db/db</i> mice in the metabolic (MET) and neuronal (NEU) phases of diabetic neuropathy. _____ | 125 |
|---|-----|

CHAPTER 6

| | |
|--|-----|
| Table 6.1. List of some advantages of the T2D <i>db/db</i> mouse model of diabetic neuropathy. _____ | 138 |
|--|-----|

| | |
|---|-----|
| Table 6.2. List of some disadvantages of the T2D <i>db/db</i> mouse model of diabetic neuropathy. _____ | 138 |
|---|-----|

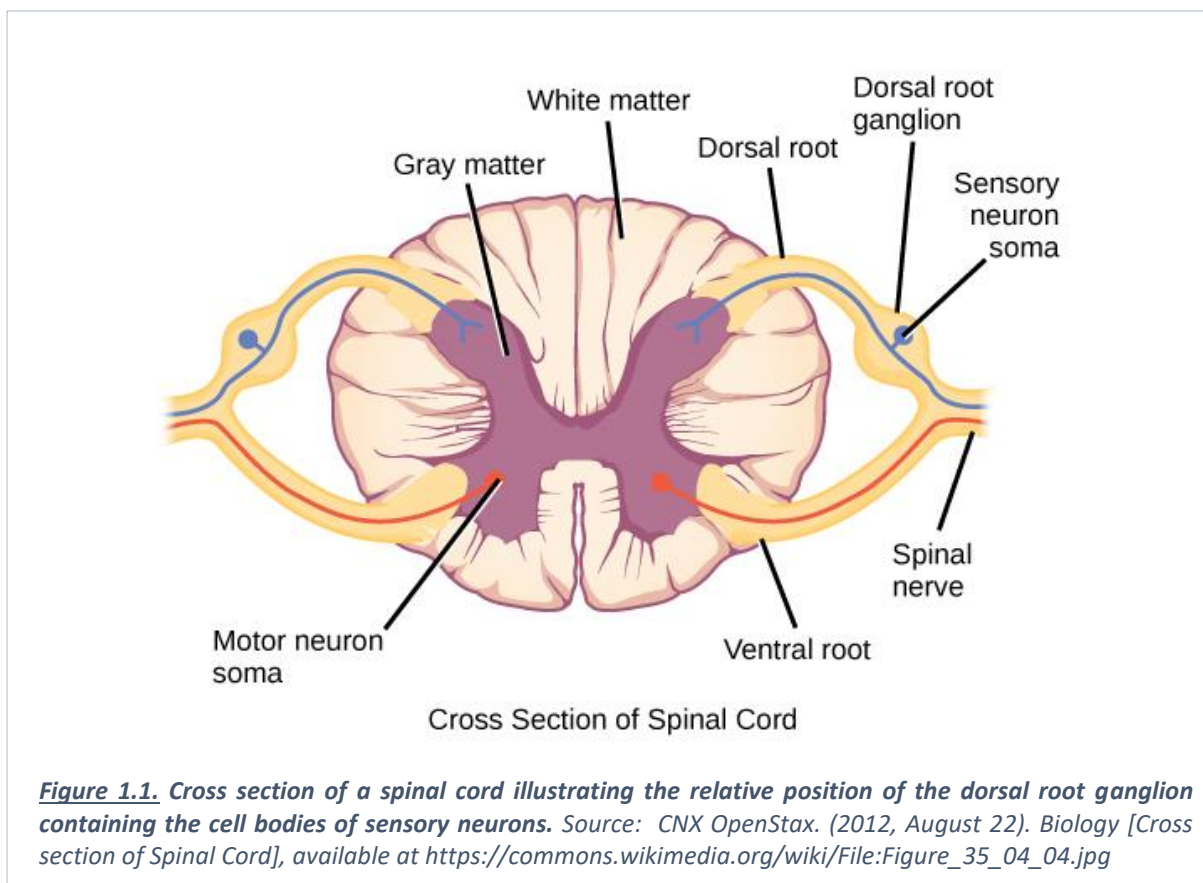
CHAPTER 1

INTRODUCTION

1.1. The nervous system and dorsal root ganglia (DRG) neurons

The nervous system is the most complex body system with a highly organised structure. It is composed of two major parts: the central nervous system (CNS), constituting the brain and spinal cord; and the peripheral nervous system (PNS), comprising all the nerves connecting the CNS to all organs, tissues and skin. The PNS contains sensory (afferent) neurons responsible for conveying sensory stimuli to the CNS, where the information is processed and a response to the stimuli is generated. The response signal is then relayed through efferent neurons and expressed in the form of movement¹.

The sensory branch of the PNS comprises an intricate network of sensory neurons and pathways responsible for transducing and transmitting information that organisms can “feel”. The cell bodies of sensory neurons are contained within small, ball-like structures called ganglia. These can be located at the base of the skull, innervating the head and face, called trigeminal ganglia (TG). The cell bodies of the neurons innervating the rest of the body reside



in ganglia along the spinal column called dorsal root ganglia (DRG) – the focus of this thesis (Figure 1.1). The pseudounipolar nature of DRG neurons somata means a single afferent fibre (axon), extends briefly from the cell body and then bifurcates into: a short central branch,

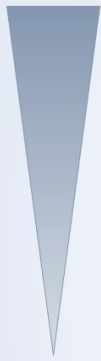
projecting into the CNS through the spinal cord; and a longer peripheral branch, innervating peripheral tissues and terminating in the skin, viscera, tendons, bones and muscles^{1,2}.

1.1.1. DRG neurons: heterogeneity and classification

Sensory neurons relay complex information from an abundant variety of innocuous (harmless) and noxious (painful) stimuli to the CNS. This richness of sensory potential is supported by the complex heterogeneity of DRG neurons. The cell bodies of sensory neurons are intermingled together within the DRG, however they are organized into a number of types and subtypes, each specialised for the detection of distinct stimuli. These include neurons sensing body movement and position (proprioceptors), touch and pressure (mechanoreceptors), itch (pruriceptors), temperature (thermoreceptors) and pain (nociceptors). Although a certain level of distinct categorisation exists, sensory neurons can also be “polymodal”, or able to integrate multiple modalities, e.g., thermal and mechanical stimuli. Additionally, up to 25% of DRG nociceptors are normally dormant and only activated upon injury and are thus called “silent nociceptors”^{3,4}.

The basis for the classification of DRG neurons was formed as early as the 1920s by Gasser and Erlanger – the first to show a relationship between DRG neurons soma diameter, axon myelination degree, signal conduction velocity and fibre projection targets within the spinal cord lamina. They established that the smaller the soma diameter, the less the myelin sheathing and the slower the conduction velocity but the higher the excitation threshold is, and vice versa (Figure 1.2)^{5,6}. From their morphological and electrophysiological observations arose the conventional DRG sensory neurons classification as it is known today: mammalian sensory neurons can be categorised into three general types: A β -fibres, A δ -fibres and C-fibres. Further behavioural studies correlated certain modalities with each fibre class⁵.

Table 1.1. Table summarising the relationship between neuronal properties and features. CV, conduction velocity; S, small; M, medium; L, large sizes of mouse DRG neurons. Based on Basbaum et al. (2009) and Li et al.

| Myelin | CV | Excitation threshold | Soma size | Fiber class | Modality | Dorsal horn termination lamina |
|---|---|---|---|--|--|--------------------------------|
|  |  |  |  | A α A β -LTMR | Proprioception Mechanoreception | VII, VIII III - V |
| | | |  | A δ -LTMR | Mechanoreception | III |
| | | |  | A δ myelinated fibers | Nociception Thermoception Pruriception | I, V |
| | | | | C (non-peptidergic) C (peptidergic) C-LTMR | | Mechanoreception |

A α -fibres are the largest in diameter, with conduction velocities in the range of 80 – 120 m/s. Defined by Gasser and Erlanger as motor nerves, the sensory neurons of the proprioceptive modality are usually denoted by the A α -fibre type. They project into the deeper laminae of the spinal cord ⁵.

A β -fibres have large soma diameter, heavily myelinated and with fast conduction velocities (30 – 70 m/s). The majority have low thresholds of activation and are dedicated to the detection of innocuous mechanical stimuli, such as touch and vibration, stretch and hair deflection ⁷. Of note, a significant proportion (e.g. ~20% of A-fibres in rat) of A β -fibres are A β -nociceptors, conducting in the A β conduction velocity range ⁸. In the spinal cord lamina, A β -fibres project into laminae III-V ⁹.

A δ -fibres have thin myelination and hence slower signal conduction velocity (5 – 30 m/s) than A β -fibres. Their size distribution in DRG is skewed, with populations of small- and medium-sized cells. In the body, A δ -fibres innervate mostly superficial organs (e.g. the skin). A δ -fibres are associated with the detection of innocuous as well as noxious stimuli. Therefore, they include A δ low-threshold mechanoreceptors (LTMRs) and A δ nociceptors, responding to noxious mechanical and heat stimuli ¹⁰. A δ nociceptors can be further divided into Type I and

Type II A δ -mechano-heat (AMH) units according to the degree of sensitivity to either stimulus. Type I AMH are sensitive to chemical stimuli and have lower threshold to mechanical and higher threshold to heat (>53°C) stimuli. Hence, they are suggested to mediate first pain to noxious mechanical stimuli. In contrast, Type II AMH have lower heat (<46°C) and higher mechanical threshold and are thus suggested to serve the first pain sensation to noxious heat¹¹. Activation of A δ -nociceptors by noxious thermal or mechanical stimuli results in short-lasting, prickling type of pain. In the spinal cord, A δ -fibres terminate in laminae I, V (A δ nociceptors) and III (A δ -LTMRs)¹⁰.

C-fibres constitute over 50% of all DRG neurons and are of the smallest soma diameter. Their axons are unmyelinated and the signal conduction velocity ranges between 0.5 – 2 m/s. They are activated by one or a combination of two or more modalities, including temperature shifts, pruritogens, chemical irritants and mechanical pressure. Their high activation thresholds to these stimuli render the majority, but not all, of them nociceptors. Nociceptive C-fibres innervate deep somatic structures, such as the muscles and joints¹². While A δ -fibre nociceptors convey acute and localized nociception, called ‘first’ or fast pain, nociceptive C-fibres propagate ‘second pain’ which is more diffuse, dull and longer lasting¹³. A portion of C-fibre neurons, termed C-LTMRs, are responsible for propagating innocuous touch stimuli⁹. Centrally, C-fibres project into the superficial laminae I-III.

Albeit still used today, fibre classification of DRG neurons does not reflect the full heterogeneous spectrum of neuronal function and hence is not an adequate functionality predictor on its own. Neurochemical markers and molecular classifications of DRG neurons have become key in building a more complete picture. A comprehensive summary of somatosensory cell type markers is presented in [Table 1.2](#).

More recently, transcriptomic techniques such as microarray, single-cell PCR and RNA sequencing (scRNA-seq) have produced their own elaborate DRG classifications. Usoskin et al. used scRNA-seq to analyse 622 DRG neurons, detecting 3900 ± 1880 genes per neuron and distributing the neurons into 11 molecularly distinct subtypes with *in vivo* validation of the predicted subpopulations¹⁴. Not long after them, Li et al. performed an even more in-depth sequencing of 197 DRG sensory neurons detecting 10950 ± 1218 genes per neuron and generating 17 molecularly distinct neuronal subtypes (however, not *in vivo* validated)¹⁵. Their work was later reanalysed and their predicted number of classes reduced to 9 subtypes which largely overlapped with the predicted subtypes by Usoskin¹⁶. Most recently, Zeisel et al. published a comprehensive scRNA-seq analysis of 1580 DRG neurons, which, merged with

that

Table 1.2. Summary of the most commonly used markers for neuronal subpopulations. Source: Pichon and Chesler 2014

of

| Marker | Sensory cell type |
|----------------------|---|
| Parvalbumin | Proprioceptors and A β -fibres |
| CGRP | Peptidergic C fibres, subpopulation of A δ -fibres |
| Substance P | Peptidergic C fibres |
| NF200 | Myelinated A δ -fibres, A β -fibres and proprioceptors |
| IB4 | Non-peptidergic C-fibres |
| Trpv1 | Small diameter C-fibres (heat & pain) |
| Trpm8 | Small diameter C-fibres (cold & pain) |
| MrgprD | Small diameter C-fibres (noxious mechanical,pain) |
| MrgprA3 | Small diameter C-fibres (itch) |
| MrgprB4 | Small diameter C-fibres (innocuous mechanical) |
| VGlut3 | Non-peptidergic C-fibres (innocuous mechanical, cooling) |
| TH | Non-peptidergic C-fibres (innocuous mechanical, cooling) |
| TrkB | A δ -fibres (innocuous mechanical, cooling) |
| Npy2r | A β -fibres (innocuous mechanical) |
| Chondrolectin | A β -fibres (innocuous mechanical) |
| DOR | Subpopulations of non-peptidergic C fibres and myelinated NF200+ fibres |

Usoskin's, delivers the most elaborate molecular classification of DRG sensory neurons to date, with a total of 18 neuronal subtypes identified ¹⁷.

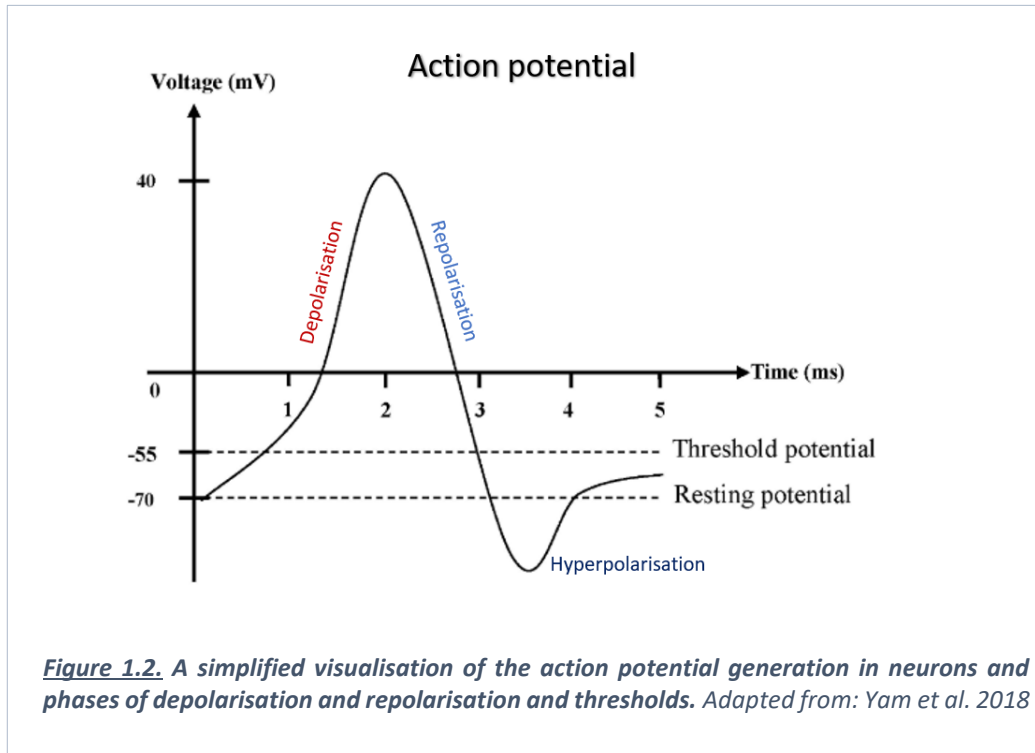
1.1.2. DRG neurons excitability

A non-firing, or 'resting' neuron maintains an electrochemical gradient across its membrane called a resting membrane potential (RMP). It is determined by the uneven distribution of sodium (Na⁺), potassium (K⁺), chloride (Cl⁻), calcium (Ca²⁺) and organic anions across the membrane. The RMP is established by the difference in ion concentrations inside and outside the neuron and the relative permeabilities of the membrane to different ions. At rest, there are more extracellular Na⁺ ions than intracellular K⁺ ions. This concentration difference is maintained by Na⁺/K⁺ pump cycles, exchanging 3 Na⁺ out for 2 K⁺ into the cell.

At rest, the membrane is more permeable to K⁺ than Na⁺, ions, letting them diffuse down their concentration gradient to the outside of the cell. Eventually, the free movement of K⁺ ions,

unbalanced by the movement of Na^+ to the inside, will cause the neuron to have negative charge inside and positive charge outside. Due to the established extracellular/intracellular charge difference, the excess negatively charged ions on the inside are attracted to the outside and vice-versa, accumulating along the inside and outside surfaces of the membrane and establishing a negative membrane potential. The membrane is 'polarised', causing the RMP of an average neuron to be around -70mV (Figure 1.2). Stimulus detection causes membrane depolarisation, which even small can activate some VGSCs and increase the Na^+ permeability of the membrane, producing even greater depolarisation. The 'threshold' potential ($\sim -55\text{mV}$) of a neuron is the critical point at which the membrane is depolarised to elicit an action potential (AP). During its depolarised state, the membrane shifts its permeability from K^+ to Na^+ ions, influencing the reversal of the charge difference across it. A critical component of the AP is the influx of Ca^{2+} ions through voltage-gated Ca^{2+} channels (VGCCs), important for the activation of K^+ channels (key during repolarisation) and transmitter release^{2,18}. Following AP generation, the neuron needs to engage cellular mechanisms for Ca^{2+} ion clearance to avoid Ca^{2+} overflow in the cell and initiate repolarisation. Most of the intracellular Ca^{2+} is cleared through extrusion via the transmembrane $\text{Na}^+/\text{Ca}^{2+}$ exchanger or Ca^{2+} ATPase. Alternatively, Ca^{2+} ions can also be sequestered through uptake by the neuronal endoplasmic reticulum via its own transmembrane Ca^{2+} ATPases or into mitochondria¹⁹. All Ca^{2+} clearance mechanisms require energy in the form of ATP to shuttle Ca^{2+} ions out of the neuronal cytoplasm and play an important protective role and influence the shape of the Ca^{2+} signal and thus AP^{19,20}.

The pathway of the signal propagation follows three main steps: transduction, transmission and perception. Each of them is carried out through the highly coordinated activation and deactivation of all the different ion channels across the membrane, allowing the external stimulus to travel through the PNS and be perceived and processed in the CNS. This process will be reviewed in more details in the context of pain signalling in the next section of this chapter along with some of the key channels and receptor regulators in the signalling pathway.



1.2. Pain: the good and the bad

1.2.1. The pain signalling pathway

The ability to detect, transmit and perceive pain is a key protective mechanism essential for one's survival. The process of pain signalling is called nociception. It starts with a noxious stimulus (chemical, mechanical or thermal) being detected at the terminals of nociceptors. The detection of the stimulus activates ion channels and receptors such as transient receptor potential activated (TRP) channels. This leads to the influx of Na^+ which starts depolarizing the membrane, bringing it closer to the activation threshold of voltage-gated sodium channels (VGSCs) which act to amplify the signal. Once the threshold potential is reached, local VGSCs open simultaneously resulting in complete membrane depolarization and peak potential. The external stimulus is transduced into an action potential (AP)²¹. VGSCs then begin inactivating and voltage-gated potassium channels (VGKCs) and K^+ leakage channels open allowing K^+ efflux. This initiates membrane repolarization and subsequently hyperpolarization. Finally, the Na^+/K^+ pump takes over to restore and maintain the RMP (Figure 1.2). In the meantime, the AP generated is propagated up the axon driven by the same sequence of ion channels opening and closing akin to a chain reaction, going through the DRG cell body and eventually reaching the dorsal horn of the spinal cord. Once at the nociceptor's presynaptic terminal, the AP

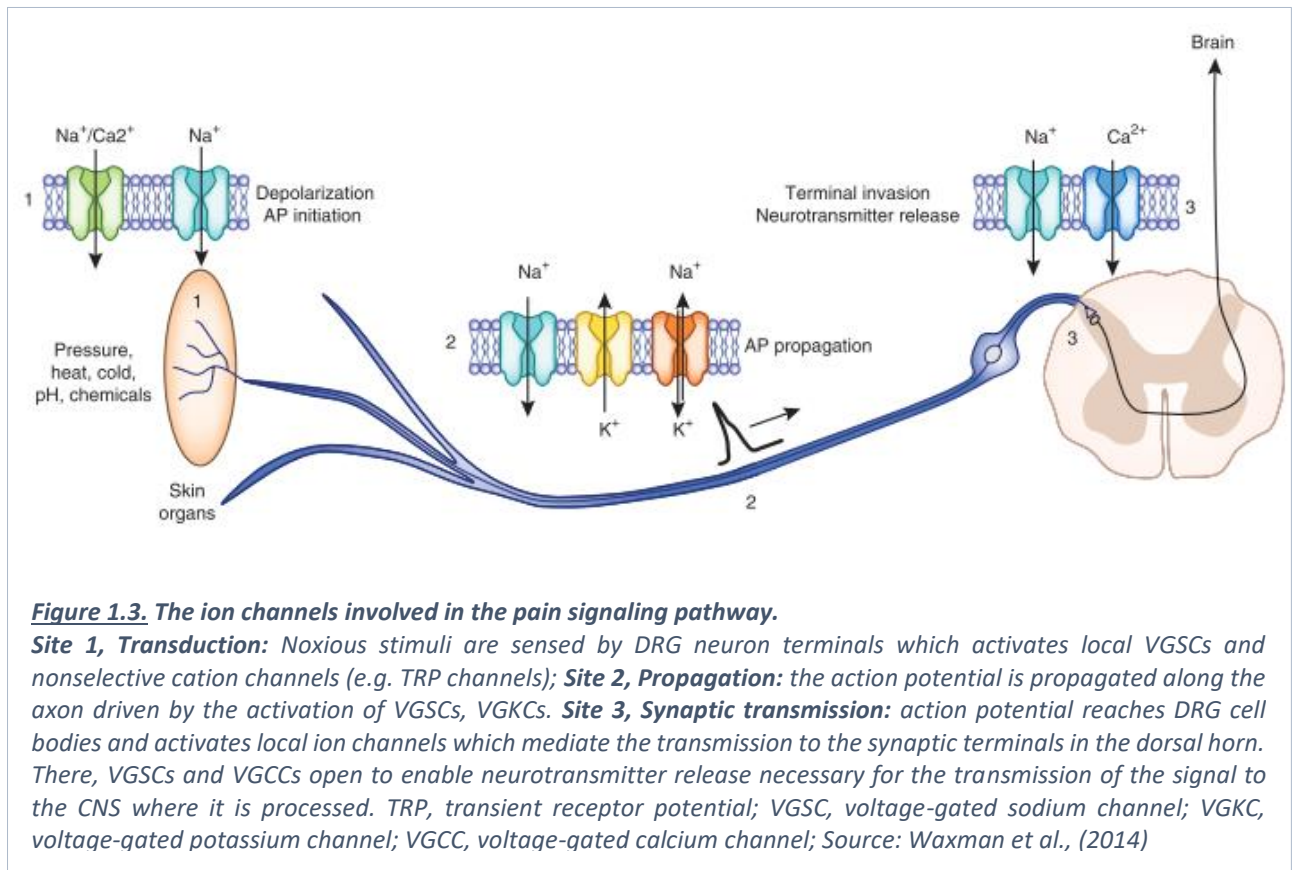
causes VGSCs there to open and Na^+ to flood in, which in turn activates local voltage-gated calcium channels (VGCCs). This results in calcium influx, bringing on a release of neurotransmitters such as substance P, CGRP or glutamate. The AP is thus passed over to the postsynaptic terminal of a second-order neuron (interneuron), completing the synaptic transmission. Finally, from there the signal can be propagated to the brain, where the site of pain perception and processing lies ²¹.

1.2.2. Pain as a disease

Dysregulation in any of the signalling steps outlined above can lead to abnormal pain signalling producing neuropathic pain. Unlike nociceptive pain, which is transient in nature and benefits the individual, neuropathic pain is sustained, usually chronic and evolving throughout the neuropathy duration. In its pathological state, pain becomes a serious disease affecting 7-10% of people worldwide^{22,23}. Neuropathic pain can arise from a direct injury to the sensory nerves or as a complication of a disease such as diabetes mellitus and other metabolic diseases²⁴; cancer and chemotherapy²⁵; HIV-infection²⁶, leprosy²⁷ and immune and inflammatory responses²⁸ amongst others²⁹. Damage to different pathway components can produce different signalling impairments such as decreased or increased AP firing thresholds, causing hyper- and hypoexcitability, respectively; dysregulated firing duration and/or degree and hence pain intensity (hyper- or hypoalgesia) or inappropriate nociceptive firing in the presence of harmless stimuli (allodynia) or in the absence of a stimulus altogether (spontaneous pain episodes)³⁰.

1.2.3. DRG-expressed channels and receptors involved in pain

From noxious stimuli detection to pain perception, pain signalling is a highly organised and controlled process. It relies on the appropriate expression and function of different voltage-gated sodium, potassium and calcium channels, leak channels and ligand-gated channels



(TRPs and acid-sensing ion channels). Among the vast diversity of ion channels implicated in pain signalling, several specific families and subtypes have been demonstrated as key regulators of sensory neurons excitability (Figure 1.3). Channel subtype-specific changes in distribution, density and kinetics are the main drivers of abnormal activity in the afferent neurons^{21,31,32}. Genetic and pharmacological studies have validated several of them as promising drug targets in human conditions of pain signalling malfunction^{21,32-34}. These include DRG-expressed voltage-gated ion channels (VGSCs, VGCCs, VGKCs), channels of the TRP family and ligand-gated ion channels and leak channels. Those of them relevant to the experiments in this thesis will be discussed in more detail next.

1.2.3.1. Voltage-gated sodium channels

VGSCs regulate AP firing in all electrically excitable cells, such as skeletal and cardiac muscle cells and neurons. Their main role in neurons is to initiate, amplify and propagate the AP. The major functional Na⁺-conducting component of VGSCs is formed by their α -subunit³⁵, while their kinetics and biophysical properties are regulated by their β -subunits³⁶. In mammals, there are nine VGSC α -subunits and thus nine different VGSC isoforms (Na_v1.1-Na_v1.9) sharing overall structural and gating motifs but differing in their expression patterns, pharmacological and functional signatures (table 1.3). A 10th VGSC isoform has also been identified (Nax), however it does not share the voltage-gating properties of the rest³⁷.

Table 1.3. Voltage-gated sodium channel isoforms discovered to date with respective gene, tissue distribution and sensitivity to tetrodotoxin (TTX). TTX-S, tetrodotoxin-sensitive; TTX-R, tetrodotoxin-resistant; TG, trigeminal ganglia; SCG, superior cervical ganglia; ND – not determined. Source: Cummins et al. (2020)

| Channel | Gene | Tissue distribution | TTX sensitivity |
|---------------------|--------|----------------------|-----------------|
| Na _v 1.1 | SCN1A | DRG, TG, CNS | TTX-S |
| Na _v 1.2 | SCN2A | CNS | TTX-S |
| Na _v 1.3 | SCN3A | Foetal DRG, CNS | TTX-S |
| Na _v 1.4 | SCN4A | Skeletal muscle | TTX-S |
| Na _v 1.5 | SCN5A | Heart muscle | TTX-R |
| Na _v 1.6 | SCN8A | DRG, TG, CNS | TTX-S |
| Na _v 1.7 | SCN9A | DRG, TG, SCG | TTX-S |
| Na _v 1.8 | SCN10A | DRG, TG | TTX-R |
| Na _v 1.9 | SCN11A | DRG, TG | TTX-R |
| Nax | SCN7A | Enteric, lung, nerve | ND |

VGSCs have different sensitivity to pore-blocking toxins, the most extensively used of which is tetrodotoxin (TTX). Accordingly, it is used to differentiate TTX-sensitive (TTX-S) from TTX-resistant (TTX-R) VGSCs. Sodium channels of the PNS can be both TTX-S and TTX-R^{38–40}. Distinct TTX sensitivity has been used to distinguish VGSC biophysical properties and

contributions, particularly in nociceptive neurons. By and large, TTX-S VGSCs are characteristic with fast activation and inactivation, whereas TTX-R channels are slowly activating and inactivating⁴¹.

Five VGSC isoforms are expressed in the DRG (Na_v1.1, Na_v1.6-1.9) and of these, three (Na_v1.7-1.9) are expressed relatively specifically in nociceptors. Although virtually all isoforms have been implicated in pain, the contribution to nociception of Na_v1.3, Na_v1.6, Na_v1.7, Na_v1.8, and Na_v1.9 has been the most extensively evidenced^{42,43}. The next part of this chapter will explore their role in nociception and pain disorders in more detail by discussing the expression and biophysical properties of each as well as evidence from clinical and animal studies.

- *Na_v1.3*

Albeit not as strongly implicated in pain as the rest of the channels discussed in this section, Na_v1.3 is of particular interest as a pain target due to its circumstantial expression pattern. Namely, this channel is usually not detectable in the adult, fully developed nervous system but its expression is upregulated in DRG neurons as well as second- and third-order neurons of the dorsal horn and thalamus under certain pathological conditions such as peripheral nerve inflammation and transection^{44,45}. Na_v1.3 has fast activation and inactivation and rapid repriming kinetics as well as persistent current that contribute to spontaneous ectopic discharges and sustained repetitive firing in injured neurons³¹. Due to the absence of isoform-selective and safe blockers, evidence of its involvement in neuropathic pain stems from genetic experiments. Antisense-driven Na_v1.3 knockdown studies show both attenuation of pain⁴⁶ and no effect⁴⁷. More recently, knockdown based on adeno-associated virus delivery of Na_v1.3 short hairpin RNA has been demonstrated to produce amelioration of pain behaviour in rodent models of neuropathic pain⁴⁸ as well as diabetic neuropathy⁴⁹.

- *Na_v1.6*

The TTX-S channel Na_v1.6 is the most abundantly expressed isoform in the CNS. In the PNS, it is present in all parts of the peripheral nerves, but it is especially abundant in the nodes of Ranvier, the microscopic myelination gaps along an axon, in myelinated DRG fibres. It is expressed constitutively in all DRG sensory neurons, with higher concentration in large, NF200+ neurons⁵⁰. In fact, Na_v1.6 has been shown to contribute to up to 60% of Na⁺ currents in large DRG compared to 34% in small DRG neurons⁵¹. It has a more hyperpolarised activation voltage compared with other VGSC isoforms and mediates persistent and resurgent Na⁺ currents contributing to repetitive AP firing^{52,53}. The role of Na_v1.6 in pain signalling has been established mainly through genetic studies. While gain of function mutations are linked to trigeminal neuralgia in humans⁵⁴, Na_v1.6-KO attenuates neuropathic pain in mice⁵¹ and

Na_v1.6-knockdown decreases TTX-S resurgent DRG currents and mechanical allodynia^{55,56}. Emerging evidence has pointed to the differing temporal upregulated expression of Na_v1.6 in different stages of neuropathic pain. Different models of neuropathic pain, including nerve injury and diabetic neuropathy, show decreased or unchanged levels of expression of Na_v1.6 in DRG in the first 4 weeks of pain^{57,58}, whereas at later stages there appears to be a consensus over the upregulated expression of Na_v1.6 in DRG neurons^{59,60}.

- *Na_v1.7*

Na_v1.7 is highly expressed in the PNS, predominantly in DRG, TG and sympathetic neurons. In DRG neurons, it is detected mainly in A β -fibres and C-fibres (nociceptors), along the entirety of the neuron^{61,62}. Other excitable cells expressing Na_v1.7 include myenteric neurons, visceral sensory neurons and neurons of the olfactory sensory system^{63,64} as well as in the hypothalamus of rodents⁶⁵. In non-excitable cells, it has been demonstrated to have a functional role in the pancreatic islet β -cells of some species⁶⁶.

Na_v1.7 is TTX-S and, like the rest of the channels from this category, is characteristic with rapid activation and inactivation kinetics. However, it has a distinct slow recovery rate from inactivation, making it unlikely to contribute to repetitive firing^{53,67}. Na_v1.7 also inactivates slowly at negative membrane potentials, which means it can remain open for longer at potentials close to RMP. Thus, it contributes to Na⁺ currents at RMP, generating “ramp currents”, important for recruiting other VGSCs (such as Nav1.8) to elicit an AP⁵³. These specific biophysical properties, together with its high expression in fibre terminals, render Na_v1.7 an AP generator or ‘threshold’ channel, setting the gain in nociceptors.

The first clues for Na_v1.7 implications in pain signalling were provided by genetic and functional profiling studies of mutations in the gene encoding it – *SCN9A*. Missense mutations in *SCN9A* produce inherited erythromelalgia (IEM), a disorder presenting with severe burning pain in the distal extremities in response to mildly warm stimuli (thermal hyperalgesia)^{68,69}. The exaggerated thermal pain phenotype is presumed to be the result of a gain of function (GoF) mutations in the *SCN9A* gene causing hyperpolarized activation of Na_v1.7 bringing its activation threshold further down. Being easier to activate, even small depolarizing stimuli are sufficient to trigger Na_v1.7 opening in nociceptors causing allodynia and hyperexcitability^{70,71}. Another dominant GoF mutation in the *SCN9A* gene, which impairs Na_v1.7 rapid inactivation, causes a syndrome known as paroxysmal extreme pain disorder⁷². The depolarising shift in the channel’s fast inactivation produces an increase in resurgent Na⁺ currents leading to enhanced DRG excitability^{73,74}. Patients suffering from this disorder experience extreme rectal, ocular and mandibular pain and erythema⁷². Other GoF *SCN9A* mutations have been identified

to occur in up to 30% of patients with diagnosed small-fibre neuropathy, impairing Na_v1.7 kinetics in both directions, i.e. hyperpolarising its activation potential and depolarising its inactivation potential in nociceptive A δ - and C-fibres⁷⁵. GoF Na_v1.7 variants have also recently been associated with diabetic neuropathy⁷⁶ - discussed in more detail later. The increased Na_v1.7 activity in these subjects produces spontaneous firing in DRG neurons causing severe pain.

In contrast, loss of function (LoF) recessive mutations in the *SCN9A* gene have been linked to channelopathy-associated insensitivity to pain (CIP). Affected individuals present with normal sensitivity to innocuous stimuli but display painless wounds, fractures and childbirth^{77,78} as well as, curiously, an inability to smell (anosmia)⁶³. In this case, the mutations produce a truncated variant of the Na_v1.7 channel which is not functional. The function of the small fibres is impaired while that of large fibres is preserved. Further to that, a recent study investigating the role of Na_v1.7 in CIP patients in more depth showed that the absence of a functional Na_v1.7 leads to structural changes in the affected afferents as well. They reported a significant decrease in intraepidermal nerve fibre (IENF) density of the distal leg and thigh of patients, implying a potential role of Na_v1.7 in long-term structural integrity in human nociceptors, particularly in the distal terminals⁷⁸. Additional links between Na_v1.7 and human pain disorders have also emerged from studies showing that single nucleotide polymorphisms in the Na_v1.7 gene lead to a subtle increase in nociceptor excitability and increased pain sensitivity in pain disorders^{79,80}. Albeit extremely rare, collectively, these mutations strongly support the importance of Na_v1.7 in the pain signalling pathway and as a target for pain relief.

Clinical case data has been further supported by animal studies. Na_v1.7-knock-out (KO) mice have aided significantly in the understanding of the mechanisms of Na_v1.7 role in pain. Originally, a Na_v1.7^{-/-} global KO in mice was lethal due to producing pups unable to feed. It was later demonstrated that this was due to the high expression of Na_v1.7 in olfactory sensory neurons in rodents⁶⁴. Knocking the channel out completely prevented blind new-born pups from relying on their sense of smell to feed. This insight allowed for the successful generation of a robust global Na_v1.7-KO model in 2014 by manually supporting KO mouse pups feeding⁸¹. The optimised Na_v1.7-KO model produced mice with near complete acute, inflammatory and neuropathic pain deficit.

Tissue-specific Na_v1.7-KO mutants utilising the Cre-recombinase-loxP system have also been available for the last decade. The first evidence of Na_v1.7 function in pain from such studies was supplied by a KO mouse whereby Cre- was driven specifically into Na_v1.8-expressing neurons, i.e. small-diameter nociceptors, since Nav1.8 is predominantly expressed there. The

conditional deletion of $Na_v1.7$ led to a dramatic loss of mechano- and inflammatory pain sensitivity⁸². Other tissue-specific $Nav1.7$ -KO models employing alternative DRG-targeting approaches (e.g. DRG-specific advillin, or neural crest-specific protein *Wnt1*) produced similar phenotypes^{83,84}.

Of note, not long ago it was demonstrated that there exist $Na_v1.7$ independent pain states. One case study reported a unique CIP patient experiencing chronic neuropathic pain following pelvic fractures and lumbar nerve impingement where $Na_v1.7$ signalling was intact⁸⁵. Similarly, a different study showed that $Na_v1.7$ was not required for the phenotype of chemotherapy-induced or cancer-induced bone pain in a mouse model⁸⁶ suggesting that similar pain phenotypes can be driven by different molecular mechanisms.

Overall, $Na_v1.7$ has been strongly established as a key regulator in DRG excitability, specifically in nociceptors. Its dysregulation has been extensively demonstrated to contribute to abnormal pain signalling in animal experiments and patients⁷⁸. Thus, it has remained as, perhaps, the most studied target for analgesic drugs with various $Na_v1.7$ channel blockers being developed (discussed in more detail in section 1.3.3.2.)

- *Na_v1.8*

Encoded by the *SCN10A* gene, $Na_v1.8$ is expressed in sensory neurons in the DRG, TG as well as nodose ganglion neurons^{87,88}. In the DRG, it is expressed in up to 90% of both non-peptidergic (IB4+) and peptidergic (IB4-) small nociceptive fibres⁸⁹, however it has been shown to be expressed in large myelinated neurons, including LTMR C- and $A\beta$ fibres responsible for touch sensation⁹⁰. Elsewhere, it is detected in high quantities in intracardiac neurons where it plays a significant role in cardiac electrophysiology⁹¹. $Na_v1.8$ is of the TTX-R family of VGSCs, but it is characteristic with its own unique biophysical properties. Compared to $Na_v1.9$ and TTX-S channels, $Na_v1.8$ is distinguished with a more depolarized activation threshold and slow inactivation. What this means is that: 1) $Na_v1.8$ can be activated only following the activation of a TTX-S channel and 2) $Na_v1.8$ channels can remain active long after other VGSCs have been inactivated, contributing to most of the generated Na^+ current upon depolarisation^{92,93}. $Na_v1.8$ also recovers quickly from inactivation and thus, contributes to high frequency AP firing when membrane depolarisation is sustained⁹².

Several GoF mutations have emerged from patient cases. An international coalition from 2012 conducted genetic analyses of 104 small-fibre neuropathy patients. No *SCN9A* ($Na_v1.7$) mutations were identified, but 7 *SCN10A* mutations were described in 9 of the patients. All of them shared similar shifts in the $Na_v1.8$ channel's kinetics, including hyperpolarization of its activation threshold and acceleration in its recovery from inactivation⁹⁴⁻⁹⁶. This lowered the AP

generation threshold and increased the rate of AP firing, thus producing high-frequency spontaneous firing even in the absence of stimuli, culminating in DRG hyperexcitability.

Natural *SCN10A* LoF mutations have not yet been identified in humans, therefore knowledge of $\text{Na}_v1.8$'s role in pain has been derived from genetic studies on animal models. The global $\text{Na}_v1.8\text{KO}$ mouse showed only moderate analgesia to painful stimuli⁹⁷. In a later study, a $\text{Na}_v1.8\text{KO}$ mouse model of neuropathic pain displayed no change in its painful phenotype⁹⁸. These observations contradict those obtained from mice with genetically ablated neurons expressing $\text{Na}_v1.8$ channels, where animals showed profound loss of pain⁹⁹; or knocked-down $\text{Na}_v1.8$ channel, where TTX-R current was reported to be significantly reduced and spinal nerve ligation-induced neuropathic pain behaviour reversed¹⁰⁰. This discrepancy was attributed to a key compensatory mechanism being triggered in the global $\text{Nav}1.8\text{KO}$, whereby $\text{Na}_v1.8$ absence induced upregulation of $\text{Na}_v1.7$ expression and hence TTX-S current, thus preserving the neuropathic pain phenotype⁸⁷. However, in a later study, a $\text{Na}_v1.7/\text{Na}_v1.8$ double KO mouse model displayed reduced inflammatory pain and impaired mechanical and thermal acute pain thresholds but developed normal levels of neuropathic pain, implicating $\text{Nav}1.8$ is not necessary for nerve injury-induced pain¹⁰¹.

Interestingly, Dib-Hajj et al. (1996) observed that $\text{Na}_v1.8$ expression and TTX-R current is downregulated in injured DRG neurons (following transection of the peripheral nerve), however they were upregulated in neighbouring uninjured neurons¹⁰². A similar conclusion was also reached by Gold et al. (2003) who observed a significant redistribution of $\text{Na}_v1.8$ channels to uninjured neurons adjacent to injured fibres of the sciatic nerve. This was accompanied by an increase in the TTX-R current, particularly in uninjured C-fibres and partially in thinly myelinated $\text{A}\delta$ -fibres following injury, leading to spontaneous activity in these neurons¹⁰³. Remarkably, Coward et al. (2000) established a time-dependent shift in $\text{Na}_v1.8$ involvement in such neuropathic pain. Overtime, post-injury $\text{Na}_v1.8$ upregulation and hyperexcitability affected not only uninjured but also the injured nociceptors as well. Therefore, considering neuropathic pain in particular, $\text{Na}_v1.8$ might be involved via a temporal role shift from intact to injured neurons as the injury progresses¹⁰⁴. In contrast to neuropathic pain, the contribution of $\text{Na}_v1.8$ to inflammatory pain is better established. Different inflammatory mediators, such as NGF, $\text{TNF}\alpha$ and other cytokines, have been evidenced to modulate $\text{Na}_v1.8$ biophysical properties and causing hyperexcitability in DRG neurons^{98,105-108}.

- *Na_v1.9*

The other DRG-expressed TTX-R channel is $\text{Na}_v1.9$, encoded by the *SCN11A* gene. Unlike $\text{Na}_v1.8$, however, it is activated at low voltage potentials (approx. -70mV), close to the RMP

and produces a persistent current ¹⁰⁹. Na_v1.9 is expressed in the soma of small-diameter DRG and TG neurons. Expression in the PNS is particularly concentrated in non-peptidergic nociceptors ^{110,111}. The specific biophysical properties of Na_v1.9 and its distribution along sensory neurons suggest it may determine the activation threshold of small DRG neurons ¹⁰⁹.

The role of Na_v1.9 in neuropathic pain is not fully understood and the literature remains controversial. In humans, 7 different mutations have been identified in the *SCN11A* gene in peripheral neuropathy patients which modified the channel properties via various mechanisms. These include reducing the current threshold and increasing the firing frequency thus increasing DRG excitability and causing patients to experience episodic chronic pain ^{112–114} and, in the case of some – cold pain ¹¹⁵. Nerve-injury models of Na_v1.9-null mice including partial sciatic nerve injury ¹¹⁶, chronic constriction injury ¹¹⁷ and spinal nerve transection ⁸⁶, demonstrated no change in the pain-thresholds of the animals. In contrast, similar to Na_v1.8, Na_v1.9 expression and current in sensory neurons has been reported to be significantly lower in different animal models of neuropathic pain, including in DRG ^{118,119} and TG ¹²⁰ neurons.

Inflammatory pain, on the other hand, has been strongly linked to the presence of Na_v1.9. Several studies assessing the effects of a great diversity of inflammatory agents on Na_v1.9KO mice were all consistent in their reports, observing reduction in the pain behaviour of these animals ^{116,121–123}. It is speculated, that inflammatory mediators act via a G-proteins-dependent mechanism to increase Na_v1.9 persistent current and lead to spontaneous activity in affected sensory neurons ¹²⁴.

From all of the above, DRG-expressed VGSCs contribute greatly to various pain states and represent attractive targets for novel analgesics in development. Characterising the changes in their function in models of neuropathic pain is, therefore, essential for the development of better-targeted and safer therapies. However, they are only one avenue of research into neuropathic pain.

1.2.3.2. Transient receptor potential cation channels: TRPV1 and TRPA1

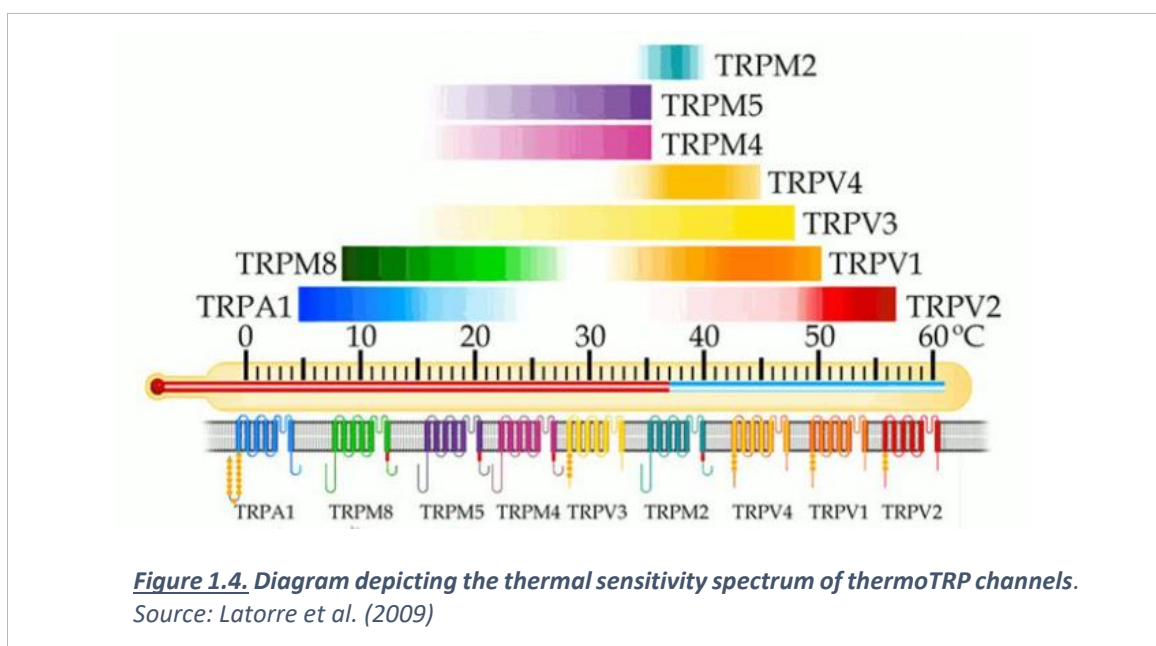
External stimuli are transduced into APs via the activation of another group of specific cation-conducting channels expressed in the neuronal membrane. These are the superfamily of transient receptor potential (TRP) ion channels which contribute to sensory perception in animals. Most lately, the great diversity within TRP channels was categorised into nine animal subfamilies: TRPA (ankyrin), TRPV (vanilloid), TRPVL (vanilloid-like), TRPC (canonical), TRPN (no mechanoreceptor potential C), TRPM (melastatin), TRPS (soromelastatin), TRPML (mucolipin) and TRPP (polycystin). Each of the subfamilies comprises several subtypes of

channels with distinct structural homology giving rise to specific signal integration and regulation functions. Members of the TRP subfamilies are activated by a great range of stimuli, including photosensation, mechanosensation, thermosensation and nociception, some integrating two or more modalities. Thus, they are key polymodal cellular sensors (for in depth reviews see ^{125,126}).

ThermoTRP channels represent those members of the families that are particularly sensitive to temperature. Of all TRP channels, nine are characteristic with differing ranges of activation temperatures (Figure 1.4). TRPV1-4, and TRPM2, 4 and 5 are heat-activated, while TRPA1 and TRPM8 are cold-activated ¹²⁷. Of these, two have received a great amount of interest and have been implicated in nociception the most ^{128,129}. Since functional changes in the same two TRP channels are also the focus of part of the upcoming experiment chapters, the rest of this section will cover the properties and role in pain of these two channels, namely TRPV1 and TRPA1.

- *TRPV1*

The TRPV1 (transient receptor potential cation channel subfamily V member 1) channel is the first channel of the TRP family to be cloned and have its structure resolved. To date, it is also the most studied member of the TRP superfamily due to its intriguing polymodality and role in pain ¹³⁰. Encoded in humans by the *TRPV1* gene, it is a nonselective cation channel with a ligand- and heat-gated mechanism. In the nervous system, it is mainly expressed in the TG and DRG sensory neurons and cranial nerve cervical ganglia neurons innervating organs in the head ^{130,131}. In primary afferents, TRPV1 is distributed throughout, from the skin-terminating



free endings (highest density), along the axons and in the cell bodies, with especially high

expression rates in small-diameter peptidergic nociceptors demonstrated using reporter mice (up to ~82% in the adult mouse DRG) ¹³².

The structure of TRPV1 has been studied extensively ¹³⁰ due to its sophisticated gating, regulation and ion selectivity mechanisms. TRPV1 is a cation-permeable channel with a strong preference for Ca^{2+} ions (10-fold more Ca^{2+} conductance than other ions). Upon TRPV1 activation, a strong Ca^{2+} and moderate Na^{+} influx is triggered, depolarising the membrane which, if strong enough, can lead to the activation of voltage-gated ion channels (such as $\text{Na}_v1.7$) and thus generate an AP ¹³³.

A homotetrameric membrane protein, TRPV1 possesses a distinct structural complexity to which it owes its vulnerability to a range of different stimuli categories. These include vanilloids (capsaicin, resiniferatoxin), lipids, noxious heat ($\geq 43^\circ\text{C}$) and acidic solutions (protons) ($\text{pH} < 6.0$) ¹³⁴. Interestingly, each group of stimuli has its distinct site of action on TRPV1. For example, vanilloids are lipophilic and have been shown to diffuse through the lipid membrane and bind to an intracellular site on TRPV1 ^{135,136}. Protons, on the other hand, act exclusively on an extracellular acidic site of the channel ^{137,138}, while high temperatures critically change the proximal region of the C-terminus ¹³⁸. The segregation of active sites allows for each stimulus to trigger channel gating alone but also for two or more stimuli to act together and cooperate to potentiate the channel. For instance, when pH is low, for example during tissue acidosis following an injury, local TRPV1 channels have lowered temperature activation thresholds so that they can be activated at as low as room temperature ¹³⁹⁻¹⁴¹. This facilitates TRPV1 activation, thus sensitising nociceptors during moderate acidosis in ischemic or inflamed nerve tissues, contributing to allodynia and/or hyperalgesia ¹⁴⁰.

TRPV1 has been strongly linked to nociception. Upon an injury, various inflammatory molecules (such as bradykinin and prostaglandin E2) are released which together with cytokines and neurotrophins have been shown to sensitise TRPV1 to its stimuli through phospholipase C, protein kinase A (PKA) or C (PKC) pathways ¹⁴²⁻¹⁴⁵; or even directly activate it (such as some lipid mediators) ^{146 147}. Evidence for the role of TRPV1 in inflammatory pain comes from experiments with TRPV1-null mice. The mutant mice showed no capsaicin-induced pain behaviour and had attenuated inflammation-induced thermal hyperalgesia and did not respond to noxious heat ^{148,149}. These observations were confirmed by pharmacological experiments with mice injected with a TRPV1 antagonists (such as capsazepine), also reporting attenuated thermal hyperalgesia under inflammatory conditions ^{148,150}.

In neuropathic pain, the evidence of TRPV1 contribution is still contradictory. In TRPV1-null mice, pain perception does not change following nerve damage ^{148,151}. However, several animal

models of neuropathic pain exhibit decreased pain following pharmacological inhibition of TRPV1^{152,153}. In addition, development of sustained thermal hyperalgesia has been correlated with the increased expression of TRPV1¹⁵⁴. Finally, TRPV1 has been implicated in neuropathic pain arising as a complication from certain conditions. Elevated expression levels of the thermo channel in DRG and dorsal horn have been reported in diabetic neuropathy and cancer-induced chronic pain models, correlating with hyperalgesia behaviour^{58,155,156}. Therefore, targeting TRPV1 for pain alleviation may prove promising. In fact several TRPV1-targeting ligands have been in development and focus appears to be equally on agonists as well as antagonists¹⁵⁷.

- *TRPA1*

Another well-studied TRP channel is the TRP ankyrin 1 (TRPA1) channel. TRPA1 is expressed in the sensory neurons of the DRG and TG¹⁵⁸, predominantly in, non-peptidergic (IB4+) nociceptors¹⁵⁹. It is often co-expressed with TRPV1 in a subset of nociceptive neurons¹⁶⁰ and has been suggested to interact with it and form a heteromeric channel¹⁶¹. Being a Ca²⁺-permeable channel, upon TRPA1 activation intracellular Ca²⁺ levels increase drastically leading to neuronal excitation¹⁵⁸.

Much like TRPV1 and other thermoTRPs, it is activated by a range of stimuli, individually as well as simultaneously. These include mechanical perturbations¹⁶², exogenous irritants such as cinnamaldehyde (compound in cinnamon), cannabinoids, acrolein (present in tear gas), menthol and allyl isothiocyanate (AITC, found in wasabi, radish and mustard)^{163–165}; as well as endogenous molecules released upon tissue damage and inflammation¹⁶⁵. In addition to being a chemosensor, TRPA1 has been implied to be activated by cold temperatures (~17°C), demonstrated clearly *in vitro*^{160,166,167}. However others using heterologous expression systems^{163,168} as well as TRPA1-null mice¹⁶⁹ report contradicting findings on its ability to be activated by noxious cold, leaving the role of TRPA1 as a cold sensor highly controversial. Of note, TRPM8 is also activated by menthol and cool temperatures (~25°C), shaping a separate population of cells specialised for low temperature sensing¹⁷⁰.

With high expression levels in nociceptors, TRPA1 has been implicated in acute, inflammatory and neuropathic pain. The role of TRPA1 in inflammatory hypersensitivity was first reported in a study demonstrating its contribution to the excitatory effects on nociceptors induced by the inflammatory mediator bradykinin¹⁶⁴. These results were confirmed by a pivotal study showing decreased formalin-induced nociceptive response in rodents following TRPA1 pharmacological blockade and genetic deletion¹⁷¹. Adopting the same methods, TRPA1 was

documented to be involved in mechanical and cold hypersensitivity associated with inflammation as well ^{172–174}.

The involvement of TRPA1 in neuropathic pain was initially suggested by observations made in spinal nerve ligated mice, where TRPA1 was downregulated in injured L5 DRG but upregulated in uninjured L4 DRG (much like the case with Nav1.8 in the same nerve injury model, see section 1.2.3.1, *Nav1.8*) ¹⁷⁵. Similar redistribution of TRPA1 expression was noted in other nerve injury models ^{176–178}. Several TRPA1 antagonists ^{179,180} and TRPA1^{-/-} animal models ^{181–183} have shown attenuated allodynia and hypersensitivity after peripheral nerve injury. TRPA1 has been implicated in diabetic neuropathy: its inhibition reduces mechanical allodynia and hypersensitivity in rat diabetic neuropathy models ¹⁸⁴, while methylglyoxal, an abundant glucose metabolite during diabetes, has been shown to activate TRPA1, contributing to hyperalgesia ¹⁸⁵.

1.2.3.3. Purinoceptors: *P₂X* purinoceptor 3 (*P₂X₃*)

The *P₂X* purinoreceptor family includes ligand-gated ion channels activated by binding of extracellular adenosine 5'-triphosphate (ATP). Apart from providing energy for cellular processes, ATP also acts as an important intercellular messenger released locally by damaged tissues. It binds *P₂X* receptors expressed by sensory neuronal terminals and cell bodies in the periphery and interneurons in the dorsal horn ^{186,187}. There are seven different *P₂X* subunits (*P₂X₁₋₇*) expressed in DRG, TG and nodose ganglia. Amongst them, *P₂X₃* is the only subtype selectively expressed in small C-fibre nociceptors, particularly the non-peptidergic subpopulation ^{188,189}. *P₂X₃* is a trimeric cation channel contributing to up to 96% of ATP-induced responses in DRG sensory neurons ¹⁸⁶. Upon ATP binding, *P₂X₃* channels activate and are desensitized within milliseconds, however ATP dissociation and desensitization recovery can take minutes thus limiting repetitive AP firing ^{190,191}.

Pharmacological studies using *P₂X₃* selective antagonists ^{192–195} and animal studies using *P₂X₃*-deficient ^{196,197} or *P₂X₃*-selective-antisense-treated animals ^{198–200} have demonstrated that *P₂X₃*, along with its heteromeric assembly with *P₂X₂* (forming *P₂X_{2/3}*), are responsible for transmitting persistent, inflammatory and neuropathic pain. For example, the intraplantar flinching in *P₂X₃*^{-/-} mice was reduced in response to α,β -MeATP and formalin (used to induce inflammatory pain in animals) ¹⁹⁷, indicating a strong role of DRG *P₂X₃* receptors in inflammatory pain. Antisense-driven knockdown of *P₂X₃* confirmed these findings and demonstrated reversal of mechanical allodynia in different neuropathic injury models ^{199,200}. Thus, *P₂X₃* has emerged as a promising target for treating pain conditions and several

antagonists are in development for treating migraine, itch-associated pain and cancer pain^{201–204}.

To summarise, these sections highlighted the importance of several VGSCs, TRPV1, TRPA1 and P2X3 in nociception and pathological pain promoting further research into their function during chronic pain conditions. These channels form an attractive cohort of targets for efficient molecules that can downregulate their function to alleviate pain and have an important function as markers of sensory subtypes in DRG characterizing experiments. The study presented here focuses on targeting the activation of VGSCs, TRPV1, TRPA1 and P2X3 in order to investigate their contribution, as well as that of the neuronal subpopulations they mark, to neuronal excitability changes during diabetic neuropathy – the topic of the next section of this chapter.

1.3. Diabetic neuropathy and pain

Diabetes mellitus is an umbrella term covering a group of metabolic disorders leading to impaired glucose uptake and metabolism by the body. In a healthy organism, its metabolization involves several steps, simplified and summarised in [Figure 1.5](#). Glucose molecules are obtained from food and metabolised in cells to release energy. Their uptake by the cells from the blood relies on the adequate function of the anabolic hormone insulin, secreted by the pancreatic β -cells. Its role is to bind to its receptor on the cell membrane of hepatocytes, skeletal muscle cells and promote glucose absorption from the blood primarily for energy generation (ATP). If not utilized for energy, excess glucose is stored in the form of glycogen (chains of glucose molecules) in the muscle and liver tissue or triglycerides (fat) in adipose tissue^{205,206}.

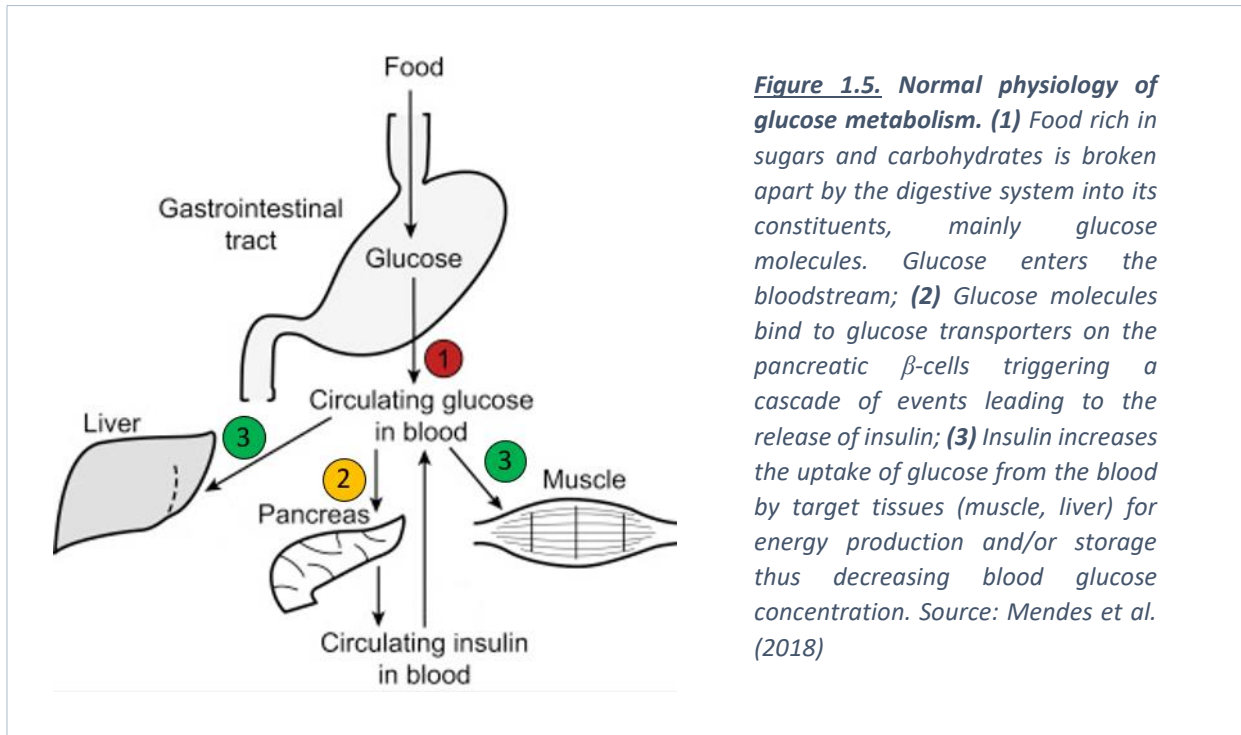


Figure 1.5. Normal physiology of glucose metabolism. (1) Food rich in sugars and carbohydrates is broken apart by the digestive system into its constituents, mainly glucose molecules. Glucose enters the bloodstream; (2) Glucose molecules bind to glucose transporters on the pancreatic β -cells triggering a cascade of events leading to the release of insulin; (3) Insulin increases the uptake of glucose from the blood by target tissues (muscle, liver) for energy production and/or storage thus decreasing blood glucose concentration. Source: Mendes et al. (2018)

1.3.1. Diabetes

The main characteristic of all diabetic disorders is impaired insulin signalling rendering the body unable to regulate blood glucose levels. The result is chronic hyperglycaemia, or elevated blood glucose. If uncontrolled, prolonged hyperglycaemia can lead to disabling and even fatal acute and chronic complications including cardiovascular disease, kidney damage (nephropathy), eye disease (retinopathy) and nerve damage (diabetic neuropathy)^{207,208}.

Although diabetic complications are all predominantly caused by excess blood glucose, the cause of hyperglycaemia can be different, giving rise to the two main distinct forms of diabetes: type 1 (T1D) and type 2 diabetes (T2D). In order to understand the underlying mechanisms of diabetic neuropathy and address its research and treatment adequately, one must first consider T1D and T2D as the distinct, if not opposite in some respects, diseases that they are, which is the aim of this chapter section. A brief outline of the characteristics of each is given in table 1.4

Table 1.4. Summary of the main characteristics for diabetes type 1 and 2. Adapted from Ozougwu O. (2013).

| | Type 1 Diabetes | Type 2 Diabetes |
|-----------------------------|---|--|
| Prevalence | ~ 10 % | ~ 90 % |
| Onset | Sudden | Gradual |
| Age of diagnosis | Mostly children | Mostly adults |
| Body mass | Low to normal | High to obese |
| Blood glucose levels | High | High |
| Blood insulin levels | Low or absent | High initially, then decreasing |
| Insulin resistance | No | High |
| Autoantibodies | Present | No |
| Symptoms | <ul style="list-style-type: none"> • Abnormal thirst & frequent urination • Sudden weight loss • Fatigue • Chronic hunger • Blurred vision • impaired wound healing | <ul style="list-style-type: none"> • Excessive thirst & urination • Weight gain • Fatigue • Blurred vision |
| Complications | <ul style="list-style-type: none"> • Ketoacidosis • Neuropathy • Retinopathy • Nephropathy • Cardiovascular disease | <ul style="list-style-type: none"> • Neuropathy • Retinopathy • Nephropathy • Cardiovascular disease |
| Treatment | Insulin supplementation | Lifestyle and diet changes, thiazolidinedione, metformin, sulfonylureas, insulin (later stages) |

1.3.1.1. Type 1 Diabetes – an autoimmune response

T1D is now well-recognised as a chronic autoimmune disorder, characteristic with immune-mediated destruction of the insulin-producing pancreatic β -cells. Their absence leads to a marked deficiency in insulin secretion (Figure 1.6b). With no circulating insulin to regulate blood glucose levels, hyperglycaemia develops. With insulin unavailable, target cells cannot uptake any of the abundance of glucose and become starved and unable to produce energy leading to rapid weight loss despite an increase in appetite amongst other symptoms (Table 1.3). The underlying causes for this devastating process are believed to include a combination of genetic susceptibility (with multiple genes altered, typically ones encoding components of the immune system) and environmental factors, commonly viral infections, toxins or diet, that trigger an autoimmune response²⁰⁹. The prevalence of T1D is approximately 10% of diabetic cases with highest incidence in children and adolescents^{209,210}. Diagnosis of both diabetes

types requires fasting blood glucose levels over 7 mmol/L and blood glycated haemoglobin levels of 6.5% or higher. To distinguish it from T2D, T1D diagnosis also requires detection of diabetes-associated autoantibodies, which can be present up to years before symptomatic onset²¹¹. Daily insulin supplementation begins immediately following diagnosis and is normally efficient at controlling the disease. Patients usually develop chronic T1D complications over approximately 10 years from diagnosis, depending on blood glucose levels management and the degree of blood vessels damage²⁰⁹. The prevalence of symptomatic diabetic neuropathy in T1D patients is substantial and consistent. Two large scale studies from 2020 established an average 11-13% prevalence estimate of symptomatic diabetic neuropathy in T1D population, with the proportion approximating 20% in older subgroups^{212,213}.

1.3.1.2. Type 2 Diabetes – a lifestyle problem

In contrast, T2D does not involve an autoimmune response, but is rather more tightly influenced by environmental factors, with an especially strong link to the global obesity pandemic^{214,215}. In T2D, initially, insulin is still being produced and secreted, however it cannot exercise its effect on target cells (muscle and liver). This state of cell insensitivity to the hormone is termed “insulin resistance” (IR) and is the key component distinguishing T2D from T1D pathophysiology. Thus, target cells remain “closed” for the high glucose flow from the blood. Ironically, the body’s response to IR is to secrete even more insulin, which over time leads to β -cell failure and inadequate insulin production²¹⁶.

While genetics, advancing age and ethnicity have been shown to be potential risk factors in T2D²¹⁷, the driving force behind IR is mainly high sugar and processed carbohydrate consumption, sedentary lifestyle and obesity and usually IR develops many years before T2D is diagnosed^{215,218–220}. When the sugar intake is chronically excessive and exceeding energy demands, the cells in a healthy body metabolise and store the excess as glycogen (in muscle and liver cells) and triglycerides (in liver and adipocytes). With time, muscle and liver cells reach full glycogen storage capacity and thus become irresponsive to insulin attempts to store more incoming glucose. Still, the body prioritises lowering blood glucose levels, so the excess sugar can now only be metabolised into free fatty acids and deposited into new fat cells, continuing to increase body weight²²¹. Thus, in T2D blood levels of glucose as well as insulin (hyperinsulinemia) and triglycerides (dyslipidaemia) are abnormally high^{222222–224}. With these two additional pathophysiological elements, T2D already differs significantly in its natural history from T1D. Although symptoms largely overlap between the two types,

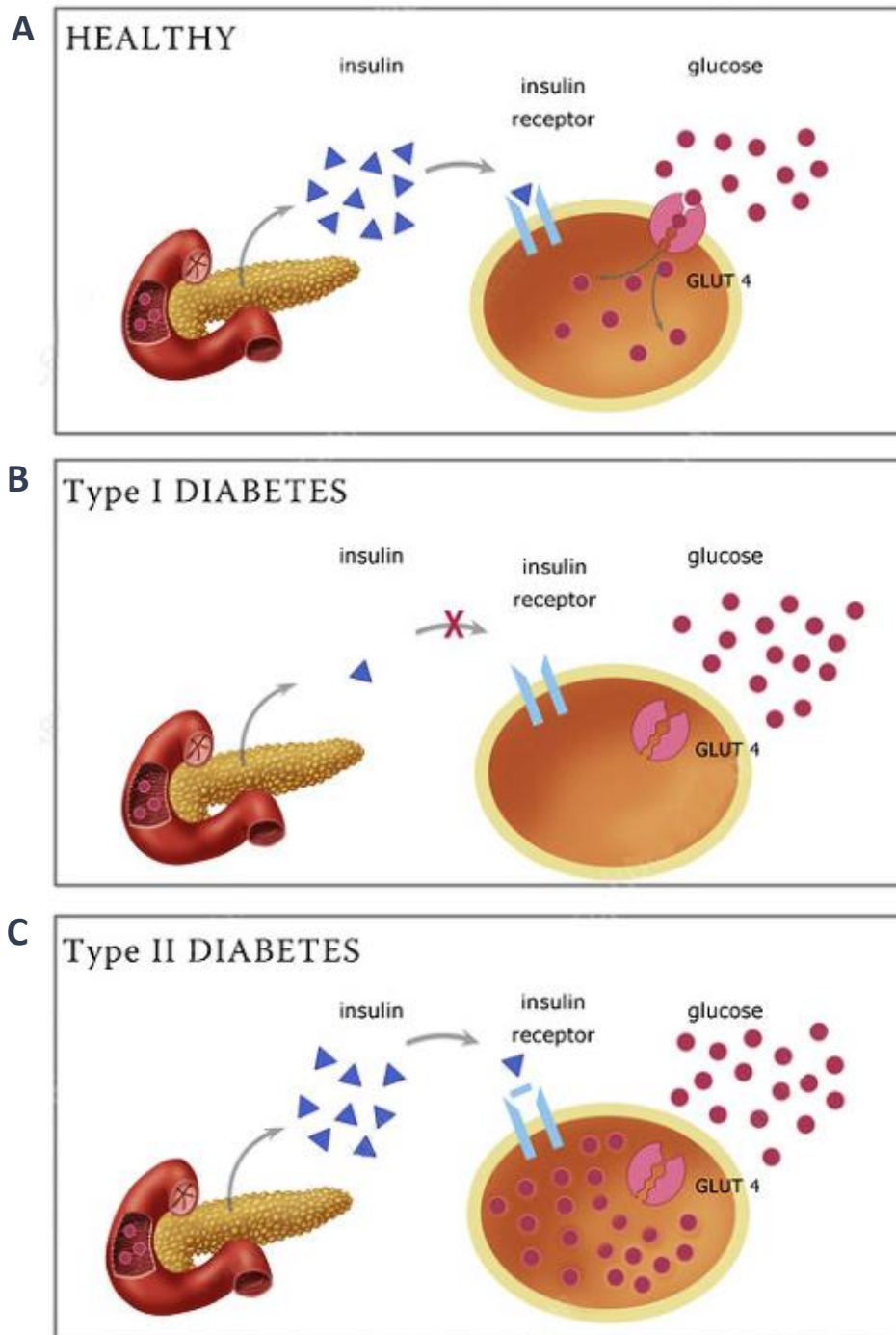


Figure 1.6. Insulin production compared between healthy, type 1 diabetes and type 2 diabetes setting. Insulin (blue triangles) is released by pancreatic β cells to allow glucose (red circles) uptake by target cells through glucose transporters (GLUT 4, pink). In a T1D scenario, insulin production is impaired leading to deficiency in insulin signaling to target tissue and no glucose uptake. In a T2D setting, insulin is still being produced, however target tissues are saturated with glucose, preventing insulin binding to its receptor and inhibiting further glucose uptake. In both T1D and T2D glucose is not cleared from the blood, leading to hyperglycemia. While in T1D cells are starved, leading to overall weight loss. Adapted from: Monica Schroeder, Science photo library, in T2D excess glucose is diverted to de novo adipose cells generation, contributing to weight gain and in severe cases obesity. Source: Monica Schroeder/Science Photo Library, available at: <https://www.sciencephoto.com/media/706546/view>

T2D typically has a much less dramatic presentation, occasionally developing

asymptomatically for a prolonged time ²¹⁵.

Ninety percent of diabetic patients suffer from T2D. It is most common in older adults (age 40+) but has been increasingly more often diagnosed in young adults and children due to the worldwide rise in sedentary lifestyle and energy-dense diets. These circumstances are also propelling the overall T2D high and rising prevalence worldwide ²²⁵.

1.3.2. Diabetic neuropathy

Diabetic neuropathy (DN) is the most common complication arising from diabetes. DN is an impairment of the nerves of the body, caused mainly by prolonged hyperglycaemia damaging the microvasculature supplying the nerves (*vasa nervorum*). This can alter the functions of proximal and distal sensory, motor and autonomic nerves and thus damage virtually any organ system of the body causing a wide variety of symptoms ²²⁶. Worryingly, it is also the most problematic diabetic complication with statistics placing it as the most widespread form of neuropathy in developed countries. Approximately 50% of diabetic patients develop some type of nerve impairment, with neuropathy onset correlating positively with diabetes duration ^{227,228}. DN accounts for more patients hospitalised than all other diabetic complications combined and is the leading cause of lower limb amputations ²²⁹. It thus represents a great economic burden for any healthcare system as well as the patients themselves ²²⁸.

The most common type of DN is a symmetric neuropathy of the peripheral, predominantly sensory neurons or “distal symmetric polyneuropathy”. Since this form is the focus of this thesis, from here on and throughout, “DN” shall refer to distal symmetric polyneuropathy. It initially affects the distal nerves, innervating the feet and hands and gradually spreads proximally following the “stocking-glove” distribution model ²³⁰. Symptoms include paraesthesia (prickling sensation), dysesthesia (abnormal sensations), pruritus (itching), sensory loss, numbness and loss of balance. However, one particular symptom is deemed so debilitating and characteristic for patients that has defined a separate neuropathic condition stemming from DN. Pain during DN is experienced by 8 to 50% of DN patients and is clinically termed as painful diabetic neuropathy (PDN) ²³¹. Patients suffering with PDN describe pain as burning, shooting, stabbing, dull and aching, usually exacerbated at night. Frequently, PDN patients present with allodynia and hyperalgesia ²³². Although symptoms and progression of DN vary from patient to patient, it has been proposed that, overall, positive symptoms (prickling, tingling, pain) are characteristic of the early stages of DN, while negative symptoms (numbness, loss of sensation) are typical of the late stages, with possible extension of pain symptoms into the advanced DN phase ^{233,234}.

T1D long-term complications largely overlap with those seen in T2D in their detriment and intensity. For decades, DN in T1D and T2D has been considered to be one and the same disease brought about by a shared underlying master mechanism – hyperglycaemia. However, accumulating evidence points to differences in the pathophysiology underlying T1DN and T2DN^{231,233,235–239}. The next section discusses the common and contrasting features of the two diabetes forms and how they may impact the neuropathy progression in each.

1.3.2.3. T1D and T2D inconsistencies

Diabetes is ranked 5th globally in disease incidence, affecting 1 in 11 people²²⁵. Albeit the lifetime incidence of neuropathies is estimated to be between 10% and 50% for both T1D and T2D²²⁸, the superior global prevalence of T2D over T1D (90% vs 10%, respectively)²⁴⁰ makes T2D-associated nerve damage the most common and imperative cause of neuropathies. Logically, therefore, if the focus is on treating DN in T2D patients, this prompts the use of T2DN pre-clinical models over T1DN ones to dissect the underlying mechanisms driving the disease's progression. Yet, our understanding of painful DN pathology has mostly been obtained from streptozotocin (STZ)-induced diabetes in rats, a model of T1D^{241,242}. Pre-clinical model selection has been speculated as an important reason for the failure of translating drug efficacy from pre-clinical animal models to patients²⁴². For example, the involvement of oxidative stress²⁴³, the polyol pathway²⁴⁴ and aldose reductase²⁴⁵ was confirmed largely by studies using the STZ rat (also reviewed in²⁴⁶). Subsequently, the STZ rat was also implemented as a pre-clinical DN model for the development of aldose reductase inhibitors as a potential DN-modifying treatment. Indeed, in STZ rats, the novel family of drugs corrected DN-induced nerve structure and nerve conduction velocity (NCV) impairments²⁴⁷. Yet, despite the promising pre-clinical data, all clinical trials failed to replicate the drug's pre-clinical efficacy. A meta-analysis of 32 aldose reductase inhibitor clinical trials showed that participants were predominantly T2D patients and diagnostic criteria for diabetes were not even stated in most of the studies included, highlighting the lack of discrimination between the diabetes types²⁴⁸. A very similar drug development course was followed by PKC inhibitors. Most of the pre-clinical success noticed with this drug class was obtained from STZ rodents, however, PKC inhibitors were ineffective in the treatment of DN in human patients²⁴⁹.

Evidence for fundamental differences in the underlying mechanisms of T1DN and T2DN is also provided by clinical research with patients. In 2012, Callaghan et al. published a comprehensive systematic review of 17 clinical studies investigating the effects of glycaemic control on DN development in T1D and T2D. It was concluded that intensive glycaemic control significantly decreases risk and progression of DN in T1D patients but was only moderately

beneficial in T2DN patients ²⁵⁰. Their analysis shows that hyperglycaemia alone is not the driving force of DN in T2D. What is more, it strongly accentuates on the concept of T1DN and T2DN being separate disease entities ²³⁶. Furthermore, painful symptoms have been shown to have higher prevalence in T2D patients than T1D ^{231,239,251}. In one of the largest cohort observational clinical studies (n = 15,692) of diabetic UK patients, Abbott et al. demonstrated that the adjusted risk of painful neuropathy in T2D is double that of T1D patients ²³¹.

What is more, these observations confirm those reached in studies conducted by Sima and Kamiya investigating DN in T1D and T2D rat models of each. They demonstrated that T1DN is much more severe than T2DN, with bigger decrease in NCVs and thermal sensitivity latencies as well as more acute IENF damage and loss, all reversible with an insulinomimetic compound ^{233,252,253}. Others showed that in contrast to T1D animals, limited amelioration to the DN phenotype was seen in *db/db* mice too, even when administered 3 times higher doses of insulin than T1D animals ²⁵⁴. The contrasting effects of insulin intervention were attributed to the different insulin levels, actions and signalling impairments in the two diabetic types. These conclusions were a strong indicator of different mechanisms driving DN in T1D and T2D. Factors other than hyperglycaemia are now being widely discussed as contributors in the development of T2DN with the main focus falling on metabolic syndrome components including dyslipidaemia ²⁵⁵, inflammation ²⁵⁶ and IR ²⁵⁷.

In the next sections, I will address the pathways, conventional and emerging, known to be dysregulated during DN, some of which are common for both diabetic types, while others are more characteristic of T2DN.

1.3.3. Mechanisms implicated in (painful) diabetic neuropathy

Although DN development varies amongst individuals, it is generally accepted that it follows a specific temporal and spatial progression. The earliest changes during DN are believed to affect the C-fibres leading to an axonal degeneration/regeneration cycle ²⁵⁸. This causes 'positive' symptoms such as pain, tingling, allodynia and hyperalgesia ²⁵⁹. Overtime, degeneration prevails resulting in the loss of C-fibres, as well as A δ -fibres and consequently diminished pain sensation. As DN progresses, myelinated A-fibres undergo a demyelination/remyelination cycle until complete destruction of the myelin sheath ^{258,260,261}. The loss of protection and nutrient supply by the supporting Schwann cells (SCs) (constituting the myelin) ²⁶¹ leads to direct axonal degeneration, resulting in impaired proprioception and touch sensation ²³⁴.

For a long time, DN was argued to either originate from metabolic abnormalities within the nerve and Schwann cells or develop secondary to diabetic microvascular complications. It is now believed that DN pathogenesis is shaped by an intricate interplay between both vascular and metabolic factors at all stages of the disease. Hyperglycaemia, dyslipidaemia and insulin's abundance (hyperinsulinemia, T2D) or absence (insulinopenia, T1D) all affect both the microvasculature and the nerves themselves. The next part of this chapter will look into these mechanisms in more detail.

1.3.2.1. Damage to the microvasculature supplying the neurons

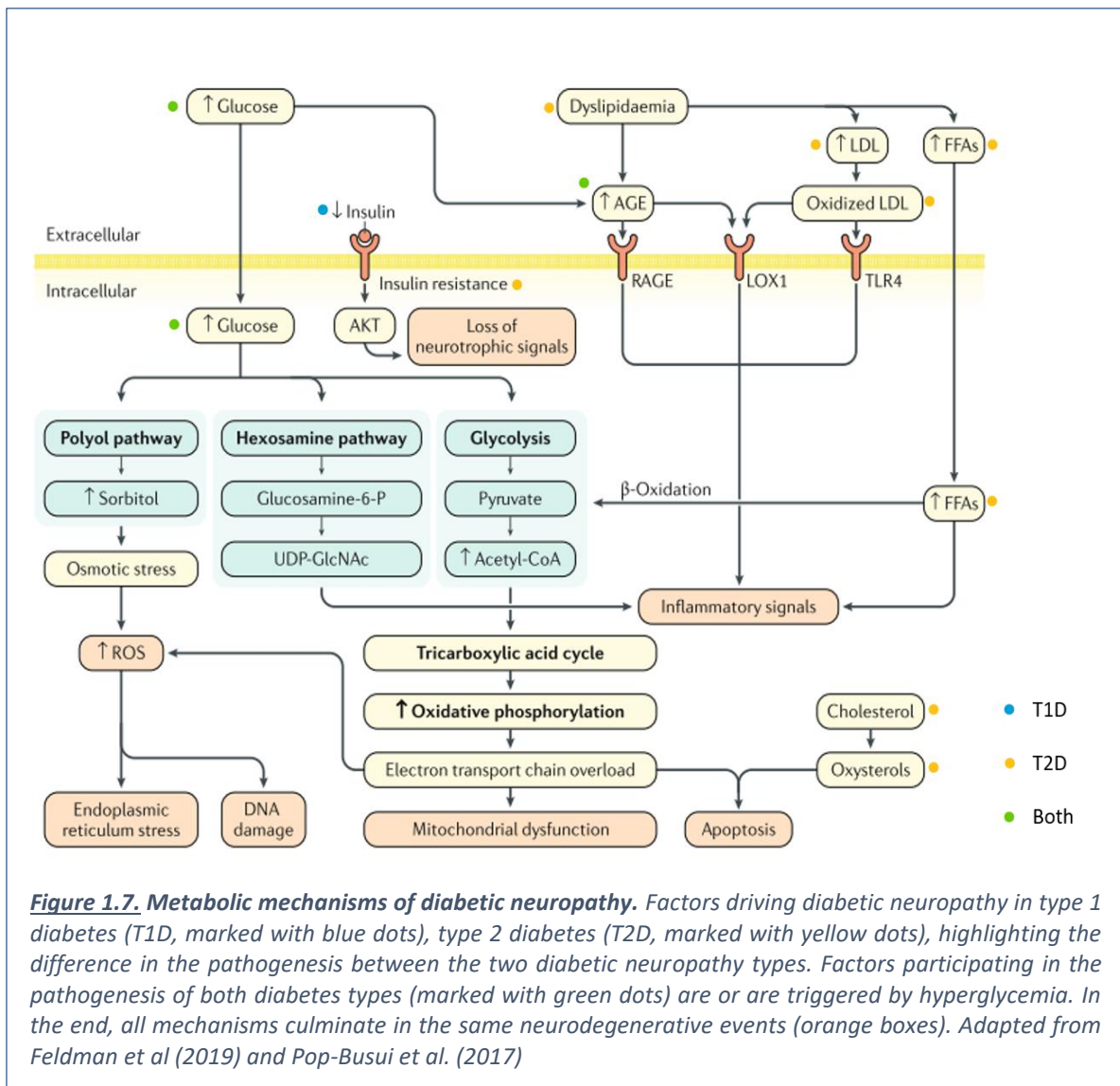
Blood vessels and nerves rely on one another to upkeep their normal function: nerves depend on adequate blood flow for oxygen and nutrient supply and blood vessels depend on normal nerve function for flow dynamics regulation²⁶². Excess blood glucose damages smaller blood vessels (microvasculature) early on in diabetes progressing towards major blood vessels and the heart (macrovasculature) in later stages. The increased number of glucose molecules per millilitre of blood flowing through damages the endothelial cells lining the inside walls of capillaries supplying the neurons. This leads to increased cell proliferation (hyperplasia), thickening of the walls and thus narrowing of the lumen^{263,264}. Peripheral perfusion to the nerves is severely reduced leading to neuronal ischemia. Glucose-induced microvascular injuries underlie the development of DN, retinopathy and nephropathy²⁶⁵. The critically low oxygen levels (hypoxia)²⁶⁶ to the neurons results in progressive neurodegeneration^{265,267,268}.

With the extremities (fingers, toes) and also retina, being supplied by the smallest and thus most vulnerable capillaries, these areas are typically the first to be affected and to present with neuropathic symptoms. The role of vascular factors in DN etiology has been confirmed in experiments with diabetic rats where vasodilators corrected NCV deficits caused by microvascular complications^{269,270}. The role of microvascular damage is further supported by clinical trials employing drugs targeting vascular changes in DN patients, reporting slowing of the progression of neuropathy and/or improving nerve function²⁷¹⁻²⁷³.

1.3.2.2. Metabolic pathways

Microvascular complications lie in the heart of the pathogenesis of DN. Triggered by hyperglycaemia, a collection of detrimental metabolic pathways is initiated that contribute to the damage of the vasa nervorum. Research suggests that hyperglycaemia drives microvascular damage through multiple cellular mechanisms, including the formation of advanced glycation end products (AGEs), oxidative stress, polyol pathway, protein kinase C (PKC) pathway and others²⁶⁷. Neurons are damaged not only by the dysfunctional blood

supply but also directly by the same hyperglycaemia-triggered pathways that damage endothelial cells. These will be discussed in the next sections in the context of direct neuronal damage, however the mechanisms by which these processes cause damage in neuronal and endothelial cells overlap. Figure 1.7 shows a schematic summary of the main detrimental metabolic pathways involved in neurodegeneration.



- *Dyslipidaemia*

DRG neurons and SCs metabolise free fatty acids (FFAs) as well as glucose for energy. FFAs are processed by β -oxidation into nicotinamide (NADH) and flavin (FADH₂) adenine dinucleotide + hydrogen, which are then used by the mitochondria to produce ATP through oxidative phosphorylation²⁷⁴. Low levels of ROSs are generated as a by-product of this

process, usually rapidly cleared by endogenous antioxidants. However, under T2D conditions, there is an excess of FFA entering this cycle thus leading to ROS overproduction²⁷⁵, mitochondrial overload and eventually failure, causing metabolic and oxidative damage to SCs and DRG neurons²⁷⁶. Levels of cholesterol are also reported to be increased in the plasma of T2D patients²⁷⁷ (hypercholesterolemia). Similarly, excess cholesterol metabolism leads to the accumulation of oxysterols. Oxidised low-density lipoproteins (LDLs), in particular, are able to bind specific receptors such as oxidized-LDL-receptor 1 (LOX1), toll-like receptor 4 (TLR4) and RAGEs, initiating a cascade of events driving apoptosis such as caspase 3 activation and DNA degradation. This all contributes to inflammation and ROS accumulation and ultimately SC impairment and neurodegeneration (Figure 1.7).

- *Insulin signalling*

The metabolic mechanisms underlying DN that are most investigated are predominantly concerning signalling pathways triggered in response to hyperglycaemia that lead to cellular damage (polyol pathway, glycation of proteins, oxidative stress and others). However, it is important to remember that hyperglycaemia is the result of the primary diabetic insult – impaired insulin signalling. Insulin's complete absence (T1D, late T2D) or abundance (early T2D) has been increasingly reported to contribute to the symptoms of T1DN and T2DN as a main hyperglycaemia driver but also through direct effects on neurons²⁷⁸.

Neurons do not rely on insulin for glucose absorption but take it up via a concentration gradient-mediated manner through membrane-expressed glucose transporters (GLUT)²⁷⁹. However, insulin receptors are still expressed by sensory neurons in DRG cell bodies and axons²⁸⁰⁻²⁸². They are predominantly expressed by small nociceptors with approximately 68% of TRPV1-positive neurons expressing the insulin receptor²⁸³. Neuronal expression of the receptor for insulin implicates direct signalling dynamics between the hormone and the PNS. Indeed, for a couple of decades insulin has been well-established as a potent neurotrophic factor, essential for supporting normal neuronal health, growth and function as well as increase in neuronal survival²⁸⁴⁻²⁸⁶. *In vitro*, insulin supplementation has been demonstrated to increase the rate of neurite generation, length and area in both embryonic sensory neurons and adult DRG²⁸⁷. Similar results were obtained from *in vivo* studies on nerve injury models²⁸⁸⁻²⁹⁰. Experiments with rat DRG neurons also show that insulin sensitises TRPV1 by lowering the activation threshold and increasing its translocation to the membrane. Such TRPV1 alterations are established to contribute to early T2DN positive symptoms, suggesting a direct effect of insulin on neuronal excitability²⁹¹⁻²⁹³. Therefore, disruption in insulin-neuron signalling can be impair neuronal function and contribute to DN just as much as hyperglycaemia itself.

In order to evaluate the damaging effects of dysregulated insulin signalling on the nerves independently from the effects of glucose in a diabetes setting, one must experimentally sever the intimate physiological connection between insulin and blood glucose levels. Achieving this has proven challenging, however several studies succeeded and supply the literature with perhaps the strongest evidence of insulin's role in T1DN. STZ-injected rats develop robust T1D and DN^{294,295}. However, the response to STZ can be variable and sometimes STZ injection produces a unique phenotype of normal glucose levels (euglycemic) and significantly decreased serum insulin. Romanovsky et al. benefited from this abnormal STZ reaction and used this cohort of euglycemic rats for their study into the effects of insulin unavailability on neuronal health. Despite not being hyperglycaemic, these rats developed sensory abnormalities just like animals with high blood glucose levels. They presented with mechanical hyperalgesia which was correlated with insulin deficiency and reversed with low dose insulin injections^{296,297}. Similar observations were made in another low insulin/normal glucose animal model, the Goto-Kakizaki rat, where severe DN symptoms were apparent after 18 months of T1D development²⁹⁸. The findings of these two studies support a dependence of neurons on insulin for normal cellular health. More importantly, this may explain the marked improvement of nerve signalling seen in T1DN animal models and beneficial effects seen in T1DN following insulin supplementation, but not T2DN patients, where insulin levels are usually higher than normal²⁹⁹. These studies provide evidence for a strong connection between insulin's direct signalling to neurons and neuropathic complications, but only in the context of T1DN.

T1D and T2D can be viewed as opposing diseases in view of the insulin availability in each in the initial stages of the disease. In T2D, insulin overproduction and skeletal muscle IR is detected up to 10 years before diagnosis and lasts for the earlier stages of the disease³⁰⁰. Neurons have also been demonstrated to develop IR *in vitro*^{301,302} and in animal models of T2DN²⁸⁶ but not yet in humans. PNS IR in animal models of T2DN was shown to correlate with reduced neurite outgrowth³⁰³. Therefore, neuronal IR is another component speculated to contribute to neuronal insulin deficiency and the following neuronal damage in T2DN.

Overall, emerging research implicates insulin signalling as a glucose-independent trigger to the progression of DN in both diabetes types, be it due to insulinopenia or insulin resistance.

- *Polyol pathway*

Neuronal glucose uptake is insulin-independent and neurons rely solely on the direct glucose supply by the microvasculature²⁷⁹. Thus, vascular barriers are also their only protection against glucose toxicity in a state of hyperglycaemia. Therefore, during hyperglycaemia, when endothelial cells lining the blood vessels are damaged, neuronal intracellular glucose

concentrations are also abnormally high. Then, instead of undergoing normal metabolism through glycolysis, glucose is diverted to metabolic pathways that can result in neurotoxicity³⁰⁴.

The polyol pathway is one of the first proposed mechanisms underlying hyperglycaemia-induced neuropathy. Under hyperglycaemic conditions, hexokinase (the first step in the glycolysis pathway) is saturated with glucose and another glucose-converting enzyme, aldose reductase (AR) takes over. AR converts excess glucose to sorbitol which accumulates intracellularly due to its low membrane permeability (Figure 1.7). Sorbitol is an osmolyte and increased intracellular sorbitol concentrations generate intracellular osmotic stress. In response, the neuron begins compensatory efflux of taurine and myoinositol³⁰⁵. Myoinositol is an essential component of Na⁺/K⁺ ATPase and its depletion from neurons leads to impaired neuronal physiology^{306–309}. AR activity also depletes cellular stores of reduced nicotinamide adenine dinucleotide phosphate (NADPH), a proton donor for reactions generating nitric oxide and regenerating glutathione (antioxidant). This consequence of the polyol pathway activation defines the “metabolic flux” hypothesis (see³⁰⁹). It contributes to the generation and reduced clearance of cytoplasmic reactive oxygen species (ROS) which mediate intracellular injuries, discussed next.

- *Oxidative stress and reactive oxygen species (ROS)*

Oxidative stress is promoted by two glucose-driven events: ROS generation and the impairment of ROS scavenging mechanisms. During hyperglycaemia, mitochondria in neurons are overwhelmed and glucose oxidative metabolism increases. This generates superoxide (O₂⁻) which is converted to hydrogen peroxide (H₂O₂) by superoxide dismutase and, under normal conditions, H₂O₂ itself is metabolised by glutathione peroxidase (GP) to harmless water. However, as mentioned above, during hyperglycaemia the polyol pathway uses up NADPH, which is needed in the glutathione cycle, and thus prevents GP from converting H₂O₂ to water. H₂O₂ is then diverted to conversion into superhydroxyl free radicals (•OH) exerting oxidative stress in the neuron^{310,311}. Moreover, H₂O₂ and O₂⁻ can react with nitrite to produce peroxynitrite which causes nitrosative stress to the cell³¹². Oxidative and nitrosative stress result in triggering DNA-strand breaks which activate poly(ADP-ribose) polymerase (PARP). This protein is involved in DNA repair and its action depends on NAD⁺. Overactivation of PARP depletes cellular NAD⁺, also augmented by the polyol pathway. This slows down glycolysis, electron transport and ATP-generation rates resulting in neuronal dysfunction and death³¹¹.

- *Disruptions of Schwann cell metabolism*

Schwann cells (SCs) are a type of glial cells supporting neurons and an essential component of the PNS. They help in the formation of the myelin sheathing of myelinated afferents as well

as the “Remak bundles” – an association of a bundle of C-fibre afferents via non-myelinating SCs ³¹³. However, the role of SCs in neuronal health goes beyond myelination as accumulating research suggest they provide active metabolic support to axons. Thus, dysregulation of SC metabolism and function, such as under diabetic conditions, will ultimately affect neuronal function and health ³¹³. SCs express GLUT through which glucose uptake is possible via an insulin-dependent manner for metabolism and energy production ³¹⁴. For example, in a healthy environment, glucose is metabolised in the SCs to lactate which is transported to the underlying axon for energy production. However, under hyperglycaemic conditions, the excess glucose activates the polyol pathway leading to the AR-dependent accumulation of sorbitol which has been suggested to lead to SC de-differentiation to immature cells, contributing to nerve demyelination and dysfunction ³¹⁵. Furthermore, SCs are highly efficient in lipid metabolism ³¹⁶. They are able to uptake FFAs, activating a sequence of events leading to ATP production. However, during T2D, where extracellular levels of FFA can be very high, there is a substrate overload, resulting in metabolic reprogramming of the SC and overproduction acylcarnitine molecules. These are then shuttled into the underlying axon, where they exercise their toxic effects, contributing to axonal degeneration ^{274,313}. These diabetes-induced alterations to SC metabolism, along with evidence for high glucose-induced oxidative damage ^{317,318} are now shaping a novel idea that the disrupted communication between SCs and their axons contributes to DN pathogenesis.

- *PKC activity*

Excess glucose increases the rate of glycolysis. In a series of biochemical reactions, this eventually leads to the overproduction of complex molecules such as 5-diphosphate-N-acetylglucosamine (GlcNac) and diacylglycerol (DAG) ³¹⁹. GlcNac reacts with transcription factors to promote lipid dyshomeostasis, inflammation and peripheral nerve injuries ³²⁰. Similarly, DAG accumulation in the nerves has also been shown to lead to neuronal damage via activating PKC. Its activation can cause a myriad of metabolic complications through increasing neuronal IR and disturbing Na⁺/K⁺ ATPase function and thus signal propagation. It has also been demonstrated to impair expression of genes associated with vascular function thus contributing to the microvascular complications surrounding neurodegeneration ³²¹.

- *Protein glycation and advanced glycation end products (AGEs)*

Excess glucose levels lead to its reaction with amino acids of proteins to generate potentially detrimental products known as advanced glycation end-product (AGEs) (Figure 1.7). AGEs have been shown to accumulate in the peripheral nerves of T2D patients with DN ³²². AGEs can cross-link essential proteins thus preventing them from functioning properly. Furthermore,

AGEs react with AGE receptors (RAGEs) on neurons initiating downstream signalling cascades partially mediated by nuclear factor (NF) κ B activation, leading to neuronal dysfunction and loss of nerve cells. This can eventually result in reduced nociception. Events such as vasoconstriction, inflammation and loss of neurotrophic support have also been reported to occur in rodent PNS as a consequence of AGE-RAGE activation ^{323,324}.

- *Inflammation*

The array of cellular imbalances underlying DN discussed so far are also powerful triggers of systemic inflammation in peripheral tissues, including the nerves. Indeed, the role of the immune system components has been established in DN patients. For example, T2D patients who have DN show higher levels of inflammatory cytokines in their plasma compared to non-diabetic patients and T2D patients without DN ³²⁵.

In the last decade, pre-clinical experiments and clinical studies have provided strong evidence for the role of inflammatory processes in DN of both diabetes types ^{255,256}. The proposed mechanism states that glucose-, insulin- and lipid metabolic abnormalities kick-start cycles of oxidative/nitrosative, endoplasmic and mitochondrial stress that in turn cause cellular damage in the neuron. Neuronal injuries activate multiple downstream kinases (including PKC) and redox-sensitive transcriptional factors, such as NF- κ B which is responsible for the regulation of genes associated with the immune response of the body ³²⁶. Activated regulation factors trigger a surge of cytokine and chemokine production which enhance existing inflammatory responses but also feed back to and amplify the whole process by triggering more cellular stress ³²⁷. This cascade of events targets not only neurons but endothelial cells of the blood vessel walls supplying the nerves, thus further feeding into the vicious damage loop ^{255,326}. This idea is supported by pre-clinical ^{328–330} and clinical ^{325,327,331–335} studies. A couple of studies demonstrated not only that DN patients have increased serum levels of inflammatory cytokines and markers of endothelial dysfunction, but that these were even further increased in patients with PDN ^{325,336}, adding to similar evidence from studies with T2DN animal models ³³⁷. One mechanism by which this is believed to occur is the modification of channels and receptors implicated in pain by inflammatory molecules. For instance, the expression density and activation thresholds of TRPV1 and TRPA1 have been demonstrated to be modulated during inflammation by a range of kinases thus sensitizing nociceptors to painful stimuli following injuries ^{142,338–341}. Such and other dysregulations in ion channel activity during DN will be discussed in the next, final part of this section. Collectively, these observations strongly implicate that inflammatory processes during diabetes contribute greatly to DN and pain directly as well as indirectly through feeding into other neurodamaging pathways.

1.3.2.3. Ion channel alterations

As discussed in more detail earlier, ion channels expressed by sensory neurons set and govern the overall neuronal excitability. The carefully regulated activity and expression of each channel creates a fine balance upon which the normal functioning of the PNS relies. Their plasticity, however, allow for modifications of their expression, trafficking and kinetics that may result in changes in neuronal excitability. Increased excitability of nociceptors due to such ion channel alterations is one of the most widely implicated mechanisms underlying pain during DN³¹³.

Diabetes triggers multiple signalling pathways that often work together to promote different post-translational modifications of ion channels. One of the best studied reactive metabolites participating in such detrimental cascades is methylglyoxal - a protein-glycating agent and important precursor of AGEs. Its levels increase during diabetes – in fact, one study demonstrated that its concentration is especially high in patients with PDN as opposed to painless DN. Furthermore, in rodents, administration of methylglyoxal renders them hypersensitive to pain³⁴². Methylglyoxal's neuron sensitising effect has been linked to post-translational modifications of Nav1.8, depolarizing its inactivation threshold. Thus, the availability of Nav1.8 at AP threshold is increased and with that, hyperexcitability of the neurons expressing it, usually nociceptors, increases, leading to hyperalgesia³⁴². Methylglyoxal's potential to cause modifications stretches beyond VGSCs, as it has been shown to affect TRPA1 too. Like many of TRPA1's agonists, methylglyoxal is an electrophilic metabolite and is able to interact and modify critical cysteine residues on TRPA1 causing a robust activation and hyperexcitability in nociceptive neurons³⁴³. A strong link between methylglyoxal and the channels TRPA1 and Nav1.8 was demonstrated in experiments by Huang et al. (2016). They showed that subcutaneous administration of methylglyoxal in STZ rats produced nociception, which was reversed by using antagonists for TRPA1 (A967079) or Nav1.8 (A-803467). In their behavioural experiments, they confirmed the association of methylglyoxal in DN with mechanical allodynia and thermal hyperalgesia in the STZ rat³⁴⁴. TRPA1 is further implicated in PDN pathogenesis due to its strong activation by ROS – highly abundant during diabetes and further enhancing TRPA1 potentiation by methylglyoxal³⁴⁵.

There is evidence describing altered expression levels of pronociceptive channels, including P₂X₃³⁴⁶, TRPV1^{58,156}, certain VGKCs³⁴⁷ and VGSCs^{60,348–351}, albeit, historically, the studies have not been consistent in their findings. For instance, in a comprehensive report by Craner et al. (2002), expression levels of VGSCs in a T1D rat model were investigated to reveal a significant upregulation of Nav1.3, Nav1.6 and Nav1.9, downregulation of Nav1.8 and no change in

Nav1.1 and Nav1.7³⁴⁸. These observations are in accordance with others who also report upregulated Nav1.3 expression^{58,352} and downregulated Nav1.8 expression^{58,353} in diabetic animals. However, they contrast with studies describing significant increase in both TTX-S and TTX-R currents and upregulated levels of both Nav1.7 and Nav1.8 in DRG cell bodies of diabetic rodents^{58,349–351,354,355}. Albeit their exact nature is still debated, dysregulated channel expression, particularly of VGSCs, has been agreed to have a key role in the development of neuropathic pain during DN.

Painful manifestations vary vastly between DN patients - some develop painful symptoms as early as pre-diabetes while others never show a painful phenotype³⁵⁶. Apart from the differences between the diabetes forms that may contribute to such variance, genetic variances in certain VGSCs have also emerged as possible modulators of an individual's risk of developing pain during DN. Nav1.7 has been of particularly great interest as a key determinant of neuronal excitability. Specifically, GoF mutations in this channel in a diabetes setting have been suggested to produce increased DRG sensitivity. Indeed, multiple variants have been discovered in the past years that were associated with PDN^{75,357–359}. Furthermore, a dozen of rare Nav.1.7 variants were recently identified in PDN patients, which correlated with earlier diagnosis of PDN, a more severe painful phenotype and greater mechanosensitivity⁷⁶. Finally, a newly emerging curious hypothesis implicates Nav1.7 along with Nav1.3 in a cause-effect relationship between diabetes and painful neuropathy. The notion arises from the fact that these TTX-S channels are expressed in both DRG as well as pancreatic islet cells. It is therefore postulated as a possible model that diabetes as a metabolic disease and peripheral neuropathy arise as a result of dysregulation in Nav1.3 and Nav1.7 due to genetically inherited mutations. When both channels are dysfunctional, they render both sensory neurons and pancreatic cells more susceptible to damage, making diabetes and neuropathy go hand in hand. Albeit intriguing, this concept is still in its early stages^{360–362}.

1.3.4. Current diabetic neuropathy treatments

Diabetic neuropathy is the most debilitating complication of diabetes associated with the highest risk of mortality³⁶³. Yet, despite the advancing understanding of the underlying pathophysiological mechanisms, to date, there are no approved disease-modifying or reversing pharmacological therapies for DN²²⁶. This section will focus on the established DN-modifying interventions and currently recommended pharmacological therapies targeted at alleviating the symptoms of PDN. Novel analgesic drugs for PDN that are under development will also be briefly discussed. The section will conclude with a short discussion of the possible reasons for the lack of adequate disease-modifying therapies.

1.3.3.1. Diabetic neuropathy management

The main approach evidenced to successfully prevent or delay DN progression is glycaemic control, usually via insulin supplementation. In T1DN patients, blood glucose management has been shown to improve NCVs and vibration thresholds and, when introduced early enough, to prevent the development of clinical neuropathy²³⁵. In T1DN patients with severe neuropathy, even signs of neuropathy reversal were evident when blood glucose levels were normalised via more invasive interventions such as pancreatic and kidney transplantations.

Albeit a successful approach in T1DN patients, improving glycaemic control in T2DN patients for delaying neuropathy progression is not as effective, even when extended to up to 5 years. In fact, in the Action to Control Cardiovascular risk in Diabetes (ACCORD) study, such prolonged intervention has been shown to be detrimental for T2D subjects as it increases hypoglycaemia and excess mortality amongst intensively treated individuals^{364,365}. Glycaemic control may be of minimal benefit for improving T2DN, however its limited efficacy provides the valuable insight that hyperglycaemia is certainly not the sole major process driving neuropathy progression in T2D and other therapy targets need to be explored.

Apart from hyperglycaemia, T2D is characteristic with hyperlipidaemia and hyperinsulinemia, which have also been widely implicated in the progression of DN in T2D (see section 1.3.2.2. *Metabolic pathways*). Therapies targeted at lowering cholesterol (such as statins) or triglyceride levels (such as fibrates) have been suggested to slow DN progression in T2D patients, however no randomised clinical trials have evaluated their efficacy clinically^{366,367}. Hyperinsulinemia and insulin resistance (IR), on the other hand, are usually improved via weight management through diet and exercise regimes and in extreme cases, weight control surgical interventions (such as bariatric surgery). In fact, weight loss has been established as the safest and most efficient intervention to lead to remission of diabetes and reversal of neuropathy, with noted increase in IENFD, amelioration of small nerve fibre damage, alleviation of pain symptoms and improved microvascular function^{368,369}. The most widely prescribed pharmacological therapy targeting IR is metformin. It reduces the amount of glucose released in the blood by the liver, thus improving cellular sensitivity to insulin. However, high doses of metformin have been linked to vitamin B12 deficiency and a recent study demonstrated an inverse correlation between DN severity and vitamin B12 levels, suggesting that metformin might not be suitable for patients with severe DN phenotype³⁷⁰. Other therapies employed that target DN progression include supplementation with alpha-lipoic acid (antioxidant)³⁷¹ and improving microvascular function via blood-pressure lowering drugs (lisinopril, trandolapril)^{271,272}. The most sensible approach remains multifactorial risk factor control combining

treatments targeting multiple pathophysiological mechanisms simultaneously (hyperglycaemia, hypertension, dyslipidaemia, insulin resistance).

1.3.3.2. Management of painful diabetic neuropathy (PDN)

Up to a third of diabetes patients develop symptomatic PDN, significantly affecting their quality of life. With the lack of pharmacological interventions modifying DN, symptomatic treatment remains the best-established way for managing pain³⁷². The rapid growth in our knowledge of pain-driving pathophysiological processes has yielded a plethora of promising therapeutic targets in these pathways.

- *Approved therapies for managing painful diabetic neuropathy*

A list of the most widely prescribed pharmacological therapies targeting pain during DN is outlined in [table 1.5](#) and the treatment strategy outlined in [Figure 1.8](#). The approved and most recommended therapies target the CNS and modify the processing of the pain signal in the brain. These include anticonvulsants, antidepressants, and opioids²³⁰. The most widely prescribed anticonvulsant drugs are gabapentin and pregabalin, both acting as inhibitors of VGCCs thus reducing neuronal excitability. Recommended antidepressants are from one of two classes: serotonin and noradrenaline reuptake inhibitors (SNRIs, e.g. duloxetine, venlafaxine) or tricyclic antidepressants (TCAs, e.g. amitriptyline, nortriptyline). Both anticonvulsant^{373–376} and antidepressant^{377–380} therapies have been demonstrated to be effective at alleviating pain during diabetes and to be relatively well-tolerated. However, they are not without adverse effects, the most common of which include dizziness, confusion, fatigue and somnolence, which tend to be more severe in older patients³⁸¹. Nevertheless, generally the benefits of these drugs outweigh the side effects and anticonvulsants and antidepressants are thus currently recommended as 1st line treatments for PDN by several drug regulatory bodies³⁷⁶ ([Figure 1.8](#)).

Opioid prescription, on the other hand, remains controversial. Albeit pain relief during PDN has been achieved with opioids in clinical trials, this drug class brings serious safety concerns. Due to their nature, opioids prescribed for treatment of chronic pain can lead to addiction, misuse and abuse and are associated with increased mortality due to overdose. Therefore, opioids such as tramadol are often only recommended as a 3rd line intervention for moderate-to-severe pain and only after careful individual benefit-to-risk ratio assessment^{382,383}.

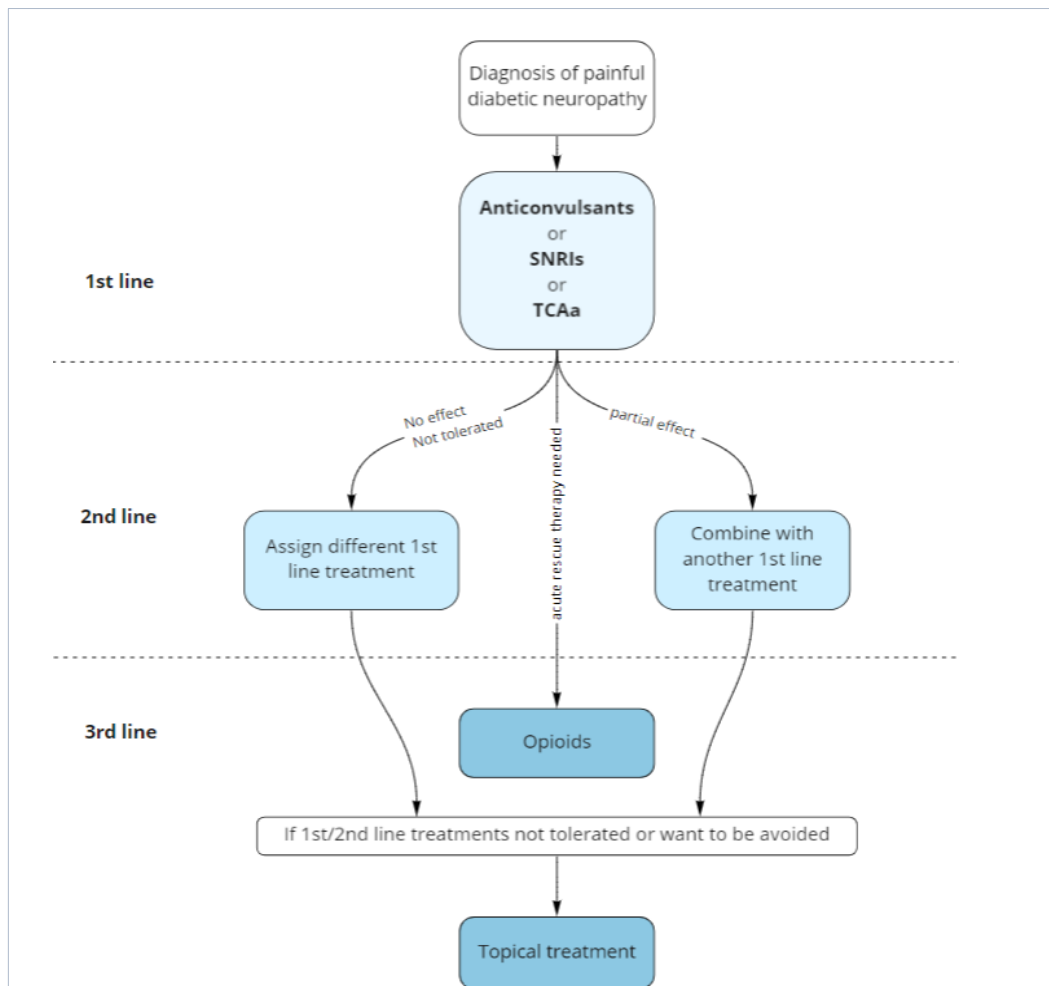


Figure 1.8. Currently established treatment strategy for painful diabetic neuropathy. Anticonvulsants, serotonin and noradrenaline reuptake inhibitors (SNRIs) and tricyclic antidepressants (TCAs) make up first- and second line treatments for painful DN. Opioids are generally avoided and only prescribed as a third line treatment in extremely severe cases. In the case of first- and second line treatments generate tolerance or generally not well-tolerated, a third line alternative or an add-on are topical treatments. Source: Feldman et al (2019)

Table 1.5. Current FDA-approved treatments for painful diabetic neuropathy with their therapeutic targets, most common side effects and serious adverse effects summarised. Adapted from Azmi et al. (2021)

| Drug | Drug class | Therapeutic target/effect | Common side effects | Serious side effects | Reference |
|---------------------------|-----------------------|--|--|---|--|
| Gabapentin | Anticonvulsant | VGCC inhibitor | Fatigue, dizziness, somnolence, headache, dry mouth, peripheral oedema, | hepatotoxicity, ataxia, Seizures following rapid discontinuation | Wiffen et al. (2017) ⁶⁴⁴ |
| Pregabalin | Anticonvulsant | VGCC inhibitor | Somnolence, dizziness, ataxia, fatigue, | Seizures (after rapid discontinuation) | Derry et al. (2019) ⁶⁴⁵ |
| Duloxetine | Antidepressant (SNRI) | inhibition of serotonin and norepinephrine reuptake in the CNS | Nausea, somnolence, dizziness, constipation, diarrhoea, dry mouth, headache, insomnia, fatigue | Seizures, hepatotoxicity, serotonin syndrome, glaucoma, myocardial infarction, cardiac arrhythmias | Lunn et al (2014) ⁶⁴⁶ |
| Amitriptyline | Antidepressant (TCA) | Same as duloxetine but less selective | Dry mouth, fatigue, headache, dizziness, insomnia, orthostatic hypotension, nausea, constipation, blurred vision, somnolence | Hepatotoxicity, heart failure exacerbation, strokes, seizures, serotonin syndrome, cardiac arrhythmias, myocardial infarction | Moore, Derry et al (2015) ⁶⁴⁷ |
| Tramadol | Opioid | Inhibition of serotonin and noradrenaline reuptake; μ -opioid receptor agonist | Somnolence, constipation, nausea, vomiting, light-headedness, dizziness, | respiratory depression, serotonin syndrome, seizures, hypertension | Duehmke et al. (2017) ⁶⁴⁸ |
| Capsaicin 8% patch | Topical | TRPV1 desensitisation | Burning, stinging, erythema, coughing, sneezing | - | Simpson et al (2017) ³⁸⁶ |
| Lidocaine 5% patch | Topical | prolongs inactivation of the fast VGSCs | Skin irritation, rashes, itching, or redness, numbness | - | Derry et al. (2014) ⁶⁴⁹ |
| Alpha-lipoic acid | Antioxidant | ROS scavenger, insulin-mimetic and anti-inflammatory activity | - | - | Agathos et al. (1999) ⁶⁵⁰ |

The severity of PDN symptoms is often robust enough to justify the implementation of CNS-modifying drugs as 1st line treatments. However, the chronic nature of DN demands long-term dependence on these therapies increasing the risk of developing drug tolerance, requiring higher doses and thus increasing adverse effects severity. Several non-CNS targeted therapies have been proposed that have shown success in relieving pain in DN. Topical treatments are a popular alternative for patients unable to tolerate the conventional systemic treatments. They also present with significantly lower risk of interactions with other medications making them a suitable option for patients with polypharmacy ³⁸⁴. The most popular topical treatments for DN pain are the capsaicin 8% patch and lidocaine 5% patch. Both have demonstrated significant pain reduction comparable to anticonvulsants and TCAs and have fewer and less serious side effects ^{385,386}. Capsaicin 8% patches are now FDA-approved for the treatment of neuropathic pain and both are proposed as 2nd or 3rd line treatments ³⁷⁶ (Figure 1.8). Nevertheless, they can cause side effects, e.g. skin irritation, rashes and, especially in the case of capsaicin, loss of IENF and altered thermal sensation, which can compromise patient compliance ³⁸⁷.

- *Novel pharmacotherapeutic agents in development*

Research into novel analgesic treatments for PDN is also focusing away from the CNS and onto the PNS. Table 1.6 presents an inexhaustible list of novel pharmacotherapeutic compounds in development for symptomatic pain relief during DN. Here, I will focus on discussing those targeted at modifying pain-associated ion channels expressed by nociceptors.

Nociceptive ion channels have become an especially attractive target for novel analgesics due to their selective expression in peripheral nociceptive neurons ³⁸⁸. This facilitates the diversion of conventional therapies towards nociceptors thus limiting detrimental CNS side effects. At the same time, affecting pain signalling at the source by the selective inhibition of specific nociceptive channels could enhance drug efficacy. Furthermore, even in the case of limited individual drug efficacy, ion channel modulators present the opportunity for combination therapies with currently approved treatments (table 1.5), whereby lower doses of both can be implemented to limit side effects while benefiting from both drugs' actions – a concept which is being explored with currently approved therapies in DN ^{389–392}.

Table 1.6. A range of novel drugs in development for the treatment of painful diabetic neuropathy. Novel analgesic pharmacological interventions are targeted at different molecules and pathways. Some have been through clinical trials and side effects have been noticed, whilst others are still in pre-clinical stages of development. Adapted from Rastogi & Jude (2021)

| Drug | Class | Known side effects | Stage of development | Reference |
|--|---|---|----------------------|--|
| PF-05089771 | Nav1.7 blocker | Headache, pneumonia, upper respiratory tract infections | Phase II | McDonnel (2018) ⁶⁵¹ |
| Vixotrigine | VGSC blocker | Headaches, dizziness | Phase II | Hinckley et al. (2021) ³⁹⁶ |
| VX-150 | Nav1.8 blocker | Nausea, headache, vomiting and dizziness | Phase II | Vertex Pharmaceuticals Incorporated. (2018) ³⁹⁸ |
| A-803467 | Nav1.8 blocker | - | Pre-clinical studies | Jarvis et al (2007) ³⁹⁹ |
| PF-01247324 | Nav1.8 blocker | - | Pre-clinical studies | Payne et al. (2015) ⁴⁰⁰ |
| Calcitonin | VGSC modulator | - | Pre-clinical studies | Ito et al. (2012) ⁶⁵² |
| A-317491 | P2X3 blocker | - | Pre-clinical studies | Jarvis et al (2002) ⁴⁰² McGraughty et al. (2003) ¹⁹⁵ |
| Sinomenine | P2X3 blocker | Injection site flare, pruritus, edema | Pre-clinical studies | Rao et al (2017) ⁴⁰³ |
| Resiniferatoxin | TRPV1 agonist | Transient burning sensation | Pre-clinical | Bishnoi et al (2011) ⁴⁰⁵ |
| Tanezumab | Humanised monoclonal IgG2 antibody | Peripheral edema, paraesthesia | Phase III | Bramson et al (2015) ⁶⁵³ |
| Pooled human immunoglobulin | Immunomodulatory agent | Allergic reactions | Phase I | Liu et al (2018) ⁶⁵⁴ |
| Botulinum Toxin A | Inhibition of sensory neurotransmitters release | Antibody formation and immune-related complications, are reported when a small amount of bont-A enters the circulatory system | Phase II | Lakhan et al. (2015) ⁶⁵⁵ Salehi et al. (2019) ⁶⁵⁶ Park, J. & Park H. (2017) ⁶⁵⁷ |
| Islet Neogenesis Associated Protein (INGAP) | Enhance nerve growth from sensory ganglia | - | Pre-clinical studies | Tam et al. (2004) ⁶⁵⁸ |
| Fidarestat | Polyol pathway inhibitor | - | Phase II | Hamada and Nakamura (2004) ⁶⁵⁹ |
| Minalrestat | Polyol pathway inhibitor | - | Pre-clinical studies | Yagihashi et al (2001) ⁶⁶⁰ |
| Sulfasalazine | NF-κB inhibitor, | Increase in gas, constipation, and diarrhea | Phase II | Berti-Mattera et al. (2008) ⁶⁶¹ ; Liedorp et al. (2008) ⁶⁶² |
| miR-146a (pro-inflammatory genes suppressant) | Micro RNA supplementation | - | Pre-clinical studies | Liu et al. (2017) ⁶⁶³ |
| VM202 | plasmid containing human growth factor | Infections, diabetic retinopathy, peripheral edema, and skin ulcers | Phase II | Kessler et al. (2015) ⁶⁶⁴ |

Of the DRG-expressed ion channels implicated in pain, Nav1.7 has perhaps been of highest interest as an analgesic target due to its high expression levels in DRG and strongly evidenced role in pathological pain conditions³³. A number of potential Nav1.7 blockers have been under development, showing promising results in preclinical studies of DN^{393,394}. However, none have yet been approved for clinical use due to their failure in clinical trials. For instance, a recent small trial of the Nav1.7 blocker PF-05089771 in PDN failed to show pain alleviation in patients³⁹⁵. Another VGSC inhibitor developed by Biogen, Vixotrigine was believed to be Nav1.7-selective but has now been redefined as a non-selective VGSC blocker³⁹⁶. Vixotrigine has shown limited efficacy but great tolerability in a phase II clinical trial for trigeminal neuralgia compared to placebo and is currently undergoing phase II trial for small fibre neuropathy in DN (ClinicalTrials.gov Identifier: NCT03339336). Interestingly, a recent study demonstrated that oxcarbazepine (a non-selective VGSC blocker) successfully attenuated pain responses in DN patients with irritable nociceptors compared to those with non-irritable nociceptors. This suggests that non-selective VGSCs might still find place in the clinical treatment of PDN provided that a more detailed patient phenotyping and hence stratification is performed³⁹⁷. Blockers of Nav1.8 have also been of interest for the pharma industry: VX-150 has been advanced to phase IIb trials after demonstrating promising efficacy and safety in small fibre neuropathy clinical trials³⁹⁸. Other Nav1.8 blockers such as A-803467 and PF-01247324 have shown promising selectivity and antinociceptive effects in preclinical studies³⁹⁹⁻⁴⁰¹. Similarly, several P₂X₃ blockers have been explored in animal studies (e.g. A-317491 and sinomenine) and have successfully relieved hyperalgesia by suppressing overexpression and overactivation of P₂X₃, however confirmation in human studies is lacking^{195,402,403}. Finally, TRP channels have been demonstrated to be particularly curious pain relief targets as both TRP-channel agonists and antagonists have shown analgesic potential⁴⁰⁴⁻⁴⁰⁸. Albeit several promising novel DN therapies are in ongoing clinical trials (table 1.6), numerous therapies targeting various pathogenic molecular mechanisms have shown great promise in preclinical studies only to fail to translate to the clinic⁴⁰⁹. In fact, analgesics in general have only 2% success rate, which is 5 times less than other therapeutic areas. The low development success rate has led to gradually decreasing interest and investment in the area of pain therapeutics further exacerbating the issue of lack of adequate pain treatments⁴¹⁰. To date, no disease-modifying pharmacotherapy has been developed for DN and the possible reasons behind this will be briefly outlined next.

1.3.3.3. Why are there no disease-modifying therapies for diabetic neuropathy?

The problem with analgesics development for treating PDN extends to DN as a whole with currently no disease-modifying therapies available and largely disappointing clinical trial outcomes²³⁰. The possible reasons behind this critical issue stretch across all steps in the drug development process from the clinical trials design all the way back to *in vitro* screening of the drug candidates. Clinical trials are recommended to introduce improvements in several aspects:

- alternative endpoints, particularly focused on monitoring small nerve fibre physiology instead of currently recommended large-fibre-focused readouts⁴¹¹;
- detailed DN diagnosis with stress on underlying pathophysiological driver(s)⁴¹¹⁻⁴¹³
- patient stratification according to key pathophysiological driver(s) of DN for enhanced, individualised therapies^{414,415}
- following on the previous two points, focus on mechanism-based drug testing approach as opposed to “one size fits all” approach

The complexity of DN poses great challenges in translating potential treatments from animal models to humans^{416,417}. Suggested improvements in this stage of the drug development include the implementation of multiple and improved preclinical screening methods with direct clinical equivalents as well as progression through several model systems⁴¹¹. However, the most fundamental issue to consider is the choice of the preclinical model: how well does it reflect the DN aspects targeted and how comparable are they to the same aspects in humans? Finally, taking yet another step back in the development process, *in vitro* drug screening would also benefit from advanced techniques with improved readout sensitivity that are able to precisely separate drug action on target from its off-target effects. Such improvement will aid in the advancement of better-targeted and safer drugs towards preclinical and clinical development stages. For more details and an extensive analysis of current drug development practices and areas of improvement, see Jin et al. (2020)⁴¹¹.

Choosing the appropriate animal model of DN and technique to evaluate its phenotype are key steps in characterising functional changes and identifying potential treatment targets in the neurons. Further considerations for animal and *in vitro* models of DN will be discussed in more details next, followed by the introduction of a novel functional assay developed in our lab which we demonstrate to have potential as a simple but sensitive drug screening tool.

1.4. Modelling diabetic neuropathy

So far, this chapter has delved into the details of DN and the known molecular mechanisms underlying its pathogenesis in order to highlight the enormity as well as depth of the clinical problem that this condition represents. Despite over 50 years of laboratory and clinical research, current treatments are far from achieving satisfactory effectiveness and safety²³⁰.

The development of high-quality therapies depends heavily on the adequate modelling of DN components *in vitro* or in animal models of pre-diabetes, T1D and T2D. To date, several *in vitro* technologies and over 20 rodent models of DN have been introduced offering the opportunity to choose the one most closely reflecting the specific DN aspects being investigated⁴¹⁸. Although, no model accurately mimics all aspects of DN as manifested in humans, *in vivo* and *in vitro* models arm researchers with the tools needed to keep advancing the understanding of the complex disease that DN is. In this section I will review some of the most common *in vitro* methods for reproducing DN conditions. Then, I will move on to discussing the most widely used T1DN and T2DN animal models. Finally, this part of the chapter will conclude with a comment on important considerations when selecting a model for DN research.

1.4.1. Modelling diabetic neuropathy *in vitro*

As the search for an effective drug to reverse or ameliorate DN progression continues, basic research focuses on unravelling the intricate molecular mechanisms propelling its development. To this end, tissue and cell culture techniques are especially instrumental because they allow for the isolated investigation of complex neuronal responses to different stimuli – a clear benefit over *in vivo* models, where a mixed-cell, global response is taking place. Other advantages of cell cultures to consider are, perhaps above all, that they allow for tight control over the extracellular environment. Thus, they are ideal for the detailed studying of a vast range of cellular processes, including cell death, neurodegeneration, hyper- and hypoexcitability and bioenergetics. With the added benefit of allowing for straightforward real-time imaging and recording, they are also useful for tracking the time kinetics of intracellular molecular events, albeit *in vivo* imaging is now possible too. These advantages render cell cultures the perfect platform for high-throughput drug screens. Finally, *in vitro* techniques usually come with fewer ethical issues than using *in vivo* models of nerve diseases, particularly when investigating pain⁴¹⁹.

The *in vitro* approach to DN research encompasses several different techniques, such as primary and immortalised cultures of dissociated neurons, organotypic explants and, more

recently, generation of neuronal cultures via the induced pluripotent stem cell (iPSC) technology.

Primary neuronal cultures are the most widely used method for investigating DN pathogenesis *in vitro*^{318,420–425}. Importantly, primary cultures of DRG neurons from an adult rat or mouse preserve the broad heterogeneity of the neuronal population within the ganglion. DRG neurons can be harvested from healthy, control animals and subjected to DN-inducing stimuli to investigate acute pathogenic responses. Alternatively, neurons can be harvested from a diabetic animal. This is an excellent example of marrying *in vivo* and *in vitro* techniques, benefiting from employing an animal model of diabetes as a DN-stimulus and an *in vitro* approach to assess the specific molecular and physiological events.⁴¹⁹ Generation of primary neuronal cultures involves the mechanical and/or enzymatic isolation of neurons into a cell monolayer which is then maintained in an optimal extracellular environment designed to mimic physiological conditions⁴²⁶.

DN entails a network of intersecting pathways driving its pathology and the choice of stimulus depends on the DN aspect under investigation. Most commonly, generating hyperglycaemic conditions is the first consideration, however, the question of the optimal glucose concentration used is still a much-debated issue in diabetes and DN studies. The physiological blood glucose concentration of healthy rodents is 4-8 mM⁴²⁷, whereas in diabetic ones levels can exceed 20 mM^{428–431}. However, the vast majority of published *in vitro* studies using neurons in general (that did not investigate diabetes) maintain neuronal cultures in standard glucose concentrations of approx. 20-30 mM, depending on the culture medium used, which can be considered a hyperglycaemic environment in a diabetes-focused study. It is, therefore, advised that modelling of diabetes *in vitro* requires 7-20 mM additional external glucose in order to not deviate from established neuronal culture protocols and still recreate hyperglycaemic conditions as accurately as possible⁴¹⁹. Other stimuli that have been successfully used in *in vitro* DN research include pro-oxidants for the assessment of oxidative stress⁴²², methylglyoxal⁴³² and lipid oxidation products for the evaluation of hyperglycaemic toxicity⁴³³, oxidized low density lipoproteins for studying hyperlipidaemia⁴³⁴ or serum from diabetic patients or animals^{342,435}.

Primary cultures are not without limitations. As neurons are non-proliferative, the yield is low and each culture requires time-consuming collection of neurons. Notably, due to the nature of the process, neuron dissection involves nerve injury, triggering a switch in cultured neurons from a “housekeeping” to a “regenerative” phenotype⁴³⁶ which should be considered when assessing neuronal excitability overtime in culture. Finally, the simplified neuronal environment

requires caution when interpreting data and demands validation of findings in an *in vivo* setting⁴¹⁹.

An alternative to primary neuronal cultures is the use of immortalised cell lines, such as SH-SY5Y^{437,438}, NTERA-2⁴³⁹ and pheochromocytoma (PC12)^{440,441} cells. Most are easy to obtain and maintain and provide an unlimited supply of a homogeneous population of cells. They have been extensively used in electrophysiological, molecular and biochemical neurophysiological research and represent a suitable platform for high-throughput drug screens necessitating vast numbers of cells. In addition, the use of cell lines eliminates the need to sacrifice animals for each culture, bringing a great ethical and time advantage. However, due to cell lines being even a further simplified culture of clonal cells, they do not reflect the heterogeneity of adult rodent neurons nor are they capable of developing processes such as dendrites and axons⁴⁴².

A promising novel technology in the research of neuronal diseases are iPSCs. By harvesting fibroblasts from patients, one can genetically reprogram them into pluripotent cells⁴⁴³ and then stimulate their differentiation into various neuronal cell types, including sensory⁴⁴⁴, and SCs⁴⁴⁵. This method holds potential for circumventing a possible problem with interspecies differences that may underlie the poor translation of drugs efficacy from established *in vitro* and *in vivo* techniques to the clinic.

The study of the intricate pathogenesis of DN has greatly benefited from *in vitro* models over the years. However, regardless of the *in vitro* model's advantages and success, findings must always be confirmed in an *in vivo* model to validate the observations when other interfering factors are also present, as they would be in the patient.

1.4.2. Experimental animal models of diabetic neuropathy

In vivo models of diabetes and DN are instrumental for the understanding of behavioural, physiological and structural DN pathology and are key drivers of progress towards successful therapy strategies. Compared to *in vitro* methods, animal models offer the advantage of susceptibility to genetic manipulations and higher system complexity. The diseases they are tailored to represent are thus closer in pathological resemblance to humans allowing for a more holistic interpretation. However, one big limitation remains the relatively short lifespan of rodents, which does not allow for the complete mimicking and investigation of the chronic aspects of human (P)DN which progresses over decades to reach irreversibility²⁴¹.

Over the years, a great diversity of rodent models of T1D and T2D have been developed and characterised (for a comprehensive review see ^{241,446,447}). Although none has yet been perfected to reflect the human disease in its full complexity, virtually all stages of human diabetes and its neuropathic complication have been reproduced by an animal model designed for the purpose ²⁴¹.

There are three established parameters by which DN is confirmed in a diabetic rodent and the animal model is recognized as useful. These represent major aspects of human DN pathology, namely:

- 1) *behaviour* – sensory abnormalities are evaluated by assessing thermal and mechanical sensitivity;
- 2) *nerve conduction velocity (NCV)* – electrophysiological measures of nerve impairment assessing motor and sensory nerve conduction;
- 3) *nerve structure* – intraepidermal nerve fibre (IENF) density in the animal's footpad is assessed to reveal anatomical evidence of fibre loss.

Two out of three need to be significantly different from control animals for a neuropathic phenotype to be confirmed ⁴⁴⁸.

There are three main approaches by which rodent models of diabetes are generated – they can be genetically induced, chemically-induced and diet-induced.

1.4.2.1. Genetically induced models of diabetic neuropathy

Transgenic rodent models have been developed for both diabetes types. The most widely used T1D genetically modified models are the non-obese diabetic (NOD) and B6Ins2^{Akita} mice ²⁴¹. NOD mice develop a T-cell-mediated autoimmune response against their β -cells caused by a polygenic immunodeficiency that they carry. Thus, they spontaneously develop T1D, consistent with the pathogenesis in T1D patients. However, due to the polygenic nature of their genetic modification, diabetes and DN progression in NOD mice is variable and affected by diet, housing conditions and the sex of the animals and DN in this model is still undercharacterised ⁴⁴⁹. Nevertheless, studies using NOD mice have reported hyperalgesia by week 8 ⁴⁵⁰ and hypoalgesia by week 12 ³¹². B6Ins2^{Akita} mice have a point mutation in the *Ins2* insulin gene impairing insulin production ⁴⁵¹ resulting in T1D by 7 weeks of age (WoA) and the gradual development of sensorimotor neuropathy ⁴⁵². NCV in this model has been reported to decrease at 16 WoA ⁴⁵², however, in another study, B6Ins2^{Akita} mice showed no NCV

impairments even at 24 WoA ⁴⁵³. Considering their current limitations, and the relatively controversial literature, DN phenotype in both NOD and B6Ins2^{Akita} mice is still unclear and requires further characterisation.

Research of T2DN has benefited from some excellent transgenic animal models. The most popular and best studied are monogenic mouse models carrying a mutation which impairs leptin signalling ⁴⁴⁷. Leptin is a hormone secreted after feeding to signal satiety and suppress appetite ⁴⁵⁴. Mutation in the leptin hormone or its receptor produce *ob/ob* and *db/db* mice, respectively. Both models develop chronic hyperglycaemia and hyperinsulinemia ^{428,455}. *Ob/ob* mice are considered as an obesity and mild T2D model and DN in this model is understudied, however, they are reported to present with thermal hypoalgesia and reduced IENF density and sensory and motor NCV at 11 WoA ⁴⁵⁵.

Db/db mice are the very first mouse model developed for the investigation of DN ⁴²⁸, shown to develop physiologically relevant T2D as early as 4 WoA. Compared to *ob/ob* mice, DN in the *db/db* mouse model has been better characterised with several studies reporting hyperalgesia and allodynia at 8-12 WoA and sensory loss at 12+ WoA accompanied by a significant decrease in motor and sensory NCV and IENF density ^{453,456-459}. However, the relatively large number of studies using this mouse model has also generated considerable inconsistencies with regards to the DN phenotype with some reporting profound sensory anomalies while others see no significant differences from control animals ⁴⁶⁰. Neuropathy severity in the *db/db* mouse is also affected by the choice of mouse strain with hyperglycaemia more stable and DN more severe in the C57BKS *db/db* than C57BL/6 *db/db* mouse ^{453,461}. Nevertheless, the progression of T2D and DN in the *db/db* mouse is considered to most closely mimic the natural history of these conditions in humans ⁴⁵³. Part of the experiments in this thesis involve the *db/db* mouse and this model will be discussed in depth in the relevant chapter (Chapter 5).

1.4.2.2. Chemically induced models of diabetic neuropathy

Rodents can also be rendered diabetic via a chemical induction process. The most common model of T1D, the streptozotocin (STZ) model, employs this approach. STZ is an alkylating compound known to selectively destroy β -cells ⁴⁶². It is injected in the animal following one of two established protocols: either in a single high dose, producing a robust DN but also bringing a high mortality rate due to severe nonspecific toxicity; or in multiple low doses – a less toxic approach producing gradual T1D but often with no or only moderate neuropathy phenotype ⁴⁶³. Although an inexpensive, easy to optimise and adequate model for T1DN research and drug tests, the induction's nature subjects animals to severe distress and potential DNA

damage – limitations that might impact measurements of pain responses and other parameters⁴⁶⁴. Furthermore, concerns have been raised over the direct neurotoxicity effects of STZ⁴⁶⁵. More recently, STZ has been shown to directly activate neuronal TRPA1 resulting in acute allodynia⁴⁶⁶. Despite its disadvantages, the diabetic STZ rat is by far the most extensively researched DN model, generating the vast majority of knowledge on the disease and its painful phenotype²⁴².

1.4.2.3. Diet-induced models of diabetic neuropathy

Drastic alterations in rodents' standard nutrition have also been employed that establish T2DN and neuropathic pain by successfully mimicking human metabolic syndrome development. Several diet modification strategies have been tried but a high fat diet (HFD), has been repeatedly demonstrated to have undeniable success at inducing T2D and neuropathy in mice⁴⁶⁷. Usually, mice on a HFD develop obesity gradually, followed by metabolic imbalances, including hyperglycaemia and moderate hyperinsulinemia until T2D is fully established. DN is close to follow with decreased sensory NCV, IENF density and thermal hypoalgesia often reported in these mice⁴⁶⁸. Although inappropriate diet is a leading cause for human T2D development too, compared to other approaches of DN induction, the diet approach can be time-consuming and its success varies due to influence from animal sex and age, diet duration, fat content and fat source. Nevertheless, diet-induced models of DN have proven useful in studies of prediabetes and obesity-associated neuropathies⁴⁶⁷.

1.4.2.4. Considerations when selecting a model

DN progression is undeniably multifactorial and a complete model has not yet been developed for either of the diabetes types. Therefore, when selecting a model, it is critical to do so with the disease aspect being investigated in mind. Further to that, model choice must also take into consideration factors such as duration and type of stimulus exposure, measurement tools, phenotype assessment techniques, and in the case of animals – their sex, age, diabetes type being induced, diet and diet duration, and degree of exposure to diabetes-inducing compounds and methods. For example, it has been well-documented, that male and female mice show significantly different DN phenotypes even when the same diabetes-induction approach is used⁴⁴⁷. Female mice are more often used as genetically NOD models of diabetes, because they develop T1D symptoms much earlier⁴⁴⁹, while male rodents are more suitable models for nutritionally-induced diabetes. Female rodents have also been reported to show a much more muted level of painful DN than males, presumed to be due to influence by specific female steroid hormones modulating the release of peptidergic neurotransmitters during pain

signalling^{469,470}. In addition, currently, an imbalance exists in the field of DN research. T1DN and its painful aspects are extensively researched (mainly in the STZ model) while clinical studies are mostly focused on T2DN cases due to their greater global prevalence. Although both diabetes forms lead to DN, it is vital that the model is of the diabetes type the findings will be translated to. Ensuring such synchronisation might contribute to closing the gap between animal and clinical studies.

The elaborate study of *in vitro* and *in vivo* models of DN would not have been possible without the development of powerful techniques and tools. To investigate the neuronal excitability of DRG neurons from *db/db* mice, I employed a functional assay previously developed in our laboratory which combines Ca^{2+} imaging and the VGSC activator veratridine. In the final section of this chapter, I will briefly outline the characteristics of the different components of this assay and discuss its experimental applications to date.

1.5. Veratridine-based calcium imaging assay for neuronal excitability assessment

The major goal in neuroscience research is the understanding of the complex patterns of neuronal activity and the physiological and molecular events underlying different neurodegenerative conditions. To address this, one must be able to record the activity and analyse the changes in excitability of nerve cells. Electrophysiology and Ca^{2+} imaging are the two most popular approaches implemented to that purpose. Electrophysiological techniques such as voltage clamp, current clamp and patch-clamping are the 'gold standard' in neurophysiology research, providing direct report of a neuron's electrical properties with high temporal precision⁴⁷¹. However, electrophysiological approaches are often invasive, usually requiring the insertion of electrodes in the cell, and limited to assessing only a small subset of neurons (most often – a single cell at a time), thus unable to monitor the neuronal dynamics in a heterogeneous population such as DRG neurons.

For the simultaneous assessment of a great number of neurons in a diverse population, a medium-to-high throughput approach is more appropriate such as Ca^{2+} imaging. Furthermore, the research for new treatments against pain has been re-targeted from the CNS towards the nociceptors in the PNS and, more specifically, the ion channels they expressed that regulate pain signalling. The development of novel, more efficient and safer analgesics creates a need to be able to single out and specifically target nociceptors with minimal or no impact on non-nociceptive cells. To that end, a suitable assay is needed that is not only high throughput but

also able to discriminate nociceptors in a heterogeneous DRG neuronal population. Calcium imaging is a technique with the potential to answer these requirements.

1.5.1. Calcium imaging technique

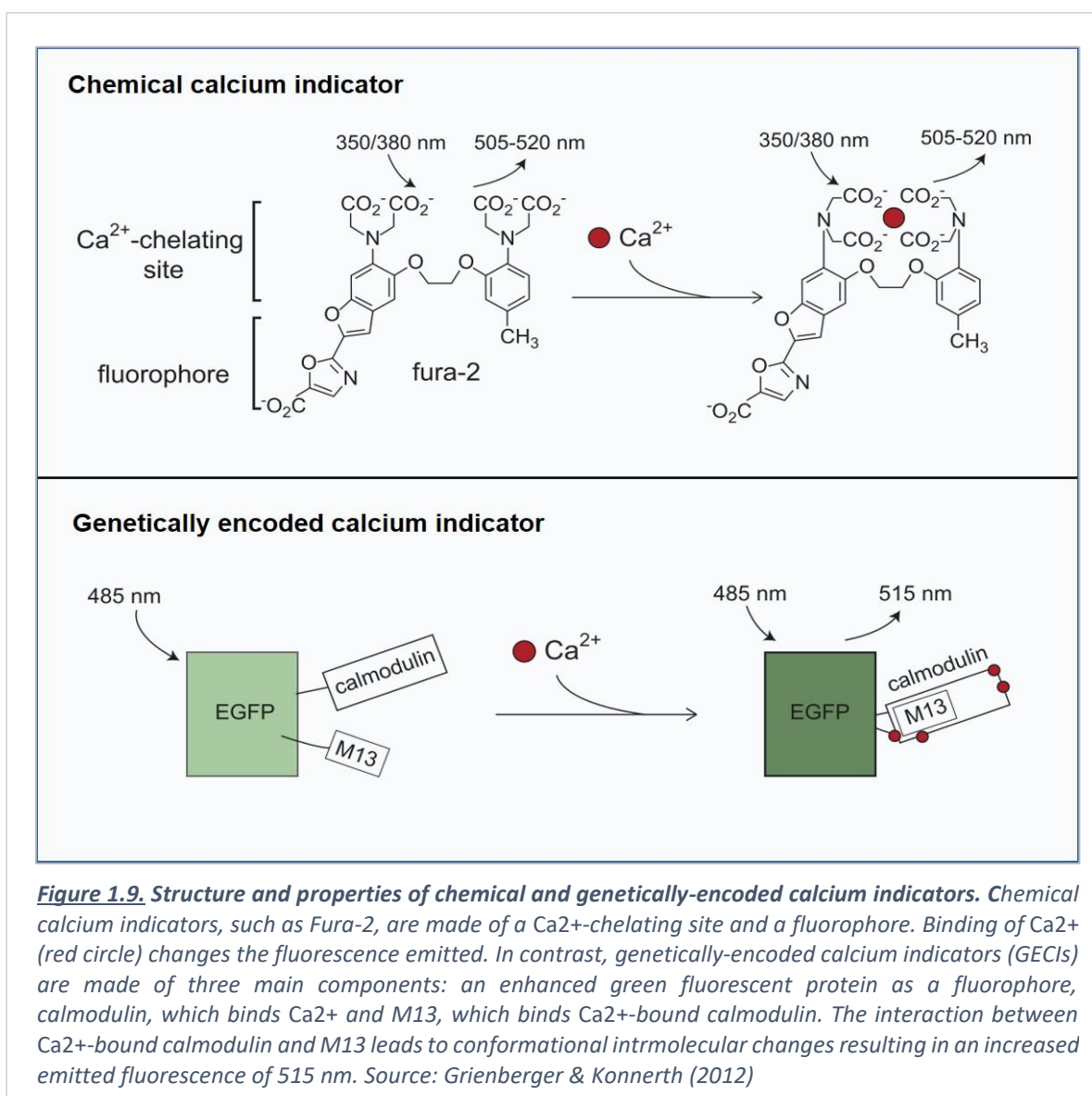
In the neuron, Ca^{2+} ions play a central role in various processes across all parts of the nerve cell. A charge carrier and an important intracellular messenger, Ca^{2+} is involved in the regulation of neuronal development, apoptosis, neurotransmitter release and membrane excitation. At rest, the intracellular Ca^{2+} ion concentration in the neuron fluctuates between 50 and 100 nM, however they can rise 100-fold during electrical activity. Therefore, the direct measurement of intracellular baseline Ca^{2+} levels as well as Ca^{2+} spikes is highly informative of a neuron's activity and excitability⁴⁷². By harnessing this neuronal property, Ca^{2+} imaging can directly visualise the Ca^{2+} status of hundreds of individual neurons simultaneously. Compared to electrophysiological methods, it does so in a less invasive way and can be used to track the activity of neurons over time. Calcium imaging has been used widely by neuroscientists to record activity in neuronal populations⁴⁷³. The imaging of Ca^{2+} ions depends highly on the use of appropriate Ca^{2+} sensor indicators. Calcium indicators allow for the real-time monitoring and recording of cellular Ca^{2+} signals *in vitro* as well as *in vivo*, discussed next.

1.5.1.1. Calcium indicators

To monitor neuronal activity based on intracellular Ca^{2+} levels, a Ca^{2+} -binding indicator is required that would enable the optical measurement of neuronal Ca^{2+} concentrations. Such indicators have been in development since the 1960s^{474,475}, but it was Tsien et al. that revolutionised Ca^{2+} imaging by introducing a series of highly sensitive fluorescent Ca^{2+} sensors. These Ca^{2+} indicators alter their spectral properties upon binding free Ca^{2+} ions. Broadly speaking, they can be classified into two main categories: chemical Ca^{2+} sensors for *in vitro* imaging⁴⁷⁶ and genetically encoded Ca^{2+} indicators (GECIs) for *in vivo* imaging⁴⁷⁷. A summary of the structure and general properties of each class is presented in the diagrams of [Figure 1.9](#).

- *Chemical calcium indicators*

The most successful example of an *in vitro* chemical Ca^{2+} indicator is the widely used high-affinity dye Fura-2. It is the result of the hybridisation of a highly Ca^{2+} -selective chelator with a fluorescent chromophore (or fluorophore) ⁴⁷⁸ (Figure 1.9). Its ester form, Fura-2AM, is its membrane-permeable derivative that freely crosses the cell membrane. Once inside the cell, cellular esterases cleave the ester bond thus “locking” the dye inside ⁴⁷⁹. Fura-2 binds Ca^{2+} ions with high affinity ($K_d \sim 145 \text{ nM}$), and has a relatively wide Ca^{2+} sensitivity, ranging between $\sim 100 \text{ nM}$ and $\sim 100 \mu\text{M}$ ⁴⁸⁰. The primary advantage of Fura-2 is that it is a ratiometric dye. The binding of free intracellular Ca^{2+} induces conformational changes in Fura-2, shifting its excitation wavelength from 380 nm (free Fura-2) to 340 nm (Ca^{2+} -bound Fura-2). Its emission



wavelength remains stable at $\sim 500 \text{ nm}$ at either excitation wavelength. The higher the intracellular Ca^{2+} concentration is, the stronger the excitation at 340 nm and the weaker the

excitation at 380 nm is. Thus, a quantitative measure of intracellular Ca^{2+} concentrations can be estimated, independently of the intracellular dye concentrations, by calculating the ratio of the emissions at the two excitation wavelengths (340/380). The ratiometric property of Fura-2 makes it a highly popular choice due to eliminating issues with variables such as variable dye concentration, unequal cell thickness, dye leaking and photobleaching ⁴⁸¹.

- *Genetically encoded calcium indicators*

After the establishment of chemical Ca^{2+} sensors, protein-based genetically encoded Ca^{2+} indicators (GECIs) were the next big breakthrough as they allowed for the imaging of neuronal activity *in vivo* ⁴⁷⁷. Their expression can be targeted to specific subpopulations of cells and maintained stable over months, allowing for the repeated observation of neurons. Thus, GECIs are invaluable in the research of nervous system development, maintenance, learning and memory. However, they remain slightly inferior to chemical Ca^{2+} indicators in terms of their signal-to-noise ratios. The most widely used form of GECIs is the single-fluorophore GCaMP family. It is composed of three main parts: a circularly permuted enhanced green fluorescent protein (eGFP) with the Ca^{2+} -binding protein – calmodulin attached on one end and a calmodulin-binding protein M13 on the other. Upon binding free Ca^{2+} , calmodulin interacts with M13, which induces a conformational change in eGFP. This results in the increase of emitted fluorescence by the fluorophore ^{477,482} (Figure 1.9). Substantial progress has been made in recent years to develop improved GECIs classes with high-affinity sensors, improved dynamics range, kinetics and better signal-to-noise ratio for the reliable detection of neurons with low activity rates ⁴⁸³.

1.5.2. Activating neurons

To record neuronal activity *in vitro*, apart from an appropriate Ca^{2+} indicator, Ca^{2+} imaging requires neuronal stimulation. This can be by a shift in extracellular conditions (e.g. temperature), electrical stimulation or pharmacological agents. Extracellular solutions with high K^+ concentration are generally used to activate neurons by depolarising the membrane potential across the whole neuronal population thus opening multiple voltage-gated ion channels simultaneously in the process. Hence, the excitability information derived by such stimulation is limited to a ‘yes or no’ interpretation and is impossible to discriminate among neuronal subtypes ⁴⁸⁴.

1.5.2.1. The constellation pharmacology approach

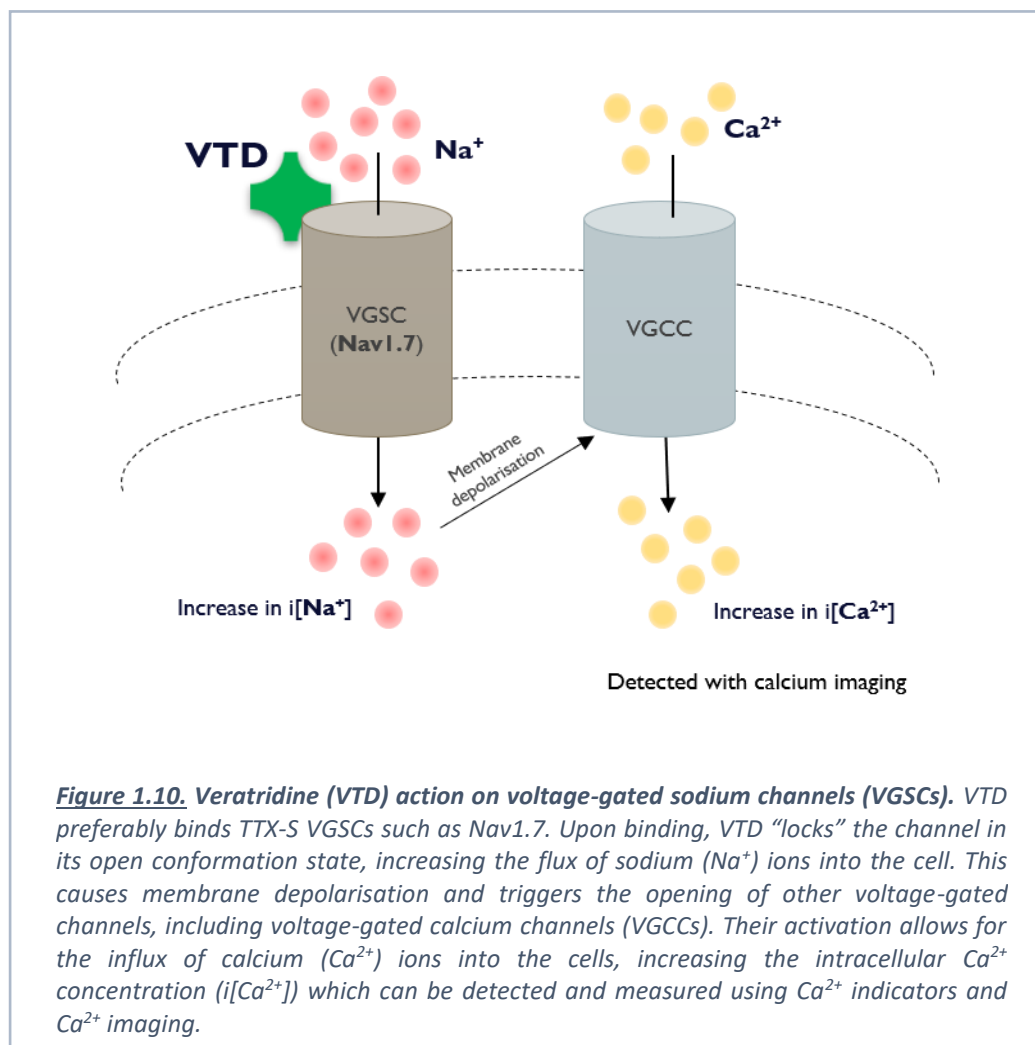
Apart from activating all neurons in a population simultaneously, separate neuronal subsets can also be targeted by applying specific pharmacological agonists. This method of “profiling”

a mixed population of neurons was popularised by Olivera et al. under the term “constellation pharmacology”^{485,486}. Specifically, they applied a variety of pharmacological agents (e.g. allyl isothiocyanate, capsaicin, histamine, ATP, menthol and acetylcholine), as well as agonists targeted at voltage-gated ion channels (e.g. TTX, tetraethylammonium – a VGKC blocker) to a heterogeneous DRG population of neurons and recorded individual responses by Ca^{2+} imaging. Based on the distinct sets of Ca^{2+} responses produced by each neuron they were able to identify and functionally characterize neuronal subtypes^{485,487}. The constellation pharmacology approach can therefore be applied not only for the functional characterisation of neuronal subtypes but also in drug screens to determine the specific selectivity of a drug, as well as the degree of any side effects. These can be established by comparing the Ca^{2+} responses induced by markers in control versus drug-treated cells⁴⁸⁸; or by pre-establishing a Ca^{2+} response template to high K^+ solution in cells and comparing the changes the drug would induce to changes induced by ion channel blockers with pre-determined specificity^{485,487,488}. Albeit highly informative, this cellular neuropharmacological approach is not without limitations. Due to its nature, this method demands the testing of multiple markers in succession in order to characterise the constellation of neuronal ion channels and receptors. The more detailed the characterisation is, the greater number of agents need to be applied, creating lengthy protocols, which cannot be supported due to limitations by other factors, e.g. the eventual photobleaching of the Ca^{2+} indicator used. The need for elaborate, pre-established Ca^{2+} response templates as well as the application of high K^+ solution as a universal neuronal activator during drug screens are further examples of drawbacks of this experimental method.

1.5.2.2. Veratridine

One pharmacological agent used in drug screens is veratridine (VTD) due to its ability to activate VGSCs. Veratridine is a lipid-soluble alkaloid toxin derived from the seeds of lilaceous plants. It was first purified in the 1950s and became commercially available as a pharmacological agent in the early 1970s. Initially used mainly as an insecticide, the interest in VTD's neurotoxic properties gradually grew sparking research into its mechanism of action on VGSCs⁴⁸⁹⁻⁴⁹¹.

Veratridine binds reversibly to the S6 VGSC segment – part of the pore domain of the channel. The toxin is selective for TTX-S VGSCs and preferably binds them in their open state. Notably, voltage-clamp experiments in neurons from rat DRG have shown that VTD can also bind TTX-R channels although the dissociation rate is much faster than TTX-S channels, leading to transient responses⁴⁹². Once bound, VTD locks the channel in its open conformation and prevents inactivation by shifting the activation threshold of the channel to a more negative potential⁴⁹³. Thus, VTD leads to an increase in intracellular Na^+ levels, depolarising the membrane and activating other voltage-gated ion channels resulting in increase in intracellular Ca^{2+} concentrations and increased overall neuronal excitability (Figure 1.10). Of note, for VTD to exercise its strong nerve depolarisation effect, the external medium needs to include Na^+ ions in its composition, as demonstrated by early experiments on frog and single nerve fibres⁴⁸⁹. With its VGSC activator profile confirmed by further electrophysiology experiments^{491,494–496}, VTD is now extensively used as a pharmacological tool in drug screening protocols to activate sodium channels and test the efficacy of VGSC blockers⁴⁹⁷.



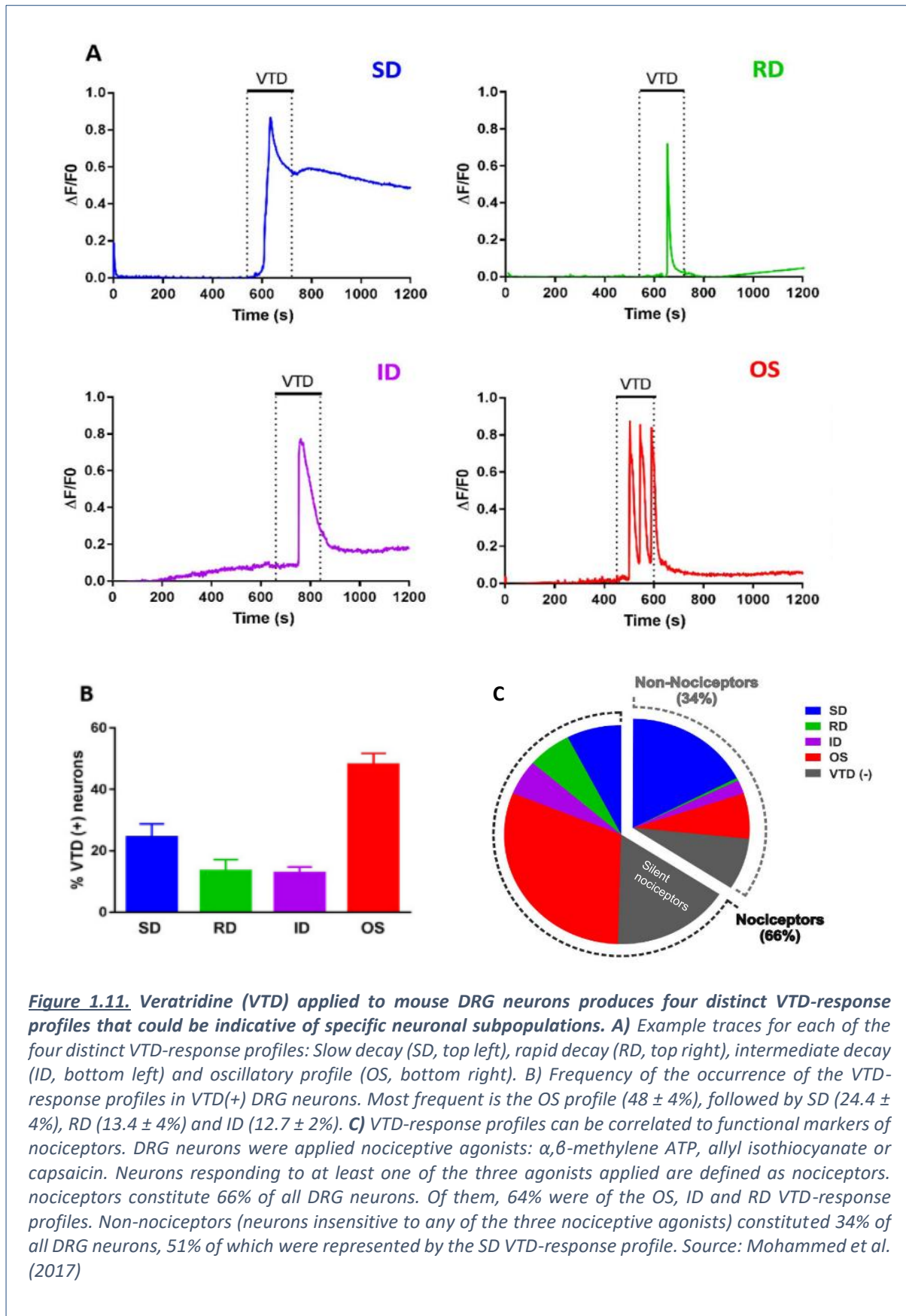
1.5.3 Veratridine-induced calcium response profiles as functional indicators of DRG neuronal subpopulations

In DRG, the TTX-S VGSCs available for VTD to bind to are Nav1.6 and Nav1.7. Of the two, Nav1.7 is the most predominantly expressed in all DRG, especially nociceptors, whereas Nav1.6, although expressed by all DRG neurons, is found mainly in large, non-nociceptive neurons⁴⁹⁸. Although VTD preferentially binds to TTX-S VGSCs, it does not have specificity to a particular isoform. Applying VTD to a mixed population of DRG neurons, therefore, would be expected to produce mixed responses based on the constellation of VGSCs (and other voltage-gated ion channels) expressed by each neuronal type.

This concept was elegantly demonstrated previously in our lab by Mohamed et al.⁴⁹⁹, in Ca²⁺ imaging experiments with VTD on mouse DRG neurons. They showed that VTD elicited heterogeneous Ca²⁺ responses. Based on their decay rate and oscillation, the responses were classified into four distinct VTD-induced Ca²⁺ response profiles: rapid decay (RD), intermediate decay (ID), slow decay (SD) and oscillatory (OS) profile with the SD and OS profiles being the most frequently occurring (Figure 1.11 A, B). Additionally, three nociceptive agonists were also applied to the neurons after VTD:

- **α,β-methylene adenosine 5'-triphosphate (ATP)** to mark non-peptidergic, IB4+ nociceptors,
- **allyl isothiocyanate (AITC)** – marker of LTMRs and some peptidergic and non-peptidergic nociceptors
- **capsaicin (CAP)** to mark peptidergic nociceptors.

The VTD-response profiles correlated with responses to the nociceptive markers (Figure 1.11 C) revealing a strong association between the OS profile and nociceptors, whereas the SD profile correlated with non-nociceptors. These observations were further confirmed by size analysis of the imaged neurons, showing that virtually all OS, ID and RD neurons are small to medium diameter, while SD was the most prevalent profile in neurons of large diameter. An additional finding of this study was that 25-30% of the identified nociceptors did not respond to VTD and were therefore presumed to be the population of high-threshold “silent nociceptors”, activated under inflammatory or nerve injury conditions⁴ (Figure 1.11 C).



Thus, the study generated the first detailed characterisation of VTD responses in DRG neurons and their correlation with neuronal subtypes. What is more, it proposed the use of the VTD response profiles as broad functional markers of neuronal subpopulation that can discriminate nociceptors from non-nociceptors. Importantly, it presented the opportunity of developing the VTD-Ca²⁺ imaging assay into a platform suitable for drug screening as well as characterisation of neuropathology phenotypes ⁴⁹⁹. The promising findings by Mohamed et al. opened the door to exploring the possibilities of this assay and laid the foundations of the project described in this thesis.

1.6. Aims

The VTD-Ca²⁺ imaging assay has shown promise as a suitable technique for neuronal characterisation. However, before it can be applied, the link between the VTD-response profiles and neuronal subpopulations needs to be strengthened further. Therefore, the first aim and its objectives of this study are

Aim 1: Validation of the VTD-Ca²⁺ imaging assay as a suitable drug screen platform (Chapter 3)

- Confirm the link between VTD-induced Ca²⁺ response profiles and neuronal subpopulations by:
 - using DRG from mice with genetically ablated nociceptors
 - using specific and non-specific VGSC blockers and analyse the VTD response profiles patterns in DRG neurons

Then, I endeavour to investigate the application of the assay as a method for characterising the neuropathological phenotype in a diabetic neuropathy model. The *db/db* mouse is one of the most popular models of type 2 diabetes, however, its diabetic neuropathy phenotype is still poorly characterised and the accumulated literature on the matter to date is highly controversial. Therefore, the second aim and objectives of the research presented here are:

Aim 2: Application of the VTD-Ca²⁺ imaging assay and nociceptive agonists to characterise changes in excitability in neuronal subpopulations under diabetic neuropathy conditions (Chapters 4 and 5).

- Characterise excitability changes in DRG neurons from healthy mice cultured *in vitro* under hyperglycaemic conditions using the VTD-Ca²⁺ imaging assay and nociceptive markers
- Characterise morphological and excitability changes in DRG neurons isolated from diabetic *db/db* mice using VTD-Ca²⁺ imaging assay and nociceptive markers. Investigate the distinct excitability changes in the two diabetic neuropathy phases in the *db/db* mouse:
 - Early diabetic neuropathy phase
 - Late diabetic neuropathy phase

CHAPTER 2

MATERIALS & METHODS

CHAPTER 2: MATERIALS & METHODS

2.1 Materials

2.1.1. Animals:

C57/BL6 adult male mice (Charles River, Margate, UK), obtained at 5-7 weeks old were used in the experiments with healthy mice outlined in this thesis. For experiments investigating effects of diabetes on DRG neurons, a total of 12 male diabetic C57BKS*db/db* mice (BKS.Cg-+Leprdb/+Leprdb/OlaHsd) were used and 12 lean littermate mice were used as non-diabetic controls (BKS.Cg-+Leprdb/-Leprdb/OlaHsd) (Envigo, The Netherlands). Animals were kept in a 12h light-dark cycle with free access to food and water. Mice were housed in groups of 3-4 and were allowed a week for acclimatisation upon arrival at the Biological Services Unit at the University of Sheffield in a temperature- ($23 \pm 2^\circ\text{C}$) and humidity- (40-70%) controlled holding room. During experimental periods, no animal was left alone in its unit for longer than 24h. All efforts were made to minimise animal suffering and reduce the number of mice used in the reported studies. All experiments with animals were conducted according to the UK Home Office Animals (Scientific Procedures) Act 1986.

2.1.2 Cell culture reagents

| Name | Supplier | Catalogue No |
|--|--------------------------|--------------|
| Albumin Bovine fraction V (BSA) | Melford | A1302 |
| Collagenase Type XI,100X (0.6 mg/mL) | Sigma | C9407 |
| Dispase, 100X (1 mg/mL) | Sigma | D4693 |
| Dulbecco's Modified Eagle's Medium/F12 with Glutamax medium (DMEM/F-12 + Glutamax) | Gibco™ life technologies | 31331-028 |
| Dulbecco's phosphate buffered saline (DPBS), without Ca²⁺ and Mg²⁺, 0.0095 M (PO₄) | Lonza | BE17-512Q |
| FBS (fetal bovine serum) – EU approved origin, origin: South America | Gibco™ life technologies | 10500-064 |

| | | |
|-------------------------------------|-------|-------|
| Penicillin/Streptomycin 100X | Sigma | P0781 |
| Poly-L-ornithine (20µg/mL) | Sigma | P3655 |

2.1.3 Pharmacological compounds

| Name | Supplier | Catalogue No | Stock concentration | Solvent |
|------------------------------------|---------------|--------------|---------------------|---------|
| 4,9-anhydrotetrodotoxin | Tocris | 6159 | 300 µM | water |
| A-803467 | Abcam | Ab120282 | 10 mM | DMSO |
| Allyl isothiocyanate (AITC) | Sigma | 377430 | 100 µM | - |
| Capsaicin | Tocris | 0462 | 10 mM | ethanol |
| Isoflurane (IsoFlo®) | Abbott | B506 | 100% | - |
| PF-04856264 | Sigma | 11916 | 10 mM | DMSO |
| PF-05089771 | Sigma-Aldrich | PZ0311 | 20 mM | DMSO |
| Veratridine | Abcam | Ab120279 | 5 mM | ethanol |
| α, β-methylene ATP | Sigma | M6517 | 10 mM | water |

2.1.4. Reagents, chemicals and solvents

| Name | Supplier | Catalogue No |
|---------------------------------------|-------------------|--------------|
| Calcium Chloride (anhydrous) | Melford | C1103 |
| D-glucose (anhydrous) | Fisher Scientific | G/0500/53 |
| Dimethylsulfoxide (DMSO) | Sigma-Aldrich | 276855 |
| Ethanol, absolute (HPLC grade) | Fisher Scientific | E/0665DF/17 |
| Fura-2, AM (20 X 50 µg unit) | Molecular Probes | F1221 |

| | | |
|---------------------------------------|-------------------|-----------|
| HEPES | Sigma | H3375 |
| Magnesium chloride (Anhydrous) | Melford | M0535 |
| Potassium chloride | Melford | P0515 |
| Sodium Chloride | Fisher Scientific | S/3160/65 |
| Sodium hydroxide | Fisher Scientific | S/4920/53 |
| Mannitol | Sigma-Aldrich | 63559 |

2.1.5. Tools, equipment and labware

| Name | Supplier | Catalogue No |
|---|------------------------------------|---------------------|
| Calcium imaging perfusion chamber | Warner instruments | RC-25F |
| Cellview™ cell culture dish, PS, 35/10MM (Glass bottom, one compartment) | Scientific Laboratory Supplies LTD | - |
| Cover glass ø16 mm (0.13-0.17 mm thick) | Scientific Laboratory Supplies LTD | MIC3310 |
| Disposable Scalpels (Surgical steel blades) | Swann-Morton | 0505 |
| Dumont #5 Forceps | Fine Science Tools, FST | 15018-10 |
| Luer-Lok syringes (50 mL) | Becton Dickinson (BD) | 300865 |
| Minisart® Syringe Filters (0.45 µm, Sartorius) | Appleton woods | 25926 |
| Portex Tubing ,30m non-sterile polythene tubing, [0.86 mm ID, 1.27 mm OD] | Fisher Scientific | 800/110/260 |

2.1.6. Solution and medium recipes

- DRG neurons digestion mix (stored at -20°)
 - Collagenase XI (0.6 mg/ml)
 - Dispase II (1 mg/ml)
 - DMEM/F-12 + Glutamax

- Standard Extracellular Ringer Solution (stored at room temperature)
 - 140 mM Sodium Chloride,
 - 4 mM Potassium Chloride,
 - 2 mM Calcium Chloride,
 - 1 mM Magnesium Chloride,
 - 10 mM HEPES,
 - 5mM D-glucose (added on the day of experiment)*
 - pH = 7.4 at 25 °C, PH is adjusted with Sodium Hydroxide

- High Potassium Ringer Solution (stored at room temperature)
 - 104 mM Sodium Chloride,
 - 40 mM Potassium Chloride,
 - 2 mM Calcium Chloride,
 - 1 mM Magnesium Chloride,
 - 10 mM HEPES,
 - 5 mM D-glucose (added on day of experiment)*
 - pH = 7.4 at 25 °C, PH is adjusted with Sodium Hydroxide

*stored at 5°C once D-glucose is added

2.2. Methods

2.2.1. Preparation of mouse dorsal root ganglia neuronal culture

2.2.1.1 Isolation of DRG

The mouse was anaesthetized using isoflurane in an anaesthetic machine, then moved to a surgical table and culled by cervical dislocation in accordance with Schedule 1 procedures of UK Animals (Scientific Procedures) Act 1986. The animal's spinal column was isolated by careful incisions along its length and unnecessary extra tissue (muscle and fat) surrounding it was gently shaved off using a scalpel. The spinal column was then cut in half longitudinally, 1-2 vertebrates

at a time, using a scalpel in order to be able to access the spinal cord. Halves of the spinal column were placed under a light microscope and spinal cord matter pushed away carefully using forceps in order to expose the sockets containing DRG underneath. Then DRGs were extracted one by one out of the spinal columns with forceps and placed into 35mm dish with PBS until end of isolation procedure. Once all DRGs were isolated, long extending axons were trimmed whilst still in PBS dish under the light microscope, using a scalpel. For experiments investigating mice with Na_v1.8-expressing neurons ablated, DRG from Na_v1.8Cre-DTA mice⁹⁹ and littermate control mice were stored in ice-cold Hibernate-A medium (Gibco) containing penicillin/streptomycin whilst being transported from University College London (approximately 5-hour journey), after which were dissociated as outlined.

2.2.1.2 DRG digestion

The PBS in the dish containing isolated and prepped DRG bodies was replaced with DRG digestion mix made up of 1 ml Dulbecco's Modified Eagle's Medium/F12 (DMEM/F12) with Glutamax medium containing Dispase (1mg/ml) and Collagenase Type XI (0.6 mg/ml). DRGs were then left in an incubator for 60 mins at 37°C and 5% CO₂ for digestion.

2.2.1.3 Dissociation of neurons and seeding

At the end of digestion time, cells were triturated 10 times to ensure tissue separation from neurons. Resulting cell suspension was then carefully layered on the surface of 1.5 ml 15% Bovine Serum Albumin (BSA) in DMEM/F12. Mixture was centrifuged for 10 minutes at 21° at 800 g (2000 rpm (rotor no. 4624/ Hettich Rotina 46R centrifuge)) set at minimum deceleration speed. The produced cell pellet was then gently washed with DMEM/F12 containing 10% Foetal Bovine Serum, 100 units/mL penicillin and 100 µg/mL streptomycin. Mixture was centrifuged once more at 200g (1000 rpm) for 3 minutes. Supernatant was removed and cells were resuspended in 60 – 100 µl of the above-described DRG culture medium and seeded on autoclaved and poly-L-ornithine- coated (20 µg/ml) 16mm glass coverslips with each seeding drop being 3-4 µl. Neurons were left in the incubator at 37°C / 5 % CO₂ for 1 hour to allow adhesion to coverslip surface. Finally, plated cells were carefully flooded with DRG culture medium and incubated for a minimum of 24h at 37 °C / 5 % CO₂ prior to experiments.

2.2.1.4. Adjustments to glucose concentration in culture for in vitro hyperglycaemia experiments

Mouse DRG neurons were cultured with standard DMEM/F12 (17.5 mM glucose) with 32.5 mM added glucose (total 50 mM) to induce hyperglycaemic, diabetic conditions; control cultures

were supplied with DMEM/F12 medium containing default amount of 17.5 mM glucose deemed optimal for neuronal survival³¹⁸ and were added 32.5 mM mannitol for osmotic control. Additional glucose administration to the culture was initiated after 1 day after culturing the neurons and maintained for up to 5 days with measurement taken on days 1, 2, 4 and 5 post - glucose addition.

2.2.2. Calcium imaging of DRG neurons

2.2.2.1. DRG cells loading with Fura-2AM

All loading of neurons with a calcium dye took place in the dark. Working concentration of 2 μ M of the calcium dye Fura-2AM was made up by mixing 1 μ l Fura-2AM stock with 1ml standard extracellular Ringer solution (see section 2.1.6. Solution and medium recipes). Using a P1000 pipette, solution was vigorously mixed for up to a minute to ensure complete solubilisation of the dye. Coverslips were carefully removed from culture plates with DRG medium and placed in a 35mm dish, up to three at a time, taking care not to overlap. They were washed once with standard extracellular Ringer solution before loaded with Fura-2AM solution and left to incubate at 37 °C / 5 % CO₂ for 30 minutes. After 30 minutes, Fura-2AM solution was removed and replaced with 1 ml standard extracellular Ringer solution and cells were left to incubate at 37 °C / 5 % CO₂ for another 15 minutes. Finally, cells were taken out and stored in an opaque container outside of incubator for another 15 minutes in order to allow for neurons to adjust to the room temperature at which calcium imaging experiments would take place.

2.2.2.2. Experimental set up

Recordings were performed at room temperature of 23 \pm 2°C. Each Fura-2AM-loaded coverslip was mounted on a recording chamber (RC-25F, Warner instruments) and slowly and carefully added 1 ml standard extracellular Ringer solution to prevent dehydration of cells. Chamber was placed on the stage of an inverted Olympus, IMT-2 microscope fitted with a 40X oil-immersion objective (Olympus, 160/-, DPlanApo40UVPL). Due to technical issues this objective was replaced with a 40X dry objective. Coverslip surface was examined to locate a suitable field of view, comprising of optimal number of cells (20 – 45) and cell density. Simple PCI6 software was used for recording set up and image acquisition with background subtraction and ratiometric measurements (F350/380 nm). Regions of interest (ROI) were obtained for each cell of interest in the selected field, as well as an additional one for the background. Neurons were excited with alternating 350 nm and 380 nm light (Cairn Dual OptoLED system) at 1.6 s intervals. Image acquisition was carried out using a Hamamatsu C4742-95 camera. Solution perfusion was carried out using a perfusion system reliant on gravity at a flow rate of 3 ml/min.

2.2.2.3. Recording of calcium responses

Upon launching of the perfusion system, a laminar stable flow across the coverslip was confirmed before recording commenced. Prior to addition of drug solutions during recording, neurons were initially perfused with standard extracellular Ringer solution for at least 5 minutes to ensure a stable initial calcium trace baseline is established. A wash of minimum of 5 minutes with standard extracellular Ringer solution was also included in between drug solution perfusions. Finally, high potassium extracellular Ringer solution (KCl, 40 mM) (see 2.1.6. Solution and medium recipes, page 66) was perfused at the end of each recording as a universal neuronal depolarising means to confirm viable neurons. Neurons unresponsive to high potassium extracellular Ringer solution were excluded from analysis.

2.2.3. Data processing and statistical analysis of calcium imaging data

2.2.3.1. Analysis of recorded calcium imaging responses

Viable neurons identified by high potassium extracellular Ringer solution were selected for analysis. All recorded traces were analysed using GraphPad Prism 8 software, also used to generate all graphs in this thesis. Calcium signal baseline was established from 30 frames of signal prior to the addition of any drugs. A calcium response to a drug was identified as an increase in F350/380 ratio of 6 standard deviations or more above the mean of the baseline. Veratridine (VTD) responses were classified according to the four VTD-response profiles, or shapes, outlined previously by Mohammed et al. (2017)⁴⁹⁹.

The fractional difference ($\Delta F/F_0$) in fluorescence was established prior to amplitude, response onset and area under the curve analysis, using the formula:

$$\frac{\Delta F}{F_0} = \frac{F_{350/380} - \text{Baseline}}{\text{Baseline}}$$

Area under the curve was calculated using a built-in analysis function in GraphPad Prism 8 implementing the 'trapezoid' principle for area under the curve measurement. The measured data included a 10-minute stretch of the recording, beginning at VTD application, due to the diversity in shapes and decay of VTD responses. Amplitude and response onsets were analysed manually using GraphPad Prism 8 for each trace individually.

2.2.3.2. Neuronal cell size analysis

Neuronal cell diameter analysis was carried out using the ImageJ software (version 1.53a for Windows). Cell circumference was obtained by manual tracing of each cell's soma outline. Cell area was then calculated by the in-built software formula. The generated cell area was then used to calculate cell diameter following the formula:

$$\text{Diameter } (d) = \sqrt{\left(\frac{4 \times \text{Area}}{\pi}\right)}$$

2.2.3.3. Statistical tests

The unit used in statistical analysis was the mouse (N). The mean percentage of responsive neurons from each culture an N produced was calculated. Upon accumulation of sufficient independent samples (independent Ns) for each experiment, means of the Ns of each experimental group were compared to each other. To test the frequency distribution of cell sizes for normal Gaussian distribution, a normality test was performed (D'Agostino-Pearson and Kolmogorov-Smirnov normality tests), which yielded normal Gaussian distribution in all cases. To calculate the significant difference between two groups, a Student's *t*-test was used. To test for significant difference in the mean values between three or more groups. one-way analysis of variance (ANOVA) with post Sidak's multiple comparison as the mean \pm standard error of the mean (SEM).

CHAPTER 3

VALIDATION OF THE DISTINCT VERATRIDINE CALCIUM RESPONSE PROFILES AS FUNCTIONAL MARKERS FOR NOCICEPTORS AND NON- NOCICEPTORS

CHAPTER 3: VALIDATION OF THE DISTINCT VERATRIDINE CALCIUM RESPONSE PROFILES AS FUNCTIONAL MARKERS FOR NOCICEPTORS AND NON-NOCICEPTORS

The research presented in this chapter has been published under the title:

“An unbiased and efficient assessment of excitability of sensory neurons for analgesic drug discovery”

Authors: Zainab A. Mohammed, Katerina K. Kaloyanova and Mohammed A. Nassar

PAIN. volume: **161**, issue: 5, pages: 1100 – 1108; doi: 10.1097/j.pain.0000000000001802,

Date: May 2020.

Published under the creative commons CC-BY license.

Authors' contribution:

I co-designed, carried out and analysed all experiments presented here, excluding experiments with knock-out mice (Figure 3A and C). Contributed to the preparation of figures. Contributed to manuscript editing and revisions.

Zainab Mohammed co-designed and carried out experiments presented in Figure 3A and C; and co-designed and contributed to carrying out experiments presented in Figures 4 and 5. Also, contributed towards manuscript editing and revisions.

Mohamed Nassar conceived, designed and supervised all experiments and prepared the manuscript.

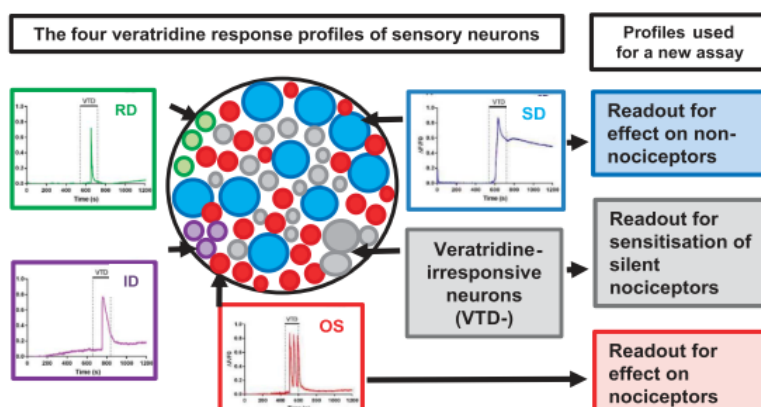


Figure 1. Assessments of the excitability of nociceptors and non-nociceptors based on veratridine-response profiles. Dorsal root ganglia (DRG) contain a heterogeneous population of sensory neurons. Nociceptors are typically small in size, express the $\text{Na}_v1.8$ channel, and respond to nociceptive compounds (eg, ATP and capsaicin). Most nociceptors responded to veratridine with an oscillatory (OS), rapid decay (RD), or intermediate decay (ID) profiles. Non-nociceptors are typically large in size, do not express the $\text{Na}_v1.8$ channel, and do not respond to nociceptive compounds. Most non-nociceptors respond to veratridine with a slow-decay (SD) profile. The percentages of the OS and SD veratridine profiles plus the percentage of veratridine-insensitive (VTD-) neurons can be used for an efficient assay of the excitability DRG neurons. Changes in the SD population reflect changes in non-nociceptors (blue, typically 15%-20% of all neurons). Changes in the OS population (red, typically 30%-40% of all neurons) reflect changes in nociceptors. Changes in the veratridine-insensitive population (gray, typically 30%-40% of all neurons) can reflect sensitisation of high-threshold and normally "silent" neurons. The 2 minor profiles, ID and RD, are mostly nociceptors but can be excluded from an assay for simplicity as both account for less than 5% to 10% of all neurons.

all spinal levels were dissected and collected in phosphate-buffered saline at room temperature. Phosphate-buffered saline was then replaced with 1-mL dissociation solution containing Dulbecco's Modified Eagle's Medium/F12 (DMEM/F12) with Glutamax (Gibco, United Kingdom), $1\times$ penicillin/streptomycin mix (Gibco), dispase (1 mg/mL, Sigma, United Kingdom), and collagenase Type XI (0.6 mg/mL, Sigma) and incubated at 37°C and 5% CO_2 for 90 minutes. Dorsal root ganglia were triturated with a P1000 pipette tip 10 times at 60 and 90 minutes. After the second trituration, the cell suspension was carefully layered on top of 15% bovine serum albumin (Melford, United Kingdom), dissolved in DMEM/F12 containing penicillin/streptomycin, and centrifuged at $800g$ for 10 minutes with the minimum deceleration speed. The cell pellet was then washed in a culture medium composed of DMEM/F12 containing 10% fetal bovine serum and penicillin/streptomycin (all from Gibco). Cells were pelleted again and then resuspended in 60- μL culture medium. A 3- μL "drop" was placed on the centre of a glass coverslip coated with D-polyornithine (20 $\mu\text{g}/\text{mL}$, Sigma). Coverslips were flooded with a 1 mL of culture medium after 15 to 30 minutes. Cells were imaged 24 to 48 hours after plating. Dorsal root ganglia from 1.8-DTA, $\text{Na}_v1.7\text{KO}$, and $\text{Na}_v1.8\text{KO}$ were placed in ice-cold Hibernate-A medium (Gibco) containing penicillin/streptomycin while being transported from UCL (about 5 hours). Dorsal root ganglia were then dissociated as above.

2.2. Calcium imaging

All recordings were performed at room temperature ($22\text{-}25^\circ\text{C}$). Dorsal root ganglia neurons were loaded with 2 μM Fura-2AM (ThermoFisher, United Kingdom) in standard Ringer solution (140 mM NaCl, 4 mM KCl, 2 mM CaCl_2 , 10 mM HEPES, 5 mM glucose, and $\text{pH} = 7.4$ with NaOH) for 30 minutes at 37°C . Coverslips were then washed with ringer solution and left for 15 minutes at $37^\circ\text{C}/5\% \text{CO}_2$ after which the Ringer was replaced. Coverslips were stored in a dark container at room temperature until imaged (within 2 hours). Cells were perfused at a flow rate of 3 mL/minute with Ringer solution for at least 5 minutes to establish a stable calcium baseline. Ringer with 40 mM KCl was perfused at

the end of recordings to identify viable neurons. Cells were imaged with a $40\times$ objective and a Hamamatsu C4742-95 camera. Cells were excited with 350 and 380 nm for ratiometric measurement of intracellular calcium using Cairn Dual OptoLED system. *Simple PCI 6* software was used for data acquisition, background subtraction, and Fura-2AM ratiometric measurement (F350/380 nm).

All drugs were made in standard Ringer solution from stock solutions of the following concentrations: veratridine (5 mM in ethanol, Abcam ab120279), capsaicin (10 mM in ethanol, Tocris 0462), α , β -methylene ATP (10 mM in water, Sigma M6517), allyl isothiocyanate (AITC; 100 μM , Sigma 377430), 4,9-anhydrotetrodotoxin (300 μM in water, Tocris 6159), PF-04856264 (10 mM in DMSO, Sigma 11916), and A-803467 (10 mM in DMSO, Abcam Ab120282).

2.3. Data and statistical analysis

Neurons were included in the analysis if they respond to 40 mM KCl. On rare occasions, neurons responded to veratridine but not KCl (or the KCl response was not clear due to the calcium signal not returning to baseline after the application of last agonist). We defined a response as an increase in (F350/380) ratio of >6 SD above the baseline. Differences in fluorescence ($\Delta F/F_0$) were calculated according to the following formula: F350/380 ratio during agonist application (F) minus the average F350/380 ratio of the 2.5 minutes before agonist application (F_0). Mean values from each experiment (each N is a culture from one mouse) were compared with each other by one-way analysis of variance (ANOVA) with Sidaks' post-test. All statistical analysis and comparisons were performed by *GraphPad Prism* software (version 7.00 for Windows).

3. Results

3.1. The oscillatory response population is highly diminished in the $\text{Na}_v1.8\text{-DTA}$ (nociceptor-ablated) model

To confirm the link between neurons with the OS profile and pain behaviour, we examined DRG from the $\text{Na}_v1.8\text{Cre-DTA}$ (1.8-DTA) mouse.¹ The $\text{Na}_v1.8$ channel is expressed in 80% to 90% of

nociceptors.^{5,21} In the 1.8-DTA mouse, Na_v1.8-expressing neurons are ablated (Fig. 2A) leading to the loss of most nociceptors and a profound loss of pain.¹ Therefore, we hypothesised that the veratridine-response profile that pertains to nociceptors (ie, OS) would be reduced in the 1.8-DTA DRG. First, we determined the percentage of remaining nociceptors in 1.8-DTA DRG using the 3 nociceptive agonists (capsaicin, $\alpha\beta$ -methyleneadenosine triphosphate, and isothiocyanate) to identify all subtypes of nociceptors as described previously.¹⁰ The percentage of neurons responding to any of the nociceptive agonists was drastically reduced from 75% in controls to just 8% in 1.8-DTA (Fig. 2B). This shows that most neurons in 1.8-DTA DRG are non-nociceptors with very few nociceptors left.

The ablation of most nociceptors caused opposing changes in the percentages of the veratridine OS and SD populations. The OS population decreased from 34% in controls to 7% (Fig. 2C). By contrast, the SD population increased from 17% in controls to 66%. This confirms that the OS population represents most nociceptors, whereas the SD population represents most non-nociceptors. Of note, the total number of veratridine-irresponsive neurons decreased

from 39% in control to 23% in 1.8-DTA (Fig. 2C). The veratridine-irresponsive population can be either nociceptors (ie, respond to the nociceptive agonists but not veratridine, yellow section in Fig. 2D) or non-nociceptors (ie, respond to neither the nociceptive agonists nor veratridine, orange section in Fig. 2D). The observed decrease in veratridine-irresponsive neurons was in fact due to the loss of almost all veratridine-irresponsive nociceptors, a population that accounted for 26% of all neurons in controls but only 0.8% in 1.8-DTA.

Results from the 1.8-DTA mouse link the reduction of the OS population in vitro to the previously described¹ pain deficits in vivo. Therefore, drugs can be screened based on their ability to reduce the OS population (an indication of potency on nociceptors) without an effect on the SD population (an indication of unwanted effects on non-nociceptors), Figure 1.

3.2. A reference veratridine-response pattern for a potent and safe analgesic

Next, we established the reference criterion by which drug potency and selectivity on nociceptors can be quickly ascertained

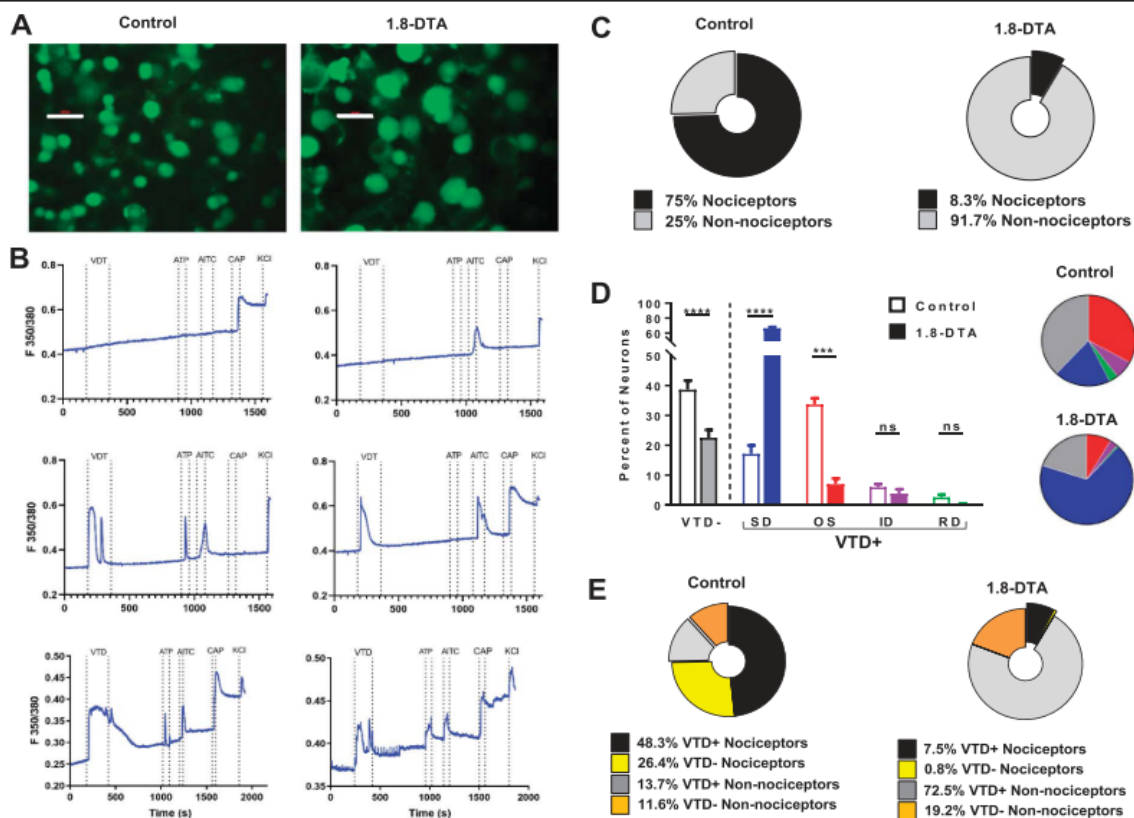


Figure 2. The OS population is reduced in mice lacking most nociceptors. (A) Representative images from control and 1.8-DTA cultures loaded with fura-2AM for imaging (contrast enhanced for both). Ablation of Na_v1.8-expressing neurons in 1.8-DTA mouse leaves behind mostly non-nociceptive large neurons. Scale bar is 50 μ m. (B) Example traces from our imaging protocol. Dashed lines indicate the periods of agonist application in recordings typically 25 to 35 minutes long. The 4 agonists and KCL are applied in the same order for all coverslips. The first row shows examples of neurons irresponsive to veratridine but respond to capsaicin and AITC, the second row shows neurons responding to veratridine and 2 nociceptive agonists, whereas the third row shows neurons responding to all 4 agonists: veratridine (VTD), capsaicin (CAP), α , β -methylene ATP (ATP), and allyl isothiocyanate (AITC). (C) In control DRG, 75% of neurons respond to one or more of the 3 nociceptive compounds and are classified as nociceptors (top) while only 8.3% do so in the 1.8-DTA confirming the loss of 89% of nociceptors. (D) Ablation of Na_v1.8-expressing neurons decreases the percentage of veratridine-irresponsive neurons, decreases the percentage of OS neurons, and increases the percentage of SD neurons. VTD- CTR = 38.6 \pm 3.1 vs VTD- DTA = 22.5 \pm 2.6; SDCTR = 17.11 \pm 2.8 vs SDDTA = 66.4 \pm 1.4; OSCTR = 33.7 \pm 2.1 vs OSDTA = 6.9 \pm 1.9; IDCTR = 5.9 \pm 1.1 vs IDDTA = 3.8 \pm 1.5; RDCTR = 2.6 \pm 0.9 vs RDDTA = 0.3 \pm 0.2%. One-way ANOVA with Sidak's test. Pie charts represent mean percentages in the histogram. (E) In control DRG, veratridine-irresponsive neurons can be nociceptors (yellow section, 26.4% of all neurons) or non-nociceptors (orange section, 11.6% of all neurons). Veratridine-irresponsive or "silent" nociceptors are almost completely lost in 1.8-DTA (become 0.8% of all neurons). Overall, there are less veratridine-irresponsive neurons in 1.8-DTA. Data for C–E are from 940 neurons from 3 control mice and 360 neurons from 4 1.8-DTA. ANOVA, analysis of variance; DRG, dorsal root ganglia.

in our assay. We base this criterion on the change to the percentages of the OS and SD populations in the $Na_v1.7$ knockout mouse where pain behaviour is lost due to a decrease in the excitability of nociceptors (as opposed to their ablation as in 1.8-DTA). $Na_v1.7$ is a VGSC that is highly expressed in nociceptors and is a critical determinant of their excitability. Deletion of $Na_v1.7$ in DRG neurons leads to profound loss of pain without adverse motor or central nervous system (CNS) effects.^{14,17} Therefore, the changes in the OS and SD populations in the $Na_v1.7$ knockout represents the effects a potent and safe analgesic would have. We used the advillin-1.7 KO mouse¹⁴ ($Na_v1.7$ KO thereafter), where $Na_v1.7$ is deleted in all DRG neurons. We hypothesized that $Na_v1.7$ deletion will cause a major decrease in veratridine-responsive neurons through a decrease in the OS but not the SD population. In the $Na_v1.7$ KO, the percentage of veratridine-irresponsible neurons increased from 51% in controls (floxed $Na_v1.7$) to 80% (Fig. 3A). This decrease in the responsiveness to veratridine was due to the reduction of the OS population, which decreased from 28% to 7% (0.25 of control). Deletion of $Na_v1.7$ rendered 3 quarters of the OS population veratridine-irresponsible. Of note, there was no significant decrease in the SD population. Therefore, drugs can be screened by our assay based on the similarity of their effect on DRG neurons to $Na_v1.7$ deletion.

To validate the use of the pattern of veratridine responses in $Na_v1.7$ KO as the criterion for a “good” analgesic, we compared it with the pattern of a would-be “bad” analgesic, a drug affecting non-nociceptors and CNS neurons. For this purpose, we used a $Na_v1.6$ channel blocker. Although conditional $Na_v1.6$ knockout suggests it

contributes to pain,³ and it is not a potential analgesic target because of its role in CNS and motor neurons.^{12,18} In DRG, $Na_v1.6$ contributes more to sodium current in large (non-nociceptive) than in small (nociceptive) neurons.³ Therefore, we hypothesised that a $Na_v1.6$ blocker will reduce the OS and SD populations, but the effect on the SD population will be greater. Low concentrations of the tetrodotoxin metabolite, 4,9-anhydro-TTX (4,9TTX), preferentially blocks $Na_v1.6$ (IC_{50} 120 times lower than $Na_v1.7$).²⁰ As expected, 300 nM 4,9TTX greatly increased the percentage of veratridine-irresponsible neurons from 42% to 68% (Fig. 3B). Unlike $Na_v1.7$ deletion, 4,9TTX reduced both the SD and OS populations, but the reduction in the SD population (0.48 of control) was greater than the reduction in the OS population (0.62 of control). Therefore, drugs that reduce the SD population may act on non-nociceptive neurons with potential unwanted physiological effects.

To test whether our assay has the potential to detect increases in neuronal excitability (ie, as a readout for changes that lead to hyperexcitability, Fig. 1), we examined veratridine responses in the $Na_v1.8$ knockout mouse ($Na_v1.8$ KO). $Na_v1.8$ is also an important determinant of the excitability of nociceptors. The global $Na_v1.8$ KO mouse, however, showed a compensatory increase in $Na_v1.7$ expression.² This is the most likely reason why the $Na_v1.8$ KO mouse does not show a major loss of pain. Because $Na_v1.8$ is expressed in nociceptors, then it is logical to assume that the compensatory increase in $Na_v1.7$ will occur in nociceptors. Therefore, we hypothesised that this compensatory increase in $Na_v1.7$ will primarily affect the OS population. In

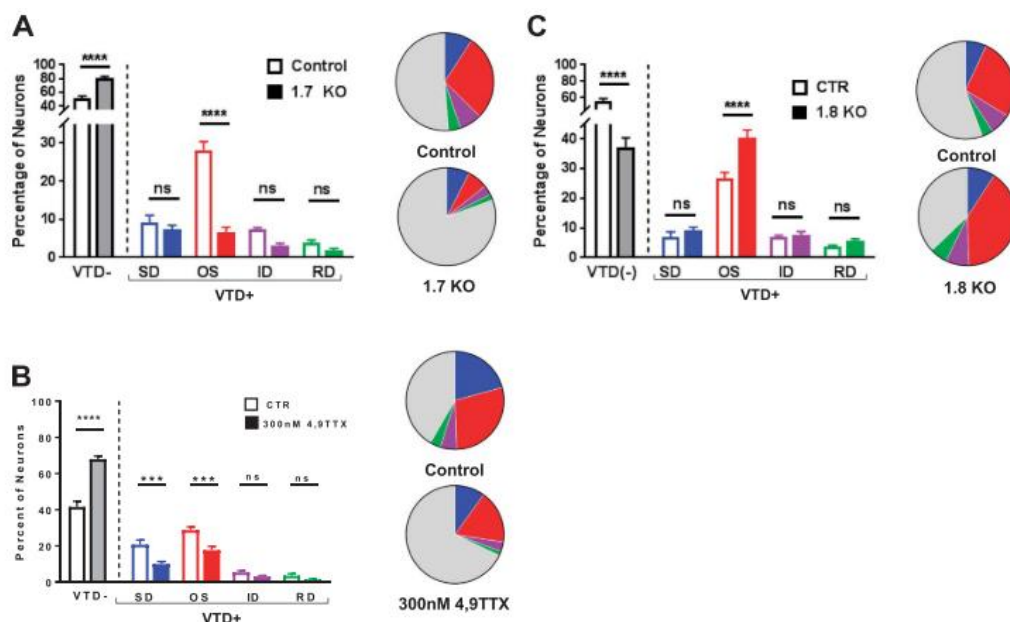


Figure 3. Reference veratridine-response patterns for “safe” and “unsafe” analgesic drugs. (A) Deletion of $Na_v1.7$ causes a major loss of pain without adverse CNS or motor effects. The veratridine-response pattern of the $Na_v1.7$ KO represents that of a safe and potent analgesic. $Na_v1.7$ deletion leads to a decrease in responsiveness to veratridine (increase VTD- population) due to a decrease in the OS population but not the SD population. VTD- CTR = 51.0 ± 3.51 vs VTD- KO = 80.4 ± 2.8 ; SDCTR = 9.1 ± 1.9 vs SDKO = 7.5 ± 1 ; OSCTR = 28.2 ± 2.2 vs OSKO = 6.7 ± 1.3 ; IDCTR = 7.4 ± 0.4 vs IDKO = 3.2 ± 0.6 ; RDCTR = 4.0 ± 0.6 vs RDKO = 1.9 ± 0.5 . One-way ANOVA with Sidak’s test. Pie charts represent mean values in the histogram. Data from 1448 neurons from 6 floxed-control mice and 1630 neurons from 6 $Na_v1.7$ KO. (B) 300 nM of the $Na_v1.6$ blocker 4,9TTX reduces responsiveness to veratridine (increases VTD-) through decreases in both the SD and OS populations. The decrease in SD is greater than that in OS. VTD- CTR = 41.6 ± 3.1 vs VTD- 4,9TTX = 68.0 ± 1.7 ; SDCTR = 20.68 ± 2.6 vs SD4,9TTX = 10.0 ± 1.5 ; OSCTR = 28.7 ± 1.8 vs OS4,9TTX = 17.6 ± 2.2 ; IDCTR = 5.4 ± 0.9 vs ID4,9TTX = 3.1 ± 0.5 ; RDCTR = 3.5 ± 1.1 vs RD4,9TTX = 1.4 ± 0.3 . One-way ANOVA with Sidak’s test. Pie charts represent mean values in the histogram. Data from 635 untreated and 927 treated neurons from 6 C57Bl6 mice. (C) The compensatory increase in $Na_v1.7$ channels in nociceptors of the $Na_v1.8$ KO increases responsiveness to veratridine (decreases VTD-) due to an increase in the OS population. VTD- CTR = 55.4 ± 3 vs VTD- KO = 37.1 ± 3.2 ; SDCTR = 6.9 ± 1.7 vs SDKO = 9.1 ± 1.1 , OSCTR = 26.7 ± 2.0 vs OSKO = 40.3 ± 2.7 , IDCTR = 7.0 ± 0.5 vs IDKO = 7.65 ± 1.1 , RDCTR = 3.6 ± 0.6 vs RDKO = 5.7 ± 0.5 . One-way ANOVA with Sidak’s test. Pie charts represent mean values in the histogram. Data from 1493 neurons from 5 littermate-control mice and 1028 neurons from 4 $Na_v1.8$ KO. ANOVA, analysis of variance.

Na_v1.8KO, the percentage of veratridine-irresponsible neurons decreased from 55% in littermate controls to 37% in Na_v1.8KO (Fig. 3B). This increase in veratridine responsiveness came from the increase in the OS population from 27% in controls to 40%. The changes in the other populations were small and highly insignificant. In other words, the compensatory increase in Na_v1.7 expression caused previously silent neurons to respond to veratridine, and that these additional neurons had the OS profile, the profile of nociceptors. These results show that our assay is sensitive to increases in Na_v1.7 and thus can be used to detect pathological changes in Na_v1.7 function (eg, gain of function mutations or painful conditions).

Collectively, our results confirm that most nociceptors respond to veratridine with the OS profile, whereas most non-nociceptors respond to veratridine with the SD profile. Only the OS population is reduced when nociceptors are ablated (1.8-DTA) or lose a critical excitability determinant (Na_v1.7KO). Importantly, the veratridine-response pattern of the Na_v1.7KO can be used as the reference for potent and safe analgesic action, a reference pattern that potential analgesics can be evaluated against before-detailed in vitro characterisation or testing.

3.3. Evaluating the potency and selectivity of subtype-specific voltage-gated sodium channel blockers using the Na_v1.7KO as reference

Several blockers of Na_v1.7 and Na_v1.8 channels have been developed and are currently in clinical trials.^{9,25} We used our assay to evaluate a candidate analgesic drug for each. PF-04856264 (PF-048) is from the arylsulfonamide class of selective Na_v1.7 blockers.¹¹ PF-048 reduced responses to veratridine at concentrations similar to or lower than those used in standard cell line-based FLIPR assays^{4,11} and shows that our assay can identify nonpore blockers such as arylsulfonamides. PF-048 at 1 μM increased the percentage of veratridine-irresponsible neurons (Fig. 4A) from 46% to 58% through a decrease in the OS population, which decreased from 26% to 17% (ie, 0.65 of control). PF-048 at 5 μM (Fig. 4B) had a greater effect, increasing veratridine-irresponsible neurons from 44% to 72% through a larger decrease in the OS population from 28% to 12% (0.43 of control). However, 5 μM PF-048 decreased the SD population from 13% to 6%. Because a reduction in the SD population was not observed in Na_v1.7KO, this suggests that PF-048 will affect non-nociceptors at a dose that does not even reduce the OS population to the Na_v1.7KO level of 0.25 of control.

The Na_v1.8 blocker A-803467 (A-80) decreases the excitability of DRG neurons.⁸ At 0.1 μM, it reduced the OS population from 25% to 12% (Fig. 4C) but without an overall increase in veratridine-irresponsible neurons (51% vs 55%). A-80 at 0.1 μM did not silence the OS population but rather prevented its multipeak oscillatory behaviour, converting them to the ID and RD profiles that respond to veratridine with a single peak (Fig. 1). A-80 at 0.3 μM increased veratridine-irresponsible neurons from 41% to 66% (Fig. 4D), through significant decreases in the OS population (from 28% to 12%) and the SD population (from 19% to 12%). These data suggest that A-80 is more potent in reducing the excitability of the OS population than PF-048, but it also affects the SD population at the higher concentration.

3.4. A combination of low concentrations of PF-04856264 and A-803467 have an additive effect on nociceptors

We suggest that our assay can be used not only to screen for novel drugs, but also to identify effective combinations of existing

ones. As a proof of concept, we used a combination of 1 μM PF-048 and 0.1 μM A-80 (Fig. 5A). When applied separately, neither reduced the SD population significantly, but their reduction of the OS population is considerably less than Na_v1.7 deletion. The combination reduced the OS population from 30% to 11%, greater than either alone. Importantly, the combination still did not significantly reduce the SD population. A direct comparison of the decreases in the OS and SD populations between the VGSC blockers used and Na_v1.7 deletion (Fig. 5B) clearly shows that the combination produced the closest effect on the OS population (reduction to 0.38 of control) to that observed in Na_v1.7KO (0.25 of control).

4. Discussion

Cell lines provide a high-throughput platform for analgesic drug discovery. However, their use leaves a knowledge gap that must be addressed on DRG neurons using lower throughput methods such as calcium imaging and patch clamping. The knowledge gap includes information on the effect of a drug on nociceptors as a whole (rather than just the molecular target of interest) and the concentrations needed for a potent effect on nociceptors with a minimal effect on non-nociceptors (as a proxy for unwanted side effects on CNS and motor neurons). We discovered that nociceptors and non-nociceptors respond to veratridine with distinct response profiles.¹⁶ Here, we show that a veratridine-based assay allows for a simultaneous assessment of drugs' action on both populations and therefore provides an efficient and more informative assay for screening for analgesics on sensory neurons. First, we discuss the results from our findings and then discuss the key advantages of our assay.

We used the 1.8-DTA mouse that has well characterised pain deficits to demonstrate the link between the loss of the OS population and loss of pain.¹ In 1.8-DTA neurons, we recorded a loss of 89% of functionally defined nociceptors (Fig. 2B), which is in agreement with the expression of Na_v1.8 in 80% to 90% of nociceptors.^{5,21} Our identification of nociceptors is based on responsiveness to one or more of 3 nociceptive agonists.¹⁶ This definition will encompass 6 of the putative 11 molecular subtypes (the NP1-3, PEP1-2, and TH types) of sensory neurons as defined in one single-cell RNA-sequencing study.²³ By our functional definition, non-nociceptors will equate to the 5 neurofilament-positive subtypes (NF1-5).²³ Ablation of nociceptors leads to the loss of 78% of the OS population, confirming that most nociceptors respond to veratridine with the OS profile. In the Na_v1.7KO mouse, nociceptors are not ablated, but their excitability is greatly reduced to the extent that the pain loss in the Na_v1.7KO is very similar to that of the 1.8-DTA.^{1,14} Not surprisingly, deletion of Na_v1.7 "silenced" 75% of the OS population (Fig. 3A), an almost identical percentage to that lost in 1.8-DTA.

Given that Na_v1.7 is expressed in all DRG neurons, why was there no significant reduction in the SD population in Na_v1.7KO? Veratridine primarily activates TTX-sensitive VGSCs, and indeed, we previously showed that TTX silences all OS and SD neurons.¹⁶ However, although Na_v1.7 is the main TTX-sensitive channel in nociceptors, non-nociceptors rely on other TTX-sensitive subtypes, namely Na_v1.1, Na_v1.2, and Na_v1.6. In the absence of Na_v1.7, these subtypes allow veratridine to activate non-nociceptors. The predominance of other TTX-sensitive subtypes in non-nociceptors explains why deletion of Na_v1.7 in all DRG neurons has no effect on touch or proprioception.¹⁴ This is also why 4,9TTX, which preferentially blocks Na_v1.6 channels, affected the SD population more than the OS population (Fig. 3B).

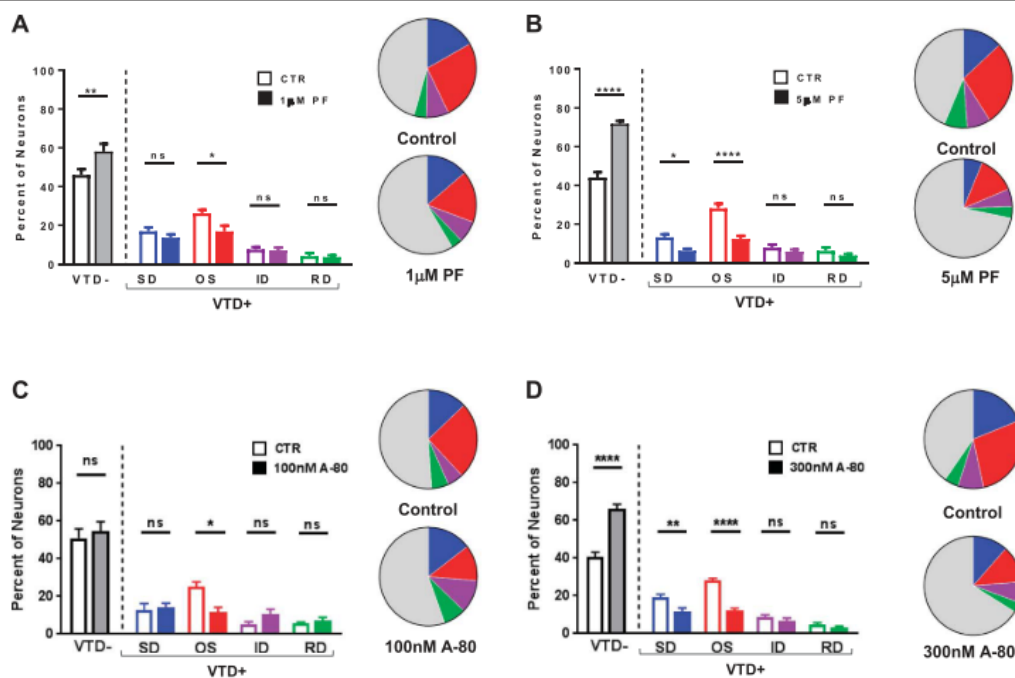


Figure 4. Evaluating the effect of PF-04856264 and A-803467 on nociceptors and non-nociceptors. (A) 1 μ M PF-048 increases the percentage of veratridine-irrespective neurons through a reduction of the OS but not the other 3 populations. VTD- CTR = 45.9 \pm 3 vs VTD- 1 PF = 58.1 \pm 4; SDCTR = 16.9 \pm 2 vs SD1PF = 13.6 \pm 1.7; OSCTR = 26.2 \pm 1.7 vs OS1PF = 16.8 \pm 3; IDCTR = 7.5 \pm 1.3 vs ID1PF = 7.0 \pm 1.4; RDCTR = 4.1 \pm 1.6 vs RD1PF = 3.6 \pm 0.9%. One-way ANOVA with Sidak's test. Pie charts represent mean values in the histogram. Data from 813 untreated and 681 treated neurons from 7 C57Bl6 mice. (B) 5 μ M PF-048 increases the percentage of veratridine-irrespective neurons through a reduction of both the OS and SD populations. 5 μ M PF-048 is equally potent on the SD and OS profiles reducing both to about 50% of control values. VTD- CTR = 44.1 \pm 2.7 vs VTD- 5 PF = 71.8 \pm 1.5; SDCTR = 13.2 \pm 1.6 vs SD1PF = 6.3 \pm 1.0; OSCTR = 28.1 \pm 2.4 vs OS5PF = 12.4 \pm 1.6; IDCTR = 7.9 \pm 1.6 vs ID5PF = 5.9 \pm 1.1; RDCTR = 6.2 \pm 1.8 vs RD5PF = 3.8 \pm 0.7%. One-way ANOVA with Sidak's test. Pie charts represent mean values in the histogram. Data from 605 untreated and 338 treated neurons from 5 C57Bl6 mice. (C) 100 nM A-80 does not change the percentage of veratridine-responsive neurons but reduces the OS population by about 50%. VTD- CTR = 51 \pm 4.9 vs VTD- 100A80 = 54.8 \pm 4.9; SDCTR = 12.9 \pm 3.2 vs SD100A80 = 14.4 \pm 2; OSCTR = 25.1 \pm 2.6 vs OS100A80 = 11.61 \pm 2.6; IDCTR = 5.2 \pm 1.3 vs ID100A80 = 10.7 \pm 2.5; RDCTR = 6.6 \pm 0.8 vs RD100A80 = 7.3 \pm 1.6%. One-way ANOVA with Sidak's test. Pie charts represent mean values in the histogram. Data from 607 untreated and 594 treated neurons from 6 C57Bl6 mice. (D) 300 nM A-80 increases the percentage of veratridine-irrespective neurons through a reduction of both the OS and SD populations. The reduction in the OS population is slightly greater than that in the SD profile. VTD- CTR = 40.8 \pm 2.3 vs VTD- 300A80 = 66.2 \pm 2.4; SDCTR = 19.1 \pm 1.7 vs SD300A80 = 11.5 \pm 2; OSCTR = 28.0 \pm 1.3 vs OS300A80 = 12.2 \pm 1.2; IDCTR = 8.5 \pm 1.5 vs ID300A80 = 6.8 \pm 1.5; RDCTR = 4.8 \pm 0.9 vs RD300A80 = 3.3 \pm 0.7%. One-way ANOVA with Sidak's test. Pie charts represent mean values in the histogram. Data from 1197 untreated and 1294 treated neurons from 7 C57Bl6 mice. ANOVA, analysis of variance.

We propose to use veratridine responses of the $\text{Na}_v1.7\text{KO}$ as the criterion VGSC blockers need to match for in vivo potency and safety. The pattern of veratridine responses we observed in vitro is due to the deletion of $\text{Na}_v1.7$ and are unlikely to be influenced by the reported increase in endogenous opioid agonism in the spinal cord.¹⁵ This is because veratridine responses are recorded from dissociated neurons after 1 day in culture (that lacks opioid-releasing spinal cord cells) and under constant Ringer flow. Our assay detected a significant increase in the number of neurons responding to veratridine in $\text{Na}_v1.8\text{KO}$, and these "unsilenced" neurons have the OS profile, demonstrating for the first time the effect of the compensatory increase in $\text{Na}_v1.7$ expression.² All of the above strongly confirms the link between nociceptors' excitability and the OS population and suggests that a reduction in the OS but not the SD population correlates with a reduction in pain without motor/CNS effects.

Our assay has several advantages over cell line-based assays and patch clamping. First, a cell line-based assay examines the effect of a condition or a drug on one target at a time, whereas our assay evaluates the overall effect on DRG neurons, including non-nociceptors. For example, while A-80 was potent in reducing excitability, we noted clear cytotoxic effects at

concentrations $>0.5 \mu\text{M}$ (not shown). The use of veratridine as a single "pan" activator of all sensory neurons has advantages over the commonly used potassium chloride (KCl). Dorsal root ganglion neurons respond to veratridine with distinct profiles that can be used to identify the main populations, whereas KCl produces a similar profile in all neurons. In addition, while 80% of $\text{Na}_v1.7\text{KO}$ neurons did not respond to veratridine, they were all KCl-positive (Fig. 3A), strongly suggesting that KCl responsiveness is a poor predictor of the excitability of DRG in in vitro assays.

Second, our assay allows for changes in the population of high-threshold or "silent" sensory neurons that are observed in vivo,¹³ to be monitored in vitro. This is possible due to the way veratridine activates sensory neurons. Veratridine acts on open VGSC at the resting membrane potential to prevent their inactivation. Neurons with low expression of threshold VGSC channels (eg, $\text{Na}_v1.7$ in DRG) or/and have a hyperpolarised membrane potential will have few open VGSC channels at resting potentials and will not respond to veratridine. We observed that between 30% and 50% of cultured DRG neurons do not respond to 3 minutes of 30 μM veratridine. Interestingly, these are similar to the percentages (38%-48%)

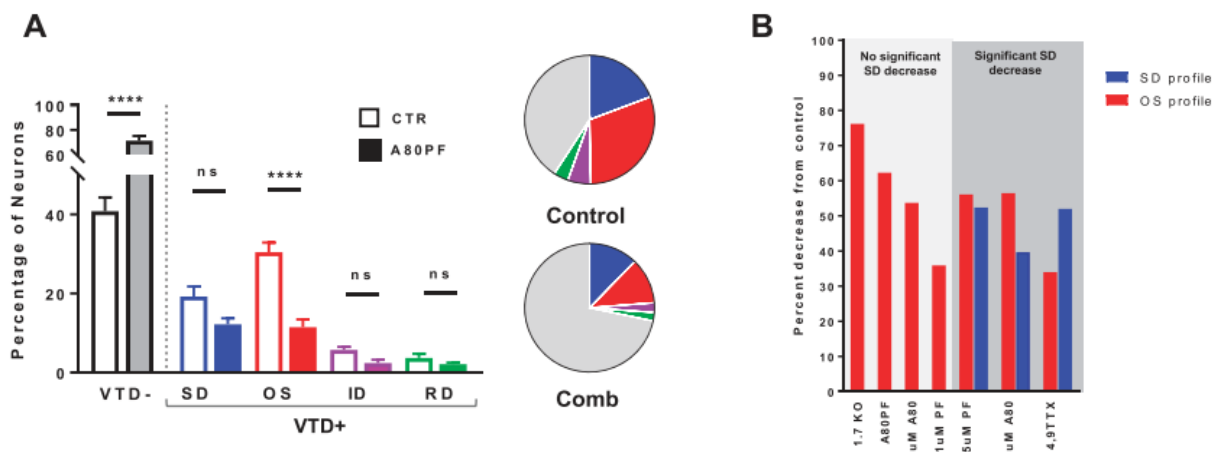


Figure 5. The additive effects of a combination of PF-04856264 and A-803467 on nociceptors. (A) A combination of 1 μ M PF-048 and 100 nM A-80 increases the percentage of veratridine-irrespective neurons through a decrease of the OS population only. VTD- CTR = 40.8 ± 3.5 vs VTD- A80PF = 71.5 ± 3.7 ; SDCTR = 19.2 ± 2.5 vs SDA80PF = 12.2 ± 1.5 ; OSCTR = 30.4 ± 2.4 vs OSA80PF = 11.5 ± 2 ; IDCTR = 5.7 ± 0.8 vs IDA80PF = 2.4 ± 0.8 ; RDCTR = 3.7 ± 0.4 vs RDA80PF = 2.1 ± 1.1 . One-way ANOVA with Sidak's test. Pie charts represent mean values in the histogram. Data from 980 untreated and 1114 treated neurons from 7 C57Bl/6 mice. (B) Comparison of the changes in the OS and SD populations caused by VGSC blockers to those of the $Na_v1.7$ KO. The higher doses of PF and A80 and 4,9TTX caused a significant reduction in the SD population. Notice that the combined action of the lower doses of the PF and A80 produced the closest reduction of the OS population to $Na_v1.7$ deletion. ANOVA, analysis of variance; VGSC, voltage-gated sodium channel.

of high-threshold "silent" DRG neurons that did not respond to 10- to 100-mA current injection *in vivo* but were unmasked by inflammation.²² Because two-thirds of veratridine-irrespective neurons responded to nociceptive markers (yellow segment in **Fig. 2D**), we speculate that the veratridine-irrespective population includes the high-threshold silent nociceptors observed *in vivo*. However, we have no data to support this hypothesis at present.

Third, our assay allows the range of plasma concentrations for a potent action on nociceptors without an effect on non-nociceptors to be determined efficiently. Both PF-048 and A-80 reduced the OS population with A-80 being 10 times more potent than PF-048. However, at the higher concentration, both reduced the SD population, an effect not observed in either $Na_v1.7$ or $Na_v1.8$ KOs but obtained from the $Na_v1.6$ blocker 4,9TTX. The concentrations at which PF-048 and A-80 affected the SD population were not much higher than those at which they did not (5 fold for PF-048 and 3 fold for A-80). The reduction of the SD population by 5 μ M PF-048 is larger than that by 0.3 μ M A-80 (**Fig. 4**). This can be explained by the greater sequence homology between the VGSC subtypes expressed in non-nociceptors to $Na_v1.7$ than to $Na_v1.8$.

Finally, our assay can be used to screen for drug combinations to obtain the most potent effect on the OS but the least effect on the SD populations. This strategy may become a necessity considering that developing potent-selective $Na_v1.7$ blockers has been a challenging task⁹; although $Na_v1.7$ has been a validated target since 2004.¹⁷ A combination strategy will be necessary when selective blockers against a single target do not produce the desired system effect. Because the pain phenotype seen in the mouse and human loss-of-function mutants^{7,14,17} results from 100% loss of $Na_v1.7$ channels, it remains to be determined what level of pharmacological block of $Na_v1.7$ is needed *in vivo* for reduced pain and if selective $Na_v1.7$ blockers can achieve this level of inhibition. Furthermore, the pain phenotype seen in the mouse and human loss-of-

function mutants seems to involve changes in other systems (ie, opioid signalling in the spinal cord¹⁵). In these situations, a selective $Na_v1.7$ blocker may not be potent enough, and combination of drugs against different targets may produce the required potency on nociceptors. As a proof of concept, we demonstrate that combining low concentrations of PF-048 and A-80 produced the closest veratridine-response pattern to that of $Na_v1.7$ KO, the reference genetic model (**Fig. 5B**). Efficient *in vitro* screening of drugs combinations against multiple targets is not possible using cell line-based expression systems. This is because a cell line has to be engineered to express multiple targets at levels similar to their native levels in DRG neurons.

Future work will focus on adapting the assay to high-throughput platforms by automating data analysis (including calculation of response onset, amplitude, and area under the curve) and making use of a nonwash protocol.²² The potential of this assay to screen for drugs for other classes of ion channels (calcium and potassium) needs to be established.

For drug screening, the assay is most useful when the primary screening criterion is the decrease in the OS population where the screening window is large, a 75% drop in the 1.7KO and 62% in the A80PF drug combination (**Fig. 5**). Although a decrease in the total number of veratridine-responsive neurons can be used as the screening criterion, the screening window is narrower (A decrease of 38% in the 1.7KO). In all cases, the screening criterion should include a requirement for minimal effect on the SD population.

In summary, we described an assay to assess the excitability of nociceptors and non-nociceptors. The assay can be used in other applications (**Fig. 6**) in addition to drug development and screening. It can be used for in-depth, long-term characterisation of excitability changes in knockout mice and models of pain pathologies (diabetes, cancer, and aging). It can be used to optimise protocols to differentiate human stem cells into the different classes of sensory neurons.²⁴ Meanwhile, all this may have the added advantage of reducing the number of animals needed for *in vitro* and *in vivo* testing.

Unbiased, medium-/high-throughput, and high content assessment of excitability of DRG neurons

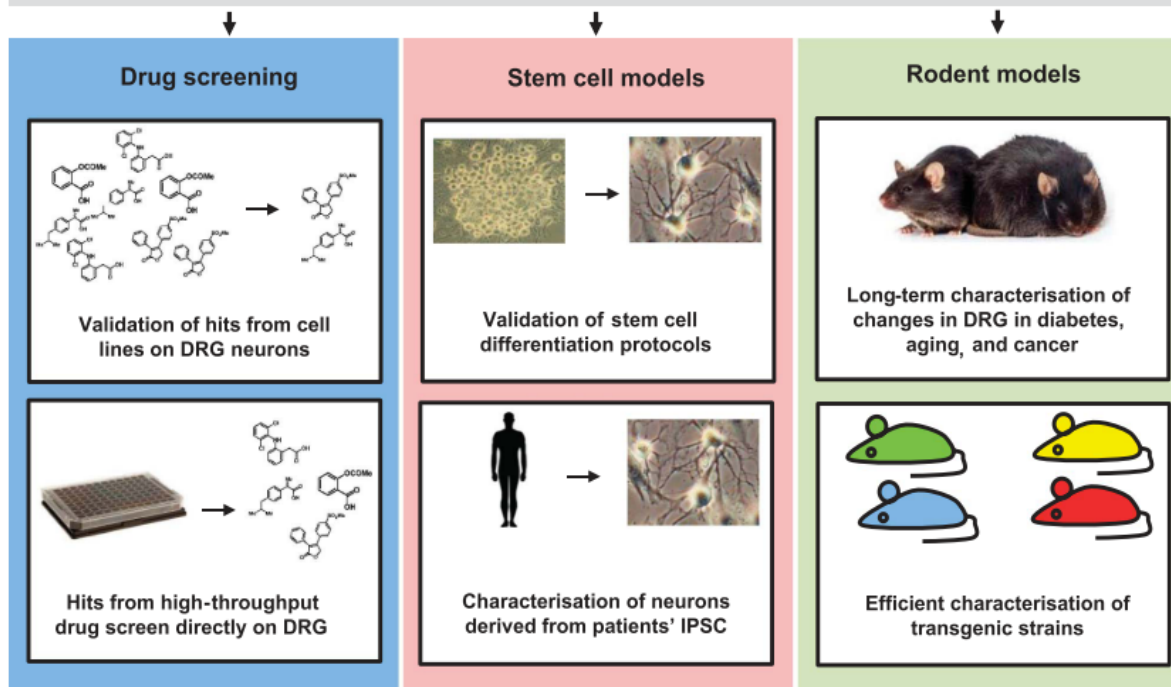


Figure 6. Applications of the veratridine-based calcium assay. The assay is a very efficient method to characterise changes in a heterogeneous population of neurons and therefore has several applications. The assay can be used to identify lead analgesic drugs either by validating hits from cell line-based screens on all types of DRG neurons or identification of hits by a direct screen on DRG neurons. The assay can be used to assess how stem cell-derived neurons compare to primary neurons of the same type more efficiently than by patch clamping. The assay can be used to compare neurons derived from patients' iPSC with known or unknown genetic mutations. The assay is suited to characterise pathologies that develop over time as in diabetes, aging, or cancer. Finally, the assay can be used to efficiently characterise changes in DRG from the large number of transgenic strains generated by phenotyping consortia. DRG, dorsal root ganglia.

Conflict of interest statement

The authors have no conflicts of interest to declare.

Acknowledgements

The authors are grateful for John N Wood, UCL, for provision of the 1.8-DTA, $Na_v1.8KO$, and $Na_v1.7KO$ transgenic mice. The authors are grateful for Yusef and Younes Nassar for proofreading the manuscript.

Author contributions: M.A. Nassar conceived, designed, and supervised experiments. Z.A. Mohammed and K. Kaloyanova codedesigned, carried out, and analysed all experiments. M.A. Nassar contributed to preparations of DRG cultures. M.A. Nassar wrote the manuscript with contributions from Z.A. Mohammed and K. Kaloyanova.

Article history:

Received 4 October 2019

Received in revised form 20 December 2019

Accepted 7 January 2020

Available online 9 January 2020

References

- [1] Abrahamson B, Zhao J, Asante CO, Cendan CM, Marsh S, Martinez-Barbera JP, Nassar MA, Dickenson AH, Wood JN. The cell and molecular basis of mechanical, cold, and inflammatory pain. *Science* 2008;321:702–5.
- [2] Akopian AN, Sivilotti L, Wood JN. A tetrodotoxin-resistant voltage-gated sodium channel expressed by sensory neurons. *Nature* 1996;379:257–62.
- [3] Chen L, Huang J, Zhao P, Persson AK, Dib-Hajj FB, Cheng X, Tan A, Waxman SG, Dib-Hajj SD. Conditional knockout of $NaV1.6$ in adult mice ameliorates neuropathic pain. *Sci Rep* 2018;8:3845.
- [4] Deuis JR, Wingerd JS, Winter Z, Durek T, Dekan Z, Sousa SR, Zimmermann K, Hoffmann T, Weidner C, Nassar MA, Alewood PF, Lewis RJ, Vetter I. Analgesic effects of GpTx-1, PF-04856264 and CNV1014802 in a mouse model of $NaV1.7$ -mediated pain. *Toxins (Basel)* 2016;8:E78.
- [5] Djouhri L, Fang X, Okuse K, Wood JN, Berry CM, Lawson SN. The TTX-resistant sodium channel $Nav1.8$ (SNS/PN3): expression and correlation with membrane properties in rat nociceptive primary afferent neurons. *J Physiol* 2003;550:739–52.
- [6] Emery EC, Luiz AP, Wood JN. $Nav1.7$ and other voltage-gated sodium channels as drug targets for pain relief. *Expert Opin Ther Targets* 2016;20:975–83.
- [7] Habib AM, Wood JN, Cox JJ. Sodium channels and pain. *Handb Exp Pharmacol* 2015;227:39–56.
- [8] Jarvis MF, Honore P, Shieh CC, Chapman M, Joshi S, Zhang XF, Kort M, Carroll W, Marron B, Atkinson R, Thomas J, Liu D, Krambis M, Liu Y, McGaraughty S, Chu K, Roeloffs R, Zhong C, Mikusa JP, Hernandez G, Gauvin D, Wade C, Zhu C, Pai M, Scanio M, Shi L, Drizin I, Gregg R, Matulencko M, Hakeem A, Gross M, Johnson M, Marsh K, Wagoner PK, Sullivan JP, Faltynek CR, Krafte DS. A-803467, a potent and selective $Nav1.8$ sodium channel blocker, attenuates neuropathic and inflammatory pain in the rat. *Proc Natl Acad Sci U S A* 2007;104:8520–5.
- [9] Kingwell K. $Nav1.7$ withholds its pain potential. *Nat Rev Drug Discov* 2019;18:321–23.

- [10] Leadley RM, Armstrong N, Reid KJ, Allen A, Misso KV, Kleijnen J. Healthy aging in relation to chronic pain and quality of life in Europe. *Pain Pract* 2014;14:547–58.
- [11] McCormack K, Santos S, Chapman ML, Kraffe DS, Marron BE, West CW, Krambis MJ, Antonio BM, Zellmer SG, Printzenhoff D, Padilla KM, Lin Z, Wagoner PK, Swain NA, Stupple PA, de GM, Butt RP, Castle NA. Voltage sensor interaction site for selective small molecule inhibitors of voltage-gated sodium channels. *Proc Natl Acad Sci U S A* 2013;110:E2724–32.
- [12] Meisler MH, Plummer NW, Burgess DL, Buchner DA, Sprunger LK. Allelic mutations of the sodium channel SCN8A reveal multiple cellular and physiological functions. *Genetica* 2004;122:37–45.
- [13] Michaelis M, Habler HJ, Jaenig W. Silent afferents: a separate class of primary afferents? *Clin Exp Pharmacol Physiol* 1996;23:99–105.
- [14] Minett MS, Falk S, Santana-Varela S, Bogdanov YD, Nassar MA, Heegaard AM, Wood JN. Pain without nociceptors? Nav1.7-independent pain mechanisms. *Cell Rep* 2014;6:301–12.
- [15] Minett MS, Pereira V, Sikandar S, Matsuyama A, Lollignier S, Kanellopoulos AH, Mancini F, Iannetti GD, Bogdanov YD, Santana-Varela S, Millet Q, Baskozos G, MacAllister R, Cox JJ, Zhao J, Wood JN. Endogenous opioids contribute to insensitivity to pain in humans and mice lacking sodium channel Nav1.7. *Nat Commun* 2015;6:8967.
- [16] Mohammed ZA, Doran C, Grundy D, Nassar MA. Veratridine produces distinct calcium response profiles in mouse Dorsal Root Ganglia neurons. *Sci Rep* 2017;7:45221.
- [17] Nassar MA, Stirling LC, Forlani G, Baker MD, Matthews EA, Dickenson AH, Wood JN. Nociceptor-specific gene deletion reveals a major role for Nav1.7 (PN1) in acute and inflammatory pain. *Proc Natl Acad Sci U S A* 2004;101:12706–11.
- [18] O'Brien JE, Meisler MH. Sodium channel SCN8A (Nav1.6): properties and de novo mutations in epileptic encephalopathy and intellectual disability. *Front Genet* 2013;4:213.
- [19] O'Connor AB. Neuropathic pain: quality-of-life impact, costs and cost effectiveness of therapy. *Pharmacoeconomics* 2009;27:95–112.
- [20] Rosker C, Lohberger B, Hofer D, Steinecker B, Quasthoff S, Schreibmayer W. The TTX metabolite 4,9-anhydro-TTX is a highly specific blocker of the Na(v1.6) voltage-dependent sodium channel. *Am J Physiol Cell Physiol* 2007;293:C783–9.
- [21] Shields SD, Ahn HS, Yang Y, Han C, Seal RP, Wood JN, Waxman SG, Dib-Hajj SD. Nav1.8 expression is not restricted to nociceptors in mouse peripheral nervous system. *PAIN* 2012;153:2017–30.
- [22] Tay B, Stewart TA, Davis FM, Deuis JR, Vetter I. Development of a high-throughput fluorescent no-wash sodium influx assay. *PLoS One* 2019;14:e0213751.
- [23] Usoskin D, Furlan A, Islam S, Abdo H, Lonnerberg P, Lou D, Hjerling-Leffler J, Haeggstrom J, Kharchenko O, Kharchenko PV, Linnarsson S, Ernfors P. Unbiased classification of sensory neuron types by large-scale single-cell RNA sequencing. *Nat Neurosci* 2015;18:145–53.
- [24] Viventi S, Dottori M. Modelling the dorsal root ganglia using human pluripotent stem cells: a platform to study peripheral neuropathies. *Int J Biochem Cell Biol* 2018;100:61–8.
- [25] Yekkiralal AS, Roberson DP, Bean BP, Woolf CJ. Breaking barriers to novel analgesic drug development. *Nat Rev Drug Discov* 2017;16:545–64.

An unbiased and efficient assessment of excitability of sensory neurons for analgesic drug discovery

Zainab A. Mohammed, Katerina K. Kaloyanova, Mohammed A. Nassar*

Department of Biomedical Science, University of Sheffield, S10 2TN, UK

*Corresponding author m.nassar@sheffield.ac.uk

CHAPTER 4

**ASSESSING EXCITABILITY
CHANGES IN DRG NEURONS
UNDER IN VITRO
HYPERGLYCEMIC
CONDITIONS**

CHAPTER 4: ASSESSING EXCITABILITY CHANGES IN DRG NEURONS UNDER IN VITRO HYPERGLYCEMIC CONDITIONS

4.1. INTRODUCTION

The first step in answering this thesis's research question: "What are the excitability changes in DRG neurons during DN?", was to validate the use of the VTD-profiles as a functional marker for nociceptors and non-nociceptors in a heterogeneous neuronal population. In the previous chapter, VTD was shown to allow for the study of changes in VGSCs and place them in the context of specific neuronal subpopulations. Hence, the VTD-Ca²⁺ imaging assay was established as a suitable tool for the discrimination of neuronal subpopulations. As a result of its validation, several potential applications arose.

For the experiments in this and the next chapter, I apply the VTD-Ca²⁺ imaging assay together with selected nociceptive agonists to characterise diabetes-induced excitability changes in DRG neurons exposed to hyperglycaemic conditions. Determining the distinct excitability changes occurring in nociceptors and non-nociceptors during DN would provide valuable insights into the pathophysiological mechanisms driving DN in sensory neurons. To this end, in the current chapter, I used the *in vitro*-induced hyperglycaemia model.

In the literature, *in vitro*-induced hyperglycaemia has been mostly used to investigate the effects of acute exposure to high glucose on DRG neurons. Such studies have contributed vastly to DN research by demonstrating decreased cell viability^{318,423,500,501}, ROS rise^{423,424,500}, cell injury⁴²³, increased Nav1.7 expression³⁵¹ and increased VGSC currents^{424,502} in DRG when exposed to high glucose concentrations for up to 48h. However, to our knowledge, there are no studies exploring the effects of extended high glucose exposure time past the 48h mark on neuronal excitability neither are there studies sorting observed excitability changes to neuronal subtypes. Since VGSC currents and expression have been observed to increase in DRG neurons as early as 18h of acute high glucose exposure^{351,424}, we hypothesised that extending the exposure time will lead to further VGSC activity increase and neuronal excitability changes. Prolonged high glucose exposure of DRG neurons should more closely mimic the chronic hyperglycaemic conditions in humans and reflect physiological DN progression. Furthermore, apart from the immediate post-translational changes induced by hyperglycaemic conditions, transcriptional changes could also have the opportunity to take place. In time periods of 24h or less, such important transcriptional changes would be missed,

therefore, culturing DRG neurons in high glucose for an extended time period would allow for their detection.

4.2. AIMS

To assess the excitability changes in DRG neurons from C57BKS mice cultured in hyperglycaemic conditions for 1, 2, 4 and 5 days by analysing calcium responses induced by the VGSC agonist VTD and the nociceptive markers ATP, AITC and CAP.

4.3. METHOD

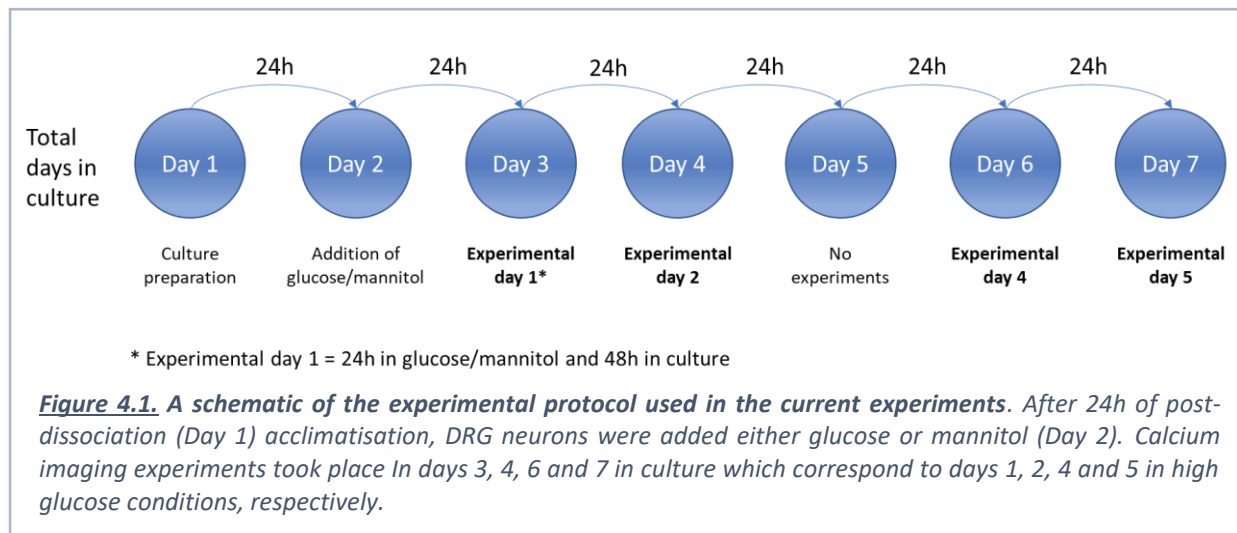
4.3.1. Glucose concentration and exposure time in *in vitro*-induced hyperglycaemia

Mouse DRG neurons were cultured with standard DMEM/F-12 (17.5 mM glucose) with 32.5 mM added glucose (total 50 mM) to induce hyperglycaemic, diabetic conditions. Control cultures were supplied with DMEM/F-12 medium containing its standard 17.5 mM glucose deemed optimal for neuronal survival³¹⁸ and added 32.5 mM mannitol as an osmolarity control to the high glucose medium. The hyperglycaemia-inducing glucose concentrations were selected on the basis of previous studies which have reported that *in vitro* glucose concentrations in the range from 30 to 45 mM lead to hyperglycaemic stress, oxidative stress, ROS elevation and cell injury in DRG neurons - all markers of DN (Table 4.1). Furthermore, 45 mM glucose treatment (1.8-fold above control) is similar to the ≥ 1.4 -fold increase in blood glucose concentration in a person diagnosed as diabetic⁵⁰³ and within the range of blood glucose concentration of diabetic mice^{428-431,504} (e.g. *db/db* mice at 10 WoA have blood glucose concentration of $\sim 32.7 \pm 2.0$ mM⁵⁰⁴, which keeps increasing as diabetes progresses uncontrolled⁴²⁸). Therefore, a total concentration of 50 mM glucose for the present experiments is consistent with other diabetic animal models and human diabetes and should ensure a clear-cut hyperglycaemia manifestation.

Table 4.1. Studies that used varying concentrations and exposure times of glucose in in vitro DRG cultures and the main conclusions reached.

| Team & Year | Type | Glucose concentration (mM) | Glucose exposure time (h) | Conclusions |
|--------------------------------------|--------------------------------|----------------------------|---------------------------|--|
| Russell et al. 1999 ³¹⁸ | Embryonic rat DRG | 30 – 330 mM | 24h- 48h | Observed concentration-dependent neuronal apoptosis and decrease in neurite outgrowth at glucose concentrations above 50 mM; optimal DRG survival and neurite growth require 25–30 mM basal glucose (optimal concentration). |
| Russell et al. 2002 ⁴²³ | Primary DRG neurons | 45 mM | 0- 24h | In vitro as in vivo, variations in administered glucose as small as 10 mM from basal value (25 mM) induce neuronal injury. |
| Singh et al. 2013 ³⁴⁹ | E4 Sprague-Dawley rat DRG | 45 mM 60 mM | 4h-24h | Short-term exposure of DRG neurons to high glucose concentrations enhance the VGSC activity and were attenuated via ROS-dependent mechanisms. |
| Leininger et al. 2006 ⁵⁰¹ | E15 Sprague-Dawley rat embryos | 45 mM | 3-6h | High glucose promotes convergence of Drp1-mediated mitochondrial fission with pro-apoptotic proteins, resulting in mitochondrial injury and apoptosis. |
| Vincent et al. 2005 ⁵⁰⁰ | E15 Sprague-Dawley rats | 45 mM | 0-24h | There were nearly identical levels of DRG neuron death at the endpoint with a 2h glucose exposure compared with prolonged hyperglycaemia for the whole 6 or 24h time course of the experiment. Programmed cell death starts as soon as 2h. |

After isolation and culturing, neurons were left to adjust for 24 hours before adding glucose or mannitol as opposed to introducing hyperglycaemia during the first cell flooding. This was to ensure that both groups had an equal opportunity to acclimatise to being in culture before the introduction of the potentially injurious effects of high glucose. After the addition of high glucose, culture was maintained for up to 5 days. Calcium imaging experiments took place at days 1, 2, 4 and 5 in high glucose. Therefore, total days in culture are equal to [days after adding glucose] + 1, e.g., day 1 of experiments is equal to 1 day in high glucose conditions and 2 days in culture overall (Figure 4.1).



4.3.2. Calcium imaging

DRG neurons were loaded with Fura-2 and responses recorded to nociceptive agonists: capsaicin (CAP, 200 nM), allyl isothiocyanate (AITC, 100 μ M) and α,β -methylene ATP (ATP, 1 μ M) as well as VGSC potentiator veratridine (VTD, 30 μ M). Standard calcium imaging protocol was followed as outlined in Chapter 2: Materials & Methods, section 2.2.2., page 68 .

4.4. RESULTS

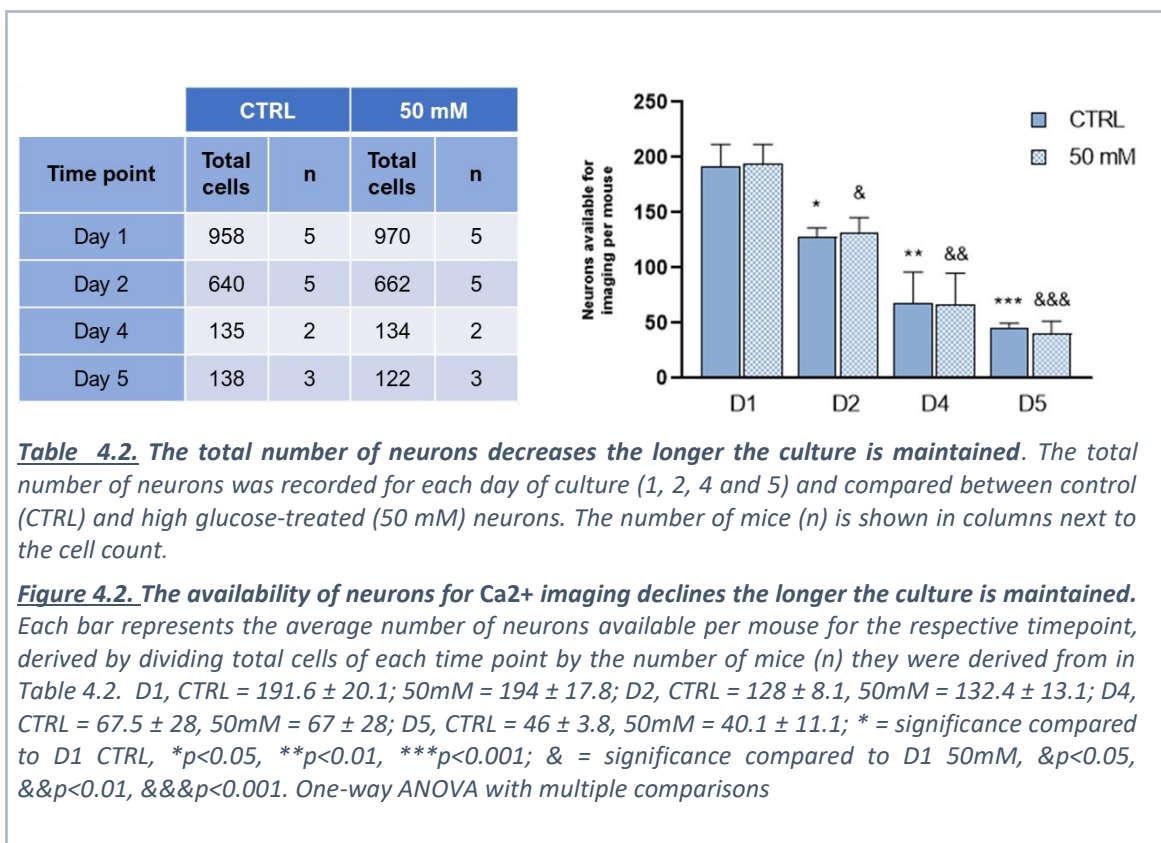
4.4.1. The number of available neurons for imaging experiments declines with time in culture

When selecting neurons for Ca^{2+} imaging experiments, firstly regions of interest (ROI) are specified around each neuron from which fluorescence intensity will be recorded. These are selected based on the neuron's health (e.g., "shiny" membrane, absence of granulation, consistent round shape), quality and positioning relative to other neurons on the coverslip. After 48h in culture, neurite outgrowth and replication of non-neuronal cells begin⁵⁰⁵. This creates overcrowded networks of overlapping neuronal processes and non-neuronal cells that obstruct the neurons in culture from being easily identified and selected for Ca^{2+} imaging in a ROI. We compared the cell yield per mouse per time point (day 1, 2, 4 and 5) in order to determine whether the number of available neurons for imaging experiments is affected with time. A neuron was defined as "available" if it was easily distinguishable, not overlapping with other culture components and hence the fluorescence it would emit would have been unobstructed. The total number of neurons for each day decreased as time in culture increased (table 4.2). Indeed, when comparing the number of available neurons per mouse for each time point, there was a significant decrease in the quantity of available cells for each

consecutive day compared to day 1, for both the control and high glucose groups (figure 4.2). The number of cells imaged for each condition was 1,871 for CTRL and 1,888 for the 50 mM group. By day 5, there was a reduction of 4.2- and 4.7-fold for CTRL and 50 mM group, respectively, compared to day 1 (CTRL: from 191.6 ± 20 in d1 to 46 ± 3.8 neurons in d5; 50mM: from 194 ± 17.9 in d1 to 40.7 ± 11 neurons in d5, $p < 0.001$). There was no significant difference in the number of neurons available between the two conditions for each day. These results demonstrated a consistent decrease in the number of neurons available for Ca^{2+} imaging experiments the longer the culture was maintained.

4.4.2. Time in culture, but not *in vitro*-induced hyperglycaemia, affects responses to nociceptive agonists

Diabetes has been shown to sensitise nociceptors in DRG neuronal populations from animal models of DN as well as in *in vitro*-induced high glucose conditions^{506–509}. Therefore, three

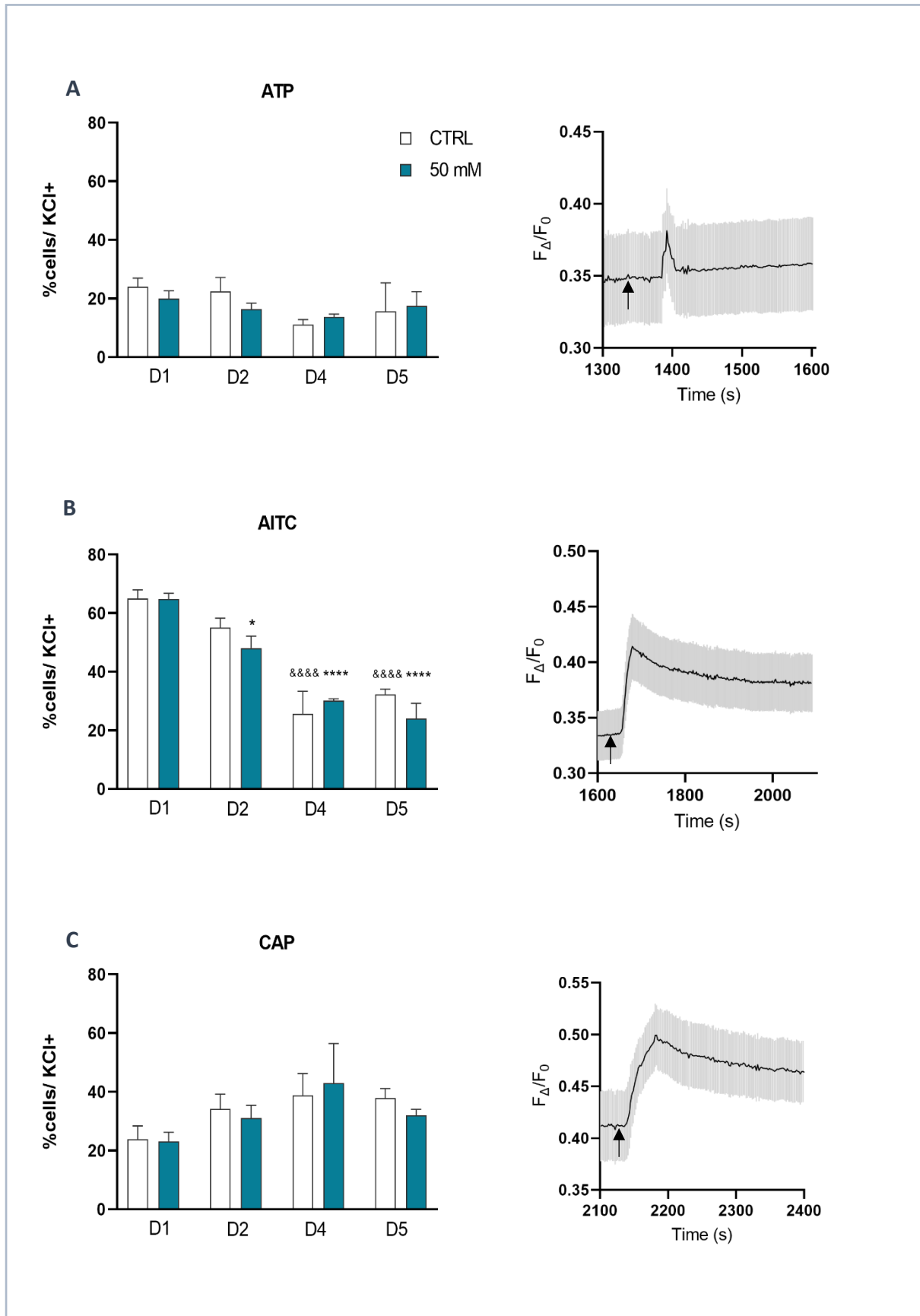


well-established nociceptive agonists were applied: α, β -methylene ATP (ATP), allyl isothiocyanate (AITC) and capsaicin (CAP), to see whether *in vitro* hyperglycaemic conditions would lead to the sensitisation of corresponding nociceptive receptor channels and the nociceptive subpopulations they mark. Agonists were applied consecutively as opposed to

added together. In the control group of neurons, responses to AITC in days 4 and 5 were significantly lower than day 1 by 2.5- and 2-fold, respectively (decrease from D1 $65 \pm 3\%$ to D4 $25.6 \pm 7.7\%$ and D5 $32.3 \pm 1.9\%$). The percentage of AITC(+) neurons between conditions within each day were not significantly different. Thus, the percentage of AITC(+) control neurons decreased significantly with time in culture (Figure 4.3 B). In the high glucose group, all days of measurements (2, 4 and 5) showed significantly lower response rates to AITC than day 1 by 1.4-, 2.2- and 2.7-fold, respectively (decrease from D1 $64.8 \pm 1.9\%$ to D2 $48.1 \pm 4.1\%$, D4 $30.2 \pm 0.7\%$ and D5 $24 \pm 5.2\%$) (Figure 4.3 B). The percentage of ATP(+) (Figure 4.3 A) and CAP(+) (Figure 4.3 C) neurons was comparable between conditions as well as overtime within each condition. Collectively, these results indicate steadily decreasing response rates to AITC in cultured DRG neurons with time, irrespective of extracellular glucose levels.

Figure 4.3. Responses of DRG neurons under control and hyperglycaemic conditions to nociceptive agonists.

A) no significant difference in the responses to ATP between conditions as well as overtime within each condition. CTRL: D1= $24.1 \pm 2.9\%$, D2= $22.4 \pm 4.8\%$, D4 = $11.1 \pm 1.7\%$, D5 = $15.65 \pm 9.7\%$; 50mM, D1 = $20 \pm 2.7\%$, D2 = $16.5 \pm 2\%$, D4= $13.8 \pm 1\%$, D5= $17.4 \pm 5\%$; **B)** The percentage of AITC(+) neurons was significantly decreasing with each day spend in culture compared to day 1 (D1) in both the control and hyperglycaemic cultures. CTRL: D1 = $65 \pm 3\%$, D2 = $55.1 \pm 3.2\%$, D4 = $25.6 \pm 7.7\%$, D5 = $32.2 \pm 1.9\%$; 50mM, D1 = $64.8 \pm 1.9\%$, D2 = $48.1 \pm 4.1\%$, D4 = $30.2 \pm 0.7\%$, D5 = $24 \pm 5.2\%$; **C)** no significant difference in the responses to ATP between conditions as well as overtime within each condition. CTRL: D1 = $23.9 \pm 4.4\%$, D2 = $34.1 \pm 5.1\%$, D4 = $38.8 \pm 7.5\%$, D5 = $37.9 \pm 3.1\%$; 50mM, D1 = $23 \pm 3.2\%$, D2 = $31.1 \pm 4.3\%$, D4 = $43 \pm 13.5\%$, D5 = $32 \pm 2\%$. * = significance compared to D1 CTRL, * $p < 0.05$, ** $p < 0.01$, *** $p < 0.001$; & = significance compared to D1 50mM, & $p < 0.05$, && $p < 0.01$, &&& $p < 0.001$. Where significance is not denoted, the difference is not significant. One-way ANOVA with multiple comparisons. Mean \pm SEM. CTRL=control (open bars); 50mM = hyperglycaemic culture (blue bars); D# = day#. ATP= α, β -methylene ATP, AITC=allyl isothiocyanate, CAP=capsaicin. On the right handside of each, intracellular calcium signal trace following stimulation with the respective agonist, averaged from all responsive neurons (24) from one experiment. Black – average trace from one experiment; grey – showing the SEM for each second of the recorded trace; black arrows indicate the time point of respective drug application.



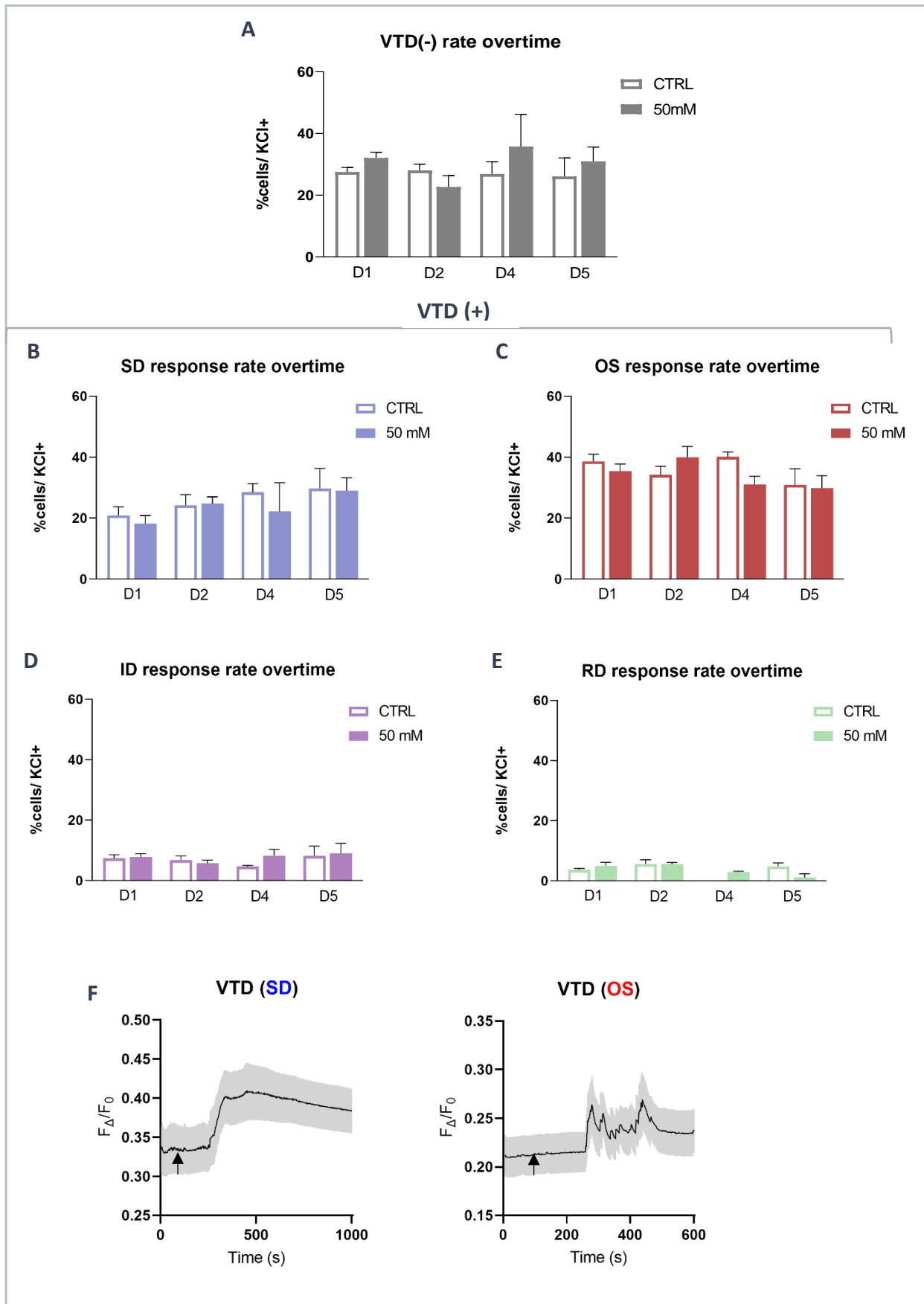
4.4.3. Time in culture leads to subtle changes in VGSC activity, affected by *in vitro* induced hyperglycaemia

High glucose concentrations have been reported to cause excitability changes in DRG neurons contributing to (P)DN³⁴⁹. We hypothesised that these changes are likely to involve modifications in VGSC activity and thus, will be detected using the VTD-based Ca²⁺ imaging assay. First, we looked at the percentage of VTD-irresponsive neurons – the percentage of VTD(-) neurons remained similar from day 1 to day 5 in culture in both the control and hyperglycaemic cultures (Figure 4.4 A). The percentage of VTD(-) neurons was also comparable between the CTRL and hyperglycaemic groups for each day, with non-significant differences. This suggests that neither hyperglycaemic conditions in this model nor time spent in culture influence overall VGSC-induced neuronal excitability.

Next, we classified the VTD(+) neurons into the four VTD-response profiles, in order to detect excitability changes within neuronal subpopulations. VTD-response profile rates overtime showed no significant differences between days within the CTRL and 50mM groups as well as between the CTRL and 50mM groups for each day (Figure 4.4 B,C,D,E).

Figure 4.4. Responses to VTD by DRG neurons cultured for 1 to 5 days in high glucose or standard conditions. Neither time spent in culture nor high glucose levels influenced the responses to VTD in cultured DRG neurons.

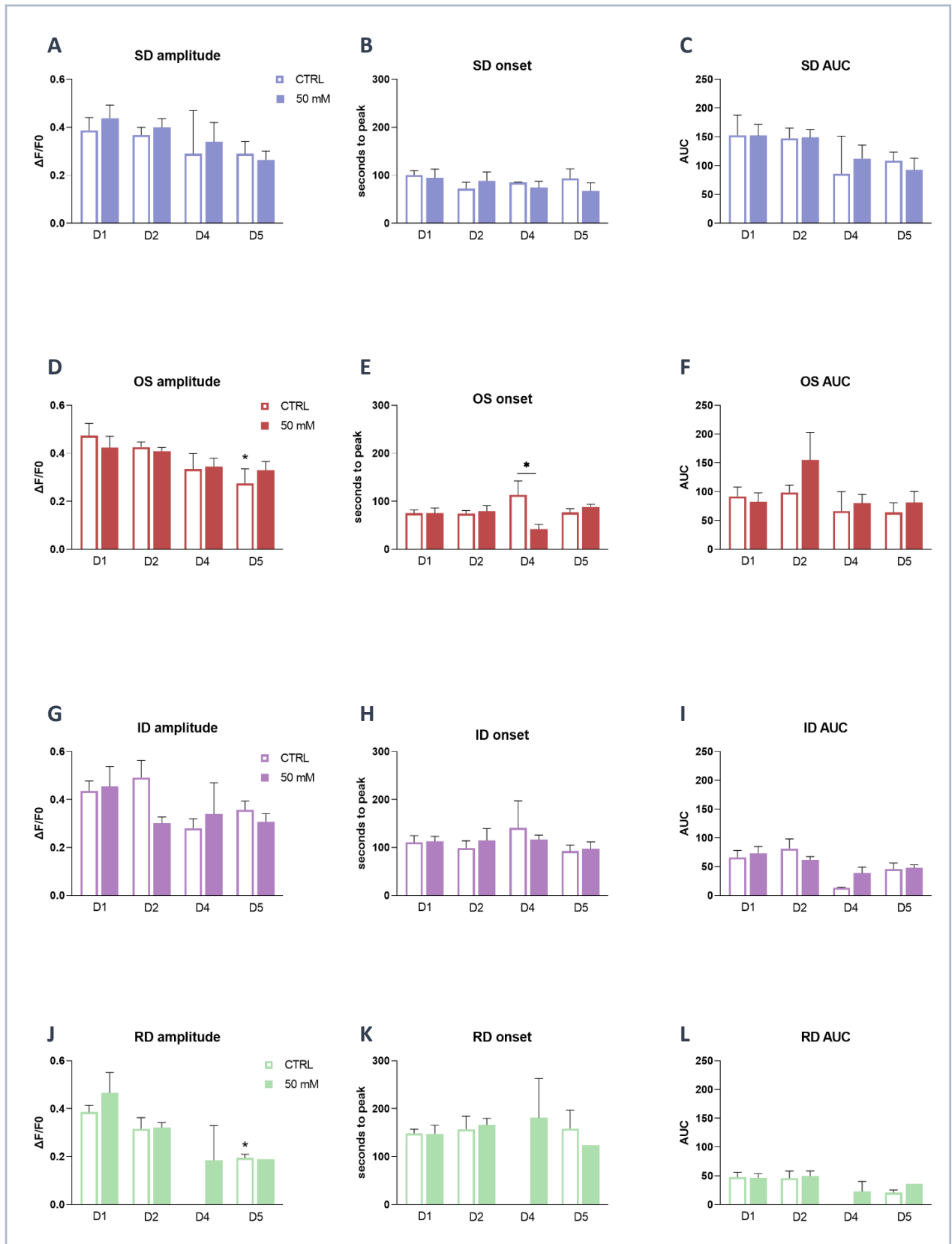
A) Percentage of VTD(-) neurons, CTRL: D1 = 27.5 ± 1.4%, D2 = 28 ± 2.1%, D4 = 26.9 ± 4%, D5 = 26.1 ± 6%; 50mM, D1 = 32.1 ± 1.9%, D2 = 22.7 ± 3.6%, D4 = 35.8 ± 10.5%, D5 = 30.1 ± 4.7%; **B)** Percentage of VTD(+) neurons of the SD profile, CTRL: D1 = 20.1 ± 2.8%, D2 = 24.2 ± 3.5%, D4 = 28.5 ± 2.9%, D5 = 29.7 ± 6.6%; 50mM, D1 = 18.2 ± 2.7%, D2 = 24.8 ± 2.2%, D4 = 22.2 ± 9.4%, D5 = 29 ± 4.2%; **C)** Percentage of VTD(+) neurons of the OS profile, CTRL: D1 = 38.6 ± 2.4%, D2 = 34.2 ± 2.8%, D4 = 40.1 ± 1.6%, D5 = 30.9 ± 5.3%; 50mM, D1 = 35.4 ± 2.3%, D2 = 39.9 ± 3.6%, D4 = 30.1 ± 2.8%, D5 = 29.9 ± 4.1%; **D)** Percentage of VTD(+) neurons of the ID profile, CTRL: D1 = 7.4 ± 1.2%, D2 = 6.8 ± 1.4%, D4 = 4.7 ± 0.5%, D5 = 8.2 ± 3.2%; 50mM, D1 = 7.8 ± 1.1%, D2 = 5.8 ± 1%, D4 = 8.3 ± 2%, D5 = 9 ± 3.3%; **E)** Percentage of VTD(+) neurons of the RD profile, CTRL: D1 = 3.7 ± 0.4%, D2 = 5.6 ± 1.4%, D4 = 0 ± 0%, D5 = 4.8 ± 1.1%; 50mM, D1 = 5 ± 1.1%, D2 = 5.6 ± 0.6%, D4 = 2.9 ± 0.3%, D5 = 1.2 ± 1.2%; Where significance is not denoted, the difference is not significant. One-way ANOVA with multiple comparisons. Mean ± SEM. CTRL = control (open bars); 50mM = hyperglycaemic culture (filled bars); **F)** Intracellular calcium signal trace following stimulation with VTD shaping the responses SD (left) and OS (right), averaged from all SD- or OS-profiled neurons (12 and 19, respectively) from one experiment.; Black – average trace from one experiment; grey – showing the SEM for each second of the recorded trace; black arrows indicate the time point of respective drug application.



Further analysis was performed of the average amplitude, time to peak and area under the curve (AUC) of the VTD responses for each of the four profiles (Figure 4.5). Significantly smaller amplitudes by 1.7-fold were observed in the OS profile in day 5 compared to day 1 of the control (decrease from d1 0.47 ± 0.06 to d5 0.27 ± 0.06 , $p < 0.05$) but not the high glucose population (Figure 4.5. D). Significant amplitude reduction by 2-fold was also evident in the RD profile between control day 1 and control day 5 neurons (decrease from d1 0.39 ± 0.03 to d5 0.2 ± 0.02 , $p < 0.05$) (Figure 4.5. J). Similar amplitude trends were evident in the SD and ID profiles, albeit non-significant (Figure 4.5. A,G). These shifts indicate a possible time-in-culture-dependent effect on the Ca^{2+} signal amplitude in untreated cells. A significantly shorter onset to peak in the OS profile was also observed in day 4 high glucose neurons compared to same day control cells (d4 CTRL = 113.3 ± 29.3 s; d4 50mM = 42.2 ± 9.7 s, $p < 0.05$), although the sample size ($n=2$) is too small for concrete conclusions (Figure 4.5. E). These observations could point towards an effect increasing time in culture exercises on VGSC activation-induced Ca^{2+} signal strength in nociceptors that is attenuated by the presence of high glucose levels.

Taken together, these results indicate no effect of high glucose conditions on the response rates of cultured DRG neurons to nociceptive agonists and the VGSC agonist VTD. However, VTD-response amplitude changes with time in culture were noticed only in the untreated population of neurons, suggesting an effect high glucose conditions on signal amplitudes of nociceptors. Furthermore, time in culture might influence the response rates to some nociceptive agonists (AITC).

Figure 4.5. Analysis of the effect time in culture and hyperglycaemic conditions have on VTD-response parameters. The amplitudes of neurons responding to VTD with the OS and RD profile were significantly smaller on the 5th day in culture in control neurons compared to day 1. **A) SD amplitude.** CTRL: D1 = $0.39 \pm 0.05\%$, D2 = $0.37 \pm 0.03\%$, D4 = $0.29 \pm 0.18\%$, D5 = $0.29 \pm 0.05\%$; 50 mM: D1 = $0.44 \pm 0.05\%$, D2 = $0.4 \pm 0.04\%$, D4 = $0.34 \pm 0.08\%$, D5 = $0.27 \pm 0.04\%$; **B) SD onset time to peak.** CTRL: D1 = $100.5 \pm 9.12\%$, D2 = $72 \pm 13.42\%$, D4 = $84.8 \pm 1\%$, D5 = $93.28 \pm 20.36\%$; 50 mM: D1 = $94.54 \pm 18.42\%$, D2 = $88.08 \pm 18.78\%$, D4 = $74.5 \pm 13.1\%$, D5 = $67 \pm 17.23\%$; **C) SD AUC.** CTRL: D1 = $152.8 \pm 35.29\%$, D2 = $147.4 \pm 17.93\%$, D4 = $86 \pm 65.4\%$, D5 = $108.8 \pm 14.73\%$; 50 mM, D1 = $152.1 \pm 19.79\%$, D2 = $149.2 \pm 13.42\%$, D4 = $112.5 \pm 23.55\%$, D5 = $92.38 \pm 20.71\%$; **D) OS amplitude.** CTRL: D1 = 0.47 ± 0.05 , D2 = 0.43 ± 0.02 , D4 = 0.34 ± 0.07 , D5 = 0.28 ± 0.06 ; 50mM, D1 = 0.42 ± 0.05 , D2 = 0.41 ± 0.01 , D4 = $0.35 \pm 0.04\%$, D5 = $0.33 \pm 0.04\%$; **E) OS onset time to peak.** CTRL: D1 = $74.78 \pm 7.16\%$, D2 = $74.44 \pm 6.28\%$, D4 = $113.3 \pm 29.25\%$, D5 = $76.58 \pm 8.07\%$; 50 mM: D1 = $74.96 \pm 10.92\%$, D2 = $79.4 \pm 11.8\%$, D4 = $42.15 \pm 9.65\%$, D5 = $88.33 \pm 5.42\%$; **F) OS AUC.** CTRL: D1 = $92 \pm 15.94\%$, D2 = $98.64 \pm 12.71\%$, D4 = $66.35 \pm 33.85\%$, D5 = $63.88 \pm 17.07\%$; 50 mM: D1 = $81.88 \pm 16.03\%$, D2 = $155 \pm 48.06\%$, D4 = $79.85 \pm 15.45\%$, D5 = $81.53 \pm 19.05\%$; **G) ID amplitude.** CTRL: D1 = $0.44 \pm 0.04\%$, D2 = $0.49 \pm 0.07\%$, D4 = $0.28 \pm 0.04\%$, D5 = $0.36 \pm 0.04\%$; 50 mM, CTRL: D1 = $0.45 \pm 0.08\%$, D2 = $0.3 \pm 0.03\%$, D4 = $0.34 \pm 0.13\%$, D5 = $0.31 \pm 0.03\%$; **H) ID onset time to peak.** CTRL: D1 = $110.7 \pm 14.01\%$, D2 = $98.62 \pm 15.14\%$, D4 = $141.2 \pm 55.85\%$, D5 = $92.4 \pm 12.81\%$; 50 mM: D1 = $112.7 \pm 10.32\%$, D2 = $114.7 \pm 24.73\%$, D4 = $116.1 \pm 9.7\%$, D5 = $97.3 \pm 14.24\%$; **I) ID AUC.** CTRL: D1 = $66.16 \pm 11.99\%$, D2 = $81.58 \pm 16.68\%$, D4 = $13.45 \pm 0.95\%$, D5 = $45.65 \pm 10.64\%$; 50 mM: D1 = $73.46 \pm 11.53\%$, D2 = $61.76 \pm 5.87\%$, D4 = $38.65 \pm 10.65\%$, D5 = $48.1 \pm 4.92\%$; **J) RD amplitude.** CTRL: D1 = 0.39 ± 0.03 , D2 = 0.32 ± 0.05 , D4 = no RD neurons recorded, D5 = 0.2 ± 0.02 ; 50mM, D1 = 0.47 ± 0.08 , D2 = 0.32 ± 0.02 , D4 = 0.19 ± 0.15 , D5 = 0.19 . **K) RD onset time to peak.** CTRL: D1 = $148.7 \pm 8.49\%$, D2 = $157 \pm 27.32\%$, D4 = no RD neurons recorded, D5 = $158.7 \pm 38.49\%$; 50 mM: D1 = $147.4 \pm 18.58\%$, D2 = $166.3 \pm 13.52\%$, D4 = $180.8 \pm 82.25\%$, D5 = $123.3 \pm 0\%$; **L) RD AUC.** CTRL: D1 = $47.72 \pm 8.51\%$, D2 = $45.98 \pm 12.31\%$, D4 = no RD neurons recorded, D5 = $20.83 \pm 4.73\%$; 50 mM: D1 = $46.3 \pm 7.79\%$, D2 = $49.74 \pm 8.64\%$, D4 = $22.55 \pm 17.85\%$, D5 = $36.1 \pm 0\%$. * = significance compared to D1 CTRL, * $p < 0.05$. Where significance is not denoted, the difference is not significant. One-way ANOVA with multiple comparisons. Mean \pm SEM. CTRL = control (open bars); 50mM = hyperglycaemic culture (filled bars); D# = day #.



4.5. DISCUSSION

In this chapter, I outlined physiological experiments with DRG neurons under *in vitro* hyperglycaemic conditions. Cells cultured in a high glucose environment over 1, 2, 4 or 5 days showed no significant changes in their excitability, nociceptor sensitivity or VTD-induced Ca^{2+} response parameters compared to control. However, a decrease in the response rate to AITC was noted in both treated and untreated neurons as time in culture increased. Furthermore, we observed decreasing amplitude of the Ca^{2+} signal in response to VTD with time in culture in control but not in hyperglycaemic neurons, indicating possible extended effect of high glucose conditions on VGSC excitability.

In vitro hyperglycaemia has been routinely used to investigate changes in excitability of DRG, however predominantly only for short-term exposure. Previous research employing short-term *in vitro* hyperglycaemia has found that high glucose levels cause an increase in TRPV1 expression and currents in DRG neurons^{506,510} as well as changes in VGSCs, including increased TTX-R current density^{424,502} and increased $\text{Na}_v1.7$ expression³⁵¹. Based on them, we expected that by inducing hyperglycaemia *in vitro* for short (1-2 days) and long-term (4-5 days) we will be able to detect changes in the VGSC and nociceptors excitability by Ca^{2+} imaging responses to different agonists. Here, *in vitro* induced hyperglycaemia did not produce the expected effects on DRG neurons excitability. However, there were differences in several values which were all associated with the time neurons had spent in culture. These findings can be summarised in the following:

- Decrease in the response rate to AITC in both high glucose-treated and control populations (Figure 4.3)
- Decrease in the VTD-induced Ca^{2+} response amplitudes of the OS and RD profiles in the control population, but not the high-glucose population of cells (Figure 4.5 D, J)

These observations are informative of possible changes in neuronal electrophysiology after maintaining neurons in culture for up to 6 days, with or without altered extracellular glucose conditions. On the other hand, these findings might be a product of the specifics of the particular protocol for culture conditions used (discussed in more detail in Chapter 6).

Neuronal dissociation and axotomy during the culturing process is injurious to neurons and has been well-documented to cause hyperexcitability in small DRG neurons via reducing AP threshold and increasing the AP duration and firing frequency⁵¹¹⁻⁵¹³. Furthermore, the electrophysiological properties of acutely dissociated neurons are different from neurons cultured for 1+ days, with VGSC (such as $\text{Nav}1.8$) and VGCC expression and current density

decreasing with time^{102,511,514}. The gradual decrease in neuronal excitability with time spent in culture could indicate neurons ‘settling’ and ‘healing’ after their excitability was increased immediately after dissociation due to its injurious nature⁵¹⁵. Here, the decreases in VTD-response amplitude in nociceptors (OS) (Figure 4.5 D) were focused in the control population, whereas the high glucose group of neurons was not affected. The lack of significant decrease in nociceptive excitability in the hyperglycaemic population suggests that the high glucose environment could be preventing DRG neurons from bringing excitability down to normal physiological levels and thus “healing”. Therefore, hyperglycaemia might render restoring normal neuronal physiology post-injury slower and more difficult. In an *in vivo* setting, wound healing has been well-documented to be delayed in diabetic rodents^{516–518} and in diabetes patients⁵¹⁹ and so it is a possibility that a similar delay may occur also to neurons healing from damage during diabetes. The slower decrease of neuronal hyperexcitability post-dissociation might translate into prolonged pain sensation post-injury caused by diabetes. Currently, no clinical studies have explored this idea specifically, however DN patients are known to present with exaggerated pain responses to harmless or mild painful stimuli (allodynia and hyperalgesia, respectively)^{234,356,520}, which could support the concept of persistent and/or exaggerated wound-induced pain in diabetes patients. In any event, these results can serve as a caution for the interpretation of Ca²⁺ imaging data using ion channel agonists when recording responses from primary DRG neuron cultures over time.

Increased activity of nociceptive ion channels, such as TRPV1, TRPA1 and P₂X₃ has also been reported in DRG neurons during diabetes^{58,343,521–523}. Here, short- and long-term exposure to high glucose conditions did not induce any significant changes in the response rates to the nociceptive agonists to these three receptors. Our results directly contradict two studies from 2018 reporting increased responses to CAP in DRG neurons cultured under high glucose conditions^{506,510}. Lam et al.⁵⁰⁶ report a significantly increased response rate to CAP in adult mouse DRG neurons cultured in high glucose conditions (25mM) glucose for 7 days. A possible reason for this discrepancy might be their choice of control and hyperglycaemic glucose concentrations of 5mM and 25mM, respectively. These are not comparable to the concentrations used in the experiments from this chapter, or the ones used in the majority of *in vitro* hyperglycaemia studies on DRG neurons^{318,423,500}. An extracellular glucose concentration of 25mM can be considered within the optimal range for neuronal survival in culture, whereas a concentration of 5mM has been demonstrated to lead to neuronal apoptosis and cellular damage⁴²³. Therefore, the higher rates of CAP responses observed by Lam et al. are likely to represent the normal neuronal function, whereas the lower values seen in the control population are likely to be indicative of a hypoglycemic effect on CAP responses. Yet,

in direct contrast to the observations by Lam et al., others, employing the same experimental glucose conditions and exposure time as them, have observed a decrease in CAP-induced Ca^{2+} influx in mature DRG neurons⁵²⁴. The second study reporting increased CAP-evoked Ca^{2+} responses is by Bestall et al. (2018) who cultured DRG from naïve adult male rats in 50 mM glucose for 24 hours. Their study is the closest to ours in experimental design, yet we report conflicting results. A possible reason for the inconsistency could be due to a species difference (rat vs mouse) and/or the fact that relatively specific DRG were isolated (T1-L5), whereas, here, all DRG were isolated for experiments indiscriminately. Finally, another *in vitro* study using 50B11 immortalised rat DRG neuronal cell line reported an increase in responses to AITC when neurons were cultured in 66 mM glucose⁵²⁵. Albeit overlapping with observations *in vivo*^{343,344}, these *in vitro* results directly contradict ours, perhaps because of the different *in vitro* culture models utilised. An immortalised DRG neuronal cell line would not possess the complete arsenal of ion channel, receptors, exchangers and proteins contributing to shaping the net response to an agonist and therefore might not necessarily generate a complete picture of the final response. Therefore, the cell line may not be representative of the same populations of neurons with decreasing sensitivity to AITC. It is, thus, yet to be confirmed whether prolonged exposure to hyperglycaemic conditions *in vitro* is a suitable method for determining functional changes in nociceptive ion channels.

Neither short- nor long-term exposure to a hyperglycaemic extracellular environment affected the VGSC excitability of DRG neurons in my experiments. A literature search found very little on the question of prolonged exposure of DRG neurons to high levels of glucose *in vitro* (40-60 mM)) and the effect on VGSCs. A number of prior studies have noted an increase in the VGSC activity through increased levels of Nav1.7 expression³⁵¹ or increased density of TTX-R currents^{349,502} of DRG neurons cultured in up to 60mM glucose for 18-24h. This corresponds to day 1 in my experiments, where no significant increase in VTD(+) cells and thus, in contrast to previous studies, no increase in overall VGSC activity was observed. There are a couple of possible explanations why these data differ. First, the studies reporting increase in VGSC activity derived their neurons from rats as opposed to the mouse neurons used here, which might account for potential interspecies differences in VGSC excitability during hyperglycaemia. However, to the best of our knowledge, there are currently no studies in literature comparing VGSC expression levels and activity between mice and rats and the VTD- Ca^{2+} imaging assay has yet to be validated in another rodent species. Second, only one study used DRG neurons from a mature rodent⁵⁰² like ours, however, only small (20-25 μm) L4-L5 DRG were selected for experiments. This, combined with the species difference (rat vs mouse here) and the very low control glucose conditions (5.5 mM) could contribute to the differences

in results reported by them and here. All other studies used embryonic DRG neuron cultures as opposed to the adult DRG neurons used here. Embryonic DRG neurons require supplementation with NGF to support neuronal survival in culture. NGF is known to alter electrophysiological properties of cultured DRG neurons⁵²⁶⁻⁵³⁰. It has also been widely implicated as a key driver of hyperalgesia during DN, with its expression levels significantly increased in DRG^{456,531}. NGF is also demonstrated to sensitise TRPV1 and increase DRG responses to capsaicin^{532,533}. Although the mechanisms of elevated NGF expression during diabetes are still unclear, it has been postulated that a hyperglycaemic environment is a trigger for increased NGF expression as a protective mechanism of tissues⁴⁵⁶. Therefore, the combination of supplemented NGF and high glucose to embryonic neurons in culture might produce a stronger hyperexcitability phenotype represented by increased VGSC activity compared to mature DRG neurons cultured in high glucose in the absence of NGF. Due to its role in DN hyperalgesia, addition of NGF to a hyperglycaemic culture could in fact be a sensible approach to recreating a physiological DN environment in a DRG culture. This and additional culture modifications to replicate DN more closely are discussed in more detail in Chapter 6 along with further limitations of the current experiment and future directions.

Taken together, the results from the *in vitro*-induced hyperglycaemia experiments are somewhat informative of events in the DRG culture when maintained for a prolonged time. Furthermore, our observation point to subtle changes hyperglycaemia might cause in VGSC excitability over extended exposure by maintaining neuronal excitability elevated after dissociation. Nevertheless, these experiments did not produce the expected, clear-cut overall increase in neuronal excitability after short- and long-term exposure to high glucose, seen in similar studies. The most likely reason for this outcome is the limited DN environment that we can be recreated in a dish which might not suffice to produce a phenotype strong enough to be detected by Ca²⁺ imaging with VTD and nociceptive agonists in our protocol. The multifactorial complexity of DN, especially T2DN, would require an individual extensive study of its own to extrapolate its components and optimise an *in vitro* T2DN model. Due to project time restrictions, it was decided to circumvent this lengthy process and opt for proceeding with investigating changes in excitability of DRG neurons derived from an *in vivo* model of diabetic neuropathy.

CHAPTER 5

ASSESSING EXCITABILITY CHANGES IN DRG NEURONS FROM DIABETIC DB/DB MICE

CHAPTER 5: ASSESSING THE EXCITABILITY CHANGES IN DRG NEURONS FROM DIABETIC *DB/DB* MICE

5.1. INTRODUCTION

The last chapter described experiments with DRG neurons under *in vitro*-induced high glucose conditions. Using an *in vitro* hyperglycaemia model to detect DRG excitability changes serves as a more ethical alternative to deriving neurons from diabetic animals. In addition, it reduces potential variability between controls and treated cells as both are isolated from the same animal as opposed to deriving diabetic cells from a diabetic animal and control cells from a healthy one. It also allows for the precise control of external glucose concentration, which varies in mouse models of diabetes and DN^{419,534}. However, inducing hyperglycaemia *in vitro* represents only one, albeit main key drivers of DN pathogenesis– the high glucose levels. Furthermore, it is closer to reflecting T1DN rather than T2DN, as T2DN is driven by additional mechanisms such as aspects of the metabolic syndrome (insulin resistance, dyslipidaemia), together with hyperglycaemia. The many subcomponents and high complexity of T2DN pathogenesis renders it extremely difficult to model *in vitro* with high accuracy⁴¹⁹. Therefore, to ensure all components of T2DN were in place, the second hyperglycaemia model I used was the T2D C57BL/*Ksdb/db* mouse model.

The C57BL/*Ksdb/db* (just *db/db* hereon) mouse is an excellent T2D model and, based on the established DN model requirements⁴⁴⁸, is recognised as one of the most robust existing models of DN⁴⁵³. Its diabetic phenotype was first discovered in 1966 by Hummel et al.⁵³⁵. It wasn't until 1995, however, that its genetic mutation was identified^{536,537}. The *db/db* mouse is a homozygous mutant knockout for the leptin receptor. Leptin is a hormone secreted by adipose cells and enterocytes in the small intestine after food intake. It controls appetite by binding to its receptor in the hypothalamus and inhibiting hunger and feeding behaviour (hence often referred to as the 'satiety hormone')^{446,536}. The *db/db* mouse carries a deletion mutation in the gene encoding the leptin receptor, resulting in leptin signalling deficiency^{536,538}. Eliminating leptin signalling leads to the mice exhibiting uncontrolled overeating behaviour (hyperphagia) simultaneous with decreased activity and thus energy expenditure. Blood insulin levels begin elevating at 10-14 days of age (DoA) followed by elevation in fasting blood glucose levels and dyslipidaemia (Figure 5.1). At 3-4 weeks of age (WoA), obesity and insulin resistance have developed and the phenotype culminates into T2D for the rest of the mouse's lifespan (Figure 5.2)⁵³⁹. The severity of the genetically induced disease causes continuous uncontrolled rise in blood glucose levels⁴²⁸ and, at later stages, critical depletion of the insulin-

secreting pancreatic β -cells⁵⁴⁰. This, in combination with the secondary derangements brought about by obesity, it leads to death by 10 months of age⁵⁴¹.

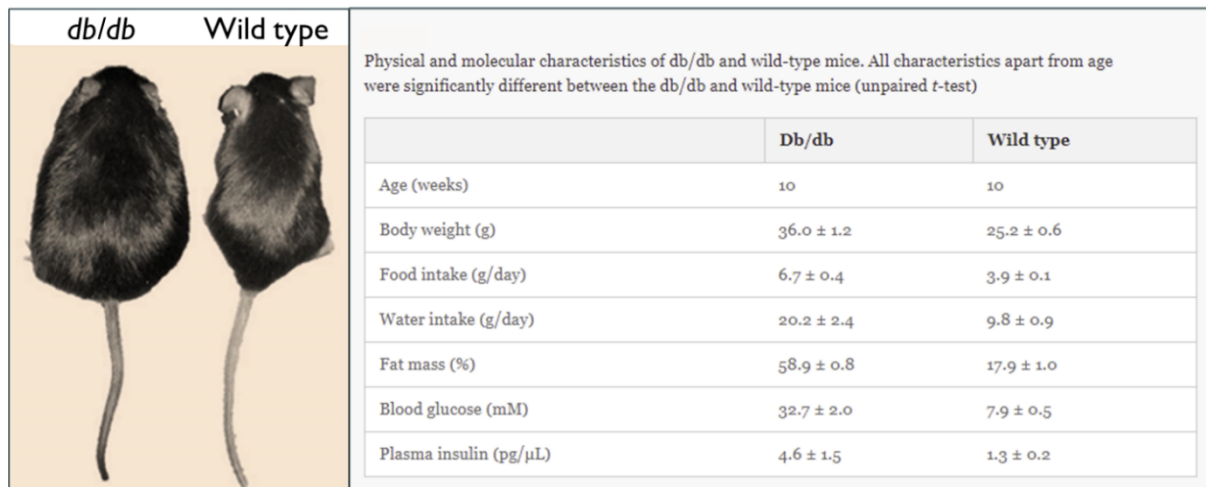


Figure 5.1. An excerpt from a paper by Guest and Rahmoune (2018) characterising the diabetic phenotype of a 10-week-old db/db mouse and comparing parameters to a wild type mouse. Source:⁵⁰⁴.

Around 8 WoA, db/db mice develop DN⁴³¹. Robertson & Sima were the first to describe the electrophysiological and morphometric changes in the nerves of db/db mice and were the first to provide a detailed characterisation of the DN phenotype in this model^{428,542}. Their research revealed the key observation that DN progression in the db/db mouse mimics closely the phases in human patients.

The early phase of DN in db/db mice develops at 8–12 WoA and is called ‘metabolic’ (MET). It was characterised by severe motor (MNCV) and milder sensory (SNCV) nerve conduction velocity impairments as well as mild axonal atrophy in both myelinated and unmyelinated fibres (Sima and Robertson, 1978; Norido *et al.*, 1984). The MET phase was later further defined behaviourally with the presence of mechanical allodynia, hyperalgesia^{456,461,507,543–546} and heat hypersensitivity^{547,548}, albeit the literature is highly controversial (see figure 5.1, Metabolic phase). In addition, a MET phase characteristic is that functional and structural deficiencies are generally reversible with metabolic interventions (usually, through glycaemic control with insulin administration)⁴²⁹.

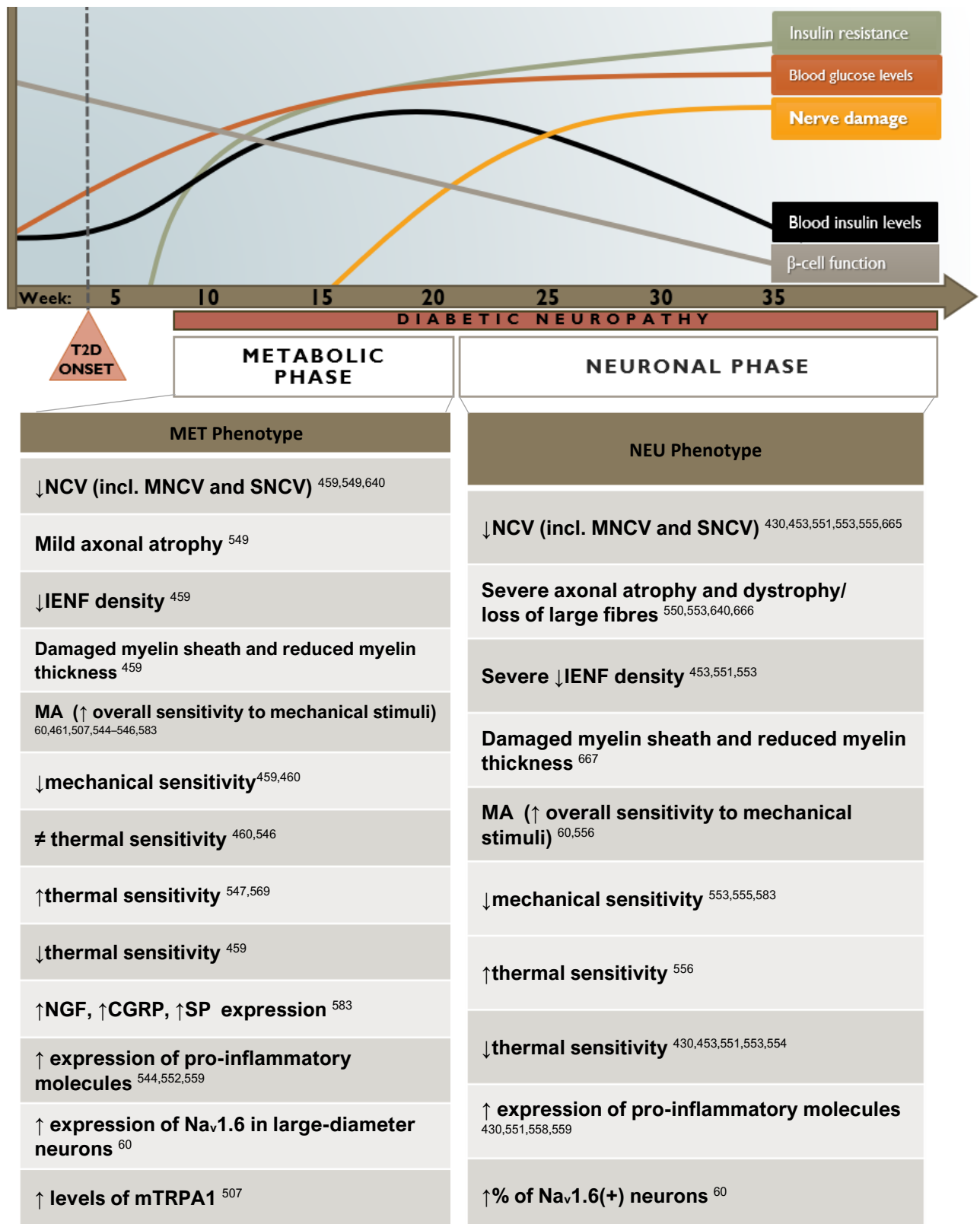


Figure 5.2. A comprehensive summary of the available molecular, physiological, behavioural and transcriptomic research on the db/db mouse model with observations categorised according to diabetic neuropathy phases observed by Sima and Robertson (1978). MA, mechanical allodynia; IENF, intraepidermal nerve fiber; NCV, nerve conduction velocity; MNCV, motor nerve conduction velocity; SNCV, sensory nerve conduction velocity; ↑ denotes an increase, while ↓ denotes a decrease Figure adapted to the db/db mouse from

<https://www.sciencedirect.com/science/article/abs/pii/S0095454305701305?via%3Dihub>

The late, 'neuronal' phase (NEU) in *db/db* mice develops from ~20 WoA and continues until the end of the mouse's life. It is characterised in the *db/db* mouse with an exacerbated MET phase phenotype of axonopathy and impaired MNCV and SNCV alongside with marked decrease of IENF density as well as loss of myelin sheathing^{428,429,453,549–553}. Most studies agree on the presence of structural nerve damage but still report contradicting behavioural findings (see figure 5.1, Neuronal phase). For example, 20+ week old *db/db* mice have been reported to present with increased mechanical and thermal sensory thresholds and hypoalgesia by some^{337,430,453,458,552–555}, however others have observed increased sensitivity to mechanical stimuli and mechanical allodynia^{544,556}.

Additionally, several microarray and RNA-Seq analyses have shown an upregulation of immune and inflammatory molecules and pathways^{430,552,557–559} in the peripheral nerves of *db/db* mice to begin as early as 8 WoA and continue throughout the rest of the DN progression contributing towards peripheral nerve fibre degeneration, as well as pain behaviour in the early stages of DN⁴⁵⁶. Finally, studies investigating the function, molecular mechanisms and expression levels of ion channels during DN in this mouse model are scarce. One study reported sustained increased expression levels of the large diameter neurons-associated VGSC Na_v1.6 in DRG of *db/db* mice from 8 WoA up until 20 WoA (end of experimental period) which was correlated to mechanical allodynia in these mice⁶⁰. More recently, Wang et al. (2018) reported no increase in total protein expression of either TRPA1 or TRPV1. However, membrane-associated TRPA1, but not TRPV1, expression was increased and activity upregulated in *db/db* mice (6-7 WoA), further linked to impaired AMPK signalling and mechanical allodynia⁵⁰⁷.

The abundance of behavioural, morphometric, and transcriptomic studies as well as the limited molecular research, has highlighted some key phenomena likely to underlie observed T2DN-associated behaviours in the *db/db* mouse, however there is no conclusive evidence on the pathophysiology of the pain during the progression of DN in T2D. Furthermore, the T1D STZ rodent is by far the most widely studied DN model, generating an imbalance in research between animal studies and clinical trials, which are largely targeting the T2D population of patients^{241,418}. This demands more intensive research into the mechanisms driving T2DN. Finally, to the best of our knowledge, there are no physiological studies investigating the functional changes in *db/db* mouse DRG neurons during the MET and NEU phases of DN. Based on the above rationale, and on the established robustness of its DN phenotype, the T2D *db/db* mouse was selected as a model of DN for these experiments.

5.2. AIMS

To assess the excitability changes and changes in size distribution in specific subpopulations of DRG neurons from C57BKS*db/db* (*db/db*) mice, isolated at two different time points: 1) early (metabolic, MET) and 2) late (neuronal, NEU) stages of diabetic neuropathy by analysing the Ca^{2+} signals generated in response to the VGSC agonist VTD and nociceptive agonists ATP, AITC and CAP.

To compare excitability changes between the MET and NEU phases of DN in this mouse model in order to track the progression of diabetic neuropathy and its effect on DRG physiology.

5.3. METHODS

5.3.1. DRG neuron culture from *db/db* mice

DRG neurons were collected from *db/db* (BKS.Cg-+Leprdb/+Leprdb/OlaHsd) mice at 8 -12 weeks of age (WoA) (metabolic phase) and 22 - 28 WoA (neuronal phase) as well as from lean, DN phase-matched control mice (BKS.Cg-+Leprdb/-Leprdb/OlaHsd). Neurons were cultured in standard DMEM medium and left to incubate for at least 24 hours before experiments.

5.3.2. Calcium imaging

DRG neurons were loaded with Fura-2 and responses recorded to nociceptive agonists: capsaicin (CAP, 200 nM), allyl isothiocyanate (AITC, 100 μ M) and α,β -methylene ATP (ATP, 1 μ M) as well as VGSC potentiator veratridine (VTD, 30 μ M). Standard calcium imaging protocol was followed as outlined in Chapter 2: Materials & Methods section 2.2.2., page 68.

5.4. RESULTS

5.4.1. The number of DRG neurons derived from *db/db* mice for each phase and condition

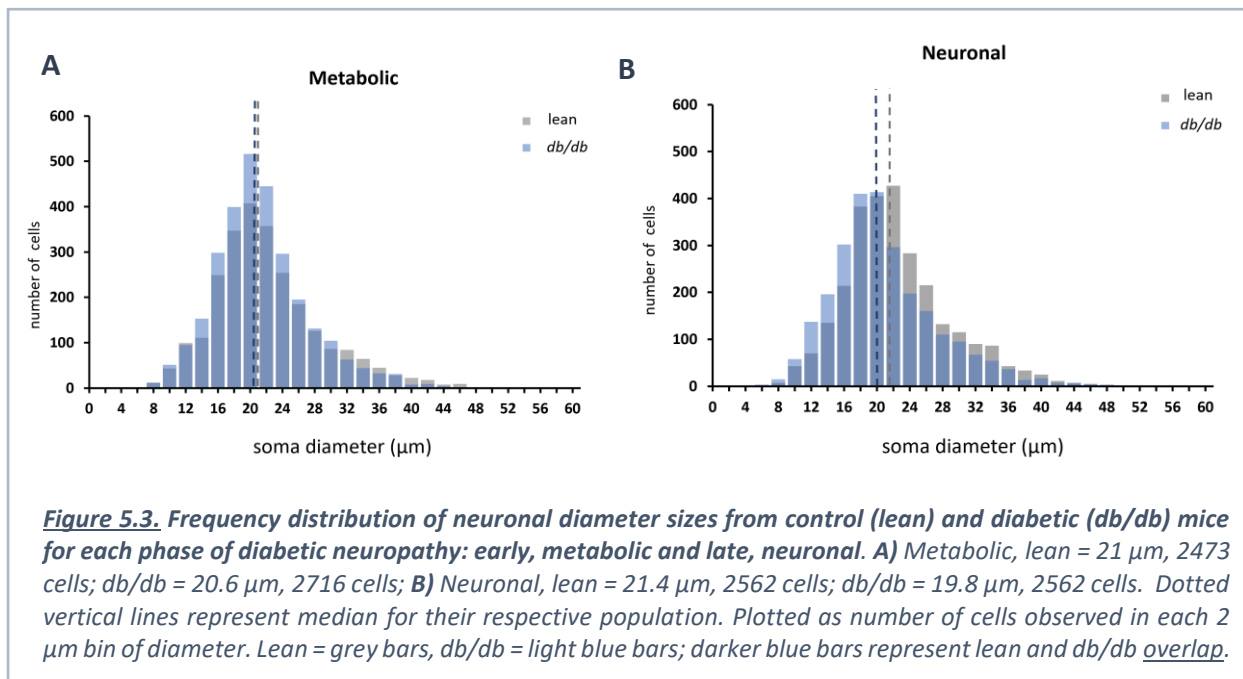
For the following experiments, 24 mice in total were sacrificed (6 MET CTRL, 6 NEU CTRL, 6 MET *db/db* and 6 NEU *db/db*). The total number of neurons imaged for each group is presented in table 5.1. The number of neurons used for these experiments from N5 and N6 in each phase and condition is generally smaller due to a diversion of some of the cells from these cultures to another set of experiments (not described in this thesis). Overall, the total numbers of neurons imaged for each phase of each condition were comparable.

Table 5.1 Number of neurons for each mouse (N) of each phase (MET or NEU) for each condition (CTRL or *db/db*). Each cell with cell count represents one mouse's total cell yield. Twenty-four mice were used in total. MET = metabolic phase; NEU = Neuronal phase; CTRL = control (lean);

| phase & condition Mouse | MET CTRL | NEU CTRL | MET <i>db/db</i> | NEU <i>db/db</i> |
|----------------------------|----------|----------|------------------|------------------|
| N1 | 496 | 425 | 521 | 409 |
| N2 | 441 | 597 | 521 | 509 |
| N3 | 267 | 326 | 610 | 384 |
| N4 | 366 | 336 | 327 | 616 |
| N5 | 270 | 463 | 338 | 374 |
| N6 | 367 | 415 | 399 | 270 |
| Total: | 2473 | 2562 | 2716 | 2562 |

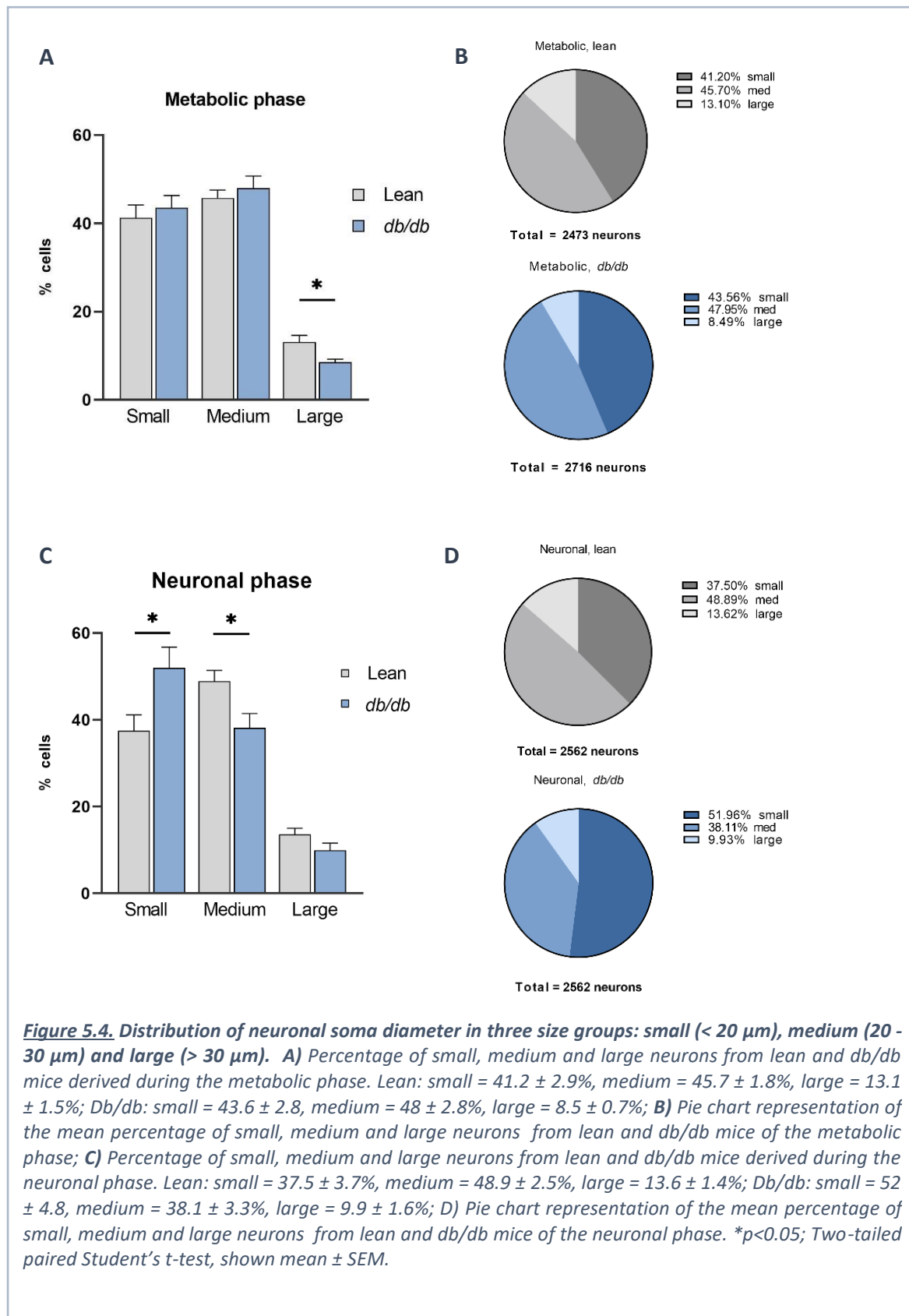
5.4.2. The overall cell size distribution is shifted towards smaller cells in DRG from *db/db* mice

The soma diameters of the DRG neurons from *db/db* and phase-matched lean control mice used for the experiments presented here were measured. Neurons from each condition group (*db/db* or lean) and phase (MET or NEU) were pooled for soma diameter analysis. Frequency distribution analysis of DRG sizes for each DN phase was performed and plotted as a histogram (Figure 5.3). In the MET phase, the median cell diameter was slightly smaller in *db/db* than in lean mice (lean = 21 μm , 2473 cells; *db/db* = 20.6 μm , 2716 cells) (Figure 5.3A). In the NEU phase, the mean cell diameter of DRG from *db/db* mice was still smaller than lean (lean = 21.4 μm , 2562 cells; *db/db* = 19.8 μm , 2562 cells), however here, the distribution of the diabetic DRG is shifted to the left (Figure 5.3B).



Neurons were classified according to their soma diameter into three categories: small- (<20 μm), medium- (20-30 μm) and large (>30 μm), consistent with diameter range groupings commonly used in other studies^{560,561} (Figure 5.4). During the MET phase, the percentage of large cells in *db/db* mice was significantly lower than that of lean cells by ~35% (lean = $13.1 \pm 1.5\%$, *db/db* = $8.5 \pm 0.7\%$; $p < 0.05$, $n = 6$ each) (Figure 5.4 A,B). The vast majority of neurons in both lean and *db/db* mice were small and medium-sized, however, there was no significant difference in the percentage of small and medium-sized cells between lean and diabetic mice in the MET phase. In the NEU phase, 52% of *db/db* DRG neurons fell in the small-sized group, compared to 37.5% of lean neurons ($n = 6$ mice from each group, $p < 0.05$) (Figure 5.4 C,D). The increased number of small-diameter cells in diabetic mice was matched by the significantly fewer medium-sized cells compared to lean (38% vs 49%, respectively, $n = 6$ each, $p < 0.05$). There was no significant difference observed in the large-sized DRG group.

Collectively, the results from both DN phases point to a shift in the size distribution of diabetic cells towards smaller-diameter and away from medium and large-diameter neurons that starts during early and progresses through late DN stages.



5.4.3. Persistent increase in the sensitivity to capsaicin in small DRG neurons from *db/db* mice

We wanted to assess DRG neurons from *db/db* mice for excitability changes in the context of nociception. To this end, we applied ATP, AITC and CAP. Each cell can respond to only one of the agonists, to a combination of any two (ATP/CAP+, ATP/AITC+ or AITC/CAP+), to all three together (all(+)) or none of them (agonist (-), or non-nociceptors). To identify if any of these specific populations is affected, we dissected the responses to the three nociceptive agonists into all 8 possible response combinations. Diabetes caused an increase of 1.8-fold in the number of neurons responding to all three agonists simultaneously (all(+)) (from $3.3 \pm 0.7\%$ to $6.1 \pm 0.9\%$, $p < 0.05$) in the MET phase (Figure 5.5A). The increase in this subpopulation, together with the non-significant increases in the rest of the CAP(+) subpopulations (Figure 5.5A), lead to a 1.2-fold increase in the percentage of total CAP(+) DRG neurons in *db/db* mice (Figure 5.5C) (from $28.4 \pm 1.8\%$ to $34.2 \pm 1.7\%$, $p < 0.05$). The total percentages of agonist(-), ATP(+) and AITC(+) *db/db* cells remained comparable to control levels (Figure 5.5C). The results from this phase indicate an early on increase in the sensitivity of DRG neurons to capsaicin, mainly occurring in one subpopulation of neurons (all(+)).

Likewise, in the NEU phase, the percentage of all(+) cells remained significantly higher than lean controls (1.9-fold, from $1.4 \pm 0.2\%$ to $2.7 \pm 0.5\%$, $p < 0.05$) (Figure 5.5B). Here, the percentage of neurons responding to CAP-only as well as ATP and CAP together (ATP/CAP) was significantly higher in *db/db* mice by 1.5-fold (from $10.2 \pm 0.9\%$ to $15.3 \pm 1.1\%$, $p < 0.005$) and 4-fold (from $0.4 \pm 0.1\%$ to $1.6\% \pm 0.4\%$, $p < 0.05$), respectively (Figure 5.5B). These rises were at the expense of cells responsive to AITC-only, the percentage of which decreased by 1.3-fold (from $35.7 \pm 1.1\%$ to $24.8 \pm 1.5\%$ $p < 0.01$). The changes in response rates within each of these individual nociceptive subpopulations brought about a significant 1.3-fold increase in the total response rates to CAP (from $31.3 \pm 1.2\%$ to $40.7 \pm 2.5\%$ $p < 0.001$) and 1.1-fold decrease in total percentage of AITC(+) DRG neurons (from $57.1 \pm 0.6\%$ to $51.3 \pm 2.1\%$, $p < 0.05$) (Figure 5.5D). These findings point to an ever persisting and increasing sensitivity of DRG neurons to CAP in the NEU phase, which seems to have spread to affect more subpopulations of neurons, coupled with a decreased sensitivity to AITC.

To further characterise the additional CAP(+) neurons in each phase, the size distribution of CAP(+) DRG neurons from *db/db* and lean mice was analysed. In the MET phase, the medians of lean and *db/db* neuron sizes were $18.8 \mu\text{m}$ ($n = 661$ cells) and $19.6 \mu\text{m}$ ($n = 928$ cells), respectively (Figure 5.6 A). The additional CAP(+) neurons in the *db/db* mice fell in the 14-26 μm diameter range (figure 5.6 A).

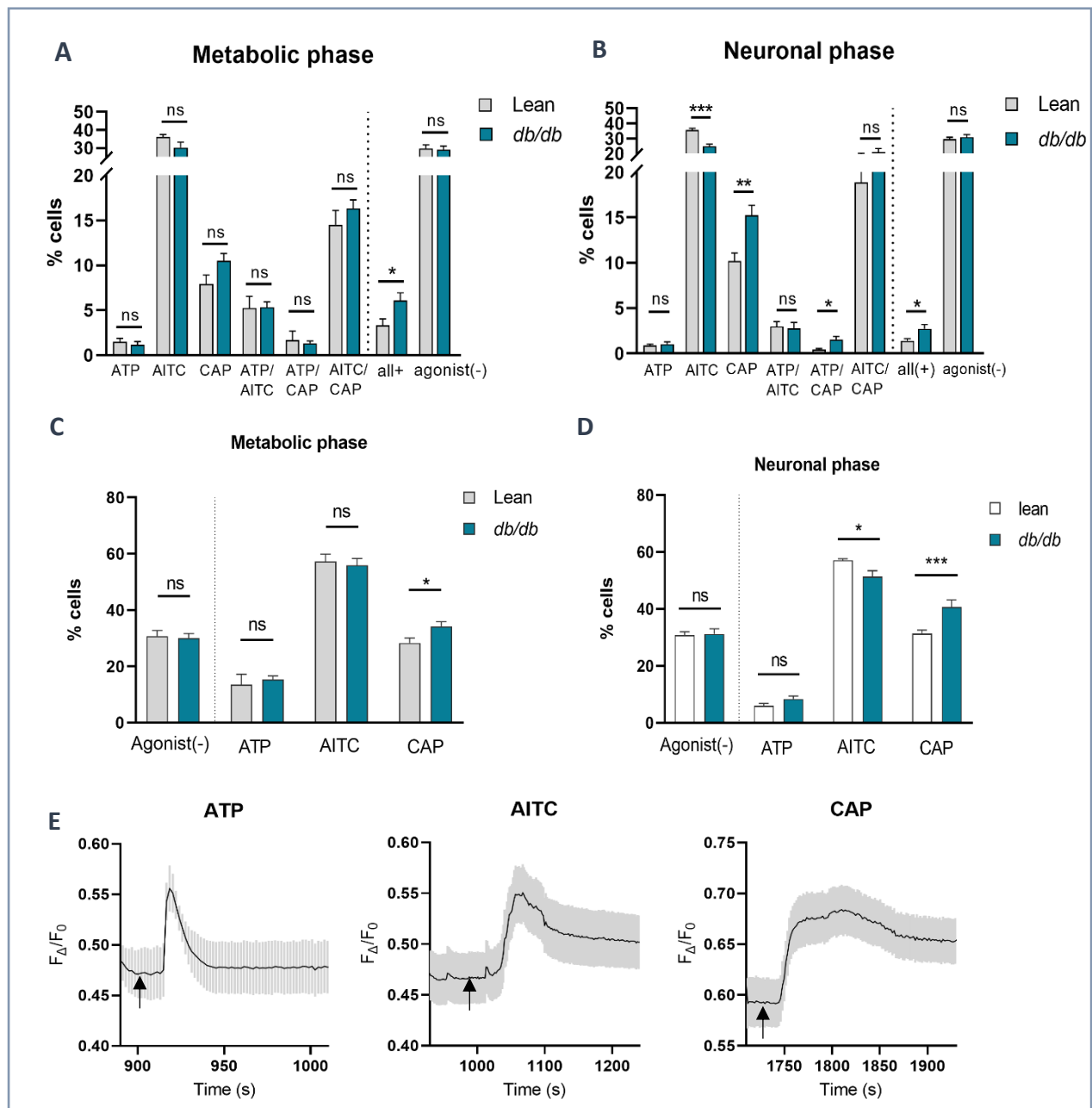
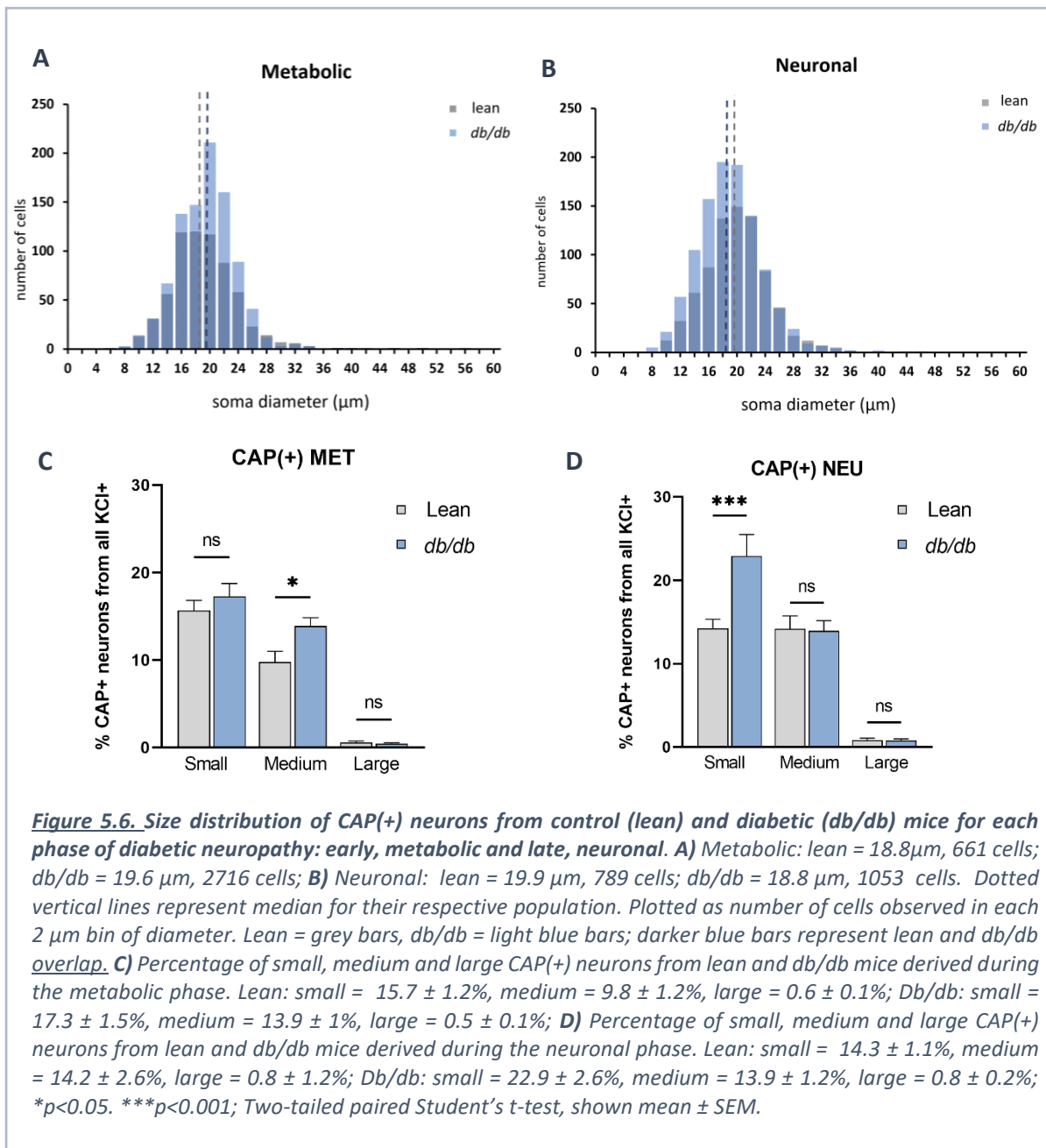


Figure 5.5. The percentage of lean and db/db-derived neurons responsive to nociceptive agonists in each phase of diabetic neuropathy. **A, B**) Percentage of neurons responsive to each nociceptive agonist individually (ATP, AITC, CAP), in combination with another (ATP/AITC, ATP/CAP, AITC/CAP), all together (all(+)) or none (agonist(-)) during the metabolic and neuronal phases. **A)** Metabolic, lean: ATP = $1.5 \pm 0.4\%$, AITC = $36.1 \pm 1.4\%$, CAP = $7.9 \pm 1\%$, ATP/AITC = $5.3 \pm 1.3\%$, ATP/CAP = $1.7 \pm 1\%$, AITC/CAP = $14.5 \pm 1.6\%$, all(+) = $3.3 \pm 0.7\%$, agonist(-) = $29.8 \pm 1.9\%$; Metabolic, db/db: ATP = $1.2 \pm 0.4\%$, AITC = $30.3 \pm 2.9\%$, CAP = $10.5 \pm 0.8\%$, ATP/AITC = $5.4 \pm 0.6\%$, ATP/CAP = $1.3 \pm 0.3\%$, AITC/CAP = $16.4 \pm 0.9\%$, all(+) = $6.1 \pm 0.9\%$, agonist(-) = $29 \pm 2\%$. **B)** Neuronal, lean: ATP = $0.9 \pm 0.2\%$, AITC = $35.7 \pm 1.1\%$, CAP = $10.2 \pm 0.9\%$, ATP/AITC = $3 \pm 0.5\%$, ATP/CAP = $0.4 \pm 0.1\%$, AITC/CAP = $18.9 \pm 1.3\%$, all(+) = $1.4 \pm 0.2\%$, agonist(-) = $29.5 \pm 1.3\%$; Neuronal, db/db: ATP = $1.1 \pm 0.2\%$, AITC = $24.8 \pm 1.5\%$, CAP = $15.3 \pm 1.1\%$, ATP/AITC = $2.8 \pm 0.6\%$, ATP/CAP = $1.6 \pm 0.3\%$, AITC/CAP = $21 \pm 2.3\%$, all(+) = $2.7 \pm 0.5\%$, agonist(-) = $30.8 \pm 1.8\%$. Two-tailed paired Student's t-test. **C, D**) Total percentage of neurons which responded to each of the three agonists irrespective of the response's nature (e.g., CAP here is the total responses when CAP, ATP/CAP, AITC/CAP and all(+)) from Figure 5.5A or C are added together). **A)** Metabolic, lean: Agonist(-) = $30.7 \pm 2.1\%$, ATP = $13.6 \pm 3.7\%$, AITC = $57.3 \pm 2.7\%$, CAP = $28.4 \pm 1.7\%$; Metabolic, db/db: Agonist(-) = $30.1 \pm 1.5\%$, ATP = $15.4 \pm 1.3\%$, AITC = $56 \pm 2.4\%$, CAP = $34.2 \pm 1.7\%$; **D)** Neuronal, lean: Agonist(-) = $30.8 \pm 1.2\%$, ATP = $6 \pm 0.8\%$, AITC = $57.1 \pm 0.6\%$, CAP = $31.3 \pm 1.2\%$; Neuronal, db/db: Agonist(-) = $31.2 \pm 1.8\%$, ATP = $8.4 \pm 1\%$, AITC = $51.3 \pm 2.1\%$, CAP = $40.7 \pm 2.5\%$. Multiple comparisons following a One-way ANOVA. * $p < 0.05$, ** $p < 0.005$, *** $p < 0.001$. Shown mean \pm SEM; **E**) Intracellular calcium signal trace following stimulation with the respective agonist, averaged from all responsive neurons (20) of one experiment. Black – average trace from one experiment; grey – showing the SEM for each second of the recorded trace; black arrows indicate the approximate time point of respective drug application.

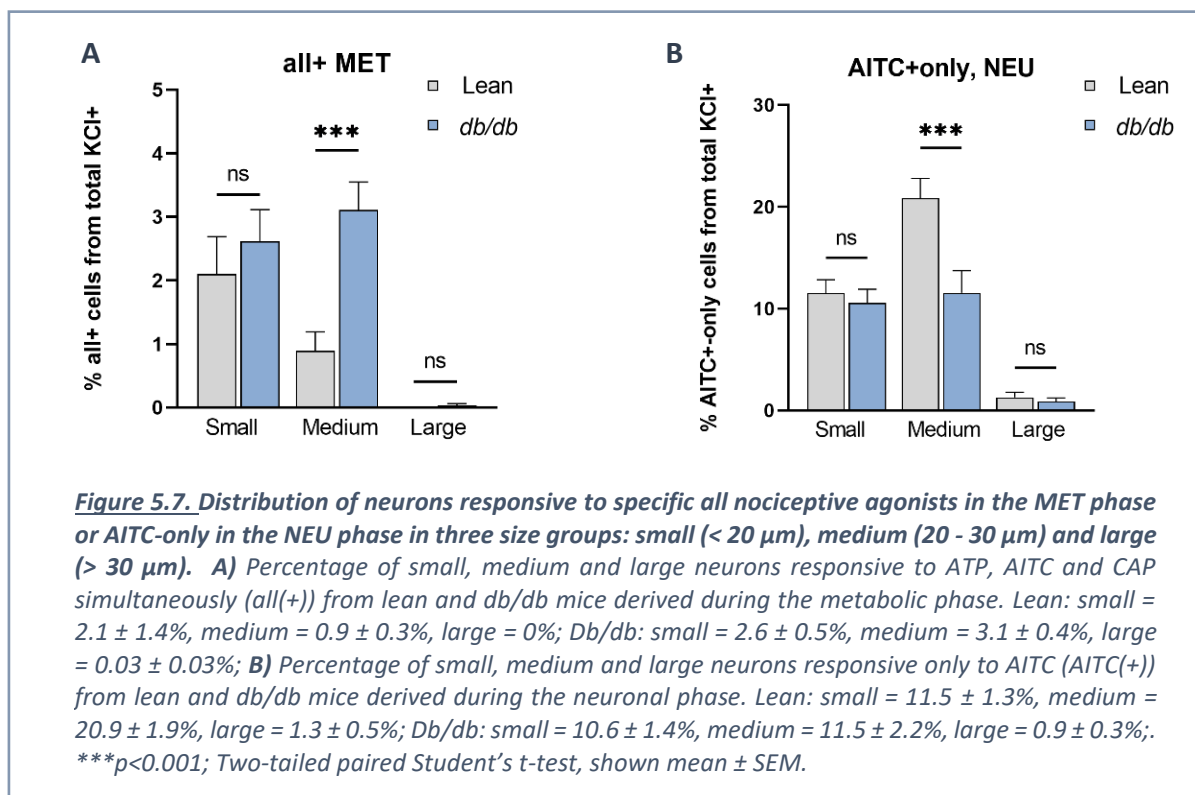


Sizes were also grouped into small medium and large. In the MET phase, there was a significant increase in the number of CAP(+) *db/db* neurons of medium-diameter (1.4-fold increase, control med 9.8 ± 1.2%; *db/db* med 13.9 ± 1%, $p < 0.05$) (Figure 5.6. C). There was no significant difference between *db/db* and control neurons of small- and large-diameter in this phase. This suggests that the increased sensitivity to CAP in *db/db* mice during the MET phase is contributed to by medium-diameter neurons but not the small or large cells. Of note, the increase in all(+) neurons in the *db/db* mice during the MET phase (Figure 5.5 A) was also contributed for by a population of medium-diameter neurons, where a significant 3.5-fold increase in the percentage of medium-sized all(+) neurons was noted (from 0.9 ± 0.3% to 3.1

$\pm 0.4\%$, $p < 0.001$) (Figure 5.7 A), further confirming the all(+) population of neurons as the main contributor to the total increase in CAP sensitivity in MET phase *db/db* mice .

In the NEU phase, the medians of lean and *db/db* neuron sizes were 19.9 μm ($n = 1053$ cells) and 18.8 μm ($n = 789$ cells), respectively, with the additional CAP(+) cells from *db/db* mice falling in the 8-20 μm diameter range (Figure 5.6 B). This translated to a significant 1.6-fold increase in the number of CAP(+) small-sized *db/db* neurons in the NEU phase (from $14.3 \pm 1.1\%$ to $22.9 \pm 2.6\%$, $p < 0.001$) (Figure 5.6 D).

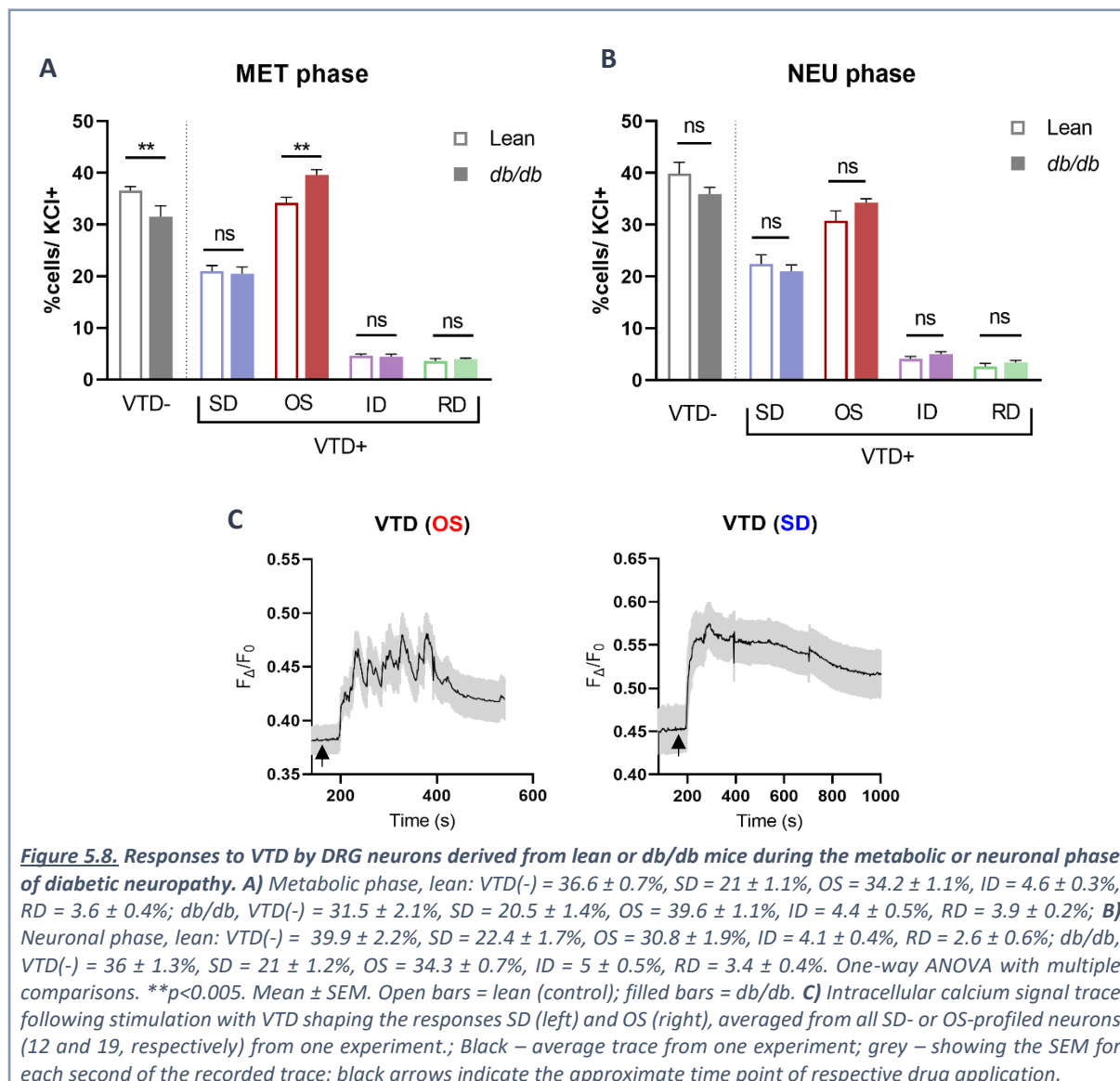
The drop in AITC(+) neurons in the NEU phase (Figure 5.5 B,D) could be correlated to a significant 1.8-fold decrease in the percentage of medium-diameter AITC(+) *db/db* neurons in the NEU phase (from $20.1 \pm 1.9\%$ to $11.5 \pm 2.2\%$, $p < 0.001$), suggesting that the neurons losing their AITC sensitivity are of medium-diameter (Figure 5.7 B).



Together, the changes in the size distribution of CAP(+) neurons during DN progression are indicating that the increasing sensitivity to CAP in *db/db* mice is dynamic, migrating from medium to smaller-diameter DRG neurons as neuropathy advances. The common medium-diameter size between the additional all(+) and CAP(+) *db/db* neurons of the MET phase strengthen the role of the all(+) subpopulation of neurons in the overall increased CAP sensitivity.

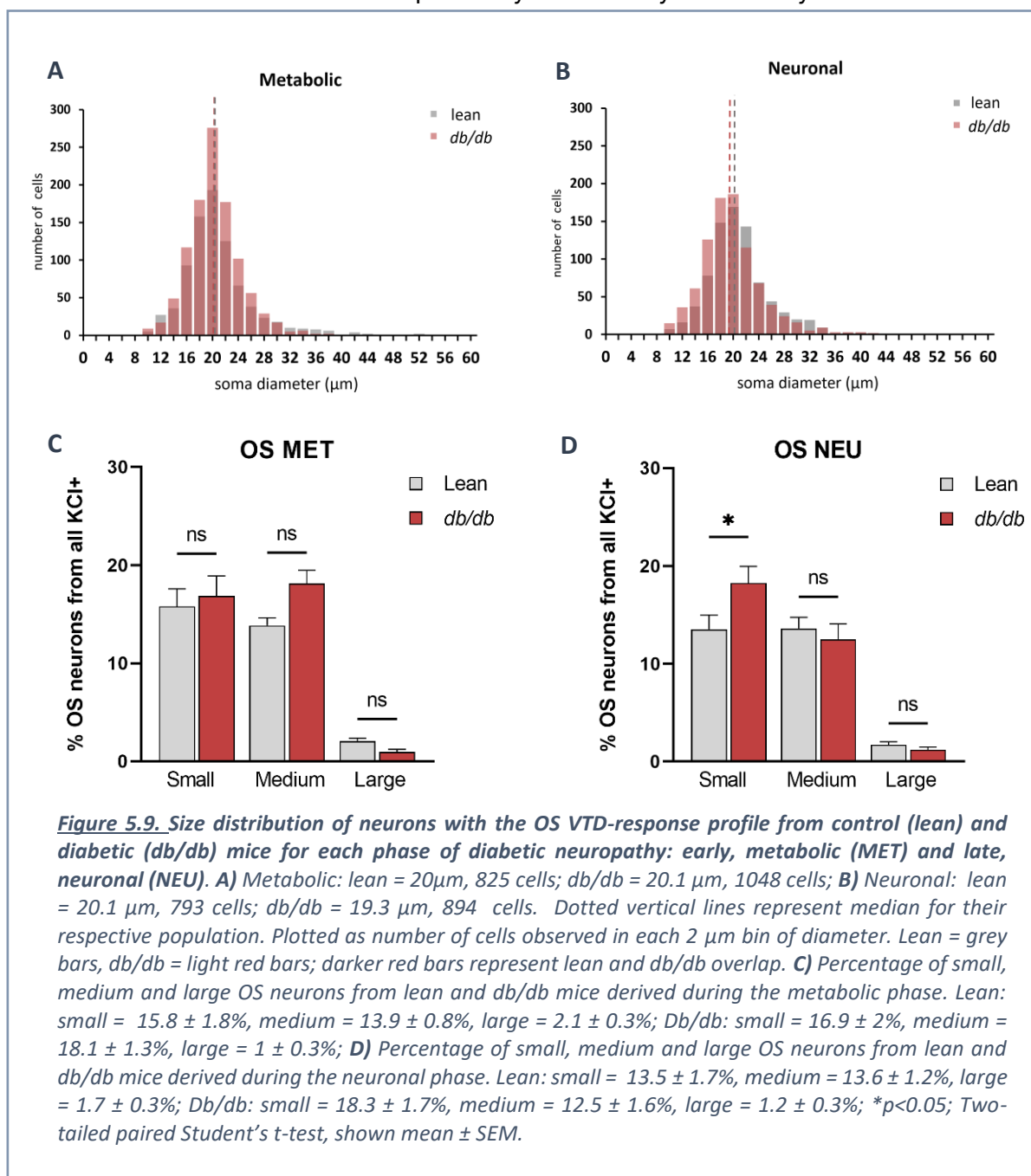
5.4.4. VGSC activity in small DRG nociceptors from *db/db* mice is increased during the course of diabetic neuropathy

Diabetic conditions have been shown to lead to an upregulation of VGSCs expression and activity, especially during early phases of neuropathy⁵⁸. We hypothesised that the VGSC excitability will have also changed in the *db/db* mice DRG neurons. We used the VTD-Ca²⁺ imaging assay to assess the VGSC excitability in nociceptors (OS VTD-response profile) and non-nociceptors (SD VTD-response profile). In the MET phase, responses to VTD showed an increase in excitability (Figure 5.8 A): the number VTD-irresponsive (VTD(-)) neurons decreased by 1.14-fold (from 36.6 ± 0.7% to 31.5 ± 2.1%, $p < 0.005$). This decrease was matched by the increase in the percentage of VTD(+) cells of the OS profile by 1.16-fold (from 34.2 ± 1.1% to 39.6 ± 1.1%, $p < 0.005$). The response rates of the SD, ID and RD VTD-response profiles were not significantly different from lean mice (Figure 5.8 A).



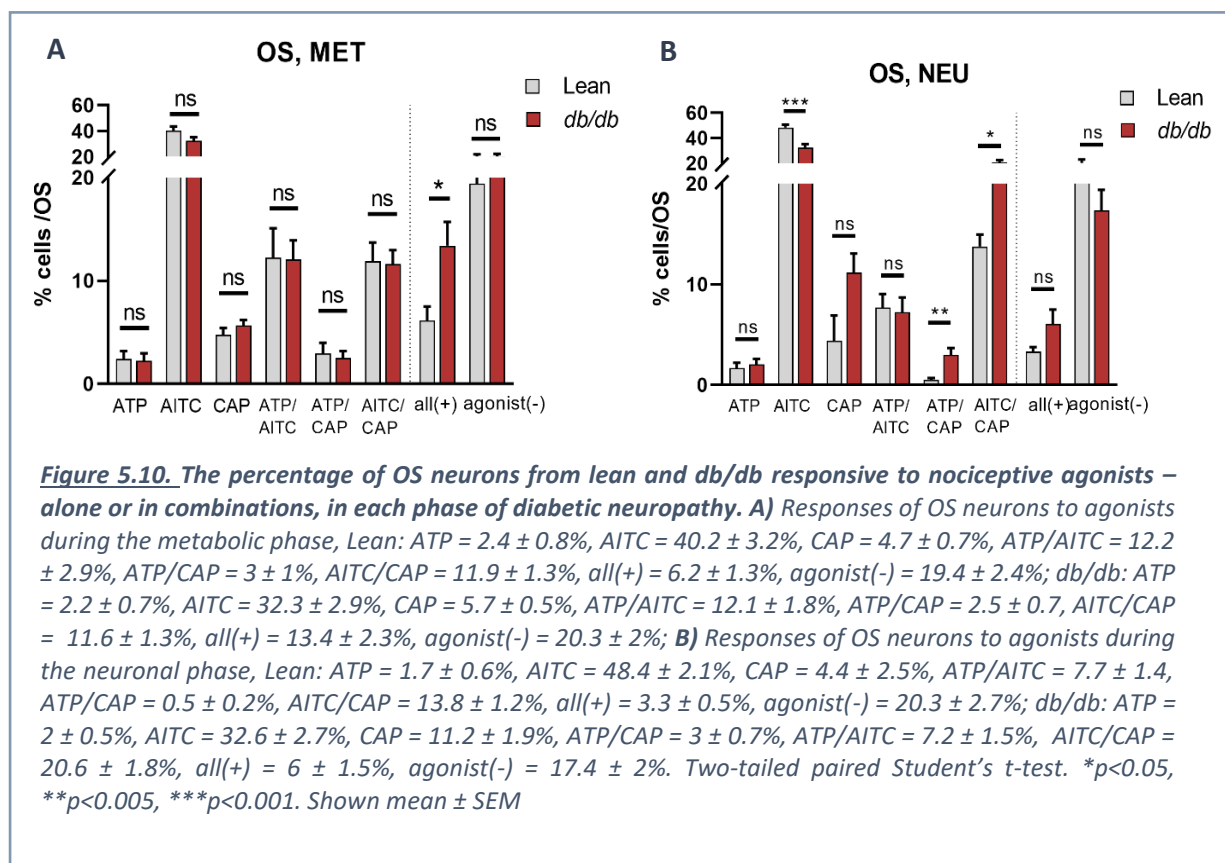
In contrast, in the NEU phase, there was no significant difference in the total response rate to VTD nor within any of the VTD-response profiles, however, albeit non-significant, a trend of increased OS responses in *db/db* neurons persisted (Figure 5.8 B). Of note, there were no significant differences in the amplitude, time to peak or AUC of calcium responses between *db/db* mice and controls (data not shown).

Analysis of the cell size distribution within the MET phase OS population (Figure 5.9 A,C) showed that there was no change in size distribution between lean and *db/db* neurons, but there were more OS *db/db* neurons in the 14-28 μm (small to medium-diameter) size range. This suggests that the additional OS neurons of the MET phase in *db/db* mice (Figure 5.8 A) are not focused in one neuronal size specifically but are likely to be mostly medium in diameter.



In the NEU phase, we saw an increase in the percentage of OS cells, however It was not significant (Figure 5.8 B). Therefore, we looked into the changes in the distribution and percentage of OS cells within the different sizes of *db/db* neurons to see whether the OS increase was focused within a particular neuronal subpopulation (Figure 5.9 B,D). There was a leftward shift in the distribution of *db/db* OS neurons, with more OS profiles in the 8-20 μm (small-diameter) diameter range (Figure 5.9 B). The additional OS neurons of the NEU phase in *db/db* mice were of small diameter – the percentage of small neurons in *db/db* mice was significantly higher than that of lean mice by 1.4-fold (lean = $13.5 \pm 1.5\%$, *db/db* = $18.3 \pm 1.7\%$, $p < 0.05$), while there was no significant difference between lean and *db/db* neurons in the small and large diameter groups (Figure 5.9 D). These insights suggest that the increase in OS neurons begins in the MET phase in small and, mostly, medium-diameter neurons and persists during the NEU phase, focusing into small-diameter neurons of *db/db* mice.

We wanted to find out whether the additional OS cells were also CAP(+). To do this, we performed isolated analysis of the OS population for the response rates to the ATP, AITC and CAP in the 8 possible combinations (Figure 5.10). In the MET phase, there was a significant increase of 2.2-fold in the percentage of all(+) OS neurons in *db/db* compared to lean mice (from $6.2 \pm 1.3\%$ to $13.4 \pm 2.3\%$, $p < 0.05$) (Figure 5.10 A). This showed that the additional OS cells of the *db/db* mice in the MET phase were of the ‘all(+)’ population, identified to be also



the main contributor to the overall increase in CAP sensitivity in that phase (Figure 5.5 A,C). The same analysis performed on the OS population of neurons in the NEU phase revealed that there was an increase in the percentage of OS neurons by responding to CAP alone by 2.5-fold (from $4.4 \pm 2.5\%$ to $11.2 \pm 1.9\%$, $p = 0.0559$) or with another agonist (ATP/CAP, 5.9-fold, from $0.5 \pm 0.2\%$ to $3 \pm 0.7\%$, $p < 0.005$; AITC/CAP, 1.5-fold, from $13.8 \pm 1.2\%$ to $20.6 \pm 1.8\%$, $p < 0.05$) (Figure 5.10 B), identified to be amongst the main contributing populations to the overall CAP increase noted in the NEU phase in *db/db* neurons (Figure 5.5 B,D). These analyses suggest it is likely that the OS subpopulations of neurons affected by increased VGSC excitability could be the same subpopulations affected by increased sensitivity to CAP in each phase of DN.

Taken together, these results suggest that DN leads to an early-phase overall increase in VGSC excitability mainly in medium-diameter DRG neurons responsive to multiple nociceptive agonists. The concentration of this increase in the OS population confirms that these changes are occurring in nociceptors. As DN progresses into the NEU phase, the increased excitability of OS neurons shifts to affect small-diameter nociceptors. The subpopulations affected by increased VGSC activity overlap with those affected by increased CAP activity, suggesting that the same subpopulation of neurons could be affected during the course of DN.

5.5. DISCUSSION

The experiments described in this chapter aimed to examine the excitability changes occurring during the course of DN in DRG neurons isolated from the well-established T2DN *db/db* mouse model. A significant loss of large neurons was observed in the early, MET phase of DN, whereas there was a leftward shift in the size distribution in the late, NEU phase of DN. There were functional changes taking place in the DRG neurons of *db/db* mice during the MET and NEU stages of DN. DRG neurons from *db/db* mice showed increased sensitivity to CAP as well as increased VGSC excitability in nociceptors in both DN phases. The neurons with increased CAP sensitivity in the MET phase were mainly of medium diameter, expressing the receptors for ATP, AITC and CAP simultaneously (P_2X_3 , TRPA1 and TRPV1, respectively), whereas those in the NEU phase were small in diameter, expressing TRPV1 alone or with another receptor. Parallel to the that, in the NEU phase there was also a significant decrease in the sensitivity to AITC, contributed by medium-diameter neurons. Collectively, these results point to distinct populations of neurons being affected by changes in excitability in each of the two DN phases: mostly medium-diameter nociceptors, expressing P_2X_3 , TRPA1 and TRPV1 in the MET phase; and small-diameter TRPV1-expressing nociceptors as well as medium-diameter TRPA1-expressing neurons in the NEU phase. To our knowledge, we are the first to perform such

physiological functional and size characterisation affected DRG subpopulations during DN in the *db/db* mouse .

5.5.1. Cell size distribution in *db/db* mice DRG through the course of diabetic neuropathy

In the current study, we show that during the MET phase, there was a significant decrease in the number of large-diameter cells, where their percentage in *db/db* mice was 1.4-fold lower than lean. In comparison, during the NEU phase of DN, diabetic mice had a significantly increased percentage of small DRG neurons (<20 μm) by nearly 1.4-fold (Figure 5.3 B). At the same time, the percentage of medium-diameter (20–30 μm) DRG neurons was reduced as well as that of large-diameter neurons (>30 μm), albeit not significantly. These observations indicate a potential loss of medium-to-large-diameter neurons during late stages of DN, that could possibly have its beginnings in the MET phase.

Our observations are consistent with those made in the NEU phase by Shi et al. (2013) who found 33% neuronal loss in sections of lumbar 5 (L5) DRG of 32/33-week-old *db/db* mice but no change in 5/6-week-old mice. The lost neurons were of medium-to-large diameter (20–40 μm , according to their size groups). This loss is correlated with hypoalgesia and hyposensitivity demonstrated by behavioural experiments⁵⁵⁵. Here, we observe a total of 16% decrease in neurons from *db/db* mice of the same size range (~11% medium + ~5% large). The discrepancy in the percentages noted by us and Shi et al. could be attributed to the difference between the DRGs selected for analysis by them (L5 only) and us (all DRGs along the spinal column length). To our knowledge, theirs is the only study that investigated the changes in the distribution of DRG neuron sizes in the *db/db* mouse and in a T2DN model in general. As summarised in Figure 5.2, most studies on the *db/db* mouse model have focused on investigating the distal (axonal) as opposed to the more central (DRG) changes induced by DN. Therefore, as far as the same mouse model of DN is concerned, the size distribution results observed here agree to some extent with those observed *in vivo*.

The little information available on diabetes-induced morphological abnormalities at the level of DRG from other animal models of DN is controversial. In STZ rat models, a significant reduction in the perikaryal volume (size of the neuronal cell body) is noted in the DRG of STZ rats but only at 1 month of induced diabetes⁵⁶². However, later, Zochodne et al. (2001) report no change in size distribution at 2 months but a significant reduction in the perikaryal volume after 12 months of induced diabetes⁵⁶³, leading to a shift of the size distribution to the left, reminiscent of the one observed in the NEU phase here. In addition, apoptosis is confirmed to occur in DRG neurons of STZ rats at 1, 3 and 12 months of age, with large neurons being

particularly vulnerable⁵⁶⁴. On the other hand, several studies confirm that loss of DRG or reduced perikaryal volume is evident only in 12-13-month-old rats with chronic DN and not in the early stages^{563,565-567}. Finally, in 10-month-old BB/Wor diabetic rats, a severe loss of small-but not large-diameter DRG has been noted³¹⁸, contradicting all previous and our own research results. Nevertheless, the vast majority of reports from the T1DN rat models outlined above are in overall agreement with the study in *db/db* mice and our results. It appears that most agree on some form of DRG neuronal loss to occur in late DN stages and predominantly in large-diameter neurons, similar to our observations. The general coherence amongst observations from T1DN and T2DN models suggests that the mechanism underlying DRG loss, at least in the late stages, is common and therefore likely to be driven by a shared mechanism underlying T1D and T2D such as hyperglycaemia. However, it remains unclear whether DRG loss preferably affects specific subpopulations and whether it is due to cell soma shrinkage^{563,565,566}, dying-back process⁵⁶⁷ or apoptosis^{318,564}, as each has been reported to occur.

5.5.2. Diabetic neuropathy leads to increasing sensitivity to capsaicin in *db/db* mouse DRG neurons

Capsaicin is an agonist for the noxious heat-gated TRPV1 channel, a non-selective cation channel and a marker of peptidergic nociceptive neurons¹³². Physiologically, TRPV1 plays a key role in the generation of thermal hyperalgesia under inflammatory or tissue injury conditions^{148,149,568}. During the MET phase of DN, our results showed an increase in the total responses to CAP (Figure 5.5 C) in medium-diameter (20-30 μm) neurons of *db/db* mice (Figure 5.6 A, B) and therefore, a likely sensitisation or increase in expression levels of its receptor TRPV1. We showed that this increase was focused within a specific neuronal subpopulation expressing P₂X₃ (ATP receptor), TRPA1 (AITC receptor) and TRPV1 simultaneously (the 'all(+)' subpopulation) (Figure 5.5 A).

In their comprehensive 2016 study, Li et al. combined transcriptomic, electrophysiological and morphological data from mouse DRG neurons and classified them into 16 molecularly distinct subtypes, each with particular set of proteins expressed¹⁵. Referencing the known expression ion channels of the identified all(+) subpopulation from our results with their categories revealed that it is likely the 'all(+)' subpopulation is of the C1 cluster – small (<30 μm according to their own size classification), mechano-heat-nociceptors, responding to noxious mechanical and thermal stimuli. Another cluster expressing P₂X₃, TRPA1 and TRPV1 together is the C10 cluster representing the large-diameter (36-42 μm) mechanoreceptors¹⁵. However, this cluster was dismissed as a possibility since the diameter of the "all(+)" neurons from our

experiments did not exceed 29 μm . Behavioural studies in *db/db* mice confirm the presence of mechanical allodynia during the MET phase of DN (week 6-8) ^{456,507,547,569}. Some report mechanical allodynia to occur together with thermal hyperalgesia (TH) ^{547,548}, consistent with the suggestion of an early stage sensitisation of mechano-heat-nociceptors. Pain of burning quality has also been reported to occur in DN patients, often in parallel to mechanical allodynia, prickling, itching, tingling and ‘electric’ pain sensation, mainly in the feet and hands ^{356,570–573}. These clinical observations agree with the early-phase behavioural data from *db/db* mice and the suggested increased overall TRPV1 activity we report in *db/db* DRG neurons.

Alternatively, referencing the all (+) subpopulation with the DRG subtypes defined by Zeisel et al. by using their online search tool for gene combinations (<http://mousebrain.org/genesearch.html>) revealed that the all(+) neurons are most likely a subpopulation of non-peptidergic neurons (particularly, the “PSNP6” group). In turn, Zeisel et al. reference their own classification with that of Usoskin’s and the “PSNP6” group corresponds to their NP3 group of neurons. Usoskin et al. describe the NP3 cluster as non-peptidergic, unmyelinated neurons of small-to-medium diameter (~20 μm). Interestingly, they strongly suggest that the NP3 DRG neurons are most likely involved in inflammatory itch and pruritus (general itching), thus suggestive of an alternative or additional function of the all(+) population in our results. Chronic pruritus has been well-documented as a symptom in DN patients, reported by 3 – 49% of diabetics ^{574,575}. Albeit not investigated as a behaviour in the *db/db* mouse model of DN, increased scratching behaviour has been reported in STZ rats and linked to DN ^{576,577}. Itch-specific neurons have been identified to be unmyelinated C-fibre nociceptors expressing the Mas1-related G-protein-coupled receptor A3 (MrgprA3) ⁵⁷⁸ as well as P₂X₃, TRPA1 and TRPV1 together ¹⁴. Albeit not the only itch-contributing neurons, they were defined as essential and sufficient for pruriception ⁵⁷⁸. The mechanism underlying the pruritus phenotype in DN is still not clear, however, mounting evidence shows that pruriception is dependent on the recruitment of TRP channels ⁵⁷⁹. Specifically, pruriception was shown to be alleviated and scratching behaviour reduced in mice after pharmacological blockade of TRPA1 and TRPV1 ⁵⁸⁰. Furthermore, inflammatory mediators, known to be upregulated during DN, such as interleukin (IL-) 2, IL-4, IL- 13, IL-31 and NGF ^{256,552,557}, have also been shown to sensitise TRPV1 and TRPA1 and contribute to itching and scratching ^{577,581}. This suggests that the increased activity of the all(+) subpopulation of *db/db* neurons in our results could be driven by their exposure to diabetes-driven inflammatory mediators in vivo and could translate to increase an increase in itch and scratching behaviour related to DN.

From the metabolic abnormalities in the early, MET phase arises progressive structural damage of the nerve fibres – the characteristic feature of the NEU phase ^{233,234}. This leads to

the well-established damage and reduction of IENF density as well as loss of myelin sheathing and slowing of NCV in animal models and patients ²⁵⁸. In contrast to the positive symptoms (pain, prickling etc.) characteristic for the MET phase, the accompanying symptoms of the NEU phase are generally negative, i.e. decreased sensory function, numbness, impaired touch and vibration perception and in some patients, mechanical and thermal hypoalgesia ^{372,520}. It is now well-documented that pain is not just a defining feature of the MET phase and can develop at any stage of DN. In fact, the more severe the sensory deficits become, the higher the risk of developing neuropathic pain episodes is ²³⁷. Moreover, one of the outcomes of IENF damage is bursts of spontaneous activity expressed as pain attacks ^{237,582}. Although the sensory deficit symptoms of DN have been well-established to originate from structural nerve damage, the mechanisms underlying the paradoxical pain during sensory deficits are still poorly understood.

Here, we report a further increase in total CAP responses, as DN progresses into the NEU phase in *db/db* mice (Figure 5.5 D). Compared to the MET phase, in the NEU phase, this total increase is contributed to mostly by small-diameter cells responding to CAP (Figure 5.6 C,D) and thus expressing TRPV1 (Figure 5.5 B). This points to the sensitisation to CAP spreading to envelop other subpopulations of DRG neurons, likely focusing on small, C-fibre nociceptors. Since the affected population in this phase is of small neurons expressing TRPV1, an increased activity in these cells could translate to increased thermal pain sensitivity *in vivo*.

Virtually all behavioural studies of *db/db* mice show increased mechanical and/or thermal pain thresholds in the NEU phase ^{430,453,553–557,583}, thus contradicting the increase in TRPV1 activity observed here. However, it is worth noting that behavioural thermal sensitivity tests in animals are performed using assays such as the ‘hot plate’, ‘Von Frey’ and ‘tail-flick’ methods. These tests rely on the cutaneous perception of stimuli and the results are, therefore, affected by the integrity of the intraepidermal innervation. Thus, an increase in thermal and mechanical thresholds is perhaps more indicative of subcutaneous IENF damage rather than any central channel alterations. The conflict between *db/db* behavioural results of decreased thermal sensitivity and the increased TRPV1 activity we report could suggest that there is an ongoing central sensitisation, upstream of the subepidermal innervation, by stimuli affecting the DRG and not the terminal ends, causing pain of different types, degrees and frequency that might not be detected via conventional animal behavioural tests.

In humans with DN, thermal hyperalgesia has been reported in some patients with mild DN early in the disease’s course ⁵⁸⁴, whereas the advanced phases of the disease are more characteristic with patients’ reports of increased thermal perception thresholds ^{356,585}.

Nevertheless, heat hyperalgesia is still experienced by some DN patients in the advanced DN stages³⁵⁶. Our results could provide a possible explanation for this by suggesting that increased TRPV1 sensitisation and/or expression in DRG is responsible for the increased responsiveness to CAP observed and thus might contribute to spontaneous heat pain. Consistent with our predictions, the most common combination reported in patients is numbness coupled with burning pain and prickling^{238,356,586}, shown by Baron et al. to occur together in 26% of tested DN patients, with the next most common sensory profile being episodic pain attacks (16%)³⁵⁶. The increased TRPV1 activity in DRG we report and the decreased sensitivity to mechanical and thermal stimuli reported by behavioural studies in *db/db* mice in the NEU phase confirm that functional changes can keep exacerbating in the soma of DRG neurons despite disconnection from the skin and impaired external inputs detection. Therefore, a continuous central sensitisation of TRPV1 in small C-fibre nociceptors could be a key player in the development of pain, specifically of burning quality, simultaneously with IENF damage and functional sensory deficits in DN patients.

What could lead to the ongoing central sensitisation of TRPV1 in DRG during DN? As mentioned, increased levels of inflammatory mediators have been reported in DRG neurons during early and late stages of DN and shown to sensitise TRPV1 by activating kinases such as PKC^{142–144,256,552,557}. Protein kinase C activation by the overproduction of glucose metabolites (such as DAG) is also one of the main mechanisms underlying DN development (see Chapter 1, section 1.3.2.2., page 34). Thus, PKC overactivation by different pathways can lead to the hypersensitisation of TRPV1 in DRG^{143,144}. The levels of one inflammatory mediator in particular – NGF, have been reported to be increased in the DRG of *db/db* mice during the MET phase, implied to contribute to the early phase painful phenotype, which could be as a result of NGF increasing TRPV1 sensitisation and expression levels³⁴⁰. Furthermore, insulin, which is abundant in the early phase of T2DN, has also been implied in increased TRPV1 activity by enhancing its translocation to the membrane and lowering its activation threshold, thus facilitating its activation by non-painful stimuli^{291–293}. Therefore, ongoing central sensitisation of TRPV1 could be a potential source of the thermal hyperalgesia and/or pruritus during the early, MET phase and of the paradoxical spontaneous pain during sensory deficits in the late, NEU phase.

5.5.3. Diabetic neuropathy leads to a decrease in the sensitivity to AITC in the *db/db* mouse DRG neurons

Parallel to the increased sensitivity to CAP, in the NEU phase, we also observed a decrease in the percentage of total responses to AITC in *db/db* mice (Figure 5.5 D). This was caused by a

significant drop in the percentage of medium-diameter DRG neurons (Figure 5.7 B) responding to AITC only (Figure 5.5 B), (expressing TRPA1). The TRPA1 channel is activated by a variety of chemicals, cold temperatures and ROS^{163,166,169}. Its role in painful DN pathogenesis has also been well-documented^{184,185,587,588}. TRPA1 is activated and sensitised during DN by diabetes-generated endogenous compound, such as methylglyoxal^{343,407,589} and conditions, such as oxidative stress³⁴⁵. This sensitisation of TRPA1 is linked to the DN phenotype of mechanical allodynia and hypersensitivity. In *db/db* mice, one group recently demonstrated that AMPK activity is impaired in DRG neurons causing an increase in membrane-associated TRPA1 and agonist-evoked TRPA1 currents and mechanical allodynia⁵⁰⁷. These findings contradict our observations of decrease in AITC response rate and hence possible TRPA1 desensitisation and/or decreased expression. However, their report on TRPA1 covers the MET phase of DN in the *db/db* mouse and not the NEU phase, where our observations take place. It is, thus, still inconclusive what changes occur in the activity of TRPA1 in the advanced DN stages in this mouse model.

The rest of the limited literature covering changes in TRPA1 activity during DN is largely focused on the STZ model of T1D and involves considerable controversy. For example, using mice with STZ-induced diabetes, Hiyama et al. demonstrated the involvement of TRPA1 in cold, but not mechanical, hypersensitivity in the early DN stage (2 weeks after diabetes induction). However, in the late stages (8 weeks after diabetes induction), mechanical hyposensitivity and loss of IENFs was shown to occur independently of TRPA1, as TRPA1-KO STZ mice developed a neuropathic phenotype comparable to WT STZ mice⁵⁹⁰. The involvement of TRPA1 in early-phase symptoms of mechanical hypersensitivity in STZ rats was further confirmed by others in the literature^{588,591}. In contrast, increased expression levels and activity of TRPA1 in the STZ mice was reported at late stages (5 weeks after diabetes induction) and correlated to itch and hypoalgesia, as revealed by the attenuated neuropathic symptoms in TRPA1-KO mice and after pharmacological blockade of TRPA1⁵⁹². Further to that, all TRPA1-related findings derived from the STZ-induced diabetes rodents have to be interpreted with caution as Andersson et al. demonstrated a direct activation of TRPA1 by STZ *in vitro* and *in vivo*, where topical administration evoked TRPA1-dependent polymodal hyperalgesia and systemic administration produced acute sensory loss⁴⁶⁶. Thus, at this time the degree and exact mechanisms underlying the involvement of TRPA1 in DN pain and sensory deficits at the different disease phases is still largely uncertain.

With the literature on the subject being scarce, we can only speculate the possible events driving the decrease in AITC responses and therefore TRPA1 activity we see here. It is unlikely that TRPA1(+) neurons acquire TRPV1 and contribute to increased CAP responses, since the

reduction in AITC responses is noted in medium-diameter cells (Figure 5.7 B), whereas the increase in CAP is contributed for by small-diameter cells (Figure 5.6 D). Had there been a functional transformation of TRPA1(+) to acquire TRPV1 activity, we would have seen an increase in medium-diameter CAP(+) cells in the NEU phase as well as small. Therefore, the decrease in AITC responses we report in the NEU phase could be attributed to decreased TRPA1 activity due to desensitisation, downregulation of TRPA1 expression or an inhibitory mechanism triggered by DN, or, alternatively, due to loss of medium-diameter TRPA1(+) neurons. Further experiments in the *db/db* mouse model tracing TRPA1 expression and activity throughout the course of DN are required to confirm or refute these theories.

5.5.4. DRG neurons from *db/db* mice have increased VGSC activity in cells with the OS VTD-response profile

DN has been well documented to alter VGSC activity and expression in sensory neurons^{350,424,593,594}. Here, we report an increase in VGSC excitability in *db/db* mice during DN (Figure 5.8). The increase in excitability was focused within the neuronal population of the OS VTD-response profile, previously confirmed to represent nociceptors^{499,595}. The increase in OS neurons was evident during both phases of DN, however, in the MET phase it occurred in small and medium nociceptors (Figure 5.9 A,C), whereas in the NEU phase it was focused only within small-diameter nociceptors (Figure 5.9 B,D).

Is it possible to identify the VGSC contributing to the OS increase? DRG neurons express several different VGSCs: Nav1.3, Nav1.6 and Nav1.7 (TTX-S), and Nav1.8 and Nav1.9 (TTX-R). All have been demonstrated to be altered and to contribute to pain during nerve injury and neuropathies^{31,360,593,596}, including DN^{351,352,424,597-600}. Veratridine preferably binds TTX-S channels in their open-state and prevents them from inactivating⁴⁹². Due to the broad selective nature of VTD for TTX-S VGSC over TTX-R and not for any VGSC isoform in particular, it is difficult to correlate the increase in OS-response neurons seen to increased activity in any specific VGSC without further supporting experiments. As each neuron expresses a 'constellation' of ion channels, changed expression levels and/or activity of any of them can shape the net VTD response and lead to an increase in a particular VTD-response profile.

Only one paper investigated the expression levels and activity of a VGSC in the *db/db* mouse DRG during DN. In 2012, Ren et al. assessed the expression levels and activity of Nav1.6 in the *db/db* mouse during the progression of DN. Nav1.6 is a TTX-S VGSC, highly expressed in large-diameter DRG neurons, predominantly involved in transmitting tactile information⁶⁰¹ but also reported to contribute to painful DN in rodent models^{58,593}. The research group reported significant and persistent (from 8 to 20 WoA) increase of Nav1.6 mRNA and protein in the DRG

of *db/db* mice. This upregulation was speculated to have been driven by the increased expression of neurotrophins and inflammatory mediators in the DRG during DN. It was also correlated with the demonstrated sustained mechanical allodynia in these mice, further implicating Nav1.6 involvement in painful DN⁶⁰. These conclusions confirmed the increased Nav1.6 expression during DN noted by Craner et al. in the STZ rat⁵⁹³. We have shown that a low dose of a Nav1.6 blocker 4.9-TTX leads to a decrease in the percentage of OS DRG neurons in WT mice⁵⁹⁵ (see Chapter 3). It is then a possibility that the VGSC activity increase in OS neurons seen in the DRG of *db/db* mice here is as a result from increased expression levels of Nav1.6 in the DRG. However, it remains rather unlikely, given that Nav1.6 is predominantly expressed in large-diameter neurons and we only noted an increase in VGSC activity in small and medium neurons. Furthermore, the 4.9-TTX blocker led to a decrease in the percentage of SD neurons as well, therefore had there been an upregulation of Nav1.6 in the DRG of our diabetic mice, we would have expected it to be reflected by an increase in the SD profile as well as the OS. It can therefore be assumed that an upregulation of Nav1.6 is unlikely to have contributed to increase in the OS-response profile seen.

The rest of the TTX-S channels in DRG, Nav1.3 and Nav1.7 upon which VTD acts directly, have both been implicated in DN and pain³⁶⁰. Nav1.3 is another TTX-S channel shown to have upregulated expression in DRG neurons, triggered by inflammation and nerve damage^{44,45,602,603}. It has also been implicated to have a role in nerve injury-related pain^{47,105,604,605}, however experiments with a Nav1.3 null mutant demonstrated that Nav1.3 is neither necessary nor sufficient for the development of such pain⁶⁰⁶. In STZ-rat models of painful DN with confirmed mechanical allodynia, Nav1.3 is reported to have lasting increased expression levels, usually accompanied by alteration in other VGSCs as well^{352,593,607}. Given the conditional upregulation of Nav1.3, it is likely that the inflammatory environment in the *db/db* mouse has increased Nav1.3 expression levels in DRG neurons, which translated in an increased VGSC activity, as detected by the increase in the OS population.

In rats with painful DN, Nav1.7 has been shown to have robustly upregulated expression in small DRG neurons^{58,350,594,608}. We have also previously suggested that increases in the OS VTD-response profile rates could be indicative of increase in the activity of Nav1.7 channel in DRG^(595, see Chapter 3). However, it is unlikely that the increase in OS VTD-profile seen in the DRG of *db/db* mice here is indicative of an increase in Nav1.7 activity or expression levels, as Nav1.7 is expressed in all DRG neurons (i.e. nociceptors and non-nociceptors). Had there been a significant increase in its expression or activity we would have expected to see this reflected by all VTD profiles.

The literature on the role of Nav1.8 in painful DN is controversial. Nav1.8 cooperates with Nav1.7 in DRG neurons, where Nav1.8 is reliant on Nav1.7's hyperpolarised activation to depolarise the membrane sufficiently for Nav1.8's activation^{92,93}. Experiments with global Nav1.8KO mice show a compensatory increase in Nav1.7 expression⁸⁷. Indeed, in diabetic animals downregulation of Nav1.8 is accompanied by an increase in Nav1.7 expression⁵⁹³. As well as downregulated³⁵³, Nav1.8 is reported to be upregulated in diabetic rat DRGs too⁵⁹⁴. In addition, one study demonstrated that Nav1.8 expression is unchanged in diabetic STZ mice but methylglyoxal, a metabolite formed by excessive glucose, causes post-translational gating modifications of Nav1.8 which, together with causing slow inactivation of Nav1.7, contribute to the painful phenotype of the diabetic mice³⁴². It could be the case that Nav1.8 activity or expression is upregulated in DRG of *db/db* mice and contributes to increase in OS. Alternatively, if Nav1.8 expression is downregulated during DN, Nav1.7 is expected to take over and sustain neuronal excitability and OS levels.

Nav1.9, a TTX-R VGSC, has also been demonstrated to be upregulated in diabetic DRG neurons from STZ rats with allodynia, where the increase of Nav1.9 mRNA and protein was observed in neurons of all sizes. The increase is greater in large-diameter neurons, whereas its expression in control DRG was primarily by small and medium-diameter neurons⁵⁹³. It is therefore unlikely that Nav1.9 solely contributed to an increase in the OS-VTD profile in small DRG neurons of *db/db*.

From all the information above, it is most likely that more than one VGSCs could have contributed to the increased OS responses we saw in *db/db* mice. Moreover, other classes of ion channels, such as VGKC and VGCC, shape the net Ca²⁺ signal response to VTD and so, any expression or functional changes in them can alter the VTD-profiles produced and contribute to the increase seen in OS profile. For example, gabapentin, a widely-prescribed VGCC blocker is effective at alleviating painful symptoms in DN patients^{374,609}. Thus, functional and expression levels in VGCC and other channels should be investigated by further functional and biochemical assays.

5.5.5. Diabetic neuropathy leads to excitability changes in specific neuronal subpopulations

A summary of the known properties of the neuronal subpopulations affected and the changes observed is presented in [Table 5.2](#) and [Figure 5.11](#). In the MET phase of *db/db* mice, the net effect was an increase in CAP-responsive cells ([Figure 5.5 C](#)) and increase in VGSC excitability ([Figure 5.8](#)). The additional CAP(+) neurons were mostly medium diameter nociceptors ([Figure 5.6 A,C](#)) expressing TRPV1, TRPA1 and P₂X₃ together (i.e., of the “all(+)” population)

(Figure 5.5 A). In the same phase, the increased VGSC activity was due to increase in the percentage of OS neurons which were also small- to medium diameter nociceptors (Figure 5.9 A,C) of the all(+) subpopulation (Figure 5.10 A). Thus, there is a considerable overlap between the properties of the subpopulations affected by increased CAP and VGSC sensitivity in the MET phase in *db/db* mice.

In the NEU phase, the net effect was an increased number of CAP-responsive cells (Figure 5.5D). Here, the additional CAP(+) cells were focused within a subpopulation of small-diameter nociceptors (Figure 5.6 B,D) expressing TRPV1 (Figure 5.5 B). Also, the increased VGSC activity was attributed to additional OS-profile cells also of small-diameter (Figure 5.9 B,D) and also expressing TRPV1 (Figure 5.10 B). Therefore, the subpopulations affected during the NEU phase in *db/db* mice also overlap in their properties.

The features of the increased VGSC excitability subpopulations largely match those of the cell subpopulations identified with hypersensitisation to CAP in each phase. This could indicate a possible correlation between the increased TRPV1 sensitivity and VGSC excitability. I.e., the same neuronal subpopulations are affected by these two phenomena in DN in the *db/db* mice: predominantly medium-diameter nociceptors expressing P_2X_3 , TRPA1 and TRPV1 together in the MET phase; and small-diameter nociceptors expressing TRPV1 in the NEU phase. In addition, the drop in AITC-responsive neurons in *db/db* mice during the NEU phase was attributed to a subpopulation of medium-diameter neurons of the OS profile expressing TRPA1. Since their parameters differ from those of the neuronal subpopulation affected by CAP(+) increase, it is likely that this is a separate effect on a different neuronal subpopulation.

Table 5.2. Summary table of the identified properties of the DRG neuronal subpopulations affected in *db/db* mice in the metabolic (MET) and neuronal (NEU) phases of diabetic neuropathy. Net effect for each phase shown in the bottom row. Green background denotes increase, whereas red background denotes a decrease observed. VTD = veratridine; VGSC = voltage-gated sodium channel; OS = oscillatory VTD-response profile.

| Phase | MET | NEU | | Population of neurons affected |
|------------------------------|------------------------------------|---------------------------------|------------------|--------------------------------|
| Expression of noc. receptors | P_2X_3 +TRPA1+TRPV1 (all(+)) | TRPV1 (alone or in combination) | TRPA1 | |
| Size (soma diameter) | small, mostly medium | small | medium | |
| VTD-response profile | OS | OS | OS | |
| Net effect | ↑ CAP responses ↑ VGSC activity | ↑ CAP responses | ↓ AITC responses | |

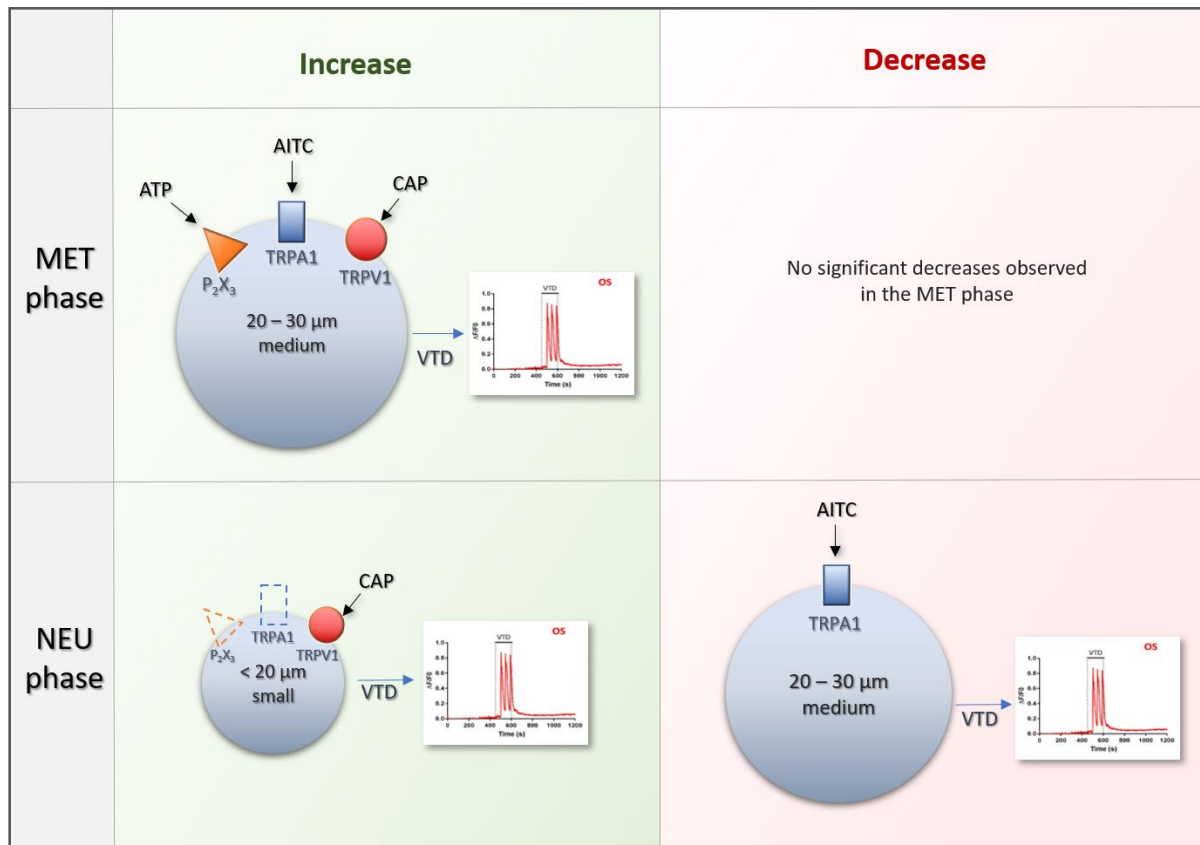


Figure 5.11. Graphic summary of the affected subpopulations of DRG neurons and their known properties in *db/db* mice in the metabolic (MET) and neuronal (NEU) phases of diabetic neuropathy. Dotted outline of receptor channels mean that the neuron might express both, one or none of them together with TRPV1. Green background denotes increase, whereas red background denotes a decrease observed.

Further experiments including tracing ion channel expression levels throughout the course of DN in the *db/db* mouse are needed in parallel to VTD-Ca²⁺ imaging to further characterise the identity of the specific subpopulations raising DRG neuronal excitability and potentially shaping a painful phenotype. The next and final chapter discusses further limitations and recommendations for future experiments to build on the results presented in this thesis.

CHAPTER 6
**LIMITATIONS & FUTURE
DIRECTIONS**

CHAPTER 6: LIMITATIONS & FUTURE DIRECTIONS

Diabetic neuropathy is a debilitating condition significantly affecting the quality of patients' life, especially if accompanied by painful symptoms. Despite decades of animal and clinical research, the multifactorial mechanisms driving the positive and negative sensations caused by DN are still poorly understood. There are no disease-modifying or reversing drugs approved and DN continues to represent a therapeutic challenge²³⁰. The only successful strategy remains diabetes prevention via glycaemic control through diet and lifestyle management. To date, several treatments have been approved for the symptomatic relief of painful DN, however first- and second-line drugs target pain pathways in the CNS and produce modest analgesia at the cost of serious, potentially fatal side effects³⁷⁶.

In recent years, research into novel analgesic agents for the treatment of pain has turned to targeting the PNS to avoid serious CNS adverse effects whilst improving drug efficacy. Several promising targets have been identified, the most popular being PNS-expressed ion channels implicated in pain for example VGSCs Na_v1.7, Na_v1.8 and Na_v1.9^{33,610}. Novel ion channel blockers or activators drugs are in development and ongoing pre-clinical and clinical studies^{393,394,399-401} (also see [Table 1.5](#)). However, a common issue is the poor translation of drug efficacy from the animal model to the DN patient with most novel pharmacotherapies failing clinical trials. For example the failed translation of aldose reductase- and PKC-inhibitors efficacy from the STZ rat model of DN to DN patients^{247,249}. To design better targeted drugs with minimal off-target effects, a better understanding of the mechanisms driving DN pathology and its modelling is required as well as a simple, efficient, medium-to-high throughput assay able to distinguish nociceptors from non-nociceptors.

Therefore, the aim of the current study was to aid this process by assessing the neuronal excitability changes occurring during DN in DRG neurons *in vitro* and from a diabetic mouse model. We expected that neuronal excitability shifts will be present at different degrees in the different subpopulations of neurons within a mixed DRG population. Therefore, first, the VTD-Ca²⁺ imaging assay was validated for its ability to discriminate nociceptors from a heterogeneous neuronal population and for its use as a potential drug screening tool, as outlined in Chapter 3. The next two chapters described following experiments exploring the application of the VTD-Ca²⁺ imaging assay in combination with other nociceptive agonists to characterise excitability changes during DN in DRG neurons from healthy mice cultured under *in vitro* hyperglycaemic conditions (Chapter 4) or DRG neurons derived from the diabetic *db/db* mouse model of DN (Chapter 5).

In this chapter, discussion will encompass advantages and future perspectives for the VTD- Ca^{2+} imaging assay regarding its optimisation and application. I will discuss the main limitations of our study with focus on the *in vitro* DN experiments and how realistic it is to replicate DN in a dish as well as using DN mouse models for assessing DRG excitability changes. Finally, the key findings and implications of the experiments will be briefly discussed with recommendations for future research.

6.1. Veratridine and Ca^{2+} imaging as a tool with multiple applications

This study began with the aim of validating the previously generated results by our lab for the use of VTD-induced Ca^{2+} responses as broad markers for DRG neuronal subpopulations. A detailed characterisation of the VTD-responses was carried out previously by our lab⁴⁹⁹. Here, using DTA mice with genetically ablated nociceptors, I demonstrated a strong link between the OS VTD-response profile and nociceptors, whilst non-nociceptors were associated with the SD profile (Chapter 3, Figure 2). Thus, the use of the VTD with Ca^{2+} imaging as a tool for assessing neuronal excitability in specific neuronal subpopulations was confirmed and the “VTD- Ca^{2+} imaging assay” was established.

6.1.2. Advantages

The VTD- Ca^{2+} imaging assay's main advantage is that it allows for the efficient screening of a heterogeneous population of neurons. Thus, the VTD response profile pattern generated integrates all responses present in the population, which would give a more realistic idea of what a drug's effect would be in a physiological environment. This contrasts with patch-clamping-based *in vitro* assays, where the investigated effect might not be detected as a result of the low-throughput screening efficiency. The ability to cover a heterogeneous population of neurons with a single assay screen is also advantageous over cell-line-based screening methods. Often the first choice in novel drug characterisations, heterologous expression systems are used to express the target protein against which drugs are screened. However, the absence of the full set of ion channels, exchangers and receptors can hide off-target effects of the compound investigated. The VTD- Ca^{2+} imaging assay is able to detect specific excitability changes in distinct neuronal subpopulations in each screen. Therefore, the development of the assay as a medium-to-high throughput screening tool in primary sensory neurons will aid in the complete characterisation of a drug's efficacy and safety profile, as it would appear in a heterogeneous population *in vivo*.

Apart from its functionality, another advantage of our system is the wealth of data generated with minimal resources and in a relatively short amount of time. For example, in our experiments with *db/db* mice, over 6 weeks of imaging experiments, a total of 10 313 neurons were imaged from 24 mice, giving an imaging efficiency of approx. 430 neurons per mouse. Such recording capacity ensured each animal made a maximum contribution to the study with minimal waste of cells. Moreover, the large numbers of neurons for each mouse contributed to the validity of the observed phenotype.

Our screening productivity is comparable to standard Ca^{2+} -imaging of DRG neurons. However, here, we employ VTD as a main neuronal exciting agent instead of a high-potassium solution (KCl), most commonly used to excite cells in Ca^{2+} imaging protocols. High-potassium solutions directly depolarise the membranes of all neurons in a DRG population, thus activating them simultaneously⁴⁸⁴. Here, due to VTD's action on VGSCs, the responses generated are shaped by the constellation of ion channels, receptors and exchangers expressed by each neuron. Therefore, neuronal responses are more nuanced and thus more informative compared to the binary “yes” or “no” information provided by responses to KCl.

Imaging Ca^{2+} responses to VTD and agonists in neurons provided us with basic information of the response rates to the drugs administered. Moreover, each recording also yielded a vast amount of data available for analysis, including measuring the amplitude of Ca^{2+} responses, time to peak and AUC. Each recording also provided an image of the neuronal population allowing for the estimation of neuronal diameter and subsequent analysis of cell size distribution. Such wealth of data allows for the in-depth multifactorial characterisation of the responses from each neuronal population imaged and hence the building of a more complete picture of the neuronal phenotype under investigation.

6.1.3. Limitations & Recommendations

Nevertheless, a major limitation of the VTD- Ca^{2+} imaging assay is the data analysis component. The diversity and abundance of information generated demands comprehensive analysis across several softwares. At present, this analysis is manual, with each neuronal trace of responses analysed individually. The process is laborious and time-consuming and manual data handling can be subject to conscious or unconscious bias.

Finally, AUC measurements are performed automatically by a software according to a method outlined in [Chapter 2: Materials & Methods, section 2.2.3.1, page 70](#). Although facilitating the analysis, the application of the same estimation formula on each trace does not produce a completely realistic picture of the AUC. The formula computes the AUC of a response to a

drug based on a pre-specified baseline, which is the average value of the signal during the 30 seconds prior to adding the drug. Assuming a perfectly steady and horizontal baseline, areas under the curve calculated will be near 100% accurate for all traces. However, occasionally, even the slightest fluorescent dye bleaching during an experiment can cause a small deviation of the resting calcium baseline and transiently or steadily shift it. If this shift is within the 30 seconds specified for baseline, they are incorporated into the baseline calculations and lead to gain or loss of estimated AUC depending on whether the trace has been shifted upwards or downwards, respectively. Albeit infrequent, such cases occur and can “pollute” the estimated overall AUC value averaged for the whole neuronal population.

Therefore, perhaps the optimisation that this assay would benefit from the most, is automation of the data analysis process. Automating the calculation and tabulation of parameters will significantly reduce human error and the time taken. Furthermore, it would allow for the integration of a more complex formula for the AUC estimation which would account for potential deviations in the baseline of the Ca^{2+} signal.

To develop a full picture of the usefulness of VTD-response profiles, the assay needs to be further developed. For example, at present, the assay has only ever been applied to mouse DRG neurons. Further characterisation using rat and human DRG (hDRG) would elucidate differences in DRG excitability between species. Transcriptomic analysis of rodent and hDRG have demonstrated different levels of expression of some pain-related ion channels. Chang et al. showed that Nav1.7 had higher expression levels in hDRG than mouse DRG, whereas mouse DRG had higher expression of Nav1.8⁶¹¹. Therefore, the VTD-response patterns produced by hDRG might be significantly different from that of rodent DRG, highlighting potential interspecies functional discrepancies. This could provide insights into why certain analgesics have shown efficacy in rodents but not in humans. Adapting the VTD- Ca^{2+} imaging assay to examine responses in hDRG would, therefore, benefit drug screening programmes.

The VTD- Ca^{2+} imaging assay can also be advanced by conducting more experiments with genetically modified animals (e.g., KO models of certain VGSCs, or knock-in for GCAMP Ca^{2+} sensors to allow *in vivo* imaging) as well as ion channel-blocking or activating drugs of various specificities. This would allow for the in-depth interrogation of each VTD-response profile and the contributing ion-channel(s) that shape it. This is of particular importance for clarifying the identity of the ID and RD profiles, which, although underrepresented, have a very distinct VTD-response shape of a single, transient peak.

Finally, experiments using DRG exposed to an inflammatory or injury-like *in vitro* environment (e.g. inflammatory soup-induced⁶¹²) would aid in the characterisation of the population of

“silent nociceptors”, believed to be “unsilenced” under such conditions^{3,4}. It is hypothesised these neurons express predominantly TTX-R channels⁴⁹⁹, but it is yet to be determined what VTD-profile they will produce once activated.

6.1.4. Applications

The confirmation of the VTD-Ca²⁺ imaging assay as a tool able to discriminate excitability changes between nociceptors and non-nociceptors has opened many doors for its potential uses. Its application as a drug screening assay was tapped into during the experiments with pharmacological channel blockers presented in [Chapter 3](#). They demonstrated that the VTD responses produced by a certain drug can be informative of its specificity to nociceptors and degree of side effects on non-nociceptors. Moreover, we demonstrated that the assay can be used for investigating the effect of combining lower doses of 2 (or more) drugs to improve efficacy and minimise off-target effects. Combination therapies have been undergoing clinical trials and, in many cases, have proven more successful than individual ones and placebo^{613–618}, however the majority are still targeting the CNS. It would be interesting to see whether such approach can be applied to novel molecules targeting PNS-expressed ion channels. This can facilitate the analgesic drug development process, whereby failed ion channel-modulating agents can be resurrected into combination therapies instead of developing novel ones. This makes the VTD-Ca²⁺ imaging assay a suitable platform for pre-clinical drug tests on primary cultures of heterogeneous neurons. Furthermore, by using a primary culture of human DRG (hDRG) neurons, this could help bridge the translational gap between pre-clinical and clinical research. Thus, VTD-Ca²⁺ imaging can be used to assess the efficacy and safety of channel blockers and activators downstream of the VGSC activation step in the process of AP generation and propagation. However, a limitation to bear in mind is that, as a drug screening tool, the VTD-Ca²⁺ imaging assay would not be able to provide information on the efficacy of drugs inhibiting initial transducing events, e.g., blockers of TRP channels. This is because signal transduction is a step prior to VGSC activation, where VTD exercises its action.

The VTD-Ca²⁺ imaging assay can also be applied for the characterisations of DRG excitability phenotype in the context of different neuropathological conditions. In [Chapter 5](#), I described and discussed experiments with DRG from the *db/db* mouse model of DN. In a DN setting, the assay was able to detect excitability changes in nociceptors expressed as increase in the percentage of neurons with the OS profile ([Figures 5.8, 5.9, 5.10](#)). The assay can be applied in other DRG-sensitisation models, such as paclitaxel-induced peripheral neuropathy⁶¹⁹ or inflammatory conditions⁶¹². It would also be interesting to compare VTD-response profiles produced by a T1DN rodent model, such as the STZ-induced model of DN, to those generated

by the *db/db* mouse. A comparison of this nature can elucidate DN-driving mechanisms in the different induced diabetes animal models and provide insights into the discrepancies seen in neuropathic complications between the two diabetes types.

Finally, the VTD-Ca²⁺ imaging assay can contribute for the validation of stem cell differentiation protocols⁶²⁰. Research efforts have been focused into the development of functional DRG cultures derived from iPSC for the study of peripheral neuropathies⁶²¹. How well such novel cultures compare to natural human DRG could be determined by comparing the VTD-response profiles both will produce. Thus, one can estimate whether the expression of the constellation of ion channels in the membrane of stem cell-derived neurons is comparable to the physiological, natural DRG neuron.

6.2. Modelling diabetic neuropathy in a dish – a realistic goal or an unfeasible challenge?

It is common practice when investigating the pathology of a disease to replicate its aspects on cultured cells *in vitro* in order to study the mechanisms in a controlled and isolated environment. *In vitro* high glucose conditions have been used as a way of modelling DN extensively and have largely contributed to our knowledge of the mechanisms underlying diabetic neuropathy and pain^{318,420–425}. In the experiments outlined in the present study, *in vitro*-induced hyperglycaemia did not produce the expected increase in neuronal excitability as increased VGSC activity^{351,424,502} or increase in responses to nociceptive agonists implied elsewhere^{506,510,525}, as the response rates remained comparable to control (Figures 4.3, 4.4). It is difficult to explain this outcome, but it might be related to differences between the age and type of the DRG used, differences in glucose concentration and exposure time used by me and others, as well as other variables in the culture conditions.

Our *in vitro* results contradict virtually all previous studies using *in vitro* high glucose conditions, which report increase in CAP-evoked currents or VGSC activity or expression^{351,424,456,502,506,510,531,622}. As discussed in detail in chapter 4, the possible reasons for these discrepancies are the extensive use of embryonic or neonatal DRGs by others^{351,424,502,506} as opposed to adult DRG used here; the use of rat DRG^{349,351,502,510} or immortalised rat DRG cell line⁶²² rather than mouse DRG used here; and the selection of specific DRG for culturing and experiments, e.g. lumbar DRGs^{502,506,510} or only those of 20-25 μm ⁵⁰² as contrasted with the isolation of DRG from the full spinal column length here, which might account for a potential “dilution” of a high glucose-driven excitability changes.

With our *in vitro* experimental design differing substantially in one or more aspects from others, we can only speculate how the conditions we introduced could be amended to achieve a high glucose-driven increase in DRG excitability. One thing to consider can be the degree and duration of hyperglycaemia exposure itself. Albeit well-supported by studies investigating its acute effects, the extracellular glucose concentration of 50mM used here might not have been potent enough to produce an effect on neuronal excitability represented by changes in VGSC activity detected in the VTD-response profile patterns generated. Also, in the present experiments, glucose concentration was increased to hyperglycaemic levels acutely after 24h and glucose in the medium was not replenished daily to maintain high concentration. DRG neurons have higher energy requirements and metabolic rates compared to other cells and tissues^{318,623}. Their energy demands are likely to be even higher than normal for the first 24h following dissociation for culture as the neuron's metabolic rate is altered to support axonal regeneration⁶²⁴. Hence, cultured neurons might metabolise the available sugar abundance and re-adapt to control glucose levels in the 24 hours before experiments begin. Although, to our knowledge, this does not seem to be a practice in similar studies, daily replenishing of glucose in the medium might be an avenue worth exploring for Ca²⁺ imaging experiments with neurons cultured for more than 24h.

Another possible explanation for the absence of a hyperexcitability phenotype in our experiments is the lack of the full spectrum of DN aspects driving neurodegeneration. Historically, DN's pathology was largely believed to be "gluco-centric". This is true to a large extent, as high blood glucose levels are toxic for the vasa nervorum, the neurons themselves and the Schwann cells supporting them. However, it is now known that glucose-independent mechanisms work in synergy with hyperglycaemia-driven processes to produce DN and pain. The major pathways were introduced in detail in [Chapter 1: Introduction, section 1.3.3](#). One of the main glucose-independent triggers of neuronal damage in a DN setting is dysregulated insulin signalling. Insulin is an important neurotrophic factor for neuronal growth and is often added to neuronal culture media for trophic support⁶²³. Poor insulin availability, as in T1D and late stages of T2D, as well as insulin overabundance, like in early T2D, both contribute to neuronal health damage, independently of hyperglycaemic conditions^{286,296–298,303}. For the experiments outlined in [Chapter 4](#), the DRG cultures were not supplied with any insulin. Thus, the *in vitro* DN conditions we designed were closer to replicating those in T1DN and late T2DN, where neurons are in an environment with excess glucose and little insulin. Supplementation of the DRG culture with excess insulin together with high glucose levels might have brought culture conditions closer to those in early T2DN and might have produced detectable neuronal excitability changes. However, adding insulin to the culture at any concentration would still

introduce its trophic support effects to the cells, which may play down or negate hyperglycaemia-induced neuronal damage. In fact, it is possible that the large quantity of available insulin, at least in the initial stages of T2D, is responsible for maintaining neuronal health and, to an extent counteract the neurodegenerative effects of hyperglycaemia during T2D. This might explain the less aggressive symptomatic expression of T2DN compared to T1DN in the early stages of diabetes^{233,252,253}. Insulin's production cessation due to β -cell destruction in T2DN advanced stages might then be responsible for the rapid progression of DN symptoms in the later stages of T2DN. This idea is reinforced in studies by Huang et al. who cultured mature sensory neurons with high insulin and normal glucose levels and reported increased hexokinase activity and ATP synthesis amongst other events. Hexokinase drives the first committed step of glycolysis, hence its upregulated activity indicates augmented glucose metabolism and energy generation⁶²⁵. In an *in vitro* hyperglycaemic setting, this could ameliorate the effects of high glucose on the neuronal health and thus mask a neuropathic phenotype. In another study, the group demonstrated that maintaining STZ-rat-derived DRG neurons in high glucose and supplementing them with insulin led to improved mitochondrial function. Furthermore, administering low dose insulin injection to STZ rats improved their sensory phenotype but without affecting hyperglycaemia in the rodent⁶²⁶. Their results call for caution when considering supplying *in vitro* cultures with insulin. Despite the growing evidence of its role in the DN pathogenesis, due to the hormone's nature it would be challenging to tease out its beneficial from neurodegenerative effects *in vitro*. Nevertheless, neuronal IR is a well-evidenced feature of T2DN⁶²⁷ and future research into modelling DN *in vitro* should explore its adequate implementation in a culture model.

NGF is another trophic factor, considered an essential component of neonatal DRG culture protocols^{628–630}. NGF expression is also upregulated in animal models of injury^{631,632} and inflammation³⁴⁰, including DN^{456,531,567,633}. In animal models of both T1DN^{531,633,634} and T2DN (*db/db* mice⁴⁵⁶), increased levels of NGF are detected and correlated to increased pain sensitivity. Although the mechanisms behind its increased expression are unclear, it is speculated that NGF levels increase during DN as a neuroprotective response to the metabolic stressors accompanying the disease⁴⁵⁶. From all of the above, neurotrophic factors such as NGF and insulin might be key drivers in the pathogenesis of DN and hence valuable components to include in an *in vitro* model, however should undergo careful consideration before being implemented and resulting outcomes should be interpreted with their trophic effects in mind.

Other components of DN pathology that have been directly introduced in *in vitro* DN models include pro-oxidants for replicating oxidative stress (Purves et al 2001), methylglyoxal for

direct glucose toxicity modelling⁴³² and oxidised LDLs to directly model hyperlipidaemia⁴³⁴. Although elucidative of the mechanism via which each might contribute to DN in isolation, no studies have yet modelled an *in vitro* DN environment incorporating several components together. Such an approach might pose difficulties, since an environment with a number of variables is less susceptible to tight control and manipulation. Nevertheless, identifying the optimal number and types of components able to be successfully and sustainably introduced in an *in vitro* neuronal environment might allow for a modelling of DN in a dish closer to that in humans.

Finally, a limitation of extending culture time to 6 days is the reduced number of neurons available for imaging with time. Twenty-four hours after plating, neurons start extending neurites and by day 3 in culture a dense axonal network is present⁵⁰⁵. In addition, proliferation of non-neuronal cells such as fibroblasts, satellite glia and SCs begins. This can obstruct neurons from being easily identified and selected for imaging experiments. The reduced availability of neurons as time in culture progresses inevitably leads to fewer cells imaged per day due to the limited number of coverslips and animals (Table 4.2, Figure 4.2). The reduced number of available neurons and hence ROIs of sufficiently good clarity for recording can be an important source of data variability. Unfortunately, to our knowledge, controlling neurite outgrowth without aggressive treatments that might introduce a phenotype is unfeasible. Future experiments might benefit from exploring compounds preventing minimising the amount of non-neuronal cells proliferation in culture, such antimitotic agents, e.g. 5-fluoro-2'-deoxyuridine^{635,636} although caution should be taken when interpreting data from cultures containing additional elements. Alternatively, the restricted number of available neurons after 2 or more days *in vitro* can be compensated for by increasing the total sample size for the time point to ensure statistically valid quantity of data.

6.3. Studying excitability of DRG neurons derived from diabetic animals

The second big aim of the present study was to assess for excitability changes present in DRG neurons derived from diabetic *db/db* mice. This was also an opportunity to explore the application of the VTD-Ca²⁺ imaging assay as a tool for characterising the excitability phenotype of DN in sensory neurons. The VTD-Ca²⁺ imaging assay detected changes in VGSC excitability expressed as an increase in the OS profile in both phases of DN in *db/db* mice (Figures 5.8, 5.9, 5.10). Nociceptive agonists revealed an increase in the sensitivity to CAP which persisted and increased into the late, NEU phase of DN (Figures 5.5, 5.6, 5.7). We speculated it is likely that the functional changes observed start in a subpopulation of small-

to-medium nociceptors and later affect small, TRPV1-expressing nociceptors as DN progresses (Table 5.2, Figure 5.11). These results implicate specific neuronal subpopulations affected at early and late stages of DN and could serve as a foundation for further research into them and the molecular mechanisms driving excitability changes. Their further characterisation will, in turn, aid the identification of specific targets for the development of pain-alleviating or DN-modifying therapies. In addition, this is the first study to investigate physiological excitability changes in the *db/db* mouse in both phases of DN.

The *db/db* mouse is perhaps the most widely used model of T2D due to the collection of advantages they bring over other diabetic models (Table 6.1). The robust development of diabetes and subsequent complications follow closely the natural progression in human patients, making them also one of the most preferred models of DN⁴⁵³. Perhaps the main advantage of this model is that DRG neurons are chronically exposed to neurodegenerative DN conditions that go beyond hyperglycaemia, including oxidative stress, hyperinsulinemia and IR, inflammation and dyslipidaemia. We and others^{431,637} have demonstrated that isolating and culturing DRG from *db/db* mice in standard medium and conditions produces a DN phenotype, hence allowing for their studying without supplementing the culture with additional elements complicating data interpretation.

Table 6.1. List of some advantages of the T2D db/db mouse model of diabetic neuropathy.

| Advantages | References |
|---|-------------------------|
| Parallels human T2D and pathogenesis to a very high degree: <ul style="list-style-type: none"> • Persistent hyperglycaemia • Obesity • Dyslipidaemia: persistent high blood cholesterol and triglyceride levels • Insulin resistance • Inflammation | 456,458,541,549,666,671 |
| Mimics human DN progression qualitatively and temporally: <ul style="list-style-type: none"> • Hyperalgesia and allodynia 8-12 weeks • Thermal and mechanical hypoalgesia after 12 weeks* • Decreased NCV • Loss of large myelinated fibres • Axonal atrophy and dystrophy • Loss, shrinkage and breakdown of myelin | |
| T2D phenotype validated with anti-diabetic drugs | 672–674 |
| Shown to exhibit a pre-diabetic state | 675 |
| Develop severe hyperglycaemia and display advanced stages of the disease without the need of any external diet or pharmacological interventions that could disturb the natural phenotype | 418,453,676 |

Table 6.2. List of some disadvantages of the T2D db/db mouse model of diabetic neuropathy.

| Disadvantages | References |
|---|-------------|
| Short lifespan (30 – 40 WoA) | 668 |
| Leptin signalling impairments are much less severe in human patients | 669 |
| Leptin-based mouse models are often infertile, and generating significant numbers is time consuming. | 447 |
| Impairment of leptin signalling might have indirect consequences on other biochemical pathways | 669,670 |
| DN phenotype depends on strain used (C57BKS vs C57BL/6) | 453,459,671 |

The *db/db* mouse does not come without some disadvantages, outlined in [table 6.2](#). Perhaps the main disadvantage, and a limitation of these experiments, is that the *db/db* mouse strain, like every genetically modified disease model, presents with lower genetic differences thus producing lower variability in DN onset and/or progression. This is in contrast to humans, where different DN patients present with different degrees and timings of functional and structural changes ⁶³⁸. Despite that, however, a similar trend is observed in both the *db/db* animal model and DN patients, whereby the early phase of DN is regulated by complex metabolic drivers producing contradicting behavioural reports in the *db/db* mouse (see [table 4.2](#)) and varying degrees of sensitivity changes in patients ⁶³⁹. On the other hand, the sensitivity loss and structural changes during the late DN phase is well documented in both, animal models ^{252,453,640} and humans ^{230,234,639}. This perhaps implicates the *db/db* mouse as a more suitable model for investigating the late, structural effects on sensory neurons during DN. However, studies reporting positive functional and behavioural changes in the animal model during early phase DN could still benefit a subpopulation of patients experiencing similar events.

DN is characteristic with its stocking-and-glove distribution, affecting the toes and feet first, followed closely by the fingers and hands ⁶⁴¹. Each dorsal horn afferent nerve is dedicated to innervating a specific area of skin or organ, i.e., its dermatome. The nerves innervating the areas affected first by DN are lumbar spinal nerves 4 and 5 (L4 and L5) for the toes and feet, and cervical spinal nerves 6, 7 and 8 as well as sacral spinal nerve 1 (C6, C7, C8 and S1, respectively) for the fingers and hands. Often, studies exploring functional and structural changes in the nerves during DN would isolate only DRG from L4/L5, noting functional and structural alterations ^{254,337,544–546,637,642,643}. In the present study, DRG from the whole length of the spinal column were isolated for studying DN. Assuming that the DN phenotype is concentrated largely in the lumbar DRG, then dissection of all DRG indiscriminately could lead to “dilution” of the neuropathic phenotype and milder excitability changes being observed as opposed to isolating specific DRGs. Future studies can explore this concept by preparing DRG cultures from specific spinal column segments of nerves evidenced to be highly affected in DN, such as the lumbar nerves. This would provide a focused investigation of DN effects on specific organs and body areas and should be interpreted as part of the bigger picture of the DN pathogenesis. It would be interesting to see a meta-analysis of studies using all DRGs as opposed to specific ones from diabetic animals and whether the results obtained via these two different approaches differ substantially.

One potential source of weakness in this study, which could have affected the neuronal excitability phenotype, is the decision to culture dissociated DRG from *db/db* mice in a

standard environment. That is, isolated DRG were not maintained in high glucose conditions, neither was insulin, NGF or other DN-characteristic elements added to the medium. Upon being faced with this choice when designing the experiments, we addressed relevant literature and established that virtually all studies using DRG from animal models of DN did not alter the culture medium to reflect DN conditions. Hence, the decision was made to undertake the same approach with the present experiments and observe the phenotype produced. Had it been the case that no significant differences were noticed between control and diabetic animal neurons, then experimental design would have been modified to introduce a modified DRG medium reflecting DN conditions. Since excitability changes were observed early in the course of the experimental period, it was agreed to proceed with the current method. However, it would be interesting to see whether maintaining neurons in a high glucose/NGF/insulin medium prior to experiments would produce a starker phenotype to the one observed here.

The scope of this study was limited to Ca^{2+} imaging experiments and some analysis of cell size and distribution. These were isolated experiments, unsupported by our own behavioural, structural, or other data. Further experiments are needed to fully understand the mechanisms underlying the DN-induced changes in neuronal excitability observed here. Is the increase in excitability in nociceptors due to altered expression and/or activity levels of a particular VGSC? Is the increase in sensitivity to CAP due to increased TRPV1 expression or simply enhanced activation? Immunohistochemistry experiments tracing changes in expression levels of ion channels during the MET and NEU phases of DN implicated would contribute to answering these questions. Are neurons from diabetic mice shrinking or apoptotic? Quantitative analysis of neurons' apoptotic tendencies throughout DN progression (e.g., using nuclei-labelling techniques) can provide insights. Further experiments would add to the physiological data provided by this research and contribute to a complete study on the DN phenotype progression in the *db/db* mouse sensory neurons.

6.4. CONCLUSION

The journey of this project started with the establishment of the VTD- Ca^{2+} imaging assay as able to discriminate between nociceptors and non-nociceptors via the VTD-response profiles generated by DRG neurons. It was then taken forward towards different applications including as a screening platform for ion channel blockers, individually or in combination, assessing their efficiency and safety. The application of the VTD- Ca^{2+} imaging assay as a tool for characterising neuropathological conditions was explored in the context of diabetic neuropathy *in vitro* as well as *in vivo*. By employing VTD- Ca^{2+} imaging as well as nociceptive agonists, we demonstrated that diabetic neuropathy produces excitability changes in distinct

subpopulation of DRG neurons from T2D *db/db* mice in the early, MET and late, NEU phase of the disease's course. This is the first detailed physiological characterisation of the diabetic neuropathy-driven excitability changes at the different phases in the T2D *db/db* mouse model. Identifying distinct neuronal subpopulations affected during DN could aid in their better targeting by novel pharmacological interventions developed. Finally, the VTD-Ca²⁺ imaging assay can have multiple applications, including as a screening platform and disease and iPSCs characterisation tool. In the future, this work can take several directions, for example focusing on the improvement of the VTD-Ca²⁺ imaging assay and its analysis process; and/or further characterisation of the *db/db* mouse model of DN and the identity of the neurons most affected during the different stages. Overall, this research hopes to eventually contribute to elucidating the complex mechanisms underlying diabetic neuropathy and aid in bridging the gap between pre-clinical and clinical research for treating this currently untreatable disease.

BIBLIOGRAPHY

1. Emery, E. C. & Ernfors, P. Dorsal Root Ganglion Neuron Types and Their Functional Specialization. (2018) doi:10.1093/OXFORDHB/9780190860509.013.4.
2. Gerhard, D. Neuroscience. 5th Edition. *Yale J. Biol. Med.* (2013).
3. Emery, E. C. *et al.* In vivo characterization of distinct modality-specific subsets of somatosensory neurons using GCaMP. *Sci. Adv.* (2016) doi:10.1126/sciadv.1600990.
4. Schmidt, R. *et al.* Novel classes of responsive and unresponsive C nociceptors in human skin. *J. Neurosci.* **15**, 333–341 (1995).
5. Gasser, H. The Classification of Nerve Fibers. (1941).
6. Gasser, H. S. & Erlanger, J. The Action Potential in Fibers of Slow Conduction in Spinal Roots and Somatic Nerves. *Exp. Biol. Med.* **26**, 647–649 (1929).
7. Lumpkin, E. A., Marshall, K. L. & Nelson, A. M. The cell biology of touch. *Journal of Cell Biology* (2010) doi:10.1083/jcb.201006074.
8. Djouhri, L. & Lawson, S. N. A β -fiber nociceptive primary afferent neurons: A review of incidence and properties in relation to other afferent A-fiber neurons in mammals. in *Brain Research Reviews* vol. 46 131–145 (Brain Res Brain Res Rev, 2004).
9. Li, L. *et al.* The functional organization of cutaneous low-threshold mechanosensory neurons. *Cell* **147**, 1615–1627 (2011).
10. Djouhri, L. A δ -fiber low threshold mechanoreceptors innervating mammalian hairy skin: A review of their receptive, electrophysiological and cytochemical properties in relation to A δ -fiber high threshold mechanoreceptors. *Neuroscience and Biobehavioral Reviews* vol. 61 225–238 (2016).
11. Djouhri, L. & Lawson, S. N. A β -fiber nociceptive primary afferent neurons: A review of incidence and properties in relation to other afferent A-fiber neurons in mammals. in *Brain Research Reviews* vol. 46 131–145 (Elsevier, 2004).
12. Yam, M. *et al.* General Pathways of Pain Sensation and the Major Neurotransmitters Involved in Pain Regulation. *Int. J. Mol. Sci.* **19**, 2164 (2018).
13. Basbaum, A. I., Bautista, D. M., Scherrer, G. & Julius, D. Cellular and Molecular Mechanisms of Pain. *Cell* vol. 139 267–284 (2009).
14. Usoskin, D. *et al.* Unbiased classification of sensory neuron types by large-scale single-cell RNA sequencing. *Nat. Neurosci.* **18**, 145–153 (2015).
15. Li, C. L. *et al.* Somatosensory neuron types identified by high-coverage single-cell RNA-sequencing and functional heterogeneity. *Cell Res.* **26**, 83–102 (2016).
16. Li, C., Wang, S., Chen, Y. & Zhang, X. Somatosensory Neuron Typing with High-Coverage Single-Cell RNA Sequencing and Functional Analysis. *Neuroscience Bulletin* vol. 34 200–207 (2018).
17. Zeisel, A. *et al.* Molecular Architecture of the Mouse Nervous System. *Cell* **174**, 999–1014.e22 (2018).
18. Yam, M. F. *et al.* General pathways of pain sensation and the major neurotransmitters involved in pain regulation. *International Journal of Molecular Sciences* vol. 19 (2018).
19. Kim, M.-H., Korogod, N., Schneggenburger, R., Ho, W.-K. & Lee, S.-H. Interplay between Na⁺/Ca²⁺ Exchangers and Mitochondria in Ca²⁺ Clearance at the Calyx of Held. *J. Neurosci.* **25**, 6057–6065 (2005).

20. P. Verdru, C. G. L. M. Na⁺-Ca²⁺ exchange in rat dorsal root ganglion neurons. *J. Neurophysiol.* **77**, 484–490 (1997).
21. Waxman, S. G. & Zamponi, G. W. Regulating excitability of peripheral afferents: Emerging ion channel targets. *Nature Neuroscience* vol. 17 153–163 (2014).
22. Bouhassira, D., Lantéri-Minet, M., Attal, N., Laurent, B. & Touboul, C. Prevalence of chronic pain with neuropathic characteristics in the general population. *Pain* **136**, 380–387 (2008).
23. Van Hecke, O., Austin, S. K., Khan, R. A., Smith, B. H. & Torrance, N. Neuropathic pain in the general population: A systematic review of epidemiological studies. *Pain* vol. 155 654–662 (2014).
24. Schreiber, A. K. Diabetic neuropathic pain: Physiopathology and treatment. *World J. Diabetes* **6**, 432 (2015).
25. Bennett, M. I. *et al.* Prevalence and aetiology of neuropathic pain in cancer patients: A systematic review. *Pain* **153**, 359–365 (2012).
26. Stavros, K. & Simpson, D. M. Understanding the etiology and management of HIV-associated peripheral neuropathy. *Current HIV/AIDS reports* vol. 11 195–201 (2014).
27. Thakur, S., Dworkin, R. H., Haroun, O. M. O., Lockwood, D. N. J. & Rice, A. S. C. Acute and chronic pain associated with leprosy. *Pain* vol. 156 998–1002 (2015).
28. Saab, C. Y., Waxman, S. G. & Hains, B. C. Alarm or curse? The pain of neuroinflammation. *Brain Research Reviews* vol. 58 226–235 (2008).
29. Colloca, L. *et al.* Neuropathic pain. *Nat. Rev. Dis. Prim.* **3**, 1–19 (2017).
30. Pasero, C. Pathophysiology of neuropathic pain. *Pain Manag. Nurs.* (2004) doi:10.1016/j.pmn.2004.10.002.
31. Rogers, M., Tang, L., Madge, D. J. & Stevens, E. B. The role of sodium channels in neuropathic pain. *Seminars in Cell and Developmental Biology* vol. 17 571–581 (2006).
32. Brederson, J. D., Kym, P. R. & Szallasi, A. Targeting TRP channels for pain relief. *European Journal of Pharmacology* vol. 716 61–76 (2013).
33. Emery, E. C., Luiz, A. P. & Wood, J. N. Nav1.7 and other voltage-gated sodium channels as drug targets for pain relief. *Expert Opin. Ther. Targets* **20**, 975–983 (2016).
34. Zamponi, G. W., Gandini, M. A. & Snutch, T. P. Voltage-Gated Calcium Channels: Molecular Targets for Treating Chronic Pain . (2019) doi:10.1093/oxfordhb/9780190860509.013.7.
35. Goldin, A. L. *et al.* Messenger RNA coding for only the α subunit of the rat brain Na channel is sufficient for expression of functional channels in *Xenopus* oocytes. *Proc. Natl. Acad. Sci. U. S. A.* (1986) doi:10.1073/pnas.83.19.7503.
36. Brackenbury, W. J. & Isom, L. L. Na⁺ channel β subunits: Overachievers of the ion channel family. *Front. Pharmacol.* (2011) doi:10.3389/fphar.2011.00053.
37. Matsumoto, M. *et al.* Channel properties of Nax expressed in neurons. *PLoS One* (2015) doi:10.1371/journal.pone.0126109.
38. Dib-Hajj, S. D. *et al.* Two tetrodotoxin-resistant sodium channels in human dorsal root ganglion neurons. *FEBS Lett.* (1999) doi:10.1016/S0014-5793(99)01519-7.
39. Sangameswaran, L. *et al.* A novel tetrodotoxin-sensitive, voltage-gated sodium channel expressed in rat and human dorsal root ganglia. *J. Biol. Chem.* (1997) doi:10.1074/jbc.272.23.14805.
40. Zhang, X., Priest, B. T., Belfer, I. & Gold, M. S. Voltage-gated Na⁺ currents in human dorsal root ganglion neurons. *Elife* (2017) doi:10.7554/eLife.23235.
41. Roy, M. L. & Narahashi, T. Differential properties of tetrodotoxin-sensitive and tetrodotoxin-

- resistant sodium channels in rat dorsal root ganglion neurons. *J. Neurosci.* (1992) doi:10.1523/jneurosci.12-06-02104.1992.
42. Dib-Hajj, S. D., Cummins, T. R., Black, J. A. & Waxman, S. G. Sodium Channels in Normal and Pathological Pain. *Annu. Rev. Neurosci.* **33**, 325–347 (2010).
 43. Goldin, A. L. Resurgence of sodium channel research. *Annual Review of Physiology* (2001) doi:10.1146/annurev.physiol.63.1.871.
 44. Waxman, S. G., Kocsis, J. D. & Black, J. A. Type III sodium channel mRNA is expressed in embryonic but not adult spinal sensory neurons, and is reexpressed following axotomy. *J. Neurophysiol.* **72**, 466–470 (1994).
 45. Hains, B. C. *et al.* Upregulation of sodium channel Nav1.3 and functional involvement in neuronal hyperexcitability associated with central neuropathic pain after spinal cord injury. *J. Neurosci.* **23**, 8881–8892 (2003).
 46. Hains, B. C., Saab, C. Y., Klein, J. P., Craner, M. J. & Waxman, S. G. Altered sodium channel expression in second-order spinal sensory neurons contributes to pain after peripheral nerve injury. *J. Neurosci.* (2004) doi:10.1523/JNEUROSCI.0300-04.2004.
 47. Lindia, J. A., Köhler, M. G., Martin, W. J. & Abbadie, C. Relationship between sodium channel Nav1.3 expression and neuropathic pain behavior in rats. *Pain* **117**, 145–153 (2005).
 48. Samad, O. A. *et al.* Virus-mediated shRNA knockdown of Na v 1.3 in rat dorsal root ganglion attenuates nerve injury-induced neuropathic pain. *Mol. Ther.* (2013) doi:10.1038/mt.2012.169.
 49. Tan, A. M., Samad, O. A., Dib-Hajj, S. D. & Waxman, S. G. Virus-mediated knockdown of Nav1.3 in dorsal root ganglia of STZ-induced diabetic rats alleviates tactile allodynia. *Mol. Med.* (2015) doi:10.2119/molmed.2015.00063.
 50. Caldwell, J. H., Schaller, K. L., Lasher, R. S., Peles, E. & Levinson, S. R. Sodium channel Nav1.6 is localized at nodes of Ranvier, dendrites, and synapses. *Proc. Natl. Acad. Sci. U. S. A.* (2000) doi:10.1073/pnas.090034797.
 51. Chen, L. *et al.* Conditional knockout of Nav1.6 in adult mice ameliorates neuropathic pain. *Sci. Rep.* (2018) doi:10.1038/s41598-018-22216-w.
 52. Cummins, T. R., Dib-Hajj, S. D., Herzog, R. I. & Waxman, S. G. Nav1.6 channels generate resurgent sodium currents in spinal sensory neurons. *FEBS Lett.* (2005) doi:10.1016/j.febslet.2005.03.009.
 53. Herzog, R. I., Cummins, T. R., Ghassemi, F., Dib-Hajj, S. D. & Waxman, S. G. Distinct repriming and closed-state inactivation kinetics of Nav1.6 and Nav1.7 sodium channels in mouse spinal sensory neurons. *J. Physiol.* (2003) doi:10.1113/jphysiol.2003.047357.
 54. Tanaka, B. S. *et al.* A gain-of-function mutation in Nav1.6 in a case of trigeminal neuralgia. *Mol. Med.* (2016) doi:10.2119/molmed.2016.00131.
 55. Xie, W., Strong, J. A. & Zhang, J. M. Local knockdown of the Nav1.6 sodium channel reduces pain behaviors, sensory neuron excitability, and sympathetic sprouting in rat models of neuropathic pain. *Neuroscience* (2015) doi:10.1016/j.neuroscience.2015.02.010.
 56. Xie, W. *et al.* Upregulation of the sodium channel Na v β 4 subunit and its contributions to mechanical hypersensitivity and neuronal hyperexcitability in a rat model of radicular pain induced by local dorsal root ganglion inflammation. *Pain* (2016) doi:10.1097/j.pain.0000000000000453.
 57. Berta, T. *et al.* Transcriptional and functional profiles of voltage-gated Na⁺ channels in injured and non-injured DRG neurons in the SNI model of neuropathic pain. *Mol. Cell. Neurosci.* (2008) doi:10.1016/j.mcn.2007.09.007.
 58. Hong, S., Morrow, T. J., Paulson, P. E., Isom, L. L. & Wiley, J. W. Early painful diabetic neuropathy is associated with differential changes in tetrodotoxin-sensitive and -resistant

- sodium channels in dorsal root ganglion neurons in the rat. *J. Biol. Chem.* **279**, 29341–29350 (2004).
59. Henry, M. A., Freking, A. R., Johnson, L. R. & Levinson, S. R. Sodium channel Nav1.6 accumulates at the site of infraorbital nerve injury. *BMC Neurosci.* (2007) doi:10.1186/1471-2202-8-56.
 60. Ren, Y. S. *et al.* Sodium channel Nav1.6 is up-regulated in the dorsal root ganglia in a mouse model of type 2 diabetes. *Brain Res. Bull.* **87**, 244–249 (2012).
 61. Toledo-Aral, J. J. *et al.* Identification of PN1, a predominant voltage-dependent sodium channel expressed principally in peripheral neurons. *Proc. Natl. Acad. Sci. U. S. A.* (1997) doi:10.1073/pnas.94.4.1527.
 62. Dib-Hajj, S. D., Yang, Y., Black, J. A. & Waxman, S. G. The Na^v 1.7 sodium channel: From molecule to man. *Nature Reviews Neuroscience* vol. 14 49–62 (2013).
 63. Weiss, J. *et al.* Loss-of-function mutations in sodium channel Na^v 1.7 cause anosmia. *Nature* (2011) doi:10.1038/nature09975.
 64. Ahn, H. S. *et al.* Nav1.7 is the predominant sodium channel in rodent olfactory sensory neurons. *Mol. Pain* (2011) doi:10.1186/1744-8069-7-32.
 65. Branco, T. *et al.* Near-Perfect Synaptic Integration by Nav1.7 in Hypothalamic Neurons Regulates Body Weight. *Cell* (2016) doi:10.1016/j.cell.2016.05.019.
 66. Zhang, Q. *et al.* Na⁺ current properties in islet α - and β -cells reflect cell-specific Scn3a and Scn9a expression. *J. Physiol.* (2014) doi:10.1113/jphysiol.2014.274209.
 67. Cummins, T. R., Howe, J. R. & Waxman, S. G. Slow closed-state inactivation: A novel mechanism underlying ramp currents in cells expressing the hNE/PN1 sodium channel. *J. Neurosci.* **18**, 9607–9619 (1998).
 68. Drenth, J. P. H. & Waxman, S. G. Mutations in sodium-channel gene SCN9A cause a spectrum of human genetic pain disorders. *Journal of Clinical Investigation* (2007) doi:10.1172/JCI33297.
 69. Yang, Y. *et al.* Mutations in SCN9A, encoding a sodium channel α subunit, in patients with primary erythromelgia. *J. Med. Genet.* (2004) doi:10.1136/jmg.2003.012153.
 70. Dib-Hajj, S. D. *et al.* Gain-of-function mutation in Nav1.7 in familial erythromelgia induces bursting of sensory neurons. *Brain* **128**, 1847–1854 (2005).
 71. Cummins, T. R., Dib-Hajj, S. D. & Waxman, S. G. Electrophysiological properties of mutant Nav1.7 sodium channels in a painful inherited neuropathy. *J. Neurosci.* (2004) doi:10.1523/JNEUROSCI.2695-04.2004.
 72. Fertleman, C. R. *et al.* SCN9A Mutations in Paroxysmal Extreme Pain Disorder: Allelic Variants Underlie Distinct Channel Defects and Phenotypes. *Neuron* (2006) doi:10.1016/j.neuron.2006.10.006.
 73. Jarecki, B. W., Piekarz, A. D., Jackson, J. O. & Cummins, T. R. Human voltage-gated sodium channel mutations that cause inherited neuronal and muscle channelopathies increase resurgent sodium currents. *J. Clin. Invest.* (2010) doi:10.1172/JCI40801.
 74. Theile, J. W., Jarecki, B. W., Piekarz, A. D. & Cummins, T. R. Nav1.7 mutations associated with paroxysmal extreme pain disorder, but not erythromelgia, enhance Nav β 4 peptide-mediated resurgent sodium currents. *J. Physiol.* (2011) doi:10.1113/jphysiol.2010.200915.
 75. Faber, C. G. *et al.* Gain of function Na^v1.7 mutations in idiopathic small fiber neuropathy. *Ann. Neurol.* (2012) doi:10.1002/ana.22485.
 76. Blesneac, I. *et al.* Rare Nav1.7 variants associated with painful diabetic peripheral neuropathy. *Pain* **159**, 469–480 (2018).
 77. Cox, J. J. *et al.* An SCN9A channelopathy causes congenital inability to experience pain.

- Nature* **444**, 894–898 (2006).
78. McDermott, L. A. *et al.* Defining the Functional Role of Na V 1.7 in Human Nociception. (2019) doi:10.1016/j.neuron.2019.01.047.
 79. Estacion, M. *et al.* A sodium channel gene SCN9A polymorphism that increases nociceptor excitability. *Ann. Neurol.* (2009) doi:10.1002/ana.21895.
 80. Reimann, F. *et al.* Pain perception is altered by a nucleotide polymorphism in SCN9A. *Proc. Natl. Acad. Sci.* **107**, 5148–5153 (2010).
 81. Gingras, J. *et al.* Global Nav1.7 Knockout Mice Recapitulate the Phenotype of Human Congenital Indifference to Pain. *PLoS One* **9**, e105895 (2014).
 82. Nassar, M. A. *et al.* Nociceptor-specific gene deletion reveals a major role for Na v 1.7 (PN1) in acute and inflammatory pain. www.pnas.org/cgi/doi/10.1073/pnas.0404915101 (2004).
 83. Hoffmann, T. *et al.* Nav1.7 and pain: contribution of peripheral nerves. *Pain* (2018) doi:10.1097/j.pain.0000000000001119.
 84. Minett, M. S. *et al.* Distinct Nav1.7-dependent pain sensations require different sets of sensory and sympathetic neurons. *Nat. Commun.* (2012) doi:10.1038/ncomms1795.
 85. Wheeler, D. W., Lee, M. C. H., Harrison, E. K., Menon, D. K. & Woods, C. G. Case Report: Neuropathic pain in a patient with congenital insensitivity to pain. *F1000Research* **3**, (2015).
 86. Minett, M. S. *et al.* Pain without nociceptors? Nav1.7-independent pain mechanisms. *Cell Rep.* **6**, 301–312 (2014).
 87. Akopian, A. N., Sivilotti, L. & Wood, J. N. A tetrodotoxin-resistant voltage-gated sodium channel expressed by sensory neurons. *Nature* **379**, 257 (1996).
 88. Sangameswaran, L. *et al.* Structure and function of a novel voltage-gated, tetrodotoxin-resistant sodium channel specific to sensory neurons. *J. Biol. Chem.* (1996) doi:10.1074/jbc.271.11.5953.
 89. Djouhri, L. *et al.* The TTX-resistant sodium channel Nav 1.8 (SNS/PN3): Expression and correlation with membrane properties in rat nociceptive primary afferent neurons. *J. Physiol.* **550**, 739–752 (2003).
 90. Shields, S. D. *et al.* Na v1.8 expression is not restricted to nociceptors in mouse peripheral nervous system. *Pain* (2012) doi:10.1016/j.pain.2012.04.022.
 91. Verkerk, A. O. *et al.* Functional Nav1.8 channels in intracardiac neurons: The link between SCN10A and cardiac electrophysiology. *Circ. Res.* (2012) doi:10.1161/CIRCRESAHA.112.274035.
 92. Renganathan, M., Cummins, T. R. & Waxman, S. G. Contribution of Nav 1.8 sodium channels to action potential electrogenesis in DRG neurons. *J. Neurophysiol.* (2001) doi:10.1152/jn.2001.86.2.629.
 93. Blair, N. T. & Bean, B. P. Roles of tetrodotoxin (TTX)-sensitive Na⁺ current, TTX-resistant Na⁺ current, and Ca²⁺ current in the action potentials of nociceptive sensory neurons. *J. Neurosci.* (2002) doi:10.1523/jneurosci.22-23-10277.2002.
 94. Faber, C. G. *et al.* Gain-of-function Nav1.8 mutations in painful neuropathy. *Proc. Natl. Acad. Sci. U. S. A.* **109**, 19444–19449 (2012).
 95. Huang, J. *et al.* Small-fiber neuropathy Nav1.8 mutation shifts activation to hyperpolarized potentials and increases excitability of dorsal root ganglion neurons. *J. Neurosci.* (2013) doi:10.1523/JNEUROSCI.2710-13.2013.
 96. Han, C. *et al.* The G1662S Nav1.8 mutation in small fibre neuropathy: Impaired inactivation underlying DRG neuron hyperexcitability. *J. Neurol. Neurosurg. Psychiatry* (2014) doi:10.1136/jnnp-2013-306095.

97. Akopian, A. N. *et al.* The tetrodotoxin-resistant sodium channel SNS has a specialized function in pain pathways. *Nat. Neurosci.* (1999) doi:10.1038/9195.
98. Kerr, B. J., Souslova, V., McMahon, S. B. & Wood, J. N. A role for the TTX-resistant sodium channel Nav 1.8 in NGF-induced hyperalgesia, but not neuropathic pain. *Neuroreport* **12**, 3077–3080 (2001).
99. Abrahamsen, B. *et al.* The cell and molecular basis of mechanical, cold, and inflammatory pain. *Science* (80-.). (2008) doi:10.1126/science.1156916.
100. Lai, J. *et al.* Inhibition of neuropathic pain by decreased expression of the tetrodotoxin-resistant sodium channel, Nav1.8. *Pain* (2002) doi:10.1016/S0304-3959(01)00391-8.
101. Nassar, M. A., Levato, A., Stirling, L. C. & Wood, J. N. Neuropathic pain develops normally in mice lacking both Nav 1.7 and Nav 1.8. *Mol. Pain* **1**, 24 (2005).
102. Dib-Hajj, S., Black, J. A., Felts, P. & Waxman, S. G. Down-regulation of transcripts for Na channel α -SNS in spinal sensory neurons following axotomy. *Proc. Natl. Acad. Sci. U. S. A.* **93**, 14950–14954 (1996).
103. Gold, M. S. *et al.* Redistribution of Nav1.8 in uninjured axons enables neuropathic pain. *J. Neurosci.* (2003) doi:10.1523/jneurosci.23-01-00158.2003.
104. Coward, K. *et al.* Immunolocalization of SNS/PN3 and NaN/SNS2 sodium channels in human pain states. *Pain* (2000) doi:10.1016/S0304-3959(99)00251-1.
105. Black, J. A., Liu, S., Tanaka, M., Cummins, T. R. & Waxman, S. G. Changes in the expression of tetrodotoxin-sensitive sodium channels within dorsal root ganglia neurons in inflammatory pain. *Pain* **108**, 237–247 (2004).
106. Gold, M. S., Reichling, D. B., Shuster, M. J. & Levine, J. D. Hyperalgesic agents increase a tetrodotoxin-resistant Na⁺ current in nociceptors. *Proc. Natl. Acad. Sci. U. S. A.* (1996) doi:10.1073/pnas.93.3.1108.
107. Fitzgerald, E. M., Okuse, K., Wood, J. N., Dolphin, A. C. & Moss, S. J. cAMP-dependent phosphorylation of the tetrodotoxin-resistant voltage-dependent sodium channel SNS. *J. Physiol.* (1999) doi:10.1111/j.1469-7793.1999.0433v.x.
108. Hudmon, A. *et al.* Phosphorylation of sodium channel Nav1.8 by p38 mitogen-activated protein kinase increases current density in dorsal root ganglion neurons. *J. Neurosci.* (2008) doi:10.1523/JNEUROSCI.4403-07.2008.
109. Cummins, T. R. *et al.* A novel persistent tetrodotoxin-resistant sodium current in SNS-null and wild-type small primary sensory neurons. *J. Neurosci.* (1999) doi:10.1523/jneurosci.19-24-j0001.1999.
110. Fang, X. *et al.* Intense isolectin-B4 binding in rat dorsal root ganglion neurons distinguishes C-fiber nociceptors with broad action potentials and high Nav1.9 expression. *J. Neurosci.* (2006) doi:10.1523/JNEUROSCI.1072-06.2006.
111. Fang, X. *et al.* The presence and role of the tetrodotoxin-resistant sodium channel Nav1.9 (NaN) in nociceptive primary afferent neurons. *J. Neurosci.* (2002) doi:10.1523/jneurosci.22-17-07425.2002.
112. Huang, J. *et al.* Gain-of-function mutations in sodium channel Nav1.9 in painful neuropathy. *Brain* (2014) doi:10.1093/brain/awu079.
113. Zhang, X. Y. *et al.* Gain-of-Function mutations in SCN11A cause familial episodic pain. *Am. J. Hum. Genet.* (2013) doi:10.1016/j.ajhg.2013.09.016.
114. Han, C. *et al.* The Domain II S4-S5 Linker in Nav1.9: A Missense Mutation Enhances Activation, Impairs Fast Inactivation, and Produces Human Painful Neuropathy. *NeuroMolecular Med.* (2015) doi:10.1007/s12017-015-8347-9.
115. Leipold, E. *et al.* Cold-aggravated pain in humans caused by a hyperactive Nav1.9 channel

- mutant. *Nat. Commun.* (2015) doi:10.1038/ncomms10049.
116. Amaya, F. *et al.* The voltage-gated sodium channel Nav1.9 is an effector of peripheral inflammatory pain hypersensitivity. *J. Neurosci.* (2006) doi:10.1523/JNEUROSCI.4015-06.2006.
 117. Hillsley, K. *et al.* Dissecting the role of sodium currents in visceral sensory neurons in a model of chronic hyperexcitability using Nav 1.8 and Nav 1.9 null mice. *J. Physiol.* (2006) doi:10.1113/jphysiol.2006.113597.
 118. Wang, H. *et al.* Chronic neuropathic pain is accompanied by global changes in gene expression and shares pathobiology with neurodegenerative diseases. *Neuroscience* **114**, 529–546 (2002).
 119. Sleeper, A. A. *et al.* Changes in expression of two tetrodotoxin-resistant sodium channels and their currents in dorsal root ganglion neurons after sciatic nerve injury but not rhizotomy. *J. Neurosci.* (2000) doi:10.1523/jneurosci.20-19-07279.2000.
 120. Eriksson, J. *et al.* Behavioral changes and trigeminal ganglion sodium channel regulation in an orofacial neuropathic pain model. *Pain* (2005) doi:10.1016/j.pain.2005.09.019.
 121. Lolignier, S. *et al.* Nav1.9 channel contributes to mechanical and heat pain hypersensitivity induced by subacute and chronic inflammation. *PLoS One* (2011) doi:10.1371/journal.pone.0023083.
 122. Leo, S., D'Hooge, R. & Meert, T. Exploring the role of nociceptor-specific sodium channels in pain transmission using Na v1.8 and Na v1.9 knockout mice. *Behav. Brain Res.* (2010) doi:10.1016/j.bbr.2009.11.023.
 123. Priest, B. T. *et al.* Contribution of the tetrodotoxin-resistant voltage-gated sodium channel Nav1.9 to sensory transmission and nociceptive behavior. *Proc. Natl. Acad. Sci. U. S. A.* (2005) doi:10.1073/pnas.0501549102.
 124. Waxman, S. G. & Estacion, M. Nav1.9, G-proteins, and nociceptors. *J. Physiol.* (2008) doi:10.1113/jphysiol.2007.149922.
 125. Latorre, R., Zaelzer, C. & Brauchi, S. Structure-functional intimacies of transient receptor potential channels. *Q. Rev. Biophys.* **42**, 201–246 (2009).
 126. Damann, N., Voets, T. & Nilius, B. TRPs in Our Senses. *Current Biology* vol. 18 R880–R889 (2008).
 127. Uchida, K. & Tominaga, M. The role of thermosensitive TRP (transient receptor potential) channels in insulin secretion. *Endocrine Journal* vol. 58 1021–1028 (2011).
 128. Tominaga, M. Activation and regulation of nociceptive transient receptor potential (TRP) channels, TRPV1 and TRPA1. *Yakugaku Zasshi* vol. 130 289–294 (2010).
 129. Tominaga, M. Nociception and TRP channels. *Handb. Exp. Pharmacol.* (2007) doi:10.1007/978-3-540-34891-7_29.
 130. Tominaga, M. & Tominaga, T. Structure and function of TRPV1. *Pflugers Archiv European Journal of Physiology* vol. 451 143–150 (2005).
 131. Cavanaugh, D. J. *et al.* Trpv1 reporter mice reveal highly restricted brain distribution and functional expression in arteriolar smooth muscle cells. *J. Neurosci.* (2011) doi:10.1523/JNEUROSCI.6451-10.2011.
 132. Cavanaugh, D. J. *et al.* Restriction of transient receptor potential vanilloid-1 to the peptidergic subset of primary afferent neurons follows its developmental downregulation in nonpeptidergic neurons. *J. Neurosci.* **31**, 10119–10127 (2011).
 133. Zeilhofer, H. U., Kress, M. & Swandulla, D. Fractional Ca²⁺ currents through capsaicin- and proton-activated ion channels in rat dorsal root ganglion neurones. *J. Physiol.* (1997) doi:10.1111/j.1469-7793.1997.067bi.x.

134. Julius, D. TRP channels and pain. *Annual Review of Cell and Developmental Biology* (2013) doi:10.1146/annurev-cellbio-101011-155833.
135. Jordt, S. E. & Julius, D. Molecular basis for species-specific sensitivity to 'hot' chili peppers. *Cell* (2002) doi:10.1016/S0092-8674(02)00637-2.
136. Jung, J. *et al.* Capsaicin binds to the intracellular domain of the capsaicin-activated ion channel. *J. Neurosci.* (1999) doi:10.1523/jneurosci.19-02-00529.1999.
137. Jordt, S. E., Tominaga, M. & Julius, D. Acid potentiation of the capsaicin receptor determined by a key extracellular site. *Proc. Natl. Acad. Sci. U. S. A.* (2000) doi:10.1073/pnas.100129497.
138. Welch, J. M., Simon, S. A. & Reinhart, P. H. The activation mechanism of rat vanilloid receptor 1 by capsaicin involves the pore domain and differs from the activation by either acid or heat. *Proc. Natl. Acad. Sci. U. S. A.* (2000) doi:10.1073/pnas.230146497.
139. Kaszas, K. *et al.* Small molecule positive allosteric modulation of TRPV1 activation by vanilloids and acidic pH. *J. Pharmacol. Exp. Ther.* (2012) doi:10.1124/jpet.111.183053.
140. Tominaga, M. *et al.* The cloned capsaicin receptor integrates multiple pain-producing stimuli. *Neuron* **21**, 531–543 (1998).
141. Caterina, M. J. & Julius, D. The vanilloid receptor: A molecular gateway to the pain pathway. *Annual Review of Neuroscience* (2001) doi:10.1146/annurev.neuro.24.1.487.
142. Chuang, H. *et al.* Bradykinin and nerve growth factor release the capsaicin receptor from PtdIns(4,5)P₂-mediated inhibition. *Nature* **411**, 957–962 (2001).
143. Crandall, M., Kwash, J., Yu, W. & White, G. Activation of protein kinase C sensitizes human VR1 to capsaicin and to moderate decreases in pH at physiological temperatures in *Xenopus* oocytes. *Pain* **98**, 109–117 (2002).
144. Numazaki, M., Tominaga, T., Toyooka, H. & Tominaga, M. Direct Phosphorylation of Capsaicin Receptor VR1 by Protein Kinase C ϵ and Identification of Two Target Serine Residues. *J. Biol. Chem.* **277**, 13375–13378 (2002).
145. Rathee, P. K. *et al.* PKA/AKAP/VR-1 Module: A Common Link of Gs-Mediated Signaling to Thermal Hyperalgesia. *J. Neurosci.* (2002) doi:10.1523/jneurosci.22-11-04740.2002.
146. Hwang, S. W. *et al.* Direct activation of capsaicin receptors by products of lipoxygenases: Endogenous capsaicin-like substances. *Proc. Natl. Acad. Sci.* **97**, 6155–6160 (2000).
147. Planells-Cases, R., García-Sanz, N., Morenilla-Palao, C. & Ferrer-Montiel, A. Functional aspects and mechanisms of TRPV1 involvement in neurogenic inflammation that leads to thermal hyperalgesia. *Pflügers Arch. - Eur. J. Physiol.* **451**, 151–159 (2005).
148. Caterina, M. J. *et al.* Impaired nociception and pain sensation in mice lacking the capsaicin receptor. *Science* (80-.). **288**, 306–313 (2000).
149. Davis, J. B. *et al.* Vanilloid receptor-1 is essential for inflammatory thermal hyperalgesia. *Nature* **405**, 183–187 (2000).
150. García-Martínez, C. *et al.* Attenuation of thermal nociception and hyperalgesia by VR1 blockers. *Proc. Natl. Acad. Sci. U. S. A.* (2002) doi:10.1073/pnas.022285899.
151. Bölcskei, K. *et al.* Investigation of the role of TRPV1 receptors in acute and chronic nociceptive processes using gene-deficient mice. *Pain* (2005) doi:10.1016/j.pain.2005.06.024.
152. Kanai, Y., Nakazato, E., Fujiuchi, A., Hara, T. & Imai, A. Involvement of an increased spinal TRPV1 sensitization through its up-regulation in mechanical allodynia of CCI rats. *Neuropharmacology* (2005) doi:10.1016/j.neuropharm.2005.05.003.
153. Yamamoto, W., Sugiura, A., Nakazato-Imasato, E. & Kita, Y. Characterization of primary sensory neurons mediating static and dynamic allodynia in rat chronic constriction injury model. *J. Pharm. Pharmacol.* (2008) doi:10.1211/jpp.60.6.0006.

154. Fukuoka, T. *et al.* VR1, but not P2X3, increases in the spared L4 DRG in rats with L5 spinal nerve ligation. *Pain* (2002) doi:10.1016/S0304-3959(02)00067-2.
155. Pan, H. L., Zhang, Y. Q. & Zhao, Z. Q. Involvement of lysophosphatidic acid in bone cancer pain by potentiation of TRPV1 via PKC ϵ pathway in dorsal root ganglion neurons. *Mol. Pain* (2010) doi:10.1186/1744-8069-6-85.
156. Pabbidi, R. M. *et al.* Influence of TRPV1 on diabetes-induced alterations in thermal pain sensitivity. *Mol. Pain* **4**, (2008).
157. Gunthorpe, M. J. & Chizh, B. A. Clinical development of TRPV1 antagonists: targeting a pivotal point in the pain pathway. *Drug Discovery Today* (2009) doi:10.1016/j.drudis.2008.11.005.
158. Takahashi, N. *et al.* Molecular characterization of TRPA1 channel activation by cysteine-reactive inflammatory mediators. *Channels* (2008) doi:10.4161/chan.2.4.6745.
159. Barabas, M. E., Kossyrev, E. A. & Stucky, C. L. TRPA1 Is Functionally Expressed Primarily by IB4-Binding, Non-Peptidergic Mouse and Rat Sensory Neurons. *PLoS One* **7**, (2012).
160. Story, G. M. *et al.* ANKTM1, a TRP-like channel expressed in nociceptive neurons, is activated by cold temperatures. *Cell* **112**, 819–829 (2003).
161. Fischer, M. J. M. *et al.* Direct evidence for functional TRPV1/TRPA1 heteromers. *Pflugers Arch. Eur. J. Physiol.* (2014) doi:10.1007/s00424-014-1497-z.
162. Corey, D. P. *et al.* TRPA1 is a candidate for the mechanosensitive transduction channel of vertebrate hair cells. *Nature* (2004) doi:10.1038/nature03066.
163. Jordt, S.-E. *et al.* Mustard oils and cannabinoids excite sensory nerve fibres through the TRP channel ANKTM1. *Nature* **427**, 260–265 (2004).
164. Bandell, M. *et al.* Noxious cold ion channel TRPA1 is activated by pungent compounds and bradykinin. *Neuron* (2004) doi:10.1016/S0896-6273(04)00150-3.
165. Bautista, D. M. *et al.* TRPA1 Mediates the Inflammatory Actions of Environmental Irritants and Proalgesic Agents. *Cell* **124**, 1269–1282 (2006).
166. Karashima, Y. *et al.* TRPA1 acts as a cold sensor in vitro and in vivo. *Proc. Natl. Acad. Sci.* **106**, 1273–1278 (2009).
167. Jaquemar, D., Schenker, T. & Trueb, B. An ankyrin-like protein with transmembrane domains is specifically lost after oncogenic transformation of human fibroblasts. *J. Biol. Chem.* (1999) doi:10.1074/jbc.274.11.7325.
168. Nagata, K., Duggan, A., Kumar, G. & García-Añoveros, J. Nociceptor and hair cell transducer properties of TRPA1, a channel for pain and hearing. *J. Neurosci.* (2005) doi:10.1523/JNEUROSCI.0013-05.2005.
169. Bautista, D. M. *et al.* TRPA1 Mediates the Inflammatory Actions of Environmental Irritants and Proalgesic Agents. *Cell* (2006) doi:10.1016/j.cell.2006.02.023.
170. McKemy, D. D., Neuhausser, W. M. & Julius, D. Identification of a cold receptor reveals a general role for TRP channels in thermosensation. *Nature* (2002) doi:10.1038/nature719.
171. McNamara, C. R. *et al.* TRPA1 mediates formalin-induced pain. *Proc. Natl. Acad. Sci. U. S. A.* (2007) doi:10.1073/pnas.0705924104.
172. Petrus, M. *et al.* A role of TRPA1 in mechanical hyperalgesia is revealed by pharmacological inhibition. *Mol. Pain* (2007) doi:10.1186/1744-8069-3-40.
173. McGaraughty, S. *et al.* TRPA1 modulation of spontaneous and mechanically evoked firing of spinal neurons in uninjured, osteoarthritic, and inflamed rats. *Mol. Pain* (2010) doi:10.1186/1744-8069-6-14.
174. da Costa, D. S. M. *et al.* The involvement of the transient receptor potential A1 (TRPA1) in the

- maintenance of mechanical and cold hyperalgesia in persistent inflammation. *Pain* (2010) doi:10.1016/j.pain.2009.12.002.
175. Obata, K. *et al.* TRPA1 induced in sensory neurons contributes to cold hyperalgesia after inflammation and nerve injury. *J. Clin. Invest.* (2005) doi:10.1172/JCI25437.
176. Katsura, H. *et al.* Antisense knock down of TRPA1, but not TRPM8, alleviates cold hyperalgesia after spinal nerve ligation in rats. *Exp. Neurol.* (2006) doi:10.1016/j.expneurol.2006.01.031.
177. Caspani, O., Zurborg, S., Labuz, D. & Heppenstall, P. A. The Contribution of TRPM8 and TRPA1 Channels to Cold Allodynia and Neuropathic Pain. *PLoS One* **4**, e7383 (2009).
178. Staaf, S., Oerther, S., Lucas, G., Mattsson, J. P. & Ernfors, P. Differential regulation of TRP channels in a rat model of neuropathic pain. *Pain* (2009) doi:10.1016/j.pain.2009.04.013.
179. Eid, S. R. *et al.* HC-030031, a TRPA1 selective antagonist, attenuates inflammatory- and neuropathy-induced mechanical hypersensitivity. *Mol. Pain* (2008) doi:10.1186/1744-8069-4-48.
180. Wei, H. *et al.* Spinal transient receptor potential ankyrin 1 channel contributes to central pain hypersensitivity in various pathophysiological conditions in the rat. *Pain* (2011) doi:10.1016/j.pain.2010.11.031.
181. Kwan, K. Y., Glazer, J. M., Corey, D. P., Rice, F. L. & Stucky, C. L. TRPA1 modulates mechanotransduction in cutaneous sensory neurons. *J. Neurosci.* (2009) doi:10.1523/JNEUROSCI.5380-08.2009.
182. Kerstein, P. C., del Camino, D., Moran, M. M. & Stucky, C. L. Pharmacological blockade of TRPA1 inhibits mechanical firing in nociceptors. *Mol. Pain* (2009) doi:10.1186/1744-8069-5-19.
183. Zappia, K. J., O'Hara, C. L., Moehring, F., Kwan, K. Y. & Stucky, C. L. Sensory neuron-specific deletion of TRPA1 results in mechanical cutaneous sensory deficits. *eNeuro* (2017) doi:10.1523/ENEURO.0069-16.2017.
184. Wei, H., Hämäläinen, M. M., Saarnilehto, M., Koivisto, A. & Pertovaara, A. Attenuation of mechanical hypersensitivity by an antagonist of the TRPA1 ion channel in diabetic animals. *Anesthesiology* (2009) doi:10.1097/ALN.0b013e3181a1642b.
185. Viisanen, H. *et al.* Pronociceptive effects induced by cutaneous application of a transient receptor potential ankyrin 1 (TRPA1) channel agonist methylglyoxal in diabetic animals: Comparison with tunicamycin-induced endoplasmic reticulum stress. *J. Physiol. Pharmacol.* (2016).
186. Burnstock, G. *P2X receptors in sensory neurones.* *British Journal of Anaesthesia* vol. 84 (2000).
187. North, R. A. Molecular physiology of P2X receptors. *Physiological Reviews* (2002) doi:10.1152/physrev.00015.2002.
188. Vulchanova, L. *et al.* P2X3 is expressed by DRG neurons that terminate in inner lamina II. *Eur. J. Neurosci.* (1998).
189. Chen, C. C. *et al.* A P2X purinoceptor expressed by a subset of sensory neurons. *Nature* (1995) doi:10.1038/377428a0.
190. Giniatullin, R. & Nistri, A. Desensitization properties of P2X3 receptors shaping pain signaling. *Frontiers in Cellular Neuroscience* (2013) doi:10.3389/fncel.2013.00245.
191. Sokolova, E. *et al.* Experimental and modeling studies of desensitization of P2X3 receptors. *Mol. Pharmacol.* (2006) doi:10.1124/mol.106.023564.
192. Honore, P. *et al.* TNP-ATP, a potent P2X3 receptor antagonist, blocks acetic acid-induced abdominal constriction in mice: Comparison with reference analgesics. *Pain* (2002) doi:10.1016/S0304-3959(01)00434-1.

193. Jarvis, M. F. *et al.* Modulation of BzATP and formalin induced nociception: Attenuation by the P2X receptor antagonist, TNP-ATP and enhancement by the P2X3 allosteric modulator, cibacron blue. *Br. J. Pharmacol.* (2001) doi:10.1038/sj.bjp.0703793.
194. Ueno, S. *et al.* Involvement of P2X2 and P2X3 receptors in neuropathic pain in a mouse model of chronic constriction injury. in *Drug Development Research* (2003). doi:10.1002/ddr.10208.
195. McGaraughty, S. *et al.* Effects of A-317491, a novel and selective P2X₃/P2X_{2/3} receptor antagonist, on neuropathic, inflammatory and chemogenic nociception following intrathecal and intraplantar administration. *Br. J. Pharmacol.* (2003) doi:10.1038/sj.bjp.0705574.
196. Cockayne, D. A. *et al.* Urinary bladder hyporeflexia and reduced pain-related behaviour in P2X3-deficient mice. *Nature* (2000) doi:10.1038/35039519.
197. Souslova, V. *et al.* Warm-coding deficits and aberrant inflammatory pain in mice lacking P2X3 receptors. *Nature* **407**, 1015–1017 (2000).
198. Inoue, K., Tsuda, M. & Koizumi, S. ATP induced three types of pain behaviors, including allodynia. in *Drug Development Research* (2003). doi:10.1002/ddr.10201.
199. Honore, P. *et al.* Analgesic profile of intrathecal P2X3 antisense oligonucleotide treatment in chronic inflammatory and neuropathic pain states in rats. *Pain* (2002) doi:10.1016/S0304-3959(02)00032-5.
200. Barclay, J. *et al.* Functional downregulation of P2X3 receptor subunit in rat sensory neurons reveals a significant role in chronic neuropathic and inflammatory pain. *J. Neurosci.* (2002) doi:10.1523/jneurosci.22-18-08139.2002.
201. North, R. A. The P2X3 subunit: A molecular target in pain therapeutics. *Current Opinion in Investigational Drugs* (2003).
202. North, R. A. & Jarvis, M. F. P2X receptors as drug targets. *Molecular Pharmacology* (2013) doi:10.1124/mol.112.083758.
203. Ginnetti, A. T. *et al.* Identification of second-generation P2X3 antagonists for treatment of pain. *Bioorg. Med. Chem. Lett.* **28**, 1392–1396 (2018).
204. Cantin, L. D. *et al.* Discovery of P2X3 selective antagonists for the treatment of chronic pain. *Bioorganic Med. Chem. Lett.* (2012) doi:10.1016/j.bmcl.2012.01.124.
205. Sonksen, P. & Sonksen, J. Insulin: Understanding its action in health and disease. *Br. J. Anaesth.* (2000) doi:10.1093/bja/85.1.69.
206. Mendes, O., Koetzner, L. & Chen, J. Nutraceutical Impact on the Pathophysiology of Diabetes Mellitus. in *Nutritional and Therapeutic Interventions for Diabetes and Metabolic Syndrome* (2018). doi:10.1016/b978-0-12-812019-4.00026-x.
207. Jean-Marie, E. Diagnosis and classification of diabetes mellitus. in *Encyclopedia of Endocrine Diseases* (2018). doi:10.1016/B978-0-12-801238-3.65822-1.
208. Deshpande, A. D., Harris-Hayes, M. & Schootman, M. Epidemiology of Diabetes and Diabetes-Related Complications. *Phys. Ther.* **88**, 1254–1264 (2008).
209. Atkinson, M. A., Eisenbarth, G. S. & Michels, A. W. Type 1 diabetes. *The Lancet* vol. 383 69–82 (2014).
210. Maahs, D. M., West, N. A., Lawrence, J. M. & Mayer-Davis, E. J. Epidemiology of type 1 diabetes. *Endocrinology and Metabolism Clinics of North America* (2010) doi:10.1016/j.ecl.2010.05.011.
211. American Diabetes Association. Diagnosis and classification of diabetes mellitus. *Diabetes Care* **35 Suppl 1**, S64-71 (2012).
212. Mizokami-Stout, K. R. *et al.* The contemporary prevalence of diabetic neuropathy in type 1 diabetes: Findings from the T1D exchange. *Diabetes Care* (2020) doi:10.2337/dc19-1583.

213. Jeyam, A. *et al.* Diabetic neuropathy is a substantial burden in people with type 1 diabetes and is strongly associated with socioeconomic disadvantage: A population-representative study from Scotland. *Diabetes Care* (2020) doi:10.2337/dc19-1582.
214. Wang, Y. C., McPherson, K., Marsh, T., Gortmaker, S. L. & Brown, M. Health and economic burden of the projected obesity trends in the USA and the UK. *The Lancet* (2011) doi:10.1016/S0140-6736(11)60814-3.
215. DeFronzo, R. A. *et al.* Type 2 diabetes mellitus. *Nat. Rev. Dis. Prim.* **1**, (2015).
216. DeFronzo, R. A. Insulin resistance, lipotoxicity, type 2 diabetes and atherosclerosis: The missing links. The Claude Bernard Lecture 2009. *Diabetologia* (2010) doi:10.1007/s00125-010-1684-1.
217. Ozougwu, O. The pathogenesis and pathophysiology of type 1 and type 2 diabetes mellitus. *J. Physiol. Pathophysiol.* **4**, 46–57 (2013).
218. Martin, B. C. *et al.* Role of glucose and insulin resistance in development of type 2 diabetes mellitus: results of a 25-year follow-up study. *Lancet* **340**, 925–929 (1992).
219. Shulman, G. I. *et al.* Quantitation of Muscle Glycogen Synthesis in Normal Subjects and Subjects with Non-Insulin-Dependent Diabetes by ¹³C Nuclear Magnetic Resonance Spectroscopy. *N. Engl. J. Med.* (1990) doi:10.1056/nejm199001253220403.
220. DeFronzo, R. A. From the triumvirate to the ominous octet: A new paradigm for the treatment of type 2 diabetes mellitus. in *Diabetes* (2009). doi:10.2337/db09-9028.
221. Glimcher, L. H. & Lee, A. H. From sugar to fat: How the transcription factor XBP1 regulates hepatic lipogenesis. *Annals of the New York Academy of Sciences* (2009) doi:10.1111/j.1749-6632.2009.04956.x.
222. Fung, J. & Teicholz, N. *The Diabetes Code: Prevent and Reverse Type 2 Diabetes Naturally.* (Greystone Books, 2018).
223. Corkey, B. E. Banting lecture 2011: Hyperinsulinemia: Cause or consequence? *Diabetes* (2012) doi:10.2337/db11-1483.
224. Rizza, R. A., Mandarino, L. J., Genest, J., Baker, B. A. & Gerich, J. E. Production of insulin resistance by hyperinsulinaemia in man. *Diabetologia* (1985) doi:10.1007/BF00279918.
225. International Diabetes Federation. *IDF DIABETES ATLAS 9th edition 2019; IDF Diabetes Atlas* <https://diabetesatlas.org/data/en/country/128/mx.html> (2019).
226. Feldman, E. L. *et al.* Diabetic neuropathy. *Nature Reviews Disease Primers* vol. 5 1–18 (2019).
227. Partanen, J. *et al.* Natural History of Peripheral Neuropathy in Patients with Non-Insulin-Dependent Diabetes Mellitus. *N. Engl. J. Med.* (1995) doi:10.1056/nejm199507133330203.
228. Hicks, C. W. & Selvin, E. Epidemiology of Peripheral Neuropathy and Lower Extremity Disease in Diabetes. *Current Diabetes Reports* vol. 19 86 (2019).
229. Margolis, D. J. & Jeffcoate, W. Epidemiology of foot ulceration and amputation: Can global variation be explained? *Medical Clinics of North America* (2013) doi:10.1016/j.mcna.2013.03.008.
230. Pop-Busui, R. *et al.* Diabetic neuropathy: A position statement by the American diabetes association. *Diabetes Care* **40**, 136–154 (2017).
231. Abbott, C. A., Malik, R. A., Van Ross, E. R. E., Kulkarni, J. & Boulton, A. J. M. Prevalence and characteristics of painful diabetic neuropathy in a large community-based diabetic population in the U.K. *Diabetes Care* (2011) doi:10.2337/dc11-1108.
232. Callaghan, B. C., Cheng, H. T., Stables, C. L., Smith, A. L. & Feldman, E. L. Diabetic neuropathy: Clinical manifestations and current treatments. *The Lancet Neurology* vol. 11 521–534 (2012).

233. SIMA, A. A. . & KAMIYA, H. Diabetic Neuropathy Differs in Type 1 and Type 2 Diabetes. *Ann. N. Y. Acad. Sci.* **1084**, 235–249 (2006).
234. Vinik, A., Casellini, C. & Nevoret, M.-L. *Diabetic Neuropathies*. Endotext (MDText.com, Inc., 2000).
235. Callaghan, B. C., Little, A. A., Feldman, E. L. & Hughes, R. A. Enhanced glucose control for preventing and treating diabetic neuropathy. *Cochrane Database Syst. Rev.* (2012) doi:10.1002/14651858.CD007543.pub2.
236. Callaghan, B. C., Hur, J. & Feldman, E. L. Diabetic neuropathy: One disease or two? *Current Opinion in Neurology* vol. 25 536–541 (2012).
237. Davies, M., Brophy, S., Williams, R. & Taylor, A. The Prevalence, Severity, and Impact of Painful Diabetic Peripheral Neuropathy in Type 2 Diabetes. *Diabetes Care* **29**, 1518–1522 (2006).
238. Spallone, V. & Greco, C. Painful and Painless Diabetic Neuropathy: One Disease or Two? *Curr. Diab. Rep.* **13**, 533–549 (2013).
239. Currie, C. J. *et al.* The financial costs of healthcare treatment for people with Type 1 or Type 2 diabetes in the UK with particular reference to differing severity of peripheral neuropathy. *Diabet. Med.* (2007) doi:10.1111/j.1464-5491.2006.02057.x.
240. Diabetes UK. Facts & Figures - Diabetes UK. 1–22 (2014).
241. Dobretsov, M., Backonja, M. M., Romanovsky, D. & Stimers, J. R. Animal models of diabetic neuropathic pain. *Neuromethods* vol. 49 147–169 (2011).
242. Apfel, S. C. Diabetic neuropathy models: Are they relevant? *Drug Discovery Today: Disease Models* (2006) doi:10.1016/j.ddmod.2006.10.014.
243. Cameron, N. E., Cotter, M. A. & Maxfield, E. K. Anti-oxidant treatment prevents the development of peripheral nerve dysfunction in streptozotocin-diabetic rats. *Diabetologia* (1993) doi:10.1007/BF00400231.
244. Cameron, N. E., Cotter, M. A., Dines, K. & Love, A. Effects of aminoguanidine on peripheral nerve function and polyol pathway metabolites in streptozotocin-diabetic rats. *Diabetologia* (1992) doi:10.1007/BF00401423.
245. Cameron, N. E. & Cotter, M. A. Dissociation between biochemical and functional effects of the aldose reductase inhibitor, ponalrestat, on peripheral nerve in diabetic rats. *Br. J. Pharmacol.* (1992) doi:10.1111/j.1476-5381.1992.tb13389.x.
246. Cameron, N. E. & Cotter, M. A. Potential Therapeutic Approaches to the Treatment or Prevention of Diabetic Neuropathy: Evidence from Experimental Studies. *Diabet. Med.* **10**, 593–605 (1993).
247. Schemmel, K. E., Padiyara, R. S. & D'Souza, J. J. Aldose reductase inhibitors in the treatment of diabetic peripheral neuropathy: A review. *Journal of Diabetes and its Complications* (2010) doi:10.1016/j.jdiacomp.2009.07.005.
248. Chalk, C., Benstead, T. J. & Moore, F. Aldose reductase inhibitors for the treatment of diabetic polyneuropathy. *Cochrane Database of Systematic Reviews* (2007) doi:10.1002/14651858.CD004572.pub2.
249. Vinik, A. I. *et al.* Treatment of symptomatic diabetic peripheral neuropathy with the protein kinase C β -inhibitor ruboxistaurin mesylate during a 1-year, randomized, placebo-controlled, double-blind clinical trial. *Clin. Ther.* (2005) doi:10.1016/j.clinthera.2005.08.001.
250. Callaghan, B. C., Little, A. A., Feldman, E. L. & Hughes, R. A. Enhanced glucose control for preventing and treating diabetic neuropathy. *Cochrane Database Syst. Rev.* **6**, CD007543 (2012).
251. Van Acker, K. *et al.* Prevalence and impact on quality of life of peripheral neuropathy with or without neuropathic pain in type 1 and type 2 diabetic patients attending hospital outpatients

- clinics. *Diabetes Metab.* **35**, 206–213 (2009).
252. Kamiya, H., Murakawa, Y., Zhang, W. & Sima, A. A. F. Unmyelinated fiber sensory neuropathy differs in type 1 and type 2 diabetes. *Diabetes. Metab. Res. Rev.* **21**, 448–458 (2005).
253. Sima, A. A. F. *et al.* A comparison of diabetic polyneuropathy in Type II diabetic BBZDR/Wor rats and in Type I diabetic BB/Wor rats. *Diabetologia* (2000) doi:10.1007/s001250051376.
254. Kan, M., Guo, G., Singh, B., Singh, V. & Zochodne, D. W. *Glucagon-Like Peptide 1, Insulin, Sensory Neurons, and Diabetic Neuropathy*. <https://academic.oup.com/jnen/article-abstract/71/6/494/2917432> (2012).
255. Stino, A. M., Rumora, A. E., Kim, B. & Feldman, E. L. Evolving concepts on the role of dyslipidemia, bioenergetics, and inflammation in the pathogenesis and treatment of diabetic peripheral neuropathy. *J. Peripher. Nerv. Syst.* **25**, 76–84 (2020).
256. Pop-Busui, R., Ang, L., Holmes, C., Gallagher, K. & Feldman, E. L. Inflammation as a Therapeutic Target for Diabetic Neuropathies. *Current Diabetes Reports* vol. 16 1–10 (2016).
257. Pierson, C. R., Zhang, W., Murakawa, Y. & Sima, A. A. F. Insulin deficiency rather than hyperglycemia accounts for impaired neurotrophic responses and nerve fiber regeneration in type 1 diabetic neuropathy. *J. Neuropathol. Exp. Neurol.* (2003) doi:10.1093/jnen/62.3.260.
258. Malik, R. A. *et al.* Sural nerve pathology in diabetic patients with minimal but progressive neuropathy. *Diabetologia* **48**, 578–585 (2005).
259. Green, A. Q., Krishnan, S., Finucane, F. M. & Rayman, G. Altered C-fiber function as an indicator of early peripheral neuropathy in individuals with impaired glucose tolerance. *Diabetes Care* (2010) doi:10.2337/dc09-0101.
260. Sveen, K. A. *et al.* Small- and large-fiber neuropathy after 40 years of type 1 diabetes: Associations with glycem ic control and advanced protein glycation: The Oslo Study. *Diabetes Care* (2013) doi:10.2337/dc13-0788.
261. Mizisin, A. P. Mechanisms of diabetic neuropathy: Schwann cells. in *Handbook of Clinical Neurology* (2014). doi:10.1016/B978-0-444-53480-4.00029-1.
262. Beggs, J., Johnson, P. C., Olafsen, A., Watkins, C. J. & Cleary, C. Transperineurial arterioles in human sural nerve. *J. Neuropathol. Exp. Neurol.* (1991) doi:10.1097/00005072-199111000-00003.
263. Østergaard, L. *et al.* The effects of capillary dysfunction on oxygen and glucose extraction in diabetic neuropathy. *Diabetologia* (2015) doi:10.1007/s00125-014-3461-z.
264. Giannini, C. & Dyck, P. J. Basement membrane reduplication and pericyte degeneration precede development of diabetic polyneuropathy and are associated with its severity. *Ann. Neurol.* (1995) doi:10.1002/ana.410370412.
265. Cameron, N. E., Eaton, S. E. M., Cotter, M. A. & Tesfaye, S. Vascular factors and metabolic interactions in the pathogenesis of diabetic neuropathy. *Diabetologia* vol. 44 1973–1988 (2001).
266. Ibrahim, S. *et al.* A new minimally invasive technique to show nerve ischaemia in diabetic neuropathy. *Diabetologia* (1999) doi:10.1007/s001250051222.
267. Barrett, E. J. *et al.* Diabetic microvascular disease: An endocrine society scientific statement. *J. Clin. Endocrinol. Metab.* **102**, 4343–4410 (2017).
268. Tesfaye, S., Malik, R. & Ward, J. D. Vascular factors in diabetic neuropathy. *Diabetologia* (1994) doi:10.1007/BF00400938.
269. Cameron, N. E., Cotter, M. A. & Robertson, S. Angiotensin converting enzyme inhibition prevents development of muscle and nerve dysfunction and stimulates angiogenesis in streptozotocin-diabetic rats. *Diabetologia* (1992) doi:10.1007/BF00400846.

270. Cameron, N. E., Cotter, M. A., Ferguson, K., Robertson, S. & Radcliffe, M. A. Effects of chronic α -adrenergic receptor blockade on peripheral nerve conduction, hypoxic resistance, polyols, Na⁺-K⁺-ATPase activity, and vascular supply in STZ-D rats. *Diabetes* (1991) doi:10.2337/diab.40.12.1652.
271. Reja, A., Tesfaye, S., Harris, N. D. & Ward, J. D. Is ACE Inhibition with Lisinopril Helpful in Diabetic Neuropathy? *Diabet. Med.* (1995) doi:10.1111/j.1464-5491.1995.tb00482.x.
272. Malik, R. A. *et al.* Effect of angiotensin-converting-enzyme (ACE) inhibitor trandolapril on human diabetic neuropathy: Randomised double-blind controlled trial. *Lancet* (1998) doi:10.1016/S0140-6736(98)02478-7.
273. Hotta, N. *et al.* Effects of the 5-HT(2A) receptor antagonist sarpogrelate in diabetic patients with complications. A pilot study. *Clin. Drug Investig.* (1999) doi:10.2165/00044011-199918030-00004.
274. Viader, A. *et al.* Aberrant schwann cell lipid metabolism linked to mitochondrial deficits leads to axon degeneration and neuropathy. *Neuron* **77**, 886–898 (2013).
275. Vincent, A. M., Russell, J. W., Low, P. & Feldman, E. L. Oxidative stress in the pathogenesis of diabetic neuropathy. *Endocrine Reviews* (2004) doi:10.1210/er.2003-0019.
276. Fernyhough, P. Mitochondrial Dysfunction in Diabetic Neuropathy: a Series of Unfortunate Metabolic Events. *Current Diabetes Reports* vol. 15 (2015).
277. Clemens, A., Siegel, E. & Gallwitz, B. Global risk management in type 2 diabetes: Blood glucose, blood pressure, and lipids - Update on the background of the current guidelines. *Experimental and Clinical Endocrinology and Diabetes* vol. 112 493–503 (2004).
278. Grote, C. W. & Wright, D. E. A role for insulin in diabetic neuropathy. *Frontiers in Neuroscience* vol. 10 581 (2016).
279. Choeiri, C., Staines, W. & Messier, C. Immunohistochemical localization and quantification of glucose transporters in the mouse brain. *Neuroscience* (2002) doi:10.1016/S0306-4522(01)00619-4.
280. Sugimoto, K., Murakawa, Y., Zhang, W., Xu, G. & Sima, A. A. F. Insulin receptor in rat peripheral nerve: Its localization and alternatively spliced isoforms. *Diabetes. Metab. Res. Rev.* (2000) doi:10.1002/1520-7560(200009/10)16:5<354::AID-DMRR149>3.0.CO;2-H.
281. Sugimoto, K., Murakawa, Y. & Sima, A. A. F. Expression and localization of insulin receptor in rat dorsal root ganglion and spinal cord. *J. Peripher. Nerv. Syst.* (2002) doi:10.1046/j.1529-8027.2002.02005.x.
282. Shettar, A. & Muttagi, G. Developmental regulation of insulin receptor gene in sciatic nerves and role of insulin on glycoprotein P0 in the Schwann cells. *Peptides* (2012) doi:10.1016/j.peptides.2012.04.012.
283. Baiou, D. *et al.* Neurochemical characterization of insulin receptor-expressing primary sensory neurons in wild-type and vanilloid type 1 transient receptor potential receptor knockout mice. *J. Comp. Neurol.* (2007) doi:10.1002/cne.21389.
284. Mielke, J. G. & Wang, Y. T. Insulin, synaptic function, and opportunities for neuroprotection. in *Progress in Molecular Biology and Translational Science* (2011). doi:10.1016/B978-0-12-385506-0.00004-1.
285. Waldbillig, R. J. & LeRoith, D. Insulin receptors in the peripheral nervous system: a structural and functional analysis. *Brain Res.* (1987) doi:10.1016/0006-8993(87)90704-9.
286. Kim, B. & Feldman, E. L. Insulin resistance in the nervous system. *Trends in Endocrinology and Metabolism* (2012) doi:10.1016/j.tem.2011.12.004.
287. Recio-Pinto, E., Rechler, M. M. & Ishii, D. N. Effects of insulin, insulin-like growth factor-II, and nerve growth factor on neurite formation and survival cultured sympathetic and sensory

- neurons. *J. Neurosci.* (1986) doi:10.1523/jneurosci.06-05-01211.1986.
288. Xu, Q. G. *et al.* Insulin as an in vivo growth factor. *Exp. Neurol.* (2004) doi:10.1016/j.expneurol.2004.03.008.
289. Toth, C. *et al.* Rescue and regeneration of injured peripheral nerve axons by intrathecal insulin. *Neuroscience* (2006) doi:10.1016/j.neuroscience.2005.11.065.
290. Guo, G. F., Kan, M., Martinez, J. A. & Zochodne, D. W. Local insulin and the rapid regrowth of diabetic epidermal axons. *Neurobiol. Dis.* (2011) doi:10.1016/j.nbd.2011.04.012.
291. Sathianathan, V. *et al.* Insulin induces cobalt uptake in a subpopulation of rat cultured primary sensory neurons. *Eur. J. Neurosci.* **18**, 2477–2486 (2003).
292. Van Buren, J. J., Bhat, S., Rotello, R., Pauza, M. E. & Premkumar, L. S. Sensitization and Translocation of TRPV1 by Insulin and IGF-I. *Mol. Pain* **1**, 1744-8069-1–17 (2005).
293. Lilja, J., Laulund, F. & Forsby, A. Insulin and insulin-like growth factor type-I up-regulate the vanilloid receptor-1 (TRPV1) in stably TRPV1-expressing SH-SY5Y neuroblastoma cells. *J. Neurosci. Res.* (2007) doi:10.1002/jnr.21255.
294. Filho, O. A. R. & Fazan, V. P. S. Streptozotocin induced diabetes as a model of phrenic nerve neuropathy in rats. *J. Neurosci. Methods* (2006) doi:10.1016/j.jneumeth.2005.06.024.
295. Jakobsen, J. & Lundbæk, K. Neuropathy in experimental diabetes: An animal model. *Br. Med. J.* (1976) doi:10.1136/bmj.2.6030.278.
296. Romanovsky, D., Cruz, N. F., Diemel, G. A. & Dobretsov, M. Mechanical hyperalgesia correlates with insulin deficiency in normoglycemic streptozotocin-treated rats. *Neurobiol. Dis.* (2006) doi:10.1016/j.nbd.2006.07.009.
297. Romanovsky, D., Wang, J., Al-Chaer, E. D., Stimers, J. R. & Dobretsov, M. Comparison of metabolic and neuropathy profiles of rats with streptozotocin-induced overt and moderate insulinopenia. *Neuroscience* (2010) doi:10.1016/j.neuroscience.2010.06.059.
298. Murakawa, Y. *et al.* Impaired glucose tolerance and insulinopenia in the GK-rat causes peripheral neuropathy. *Diabetes. Metab. Res. Rev.* (2002) doi:10.1002/dmrr.326.
299. Brussee, V., Cunningham, F. A. & Zochodne, D. W. Direct insulin signalling of neurons reverses diabetic neuropathy. *Diabetes* (2004) doi:10.2337/diabetes.53.7.1824.
300. Petersen, K. F. *et al.* Reversal of muscle insulin resistance by weight reduction in young, lean, insulin-resistant offspring of parents with type 2 diabetes. *Proc. Natl. Acad. Sci. U. S. A.* (2012) doi:10.1073/pnas.1205675109.
301. Singh, B. *et al.* Resistance to trophic neurite outgrowth of sensory neurons exposed to insulin. *J. Neurochem.* (2012) doi:10.1111/j.1471-4159.2012.07681.x.
302. Kim, B., Mclean, L. L., Philip, S. S. & Feldman, E. L. Hyperinsulinemia Induces Insulin Resistance in Dorsal Root Ganglion Neurons. (2011) doi:10.1210/en.2011-0029.
303. Grote, C. W., Morris, J. K., Ryals, J. M., Geiger, P. C. & Wright, D. E. Insulin receptor substrate 2 expression and involvement in neuronal insulin resistance in diabetic neuropathy. *Exp. Diabetes Res.* (2011) doi:10.1155/2011/212571.
304. Patel, N. J., Llewelyn, J. G., Wright, D. W. & Thomas, P. K. Glucose and leucine uptake by rat dorsal root ganglia is not insulin sensitive. *J. Neurol. Sci.* (1994) doi:10.1016/0022-510X(94)90345-X.
305. Nishimura, C., Lou, M. F. & Kinoshita, J. H. Depletion of myo-Inositol and Amino Acids in Galactosemic Neuropathy. *J. Neurochem.* (1987) doi:10.1111/j.1471-4159.1987.tb03428.x.
306. Tomlinson, D. R. & Gardiner, N. J. Glucose neurotoxicity. *Nature Reviews Neuroscience* (2008) doi:10.1038/nrn2294.

307. Gabbay, K. H., Merola, L. O. & Field, R. A. Sorbitol pathway: Presence in nerve and cord with substrate accumulation in diabetes. *Science* (80-). (1966) doi:10.1126/science.151.3707.209.
308. Greene, D. A. & Winegrad, A. I. In vitro studies of the substrates for energy production and the effects of insulin on glucose utilization in the neural components of peripheral nerve. *Diabetes* (1979) doi:10.2337/diab.28.10.878.
309. Oates, P. Aldose Reductase, Still a Compelling Target for Diabetic Neuropathy. *Curr. Drug Targets* (2008) doi:10.2174/138945008783431781.
310. Obrosova, I. G. *et al.* An aldose reductase inhibitor reverses early diabetes-induced changes in peripheral nerve function, metabolism, and antioxidative defense. *FASEB J.* (2002) doi:10.1096/fj.01-0603fje.
311. Obrosova, I. G. *et al.* Oxidative-nitrosative stress and poly(ADP-ribose) polymerase (PARP) activation in experimental diabetic neuropathy: The relation is revisited. *Diabetes* (2005) doi:10.2337/diabetes.54.12.3435.
312. Obrosova, I. G. *et al.* Role for nitrosative stress in diabetic neuropathy: evidence from studies with a peroxynitrite decomposition catalyst. *FASEB J.* (2005) doi:10.1096/fj.04-1913fje.
313. Feldman, E. L., Nave, K. A., Jensen, T. S. & Bennett, D. L. H. New Horizons in Diabetic Neuropathy: Mechanisms, Bioenergetics, and Pain. *Neuron* vol. 93 1296–1313 (2017).
314. Magnani, P. *et al.* Glucose transporters in rat peripheral nerve: Paranodal expression of GLUT1 and GLUT3. *Metabolism*. **45**, 1466–1473 (1996).
315. Hao, W. *et al.* Hyperglycemia promotes Schwann cell de-differentiation and de-myelination via sorbitol accumulation and Igf1 protein down-regulation. *J. Biol. Chem.* **290**, 17106–17115 (2015).
316. Verheijen, M. H. G., Chrast, R., Burrola, P. & Lemke, G. Local regulation of fat metabolism in peripheral nerves. *Genes Dev.* **17**, 2450–2464 (2003).
317. Vareniuk, I., Pavlov, I. A. & Obrosova, I. G. Inducible nitric oxide synthase gene deficiency counteracts multiple manifestations of peripheral neuropathy in a streptozotocin-induced mouse model of diabetes. *Diabetologia* **51**, 2126–2133 (2008).
318. Russell, J. W., Sullivan, K. A., Windebank, A. J., Herrmann, D. N. & Feldman, E. L. Neurons undergo apoptosis in animal and cell culture models of diabetes. *Neurobiol. Dis.* **6**, 347–363 (1999).
319. Eichberg, J. Protein kinase C changes in diabetes: Is the concept relevant to neuropathy? *International Review of Neurobiology* (2002) doi:10.1016/s0074-7742(02)50073-8.
320. Du, X. L. *et al.* Hyperglycemia-induced mitochondrial superoxide overproduction activates the hexosamine pathway and induces plasminogen activator inhibitor-1 expression by increasing Sp1 glycosylation. *Proc. Natl. Acad. Sci. U. S. A.* (2000) doi:10.1073/pnas.97.22.12222.
321. Geraldles, P. & King, G. L. Activation of protein kinase C isoforms and its impact on diabetic complications. *Circulation Research* (2010) doi:10.1161/CIRCRESAHA.110.217117.
322. Mišur, I. *et al.* Advanced glycation end products in peripheral nerve in type 2 diabetes with neuropathy. *Acta Diabetol.* (2004) doi:10.1007/s00592-004-0160-0.
323. Haslbeck, K. M. *et al.* Activation of the RAGE pathway: A general mechanism in the pathogenesis of polyneuropathies? *Neurol. Res.* (2007) doi:10.1179/174313206X152564.
324. Lukic, I. K., Humpert, P. M., Nawroth, P. P. & Bierhaus, A. The RAGE pathway: Activation and perpetuation in the pathogenesis of diabetic neuropathy. in *Annals of the New York Academy of Sciences* (2008). doi:10.1196/annals.1433.059.
325. Doupis, J. *et al.* Microvascular reactivity and inflammatory cytokines in painful and painless peripheral diabetic neuropathy. *J. Clin. Endocrinol. Metab.* (2009) doi:10.1210/jc.2008-2385.

326. Shoelson, S. E., Lee, J. & Goldfine, A. B. Inflammation and insulin resistance. *Journal of Clinical Investigation* (2006) doi:10.1172/JCI29069.
327. Hur, J. *et al.* The identification of gene expression profiles associated with progression of human diabetic neuropathy. *Brain* **134**, 3222–3235 (2011).
328. Wang, Y., Schmeichel, A. M., Iida, H., Schmelzer, J. D. & Low, P. A. Enhanced inflammatory response via activation of NF- κ B in acute experimental diabetic neuropathy subjected to ischemia-reperfusion injury. *J. Neurol. Sci.* (2006) doi:10.1016/j.jns.2006.03.011.
329. Cameron, N. & Cotter, M. Pro-Inflammatory Mechanisms in Diabetic Neuropathy: Focus on the Nuclear Factor Kappa B Pathway. *Curr. Drug Targets* (2008) doi:10.2174/138945008783431718.
330. Kellogg, A. P. *et al.* Protective effects of cyclooxygenase-2 gene inactivation against peripheral nerve dysfunction and intraepidermal nerve fiber loss in experimental diabetes. *Diabetes* (2007) doi:10.2337/db07-0740.
331. Herder, C. *et al.* Association of subclinical inflammation with polyneuropathy in the older population: KORA F4 study. *Diabetes Care* (2013) doi:10.2337/dc13-0382.
332. Lieb, D. C., Parson, H. K., Mamikunian, G. & Vinik, A. I. Cardiac autonomic imbalance in newly diagnosed and established diabetes is associated with markers of adipose tissue inflammation. *Exp. Diabetes Res.* (2012) doi:10.1155/2012/878760.
333. Hur, J., Sullivan, K. A., Callaghan, B. C., Pop-Busui, R. & Feldman, E. L. Identification of factors associated with sural nerve regeneration and degeneration in diabetic neuropathy. *Diabetes Care* (2013) doi:10.2337/dc12-2530.
334. Pop-Busui, R. *et al.* Sympathetic dysfunction in type 1 diabetes: Association with impaired myocardial blood flow reserve and diastolic dysfunction. *J. Am. Coll. Cardiol.* (2004) doi:10.1016/j.jacc.2004.09.033.
335. Goldfine, A. B. *et al.* Salicylate (Salsalate) in patients with type 2 diabetes: A randomized trial. *Ann. Intern. Med.* (2013) doi:10.7326/0003-4819-159-1-201307020-00003.
336. Üçeyler, N., Rogausch, J. P., Toyka, K. V. & Sommer, C. Differential expression of cytokines in painful and painless neuropathies. *Neurology* (2007) doi:10.1212/01.wnl.0000265062.92340.a5.
337. Cheng, H. T. *et al.* p38 Mediates Mechanical Allodynia in a Mouse Model of Type 2 Diabetes. *Mol. Pain* **6**, 1744-8069-6–28 (2010).
338. Patapoutian, A., Tate, S. & Woolf, C. J. Transient receptor potential channels: Targeting pain at the source. *Nature Reviews Drug Discovery* vol. 8 55–68 (2009).
339. Wang, S. *et al.* Phospholipase C and protein kinase A mediate bradykinin sensitization of TRPA1: A molecular mechanism of inflammatory pain. *Brain* (2008) doi:10.1093/brain/awn060.
340. Ji, R. R., Samad, T. A., Jin, S. X., Schmolz, R. & Woolf, C. J. p38 MAPK activation by NGF in primary sensory neurons after inflammation increases TRPV1 levels and maintains heat hyperalgesia. *Neuron* (2002) doi:10.1016/S0896-6273(02)00908-X.
341. Alessandri-Haber, N., Dina, O. A., Joseph, E. K., Reichling, D. & Levine, J. D. A transient receptor potential vanilloid 4-dependent mechanism of hyperalgesia is engaged by concerted action of inflammatory mediators. *J. Neurosci.* (2006) doi:10.1523/JNEUROSCI.5385-05.2006.
342. Bierhaus, A. *et al.* Methylglyoxal modification of Na v 1.8 facilitates nociceptive neuron firing and causes hyperalgesia in diabetic neuropathy. *Nat. Med.* (2012) doi:10.1038/nm.2750.
343. Andersson, D. A. *et al.* Methylglyoxal Evokes Pain by Stimulating TRPA1. *PLoS One* **8**, (2013).
344. Huang, Q., Chen, Y., Gong, N. & Wang, Y. X. Methylglyoxal mediates streptozotocin-induced diabetic neuropathic pain via activation of the peripheral TRPA1 and Nav1.8 channels. *Metabolism*. **65**, 463–474 (2016).

345. Andersson, D. A., Gentry, C., Moss, S. & Bevan, S. Transient receptor potential A1 is a sensory receptor for multiple products of oxidative stress. *J. Neurosci.* **28**, 2485–2494 (2008).
346. Xu, G. Y., Li, G., Liu, N. & Huang, L. Y. M. Mechanisms underlying purinergic P2X3 receptor-mediated mechanical allodynia induced in diabetic rats. *Mol. Pain* **7**, (2011).
347. Zenker, J. *et al.* Altered distribution of juxtaparanodal Kv1.2 subunits mediates peripheral nerve hyperexcitability in type 2 diabetes mellitus. *J. Neurosci.* (2012) doi:10.1523/JNEUROSCI.0719-12.2012.
348. Craner, M. J., Klein, J. P., Renganathan, M., Black, J. A. & Waxman, S. G. Changes of sodium channel expression in experimental painful diabetic neuropathy. *Ann. Neurol.* **52**, 786–792 (2002).
349. Singh, J. N., Jain, G. & Sharma, S. S. In vitro hyperglycemia enhances sodium currents in dorsal root ganglion neurons: An effect attenuated by carbamazepine. *Neuroscience* **232**, 64–73 (2013).
350. Zhang, J.-L. *et al.* Gabapentin reduces allodynia and hyperalgesia in painful diabetic neuropathy rats by decreasing expression level of Nav1.7 and p-ERK1/2 in DRG neurons. *Brain Res.* **1493**, 13–18 (2013).
351. Chattopadhyay, M., Mata, M. & Fink, D. J. Continuous δ -opioid receptor activation reduces neuronal voltage-gated sodium channel (Nav1.7) levels through activation of protein kinase C in painful diabetic neuropathy. *J. Neurosci.* **28**, 6652–6658 (2008).
352. Shah, B. S. *et al.* $\beta 3$, a novel auxiliary subunit for the voltage gated sodium channel is upregulated in sensory neurones following streptozocin induced diabetic neuropathy in rat. *Neurosci. Lett.* **309**, 1–4 (2001).
353. Okuse, K. *et al.* Regulation of expression of the sensory neuron-specific sodium channel SNS in inflammatory and neuropathic pain. *Mol. Cell. Neurosci.* **10**, 196–207 (1997).
354. Sun, W. *et al.* Reduced conduction failure of the main axon of polymodal nociceptive C-fibres contributes to painful diabetic neuropathy in rats. *Brain* **135**, 359–375 (2012).
355. Chattopadhyay, M., Mata, M. & Fink, D. J. Vector-mediated release of GABA attenuates pain-related behaviors and reduces Na V1.7 in DRG neurons. *Eur. J. Pain* **15**, 913–920 (2011).
356. Baron, R., Tölle, T. R., Gockel, U., Brosz, M. & Freynhagen, R. A cross-sectional cohort survey in 2100 patients with painful diabetic neuropathy and postherpetic neuralgia: Differences in demographic data and sensory symptoms. *Pain* **146**, 34–40 (2009).
357. Li, Q. S. *et al.* SCN9A variants may be implicated in neuropathic pain associated with diabetic peripheral neuropathy and pain severity. *Clin. J. Pain* (2015) doi:10.1097/AJP.000000000000205.
358. Estacion, M. *et al.* Ca²⁺ toxicity due to reverse Na⁺/Ca²⁺ exchange contributes to degeneration of neurites of DRG neurons induced by a neuropathy-associated Nav1.7 mutation. *J. Neurophysiol.* (2015) doi:10.1152/jn.00195.2015.
359. Rolyan, H. *et al.* A painful neuropathy-associated Nav1.7 mutant leads to time-dependent degeneration of small-diameter axons associated with intracellular Ca²⁺ dysregulation and decrease in ATP levels. *Mol. Pain* (2016) doi:10.1177/1744806916674472.
360. Yang, L., Li, Q., Liu, X. & Liu, S. Roles of voltage-gated tetrodotoxin-sensitive sodium channels Nav1.3 and Nav1.7 in diabetes and painful diabetic neuropathy. *International Journal of Molecular Sciences* (2016) doi:10.3390/ijms17091479.
361. Hoeijmakers, J. G. J., Faber, C. G., Merkies, I. S. J. & Waxman, S. G. Channelopathies, painful neuropathy, and diabetes: Which way does the causal arrow point? *Trends in Molecular Medicine* vol. 20 544–550 (2014).
362. Rush, A. M., Cummins, T. R. & Waxman, S. G. Multiple sodium channels and their roles in

- electrogenesis within dorsal root ganglion neurons. *Journal of Physiology* (2007) doi:10.1113/jphysiol.2006.121483.
363. Pop-Busui, R. *et al.* Effects of cardiac autonomic dysfunction on mortality risk in the Action to Control Cardiovascular Risk in Diabetes (ACCORD) trial. *Diabetes Care* (2010) doi:10.2337/dc10-0125.
364. Ismail-Beigi, F. *et al.* Effect of intensive treatment of hyperglycaemia on microvascular outcomes in type 2 diabetes: An analysis of the ACCORD randomised trial. *Lancet* (2010) doi:10.1016/S0140-6736(10)60576-4.
365. Calles-Escandon, J. *et al.* Effect of intensive compared with standard glycemia treatment strategies on mortality by baseline subgroup characteristics: The Action to Control Cardiovascular Risk in Diabetes (ACCORD) trial. *Diabetes Care* (2010) doi:10.2337/dc09-1471.
366. Davis, T. M. E., Yeap, B. B., Davis, W. A. & Bruce, D. G. Lipid-lowering therapy and peripheral sensory neuropathy in type 2 diabetes: The Fremantle Diabetes Study. *Diabetologia* (2008) doi:10.1007/s00125-007-0919-2.
367. Villegas-Rivera, G. *et al.* Effects of ezetimibe/simvastatin and rosuvastatin on oxidative stress in diabetic neuropathy: A randomized, double-blind, placebo-controlled clinical trial. *Oxid. Med. Cell. Longev.* (2015) doi:10.1155/2015/756294.
368. Smith, A. G. *et al.* Lifestyle intervention for pre-diabetic neuropathy. *Diabetes Care* **29**, 1294–1299 (2006).
369. Sheng, B. *et al.* The Long-Term Effects of Bariatric Surgery on Type 2 Diabetes Remission, Microvascular and Macrovascular Complications, and Mortality: a Systematic Review and Meta-Analysis. *Obesity Surgery* (2017) doi:10.1007/s11695-017-2866-4.
370. Alvarez, M., Sierra, O. R., Saavedra, G. & Moreno, S. Vitamin B12 deficiency and diabetic neuropathy in patients taking metformin: A cross-sectional study. *Endocr. Connect.* (2019) doi:10.1530/EC-19-0382.
371. Ziegler, D. *et al.* Treatment of symptomatic diabetic polyneuropathy with the antioxidant α -lipoic acid: A 7-month multicenter randomized controlled trial (ALADIN III study). *Diabetes Care* (1999) doi:10.2337/diacare.22.8.1296.
372. Pop-Busui, R. *et al.* Diabetic neuropathy: A position statement by the American diabetes association. *Diabetes Care* **40**, 136–154 (2017).
373. Sandercock, D., Cramer, M., Biton, V. & Cowles, V. E. A gastroretentive gabapentin formulation for the treatment of painful diabetic peripheral neuropathy: Efficacy and tolerability in a double-blind, randomized, controlled clinical trial. *Diabetes Res. Clin. Pract.* (2012) doi:10.1016/j.diabres.2012.03.010.
374. Backonja, M. *et al.* Gabapentin for the symptomatic treatment of painful neuropathy in patients with diabetes mellitus. A randomized controlled trial. *J. Am. Med. Assoc.* (1998) doi:10.1001/jama.280.21.1831.
375. Lesser, H., Sharma, U., LaMoreaux, L. & Poole, R. M. Pregabalin relieves symptoms of painful diabetic neuropathy: A randomized controlled trial. *Neurology* (2004) doi:10.1212/01.WNL.0000145767.36287.A1.
376. Finnerup, N. B. *et al.* Pharmacotherapy for neuropathic pain in adults: A systematic review and meta-analysis. *Lancet Neurol.* **14**, 162–173 (2015).
377. Goldstein, D. J., Lu, Y., Detke, M. J., Lee, T. C. & Iyengar, S. Duloxetine vs. placebo in patients with painful diabetic neuropathy. *Pain* (2005) doi:10.1016/j.pain.2005.03.029.
378. Wernicke, J. F. *et al.* A randomized controlled trial of duloxetine in diabetic peripheral neuropathic pain. *Neurology* (2006) doi:10.1212/01.wnl.0000240225.04000.1a.
379. Rowbotham, M. C., Goli, V., Kunz, N. R. & Lei, D. Venlafaxine extended release in the treatment

- of painful diabetic neuropathy: A double-blind, placebo-controlled study. *Pain* (2004) doi:10.1016/j.pain.2004.05.010.
380. Boyle, J. *et al.* Randomized, placebo-controlled comparison of amitriptyline, duloxetine, and pregabalin in patients with chronic diabetic peripheral neuropathic pain: Impact on pain, polysomnographic sleep, daytime functioning, and quality of life. *Diabetes Care* (2012) doi:10.2337/dc12-0656.
381. Dworkin, R. H., Jensen, M. P., Gammaitoni, A. R., Olaleye, D. O. & Galer, B. S. Symptom Profiles Differ in Patients With Neuropathic Versus Non-neuropathic Pain. *J. Pain* (2007) doi:10.1016/j.jpain.2006.06.005.
382. Franklin, G. M. Opioids for chronic noncancer pain: A position paper of the American Academy of Neurology. *Neurology* (2014) doi:10.1212/WNL.0000000000000839.
383. Giraudon, I., Lowitz, K., Dargan, P. I., Wood, D. M. & Dart, R. C. Prescription opioid abuse in the UK. *British Journal of Clinical Pharmacology* (2013) doi:10.1111/bcp.12133.
384. Maloney, J. *et al.* Comprehensive Review of Topical Analgesics for Chronic Pain. *Curr. Pain Headache Rep.* **25**, 7 (2021).
385. Wolff, R. F., Bala, M. M., Westwood, M., Kessels, A. G. & Kleijnen, J. 5% lidocaine medicated plaster in painful diabetic peripheral neuropathy (DPN): A systematic review. *Swiss Medical Weekly* (2010) doi:10.4414/smw.2010.12995.
386. Simpson, D. M. *et al.* Capsaicin 8% Patch in Painful Diabetic Peripheral Neuropathy: A Randomized, Double-Blind, Placebo-Controlled Study. *J. Pain* (2017) doi:10.1016/j.jpain.2016.09.008.
387. Nolano, M. *et al.* Topical capsaicin in humans: Parallel loss of epidermal nerve fibers and pain sensation. *Pain* (1999) doi:10.1016/S0304-3959(99)00007-X.
388. Rastogi, A. & Jude, E. B. Novel treatment modalities for painful diabetic neuropathy. *Diabetes and Metabolic Syndrome: Clinical Research and Reviews* vol. 15 287–293 (2021).
389. Yorek, M. S. *et al.* Early vs. late intervention of high fat/low dose streptozotocin treated C57Bl/6J mice with enalapril, α -lipoic acid, menhaden oil or their combination: Effect on diabetic neuropathy related endpoints. *Neuropharmacology* (2017) doi:10.1016/j.neuropharm.2016.12.022.
390. Hwang, H. S., Yang, E. J., Lee, S. M., Lee, S. C. & Choi, S.-M. Antiallodynic Effects of Electroacupuncture Combined with MK-801 Treatment through the Regulation of p35/p25 in Experimental Diabetic Neuropathy. *Exp. Neurobiol.* (2011) doi:10.5607/en.2011.20.3.144.
391. Chaparro, L. E., Wiffen, P. J., Moore, R. A. & Gilron, I. Combination pharmacotherapy for the treatment of neuropathic pain in adults. *Cochrane Database of Systematic Reviews* (2012) doi:10.1002/14651858.CD008943.pub2.
392. Tesfaye, S. *et al.* Duloxetine and pregabalin: High-dose monotherapy or their combination? the 'cOMBO-DN study' - A multinational, randomized, double-blind, parallel-group study in patients with diabetic peripheral neuropathic pain. *Pain* (2013) doi:10.1016/j.pain.2013.05.043.
393. Theile, J. W., Fuller, M. D. & Chapman, M. L. The selective Nav1.7 inhibitor, PF-05089771, interacts equivalently with fast and slow inactivated Nav1.7 channels. *Mol. Pharmacol.* (2016) doi:10.1124/mol.116.105437.
394. Moyer, B. D. *et al.* Pharmacological characterization of potent and selective Nav1.7 inhibitors engineered from *Chilobrachys jingzhao* tarantula venom peptide JzTx-V. *PLoS One* (2018) doi:10.1371/journal.pone.0196791.
395. McDonnell, A. *et al.* Efficacy of the Nav1.7 blocker PF-05089771 in a randomised, placebo-controlled, double-blind clinical study in subjects with painful diabetic peripheral neuropathy. *Pain* **159**, 1465–1476 (2018).

396. Hinckley, C. A. *et al.* Characterization of vixotrigine, a broad-spectrum voltage-gated sodium channel blocker. *Mol. Pharmacol.* **99**, 49–59 (2021).
397. Demant, D. T. *et al.* The effect of oxcarbazepine in peripheral neuropathic pain depends on pain phenotype: A randomised, double-blind, placebo-controlled phenotype-stratified study. *Pain* (2014) doi:10.1016/j.pain.2014.08.014.
398. Vertex Pharmaceuticals Incorporated. Vertex Announces Positive Phase 2 Data in Third Proof-of-Concept Study with the Nav1.8 Inhibitor VX-150. *Release Summary* <https://www.businesswire.com/news/home/20181218005223/en/> (2018).
399. Jarvis, M. F. *et al.* A-803467, a potent and selective Nav1.8 sodium channel blocker, attenuates neuropathic and inflammatory pain in the rat. *Proc. Natl. Acad. Sci. U. S. A.* **104**, 8520–5 (2007).
400. Payne, C. E. *et al.* A novel selective and orally bioavailable Nav1.8 channel blocker, PF-01247324, attenuates nociception and sensory neuron excitability. *Br. J. Pharmacol.* (2015) doi:10.1111/bph.13092.
401. Browne, L. E., Blaney, F. E., Yusaf, S. P., Clare, J. J. & Wray, D. Structural determinants of drugs acting on the Nav 1.8 channel. *J. Biol. Chem.* (2009) doi:10.1074/jbc.M807569200.
402. Jarvis, M. F. *et al.* A-317491, a novel potent and selective non-nucleotide antagonist of P2X3 and P2X2/3 receptors, reduces chronic inflammatory and neuropathic pain in the rat. *Proc. Natl. Acad. Sci. U. S. A.* (2002) doi:10.1073/pnas.252537299.
403. Rao, S. *et al.* The effect of sinomenine in diabetic neuropathic pain mediated by the P2X3 receptor in dorsal root ganglia. *Purinergic Signal.* (2017) doi:10.1007/s11302-016-9554-z.
404. Koivisto, A., Jalava, N., Bratty, R. & Pertovaara, A. TRPA1 antagonists for pain relief. *Pharmaceuticals* vol. 11 (2018).
405. Bishnoi, M., Bosgraaf, C. A., Abooj, M., Zhong, L. & Premkumar, L. S. Streptozotocin-Induced Early Thermal Hyperalgesia is independent of Glycemic State of Rats: Role of Transient Receptor Potential Vanilloid 1 (TRPV1) and Inflammatory mediators. *Mol. Pain* (2011) doi:10.1186/1744-8069-7-52.
406. Zan, Y., Kuai, C. X., Qiu, Z. X. & Huang, F. Berberine Ameliorates Diabetic Neuropathy: TRPV1 Modulation by PKC Pathway. *Am. J. Chin. Med.* (2017) doi:10.1142/S0192415X17500926.
407. Koivisto, A. *et al.* Inhibiting TRPA1 ion channel reduces loss of cutaneous nerve fiber function in diabetic animals: Sustained activation of the TRPA1 channel contributes to the pathogenesis of peripheral diabetic neuropathy. *Pharmacol. Res.* **65**, 149–158 (2012).
408. Andrade, E. L., Meotti, F. C. & Calixto, J. B. TRPA1 antagonists as potential analgesic drugs. *Pharmacology and Therapeutics* (2012) doi:10.1016/j.pharmthera.2011.10.008.
409. Malik, R. A. Why are there no good treatments for diabetic neuropathy? *The Lancet Diabetes and Endocrinology* vol. 2 607–609 (2014).
410. Thomas, D. & Wessel, C. *The State of Innovation in Highly Prevalent Chronic Diseases Volume II: Pain and Addiction Therapeutics.* www.bio.org/iareports (2018).
411. Jin, H. Y., Moon, S.-S. & Calcutt, N. A. Lost in Translation? Measuring Diabetic Neuropathy in Humans and Animals. *Diabetes Metab. J.* **45**, (2020).
412. Lauria, G. *et al.* European federation of neurological societies/peripheral nerve society guideline on the use of skin biopsy in the diagnosis of small fiber neuropathy. report of a joint task force of the european fe-deration of neurological societies and the peripheral ne. *European Journal of Neurology* (2010) doi:10.1111/j.1468-1331.2010.03023.x.
413. Williams, B. M. *et al.* An artificial intelligence-based deep learning algorithm for the diagnosis of diabetic neuropathy using corneal confocal microscopy: a development and validation study. *Diabetologia* (2020) doi:10.1007/s00125-019-05023-4.

414. Vollert, J. *et al.* Stratifying patients with peripheral neuropathic pain based on sensory profiles: Algorithm and sample size recommendations. *Pain* (2017) doi:10.1097/j.pain.0000000000000935.
415. Yarnitsky, D., Granot, M., Nahman-Averbuch, H., Khamaisi, M. & Granovsky, Y. Conditioned pain modulation predicts duloxetine efficacy in painful diabetic neuropathy. *Pain* (2012) doi:10.1016/j.pain.2012.02.021.
416. Fernyhough, P. & Calcutt, N. A. An Introduction to the History and Controversies of the Pathogenesis of Diabetic Neuropathy. in *International Review of Neurobiology* (2016). doi:10.1016/bs.irn.2016.03.012.
417. Calcutt, N. A. & Fernyhough, P. An Introduction to the History and Controversies of Animal Models of Diabetic Neuropathy. in *International Review of Neurobiology* (2016). doi:10.1016/bs.irn.2016.03.011.
418. Islam, M. S. Animal models of diabetic neuropathy: Progress since 1960s. *Journal of Diabetes Research* vol. 2013 (2013).
419. Gardiner, N. J. & Freeman, O. J. Can Diabetic Neuropathy Be Modeled In Vitro? in *International Review of Neurobiology* vol. 127 53–87 (Academic Press Inc., 2016).
420. Vincent, A. M., Stevens, M. J., Backus, C., Mclean, L. L. & Feldman, E. L. Cell culture modeling to test therapies against hyperglycemia-mediated oxidative stress and injury. *Antioxidants Redox Signal.* **7**, 1494–1506 (2005).
421. Sotelo, J. R. *et al.* An in vitro model to study diabetic neuropathy. *Neurosci. Lett.* (1991) doi:10.1016/0304-3940(91)90727-B.
422. PURVES, T. *et al.* A role for mitogen-activated protein kinases in the etiology of diabetic neuropathy. *FASEB J.* (2001) doi:10.1096/fj.01-0253hyp.
423. Russell, J. W. *et al.* High glucose-induced oxidative stress and mitochondrial dysfunction in neurons. *FASEB J.* **16**, 1738–1748 (2002).
424. Singh, J. N., Jain, G. & Sharma, S. S. In vitro hyperglycemia enhances sodium currents in dorsal root ganglion neurons: An effect attenuated by carbamazepine. *Neuroscience* **232**, 64–73 (2013).
425. Hattangady, N. G. & Rajadhyaksha, M. S. A brief review of in vitro models of diabetic neuropathy. *International Journal of Diabetes in Developing Countries* vol. 29 143–149 (2009).
426. Sleigh, J. N., Weir, G. A. & Schiavo, G. A simple, step-by-step dissection protocol for the rapid isolation of mouse dorsal root ganglia. *BMC Res. Notes* (2016) doi:10.1186/s13104-016-1915-8.
427. Wang, Z. *et al.* [Estimation of the normal range of blood glucose in rats]. *Wei Sheng Yan Jiu* (2010).
428. Sima, A. A. F. & Robertson, D. M. Peripheral neuropathy in mutant diabetic mouse [C57BL/Ks (db/db)]. *Acta Neuropathol.* **41**, 85–89 (1978).
429. Norido, F., Canella, R., Zanoni, R. & Gorio, A. Development of diabetic neuropathy in the C57BL/Ks (db/db) mouse and its treatment with gangliosides. *Exp. Neurol.* **83**, 221–232 (1984).
430. Hinder, L. M., Vincent, A. M., Hayes, J. M., McLean, L. L. & Feldman, E. L. Apolipoprotein E knockout as the basis for mouse models of dyslipidemia-induced neuropathy. *Exp. Neurol.* **239**, 102–110 (2013).
431. De Gregorio, C., Contador, D., Campero, M., Ezquer, M. & Ezquer, F. Characterization of diabetic neuropathy progression in a mouse model of type 2 diabetes mellitus. *Biol. Open* **7**, bio036830 (2018).
432. Radu, B. M., Dumitrescu, D. I., Mustaciosu, C. C. & Radu, M. Dual effect of methylglyoxal on the intracellular Ca²⁺ signaling and neurite outgrowth in mouse sensory neurons. *Cell. Mol.*

- Neurobiol.* **32**, 1047–1057 (2012).
433. Zhrebetskaya, E., Akude, E., Smith, D. R. & Fernyhough, P. Development of selective axonopathy in adult sensory neurons isolated from diabetic rats: Role of glucose-induced oxidative stress. *Diabetes* (2009) doi:10.2337/db09-0034.
434. Vincent, A. M. *et al.* Dyslipidemia-induced neuropathy in mice: The role of oxLDL/LOX-1. *Diabetes* **58**, 2376–2385 (2009).
435. Ristic, H., Srinivasan, S., Hall, K. E., Sima, A. A. F. & Wiley, J. W. Serum from diabetic BB/W rats enhances calcium currents in primary sensory neurons. *J. Neurophysiol.* (1998) doi:10.1152/jn.1998.80.3.1236.
436. Smith, D. S. & Skene, J. H. P. A transcription-dependent switch controls competence of adult neurons for distinct modes of axon growth. *J. Neurosci.* (1997) doi:10.1523/jneurosci.17-02-00646.1997.
437. Vincent, A. M., Brownlee, M. & Russell, J. W. Oxidative stress and programmed cell death in diabetic neuropathy. in *Annals of the New York Academy of Sciences* (2002). doi:10.1111/j.1749-6632.2002.tb02108.x.
438. Shindo, H. *et al.* Modulation of basal nitric oxide-dependent cyclic-GMP production by ambient glucose, myo-inositol, and protein kinase C in SH-SY5Y human neuroblastoma cells. *J. Clin. Invest.* (1996) doi:10.1172/JCI118472.
439. Pleasure, S. J. & Lee, V. M. -. NTera 2 Cells: A human cell line which displays characteristics expected of a human committed neuronal progenitor cell. *J. Neurosci. Res.* (1993) doi:10.1002/jnr.490350603.
440. Sharifi, A. M., Mousavi, S. H., Farhadi, M. & Larijani, B. Study of high glucose-induced apoptosis in PC12 cells: Role of bax protein. *J. Pharmacol. Sci.* (2007) doi:10.1254/jphs.FP0070258.
441. Lelkes, E., Unsworth, B. R. & Lelkes, P. I. Reactive oxygen species, apoptosis and altered NGF-induced signaling in PC12 pheochromocytoma cells cultured in elevated glucose: An in vitro cellular model for diabetic neuropathy. *Neurotox. Res.* (2001) doi:10.1007/BF03033191.
442. Landis, D. M. D. Culturing Nerve Cells. *Neurology* (1991) doi:10.1212/wnl.41.12.2017-a.
443. Takahashi, K. *et al.* Induction of Pluripotent Stem Cells from Adult Human Fibroblasts by Defined Factors. *Cell* (2007) doi:10.1016/j.cell.2007.11.019.
444. Chambers, S. M. *et al.* Combined small-molecule inhibition accelerates developmental timing and converts human pluripotent stem cells into nociceptors. *Nat. Biotechnol.* (2012) doi:10.1038/nbt.2249.
445. Liu, Q. *et al.* Human Neural Crest Stem Cells Derived from Human ESCs and Induced Pluripotent Stem Cells: Induction, Maintenance, and Differentiation into Functional Schwann Cells. *Stem Cells Transl. Med.* (2012) doi:10.5966/sctm.2011-0042.
446. Fellmann, L., Nascimento, A. R., Tibiriça, E. & Bousquet, P. Murine models for pharmacological studies of the metabolic syndrome. *Pharmacology and Therapeutics* vol. 137 331–340 (2013).
447. O'Brien, P. D., Sakowski, S. A. & Feldman, E. L. Mouse models of diabetic neuropathy. *ILAR J.* **54**, 259–272 (2014).
448. Biessels, G. J. *et al.* Phenotyping animal models of diabetic neuropathy: a consensus statement of the diabetic neuropathy study group of the EASD (Neurodiab). *J. Peripher. Nerv. Syst.* **19**, 77–87 (2014).
449. Leiter, E. H. The NOD Mouse: A Model for Insulin-Dependent Diabetes Mellitus. *Curr. Protoc. Immunol.* (1997) doi:10.1002/0471142735.im1509s24.
450. Gabra, B. H. & Sirois, P. Hyperalgesia in non-obese diabetic (NOD) mice: A role for the inducible bradykinin B1 receptor. *Eur. J. Pharmacol.* (2005) doi:10.1016/j.ejphar.2005.03.018.

451. Yoshioka, M., Kayo, T., Ikeda, T. & Koizumi, A. A novel locus, Mody4, distal to D7Mit189 on chromosome 7 determines early-onset NIDDM in nonobese C57BL/6 (Akita) mutant mice. *Diabetes* (1997) doi:10.2337/diab.46.5.887.
452. Choeiri, C. *et al.* Longitudinal evaluation of memory performance and peripheral neuropathy in the Ins2 C96Y Akita mice. *Behav. Brain Res.* (2005) doi:10.1016/j.bbr.2004.06.005.
453. Sullivan, K. A. *et al.* Mouse models of diabetic neuropathy. *Neurobiol. Dis.* **28**, 276–285 (2007).
454. Myers, M. G., Cowley, M. A. & Münzberg, H. Mechanisms of leptin action and leptin resistance. *Annual Review of Physiology* (2008) doi:10.1146/annurev.physiol.70.113006.100707.
455. Drel, V. R. *et al.* The leptin-deficient (ob/ob) mouse: A new animal model of peripheral neuropathy of type 2 diabetes and obesity. *Diabetes* (2006) doi:10.2337/db06-0885.
456. Cheng, H. T., Dauch, J. R., Hayes, J. M., Hong, Y. & Feldman, E. L. Nerve Growth Factor Mediates Mechanical Allodynia in a Mouse Model of Type 2 Diabetes. *J. Neuropathol. Exp. Neurol.* **68**, 1229–1243 (2009).
457. Li, M. *et al.* Neuronal nitric oxide synthase mediates statin-induced restoration of vasa nervorum and reversal of diabetic neuropathy. *Circulation* **112**, 93–102 (2005).
458. Kan, M., Guo, G., Singh, B., Singh, V. & Zochodne, D. W. *Glucagon-Like Peptide 1, Insulin, Sensory Neurons, and Diabetic Neuropathy*. <https://academic.oup.com/jnen/article-abstract/71/6/494/2917432> (2012).
459. Wang, L. *et al.* Phosphodiesterase-5 is a therapeutic target for peripheral neuropathy in diabetic mice. *Neuroscience* **193**, 399–410 (2011).
460. Wright, D. E., Johnson, M. S., Arnett, M. G., Smittkamp, S. E. & Ryals, J. M. Selective changes in nocifensive behavior despite normal cutaneous axon innervation in leptin receptor-null mutant (db/db) mice. *J. Peripher. Nerv. Syst.* **12**, 250–261 (2007).
461. Dauch, J. R., Yanik, B. M., Hsieh, W., Oh, S. S. & Cheng, H. T. Neuron-astrocyte signaling network in spinal cord dorsal horn mediates painful neuropathy of type 2 diabetes. *Glia* **60**, 1301–15 (2012).
462. Rees, D. A. & Alcolado, J. C. Animal models of diabetes mellitus. *Diabetic Medicine* (2005) doi:10.1111/j.1464-5491.2005.01499.x.
463. Ventura-Sobrevilla, J. *et al.* Effect of varying dose and administration of streptozotocin on blood sugar in male CD1 mice. *Proc. West. Pharmacol. Soc.* (2011).
464. Usman, U., Bakar, A. & Mohamed, M. A Review on Experimental Methods of Diabetic Research: Advantages and Limitations. *Annu. Res. Rev. Biol.* **7**, 100–108 (2015).
465. Romanovsky, D., Hastings, S. L., Stimers, J. R. & Dobretsov, M. Relevance of hyperglycemia to early mechanical hyperalgesia in streptozotocin-induced diabetes. *J. Peripher. Nerv. Syst.* (2004) doi:10.1111/j.1085-9489.2004.009204.x.
466. Andersson, D. A. *et al.* Streptozotocin Stimulates the Ion Channel TRPA1 Directly. *J. Biol. Chem.* **290**, 15185–15196 (2015).
467. Obrosova, I. G. *et al.* High-fat diet-induced neuropathy of pre-diabetes and obesity: Effects of 'healthy' diet and aldose reductase inhibition. *Diabetes* (2007) doi:10.2337/db06-1176.
468. Coppey, L., Lu, B., Gerard, C. & Yorek, M. A. Effect of inhibition of angiotensin-converting enzyme and/or neutral endopeptidase on neuropathy in high-fat-fed C57Bl/6J Mice. *J. Obes.* (2012) doi:10.1155/2012/326806.
469. Stavniichuk, R. *et al.* Role of 12/15-lipoxygenase in nitrosative stress and peripheral prediabetic and diabetic neuropathies. *Free Radic. Biol. Med.* (2010) doi:10.1016/j.freeradbiomed.2010.06.016.
470. Lanlua, P. *et al.* Female steroid hormones modulate receptors for nerve growth factor in rat

- dorsal root ganglia. *Biol. Reprod.* (2001) doi:10.1095/biolreprod64.1.331.
471. Scanziani, M. & Häusser, M. Electrophysiology in the age of light. *Nature* (2009) doi:10.1038/nature08540.
472. Berridge, M. J., Lipp, P. & Bootman, M. D. The versatility and universality of calcium signalling. *Nature Reviews Molecular Cell Biology* (2000) doi:10.1038/35036035.
473. Grienberger, C. & Konnerth, A. Imaging Calcium in Neurons. *Neuron* vol. 73 862–885 (2012).
474. Ashley, C. C. & Ridgway, E. B. Simultaneous recording of membrane potential, calcium transient and tension in single muscle fibres. *Nature* (1968) doi:10.1038/2191168a0.
475. Shimomura, O., Johnson, F. H. & Saiga, Y. Extraction, Purification and Properties of Aequorin, a Bioluminescent Protein from the Luminous Hydromedusan, Aequorea. *J. Cell. Comp. Physiol.* (1962) doi:10.1002/jcp.1030590302.
476. Tsien, R. Y. New Calcium Indicators and Buffers with High Selectivity Against Magnesium and Protons: Design, Synthesis, and Properties of Prototype Structures. *Biochemistry* (1980) doi:10.1021/bi00552a018.
477. Miyawaki, A. *et al.* Fluorescent indicators for Ca²⁺ based on green fluorescent proteins and calmodulin. *Nature* (1997) doi:10.1038/42264.
478. Grynkiewicz, G., Poenie, M. & Tsien, R. Y. A new generation of Ca²⁺ indicators with greatly improved fluorescence properties. *Journal of Biological Chemistry* (1985) doi:10.1016/s0021-9258(19)83641-4.
479. Oakes, S. G., Martin, W. J., Lisek, C. A. & Powis, G. Incomplete hydrolysis of the calcium indicator precursor fura-2 pentaacetoxymethyl ester (fura-2 AM) by cells. *Anal. Biochem.* (1988) doi:10.1016/0003-2697(88)90267-9.
480. Paredes, R. M., Etzler, J. C., Watts, L. T., Zheng, W. & Lechleiter, J. D. Chemical calcium indicators. *Methods* **46**, 143–151 (2008).
481. Tsien, R. Y., Rink, T. J. & Poenie, M. Measurement of cytosolic free Ca²⁺ in individual small cells using fluorescence microscopy with dual excitation wavelengths. *Cell Calcium* (1985) doi:10.1016/0143-4160(85)90041-7.
482. Nakai, J., Ohkura, M. & Imoto, K. A high signal-to-noise ca²⁺ probe composed of a single green fluorescent protein. *Nat. Biotechnol.* (2001) doi:10.1038/84397.
483. Tian, L., Hires, S. A. & Looger, L. L. Imaging Neuronal Activity with Genetically Encoded Calcium Indicators. (2012) doi:10.1101/pdb.top069609.
484. Uebele, V. N., Nuss, C. E., Renger, J. J. & Connolly, T. M. Role of voltage-gated calcium channels in potassium-stimulated aldosterone secretion from rat adrenal zona glomerulosa cells. *J. Steroid Biochem. Mol. Biol.* (2004) doi:10.1016/j.jsbmb.2004.04.012.
485. Teichert, R. W. *et al.* Functional profiling of neurons through cellular neuropharmacology. *Proc. Natl. Acad. Sci. U. S. A.* **109**, 1388–1395 (2012).
486. Teichert, R. W., Schmidt, E. W. & Olivera, B. M. Constellation pharmacology: A new paradigm for drug discovery. *Annual Review of Pharmacology and Toxicology* vol. 55 573–589 (2015).
487. Teichert, R. W. *et al.* Characterization of two neuronal subclasses through constellation pharmacology. *Proc. Natl. Acad. Sci. U. S. A.* **109**, 12758–12763 (2012).
488. Imperial, J. S. *et al.* A family of excitatory peptide toxins from venomous crassispine snails: Using Constellation Pharmacology to assess bioactivity. *Toxicon* (2014) doi:10.1016/j.toxicon.2014.06.014.
489. Ulbricht, W. Voltage clamp studies of veratrinized frog nodes. *J. Cell. Comp. Physiol.* (1965) doi:10.1002/jcp.1030660516.

490. Ulbricht, W. The effect of veratridine on excitable membranes of nerve and muscle. in *Reviews of Physiology, Biochemistry and Experimental Pharmacology* 18–71 (Springer Berlin Heidelberg, 1969). doi:10.1007/BFb0111446.
491. Catterall, W. A. Neurotoxins that act on voltage-sensitive sodium channels in excitable membranes. *Annual review of pharmacology and toxicology* (1980) doi:10.1146/annurev.pa.20.040180.000311.
492. Farrag, K. J., Bhattacharjee, A. & Docherty, R. J. A comparison of the effects of veratridine on tetrodotoxin-sensitive and tetrodotoxin-resistant sodium channels in isolated rat dorsal root ganglion neurons. *Pflugers Arch. Eur. J. Physiol.* **455**, 929–938 (2008).
493. Ulbricht, W. Sodium Channel Inactivation: Molecular Determinants and Modulation. *Physiol. Rev.* **85**, 1271–1301 (2005).
494. Barnes, S. & Hille, B. Veratridine modifies open sodium channels. *J. Gen. Physiol.* (1988) doi:10.1085/jgp.91.3.421.
495. Ulbricht, W. Effects of veratridine on sodium currents and fluxes. *Reviews of physiology, biochemistry and pharmacology* (1998) doi:10.1007/bfb0000612.
496. Wang, S. Y. & Wang, G. K. Voltage-gated sodium channels as primary targets of diverse lipid-soluble neurotoxins. *Cellular Signalling* (2003) doi:10.1016/S0898-6568(02)00085-2.
497. Felix, J. P. *et al.* Functional assay of voltage-gated sodium channels using membrane potential-sensitive dyes. *Assay Drug Dev. Technol.* **2**, 260–268 (2004).
498. Dib-Hajj, S. D., Cummins, T. R., Black, J. A. & Waxman, S. G. Sodium Channels in Normal and Pathological Pain. *Annu. Rev. Neurosci.* **33**, 325–347 (2010).
499. Mohammed, Z. A., Doran, C., Grundy, D. & Nassar, M. A. Veratridine produces distinct calcium response profiles in mouse Dorsal Root Ganglia neurons. *Sci. Rep.* **7**, 45221 (2017).
500. Vincent, A. M., Mclean, L. L., Backus, C. & Feldman, E. L. Short-term hyperglycemia produces oxidative damage and apoptosis in neurons. *FASEB J.* **19**, 1–24 (2005).
501. Leininger, G. M. *et al.* Mitochondria in DRG neurons undergo hyperglycemic mediated injury through Bim, Bax and the fission protein Drp1. *Neurobiol. Dis.* **23**, 11–22 (2006).
502. Kharatmal, S. B., Singh, J. N. & Sharma, S. S. Comparative evaluation of in vitro and in vivo high glucose-induced alterations in voltage-gated tetrodotoxin-resistant sodium channel: Effects attenuated by sodium channel blockers. *Neuroscience* **305**, 183–196 (2015).
503. Mayfield, J. A. Diagnosis and Classification of Diabetes Mellitus: New Criteria. *Am. Fam. Physician* **58**, 1355 (1998).
504. Guest, P. C. & Rahmoune, H. Characterization of the db/db Mouse Model of Type 2 Diabetes. in *Methods in Molecular Biology* vol. 1916 195–201 (Humana Press Inc., 2019).
505. Malin, S. A., Davis, B. M. & Molliver, D. C. Production of dissociated sensory neuron cultures and considerations for their use in studying neuronal function and plasticity. *Nat. Protoc.* **2**, 152–160 (2007).
506. Lam, D. *et al.* RAGE-dependent potentiation of TRPV1 currents in sensory neurons exposed to high glucose. *PLoS One* **13**, e0193312 (2018).
507. Wang, S. *et al.* Negative regulation of TRPA1 by AMPK in primary sensory neurons as a potential mechanism of painful diabetic neuropathy. *Diabetes* **67**, 98–109 (2018).
508. Pabbidi, M. R. & Premkumar, L. S. Role of Transient Receptor Potential Channels Trpv1 and Trpm8 in Diabetic Peripheral Neuropathy. *J. diabetes Treat.* **2017**, (2017).
509. Pabbidi, R. M. *et al.* Influence of TRPV1 on diabetes-induced alterations in thermal pain sensitivity. *Mol. Pain* **4**, 9 (2008).

510. Bestall, S. M. *et al.* Sensory neuronal sensitisation occurs through HMGB-1-RAGE and TRPV1 in high-glucose conditions. *J. Cell Sci.* **131**, (2018).
511. Song, Y. *et al.* Difference of acute dissociation and 1-day culture on the electrophysiological properties of rat dorsal root ganglion neurons. *J. Physiol. Biochem.* **74**, 207–221 (2018).
512. Zheng, J. H., Walters, E. T. & Song, X. J. Dissociation of dorsal root ganglion neurons induces hyperexcitability that is maintained by increased responsiveness to cAMP and cGMP. *J. Neurophysiol.* **97**, 15–25 (2007).
513. Li, Z. H., Cui, D., Qiu, C. J. & Song, X. J. Cyclic nucleotide signaling in sensory neuron hyperexcitability and chronic pain after nerve injury. *Neurobiology of Pain* vol. 6 (2019).
514. Dib-Hajj, S. D., Tyrrell, L., Black, J. A. & Waxman, S. G. Na_v1.9, a novel voltage-gated Na channel, is expressed preferentially in peripheral sensory neurons and down-regulated after axotomy. *Proc. Natl. Acad. Sci. U. S. A.* (1998) doi:10.1073/pnas.95.15.8963.
515. Wangzhou, A. *et al.* Pharmacological target-focused transcriptomic analysis of native vs cultured human and mouse dorsal root ganglia. *Pain* **161**, 1497–1517 (2020).
516. Galeano, M. *et al.* Polydeoxyribonucleotide stimulates angiogenesis and wound healing in the genetically diabetic mouse. *Wound Repair Regen.* **16**, 208–217 (2008).
517. Luo, J. D., Wang, Y. Y., Fu, W. L., Wu, J. & Chen, A. F. Gene therapy of endothelial nitric oxide synthase and manganese superoxide dismutase restores delayed wound healing in type 1 diabetic mice. *Circulation* **110**, 2484–2493 (2004).
518. Michaels, J. *et al.* db/db mice exhibit severe wound-healing impairments compared with other murine diabetic strains in a silicone-splinted excisional wound model. *Wound Repair Regen.* **15**, 665–670 (2007).
519. Brem, H. & Tomic-Canic, M. Cellular and molecular basis of wound healing in diabetes. *Journal of Clinical Investigation* vol. 117 1219–1222 (2007).
520. Callaghan, B. C., Cheng, H. T., Stables, C. L., Smith, A. L. & Feldman, E. L. Diabetic neuropathy: Clinical manifestations and current treatments. *The Lancet Neurology* vol. 11 521–534 (2012).
521. Xu, G. Y., Li, G., Liu, N. & Huang, L. Y. M. Mechanisms underlying purinergic P2X₃ receptor-mediated mechanical allodynia induced in diabetic rats. *Mol. Pain* (2011) doi:10.1186/1744-8069-7-60.
522. Pabbidi, R. M. *et al.* Influence of TRPV1 on diabetes-induced alterations in thermal pain sensitivity. *Mol. Pain* **4**, (2008).
523. Andersson, D. A., Gentry, C., Moss, S. & Bevan, S. Transient receptor potential A1 is a sensory receptor for multiple products of oxidative stress. *J. Neurosci.* (2008) doi:10.1523/JNEUROSCI.5369-07.2008.
524. Chen, X. *et al.* Long-term diabetic microenvironment augments the decay rate of capsaicin-induced currents in mouse dorsal root ganglion neurons. *Molecules* **24**, (2019).
525. Hulse, R., Riaz, H., Singhal, P., Bates, D. & Donaldson, L. VEGF165b attenuates hyperglycaemia-induced sensitisation of neuronal TRPA1 activation: implications for diabetic neuropathy. in *Proceedings of The Physiological Society* vol. Proc 37th (The Physiological Society, 2013).
526. KAYANO, T. *et al.* Chronic NGF treatment induces somatic hyperexcitability in cultured dorsal root ganglion neurons of the rat. *Biomed. Res.* **34**, 329–342 (2013).
527. Zhang, Y. H., Kays, J., Hodgdon, K. E., Sacktor, T. C. & Nicol, G. D. Nerve growth factor enhances the excitability of rat sensory neurons through activation of the atypical protein kinase C isoform, PKM ζ . *J. Neurophysiol.* **107**, 315–335 (2012).
528. Zhang, Y. H., Vasko, M. R. & Nicol, G. D. Ceramide, a putative second messenger for nerve

- growth factor, modulates the TTX-resistant Na⁺ current and delayed rectifier K⁺ current in rat sensory neurons. *J. Physiol.* **544**, 385–402 (2002).
529. Schaefer, I., Prato, V., Arcourt, A., Taberner, F. J. & Lechner, S. G. Differential modulation of voltage-gated sodium channels by nerve growth factor in three major subsets of TrkA-expressing nociceptors. *Mol. Pain* **14**, (2018).
530. Denk, F., Bennett, D. L. & McMahon, S. B. Nerve Growth Factor and Pain Mechanisms. *Annu. Rev. Neurosci.* **40**, 307–325 (2017).
531. Fernyhough, P., Diemel, L. T., Brewster, W. J. & Tomlinson, D. R. Altered Neurotrophin mRNA Levels in Peripheral Nerve and Skeletal Muscle of Experimentally Diabetic Rats. *J. Neurochem.* **64**, 1231–1237 (2002).
532. Zhang, X., Huang, J. & McNaughton, P. A. NGF rapidly increases membrane expression of TRPV1 heat-gated ion channels. *EMBO J.* **24**, 4211–4223 (2005).
533. Winter, J., Alistair Forbes, C., Sternberg, J. & Lindsay, R. M. Nerve growth factor (NGF) regulates adult rat cultured dorsal root ganglion neuron responses to the excitotoxin capsaicin. *Neuron* **1**, 973–981 (1988).
534. Han, B. G. *et al.* Markers of glycemic control in the mouse: comparisons of 6-h- and overnight-fasted blood glucoses to Hb A_{1c}. *Am. J. Physiol. Metab.* **295**, E981–E986 (2008).
535. Hummel, K. P., Dickie, M. M. & Coleman, D. L. Diabetes, a new mutation in the mouse. *Science (80-)*. **153**, 1127–1128 (1966).
536. Chen, H. *et al.* Evidence That the Diabetes Gene Encodes the Leptin Receptor: Identification of a Mutation in the Leptin Receptor Gene in db/db Mice. *Cell* **84**, 491–495 (1996).
537. Tartaglia, L. A. *et al.* Identification and Expression Cloning of a Leptin Receptor, OB-R. *Cell* vol. 83 (1995).
538. Lee, G. H. *et al.* Abnormal splicing of the leptin receptor in diabetic mice. *Nature* **379**, 632–635 (1996).
539. Lee, S. M. & Bressler, R. Prevention of diabetic nephropathy by diet control in the db/db mouse. *Diabetes* **30**, 106–111 (1981).
540. Like, A. A., Lavine, R. L., Poffenbarger, P. L. & Chick, W. L. Studies in the diabetic mutant mouse. VI. Evolution of glomerular lesions and associated proteinuria. *Am. J. Pathol.* **66**, 193–224 (1972).
541. Kobayashi, K. *et al.* The db/db mouse, a model for diabetic dyslipidemia: Molecular characterization and effects of western diet feeding. *Metabolism* **49**, 22–31 (2000).
542. Robertson, D. M. & Sima, A. A. F. Diabetic Neuropathy in the Mutant Mouse [C57BL/ks(db/db)]: A Morphometric Study. *Diabetes* **29**, 60–67 (1980).
543. Ren, Y.-S. *et al.* Sodium channel Nav1.6 is up-regulated in the dorsal root ganglia in a mouse model of type 2 diabetes. *Brain Res. Bull.* **87**, 244–249 (2012).
544. Ren, P. C. *et al.* High-mobility group box 1 contributes to mechanical allodynia and spinal astrocytic activation in a mouse model of type 2 diabetes. *Brain Res. Bull.* **88**, 332–337 (2012).
545. Chen, H. *et al.* Systemic dexmedetomidine attenuates mechanical allodynia through extracellular sign db type 2 diabetic mice. *Neurosci. Lett.* **657**, 126–133 (2017).
546. Liu, S. *et al.* CXCL13/CXCR5 signaling contributes to diabetes-induced tactile allodynia via activating pERK, pSTAT3, pAKT pathways and pro-inflammatory cytokines production in the spinal cord of male mice. *Brain. Behav. Immun.* **80**, 711–724 (2019).
547. Xu, X. *et al.* Extracellular signal-regulated protein kinase activation in spinal cord contributes to pain hypersensitivity in a mouse model of type 2 diabetes. *Neurosci. Bull.* **30**, 53–66 (2014).

548. Griggs, R. B. *et al.* Methylglyoxal and a spinal TRPA1-AC1-Epac cascade facilitate pain in the db/db mouse model of type 2 diabetes. *Neurobiol. Dis.* **127**, 76–86 (2019).
549. Robertson, D. M. & Sima, A. A. F. Diabetic Neuropathy in the Mutant Mouse [C57BL/ks(db/db)]: A Morphometric Study. *Diabetes* **29**, 60–67 (1980).
550. CARSON, K. A., BOSSEN, E. H. & HANKER, J. S. PERIPHERAL NEUROPATHY IN MOUSE HEREDITARY DIABETES MELLITUS. II. ULTRASTRUCTURAL CORRELATES OF DEGENERATIVE AND REGENERATIVE CHANGES. *Neuropathol. Appl. Neurobiol.* **6**, 361–374 (1980).
551. Pande, M. *et al.* Transcriptional profiling of diabetic neuropathy in the BKS db/db mouse: A model of type 2 diabetes. *Diabetes* **60**, 1981–1989 (2011).
552. Hinder, L. M. *et al.* Transcriptional networks of progressive diabetic peripheral neuropathy in the db/db mouse model of type 2 diabetes: An inflammatory story. *Exp. Neurol.* **305**, 33–43 (2018).
553. Fan, B. *et al.* Mesenchymal stromal cell-derived exosomes ameliorate peripheral neuropathy in a mouse model of diabetes. *Diabetologia* (2019).
554. Walwyn, W. M. *et al.* HSV-1-mediated NGF delivery delays nociceptive deficits in a genetic model of diabetic neuropathy. *Exp. Neurol.* **198**, 260–270 (2006).
555. Shi, T. J. S. *et al.* Coenzyme Q10 prevents peripheral neuropathy and attenuates neuron loss in the db-/db- mouse, a type 2 diabetes model. *Proc. Natl. Acad. Sci. U. S. A.* **110**, 690–695 (2013).
556. Wang, H. *et al.* Protection of insulin-like growth factor 1 on experimental peripheral neuropathy in diabetic mice. *Mol. Med. Rep.* **18**, 4577–4586 (2018).
557. Pande, M. *et al.* Transcriptional profiling of diabetic neuropathy in the BKS db/db mouse: A model of type 2 diabetes. *Diabetes* **60**, 1981–1989 (2011).
558. Hur, J. *et al.* Transcriptional networks of murine diabetic peripheral neuropathy and nephropathy: common and distinct gene expression patterns. *Diabetologia* **59**, 1297–1306 (2016).
559. McGregor, B. A. *et al.* Conserved Transcriptional Signatures in Human and Murine Diabetic Peripheral Neuropathy. *Sci. Rep.* **8**, (2018).
560. Herweijer, G., Kyloh, M., Beckett, E. A. H., Dodds, K. N. & Spencer, N. Characterisation of primary afferent spinal innervation of mouse uterus. *Front. Neurosci.* **8**, (2014).
561. Ruscheweyh, R., Forsthuber, L., Schoffnegger, D. & Sandkühler, J. Modification of classical neurochemical markers in identified primary afferent neurons with A β -, A δ -, and C-fibers after chronic constriction injury in mice. *J. Comp. Neurol.* **502**, 325–336 (2007).
562. Sidenius, P. & Jakobsen, J. Reduced perikaryal volume of lower motor and primary sensory neurons in early experimental diabetes. *Diabetes* **29**, 182–187 (1980).
563. Zochodne, D. W., Verge, V. M. K., Cheng, C., Sun, H. & Johnston, J. Does diabetes target ganglion neurones? Progressive sensory neurone involvement in long-term experimental diabetes. *Brain* **124**, 2319–2334 (2001).
564. Schmeichel, A. M., Schmelzer, J. D. & Low, P. A. Oxidative injury and apoptosis of dorsal root ganglion neurons in chronic experimental diabetic neuropathy. *Diabetes* **52**, 165–171 (2003).
565. Shimoshige, Y. *et al.* Thirteen-month inhibition of aldose reductase by zenarestat prevents morphological abnormalities in the dorsal root ganglia of streptozotocin-induced diabetic rats. *Brain Res.* **1247**, 182–187 (2009).
566. Kishi, M., Tanabe, J., Schmelzer, J. D. & Low, P. A. Morphometry of dorsal root ganglion in chronic experimental diabetic neuropathy. *Diabetes* **51**, 819–824 (2002).

567. Kamiya, H., Zhang, W. & Sima, A. A. Degeneration of the Golgi and neuronal loss in dorsal root ganglia in diabetic BioBreeding/Worcester rats. *Diabetologia* **49**, 2763–2774 (2006).
568. Caterina, M. J. *et al.* The capsaicin receptor: A heat-activated ion channel in the pain pathway. *Nature* **389**, 816–824 (1997).
569. Griggs, R. B. *et al.* Methylglyoxal and a spinal TRPA1-AC1-Epac cascade facilitate pain in the db/db mouse model of type 2 diabetes. *Neurobiol. Dis.* **127**, 76–86 (2019).
570. Rundles, R. W. Diabetic neuropathy: General review with report of 125 cases. *Med. (United States)* **24**, 111–160 (1945).
571. Galer, B. S., Gianas, A. & Jensen, M. P. Painful diabetic polyneuropathy: Epidemiology, pain description, and quality of life. *Diabetes Res. Clin. Pract.* **47**, 123–128 (2000).
572. Abbott, C. A., Malik, R. A., Van Ross, E. R. E., Kulkarni, J. & Boulton, A. J. M. Prevalence and characteristics of painful diabetic neuropathy in a large community-based diabetic population in the U.K. *Diabetes Care* **34**, 2220–2224 (2011).
573. Cruccu, G. & Truini, A. Sensory profiles: A new strategy for selecting patients in treatment trials for neuropathic pain. *Pain* (2009) doi:10.1016/j.pain.2009.07.004.
574. Lima, A. L., Illing, T., Schliemann, S. & Elsner, P. Cutaneous Manifestations of Diabetes Mellitus: A Review. *American Journal of Clinical Dermatology* vol. 18 541–553 (2017).
575. Ko, M. J., Chiu, H. C., Jee, S. H., Hu, F. C. & Tseng, C. H. Postprandial blood glucose is associated with generalized pruritus in patients with type 2 diabetes. *Eur. J. Dermatology* **23**, 688–693 (2013).
576. D’Almeida, J. A. C. *et al.* Behavioral changes of Wistar rats with experimentally-induced painful diabetic neuropathy. *Arq. Neuropsiquiatr.* **57**, 746–752 (1999).
577. Cheng, R.-X. *et al.* The role of Na v 1.7 and methylglyoxal-mediated activation of TRPA1 in itch and hypoalgesia in a murine model of type 1 diabetes. *Theranostics* **9**, 15 (2019).
578. Han, L. *et al.* A subpopulation of nociceptors specifically linked to itch. *Nat. Neurosci.* **16**, 174–182 (2013).
579. Toth, B. I. & Biro, T. TRP Channels and Pruritus. *Open Pain J.* **6**, 62–80 (2013).
580. Sharif, B., Ase, A. R., Ribeiro-da-Silva, A. & Séguéla, P. Differential Coding of Itch and Pain by a Subpopulation of Primary Afferent Neurons. *Neuron* **106**, (2020).
581. Xie, B. & Li, X. Y. Inflammatory mediators causing cutaneous chronic itch in some diseases via transient receptor potential channel subfamily V member 1 and subfamily A member 1. *Journal of Dermatology* vol. 46 177–185 (2019).
582. Mondelli, M., Aretini, A. & Baldasseroni, A. Distal symmetric polyneuropathy in diabetes—differences between patients with and without neuropathic pain. *Exp. Clin. Endocrinol. Diabetes* (2012) doi:10.1055/s-0031-1286296.
583. Cheng, H. T. *et al.* P38 mediates mechanical allodynia in a mouse model of type 2 diabetes. *Mol. Pain* **6**, (2010).
584. Dyck, P. J., Dyck, P. J. B., Velosa, J. A., Larson, T. S. & O’Brien, P. C. Patterns of quantitative sensation testing of hypoesthesia and hyperalgesia are predictive of diabetic polyneuropathy: A study of three cohorts. *Diabetes Care* **23**, 510–517 (2000).
585. Obrosova, I. G. Diabetic Painful and Insensate Neuropathy: Pathogenesis and Potential Treatments DIABETIC PAIN AND SENSORY LOSS: PREVALENCE, CURRENT TREATMENT OPTIONS, AND LIMITATIONS OF EXISTING ANIMAL MODELS. *Neurother. J. Am. Soc. Exp. Neurother. Diabet.* **6**, 638–647 (2009).
586. Cruccu, G. & Truini, A. Sensory profiles: A new strategy for selecting patients in treatment trials for neuropathic pain. *Pain* **146**, 5–6 (2009).

587. Koivisto, A. & Pertovaara, A. Transient receptor potential ankyrin 1 (TRPA1) ion channel in the pathophysiology of peripheral diabetic neuropathy. *Scandinavian Journal of Pain* vol. 4 129–136 (2013).
588. Wei, H. *et al.* Roles of cutaneous versus spinal TRPA1 channels in mechanical hypersensitivity in the diabetic or mustard oil-treated non-diabetic rat. *Neuropharmacology* **58**, 578–584 (2010).
589. Eberhardt, M. J. *et al.* Methylglyoxal activates nociceptors through transient receptor potential channel A1 (TRPA1): A possible mechanism of metabolic neuropathies. *J. Biol. Chem.* **287**, 28291–28306 (2012).
590. Hiyama, H. *et al.* TRPA1 sensitization during diabetic vascular impairment contributes to cold hypersensitivity in a mouse model of painful diabetic peripheral neuropathy. *Mol. Pain* **14**, 174480691878981 (2018).
591. Koivisto, A. & Pertovaara, A. Transient receptor potential ankyrin 1 (TRPA1) ion channel in the pathophysiology of peripheral diabetic neuropathy. *Scandinavian Journal of Pain* vol. 4 129–136 (2013).
592. Cheng, R. X. *et al.* The role of Nav1.7 and methylglyoxal-mediated activation of TRPA1 in itch and hypoalgesia in a murine model of type 1 diabetes. *Theranostics* (2019) doi:10.7150/thno.36077.
593. Craner, M. J., Klein, J. P., Renganathan, M., Black, J. A. & Waxman, S. G. Changes of sodium channel expression in experimental painful diabetic neuropathy. *Ann. Neurol.* **52**, 786–792 (2002).
594. Sun, W. *et al.* Reduced conduction failure of the main axon of polymodal nociceptive C-fibres contributes to painful diabetic neuropathy in rats. *Brain* **135**, 359–375 (2012).
595. Mohammed, Z. A., Kaloyanova, K. & Nassar, M. A. An unbiased and efficient assessment of excitability of sensory neurons for analgesic drug discovery. *Pain* **161**, 1100–1108 (2020).
596. Waxman, S. G. *et al.* Sodium channel genes in pain-related disorders: phenotype-genotype associations and recommendations for clinical use. *Lancet. Neurol.* **13**, 1152–1160 (2014).
597. Craner, M. J., Klein, J. P., Renganathan, M., Black, J. A. & Waxman, S. G. Changes of sodium channel expression in experimental painful diabetic neuropathy. *Ann. Neurol.* **52**, 786–792 (2002).
598. Hong, S., Morrow, T. J., Paulson, P. E., Isom, L. L. & Wiley, J. W. Early painful diabetic neuropathy is associated with differential changes in tetrodotoxin-sensitive and -resistant sodium channels in dorsal root ganglion neurons in the rat. *J. Biol. Chem.* (2004) doi:10.1074/jbc.M404167200.
599. Chattopadhyay, M., Mata, M. & Fink, D. J. Vector-mediated release of GABA attenuates pain-related behaviors and reduces Na V1.7 in DRG neurons. *Eur. J. Pain* (2011) doi:10.1016/j.ejpain.2011.03.007.
600. Zhang, J. L. *et al.* Gabapentin reduces allodynia and hyperalgesia in painful diabetic neuropathy rats by decreasing expression level of Nav1.7 and p-ERK1/2 in DRG neurons. *Brain Res.* (2013) doi:10.1016/j.brainres.2012.11.032.
601. Israel, M. R. *et al.* Na_v 1.6 regulates excitability of mechanosensitive sensory neurons. *J. Physiol.* **597**, 3751–3768 (2019).
602. Yin, R. *et al.* Voltage-gated sodium channel function and expression in injured and uninjured rat dorsal root ganglia neurons. *Int. J. Neurosci.* **126**, 182–192 (2016).
603. Black, J. A. *et al.* Upregulation of a silent sodium channel after peripheral, but not central, nerve injury in DRG neurons. *J. Neurophysiol.* **82**, 2776–2785 (1999).
604. Cummins, T. R. *et al.* Nav1.3 sodium channels: Rapid repriming and slow closed-state

- inactivation display quantitative differences after expression in a mammalian cell line and in spinal sensory neurons. *J. Neurosci.* **21**, 5952–5961 (2001).
605. Cummins, T. R. & Waxman, S. G. Downregulation of tetrodotoxin-resistant sodium currents and upregulation of a rapidly repriming tetrodotoxin-sensitive sodium current in small spinal sensory neurons after nerve injury. *J. Neurosci.* **17**, 3503–3514 (1997).
606. Nassar, M. A. *et al.* Nerve injury induces robust allodynia and ectopic discharges in Nav 1.3 null mutant mice. *Mol. Pain* **2**, (2006).
607. Cheng, K. I. *et al.* Persistent mechanical allodynia positively correlates with an increase in activated microglia and increased P-p38 mitogen-activated protein kinase activation in streptozotocin-induced diabetic rats. *Eur. J. Pain (United Kingdom)* **18**, 162–173 (2014).
608. Huang, Y. *et al.* The role of TNF- α /NF- κ B pathway on the up-regulation of voltage-gated sodium channel Nav1.7 in DRG neurons of rats with diabetic neuropathy. *Neurochem. Int.* **75**, 112–119 (2014).
609. Liampas, A. *et al.* Pharmacological Management of Painful Peripheral Neuropathies: A Systematic Review. *Pain Ther.* (2020) doi:10.1007/s40122-020-00210-3.
610. Azmi, S., Alam, U., Burgess, J. & Malik, R. a. State-of-the-art pharmacotherapy for diabetic neuropathy. *Expert Opinion on Pharmacotherapy* vol. 22 55–68 (2021).
611. Chang, W. *et al.* Expression and Role of Voltage-Gated Sodium Channels in Human Dorsal Root Ganglion Neurons with Special Focus on Nav1.7, Species Differences, and Regulation by Paclitaxel. *Neurosci. Bull.* **34**, 4–12 (2018).
612. Davidson, S. *et al.* Human sensory neurons: Membrane properties and sensitization by inflammatory mediators. *Pain* **155**, 1861–1870 (2014).
613. Deuis, J. R. *et al.* Pharmacological characterisation of the highly Na^v 1.7 selective spider venom peptide Pn3a. *Sci. Rep.* **7**, (2017).
614. Gilron, I. *et al.* Nortriptyline and gabapentin, alone and in combination for neuropathic pain: a double-blind, randomised controlled crossover trial. *Lancet* **374**, 1252–1261 (2009).
615. Hanna, M., O'Brien, C. & Wilson, M. C. Prolonged-release oxycodone enhances the effects of existing gabapentin therapy in painful diabetic neuropathy patients. *Eur. J. Pain* **12**, 804–813 (2008).
616. Gilron, I. *et al.* Morphine, Gabapentin, or Their Combination for Neuropathic Pain. *N. Engl. J. Med.* **352**, 1324–1334 (2005).
617. Simpson, D. A. Gabapentin and venlafaxine for the treatment of painful diabetic neuropathy. *J. Clin. Neuromuscul. Dis.* **3**, 53–62 (2001).
618. Holbeck, J. V. *et al.* Imipramine and pregabalin combination for painful polyneuropathy: A randomized controlled trial. *Pain* **156**, 958–966 (2015).
619. Xia, Z., Xiao, Y., Wu, Y. & Zhao, B. Sodium channel Nav1.7 expression is upregulated in the dorsal root ganglia in a rat model of paclitaxel-induced peripheral neuropathy. *Springerplus* **5**, 1738 (2016).
620. Viventi, S. & Dottori, M. Modelling the dorsal root ganglia using human pluripotent stem cells: A platform to study peripheral neuropathies. *International Journal of Biochemistry and Cell Biology* vol. 100 61–68 (2018).
621. Mittal, K. & Schrenk-Siemens, K. Lessons from iPSC research: Insights on peripheral nerve disease. *Neuroscience Letters* vol. 738 135358 (2020).
622. Hulse, R. P. *et al.* Vascular endothelial growth factor-A165b prevents diabetic neuropathic pain and sensory neuronal degeneration. *Clin. Sci.* **129**, 741–756 (2015).
623. Skaper, S. D., Selak, I. & Varon, S. Molecular requirements for survival of cultured avian and

- rodent dorsal root ganglionic neurons responding to different trophic factors. *J. Neurosci. Res.* **8**, 251–261 (1982).
624. He, Z. & Jin, Y. Intrinsic Control of Axon Regeneration. *Neuron* vol. 90 437–451 (2016).
625. Huang, T. J., Verkhatsky, A. & Fernyhough, P. Insulin enhances mitochondrial inner membrane potential and increases ATP levels through phosphoinositide 3-kinase in adult sensory neurons. *Mol. Cell. Neurosci.* **28**, 42–54 (2005).
626. Huang, T. J. *et al.* Insulin prevents depolarization of the mitochondrial inner membrane in sensory neurons of type 1 diabetic rats in the presence of sustained hyperglycemia. *Diabetes* **52**, 2129–2136 (2003).
627. Kim, B., McLean, L. L., Philip, S. S. & Feldman, E. L. Hyperinsulinemia induces insulin resistance in dorsal root ganglion neurons. *Endocrinology* **152**, 3638–3647 (2011).
628. Johnson, E. M., Gorin, P. D., Brandeis, L. D. & Pearson, J. Dorsal root ganglion neurons are destroyed by exposure in utero to maternal antibody to nerve growth factor. *Science* (80-.). **210**, 916–918 (1980).
629. Crowley, C. *et al.* Mice lacking nerve growth factor display perinatal loss of sensory and sympathetic neurons yet develop basal forebrain cholinergic neurons. *Cell* **76**, 1001–1011 (1994).
630. Huang, E. J. & Reichardt, L. F. Neurotrophins: Roles in neuronal development and function. *Annual Review of Neuroscience* vol. 24 677–736 (2001).
631. Sebert, M. E. & Shooter, E. M. Expression of mRNA for neurotrophic factors and their receptors in the rat dorsal root ganglion and sciatic nerve following nerve injury. *J. Neurosci. Res.* **36**, 357–367 (1993).
632. Brown, A., Ricci, M. J. & Weaver, L. C. NGF mRNA is expressed in the dorsal root ganglia after spinal cord injury in the rat. *Exp. Neurol.* **205**, 283–286 (2007).
633. Christianson, J. A., Riekhof, J. T. & Wright, D. E. Restorative effects of neurotrophin treatment on diabetes-induced cutaneous axon loss in mice. *Exp. Neurol.* **179**, 188–199 (2003).
634. Kamiya, H., Zhang, W. & Sima, A. A. Degeneration of the Golgi and neuronal loss in dorsal root ganglia in diabetic BioBreeding/Worcester rats. *Diabetologia* **49**, 2763–2774 (2006).
635. Cone, C. D. & Cone, C. M. Blockage of depolarization-induced mitogenesis in CNS neurons by 5-fluoro-2'-deoxyuridine. *Brain Res.* **151**, 545–559 (1978).
636. Andersen, P. L., Doucette, J. R. & Nazarali, A. J. *A Novel Method of Eliminating Non-Neuronal Proliferating Cells From Cultures of Mouse Dorsal Root Ganglia.* *Cellular and Molecular Neurobiology* vol. 23 (2003).
637. De Gregorio, C. & Ezquer, F. Sensory neuron cultures derived from adult db/db mice as a simplified model to study type-2 diabetes-associated axonal regeneration defects. *Dis. Model. Mech.* **14**, dmm046334 (2021).
638. Aring, A. M., Jones, D. E. & Falko, J. M. *Evaluation and Prevention of Diabetic Neuropathy - American Family Physician.* *American Family Physician* vol. 71 www.aafp.org/afp. (2005).
639. Baron, R., Tölle, T. R., Gockel, U., Brosz, M. & Freynhagen, R. A cross-sectional cohort survey in 2100 patients with painful diabetic neuropathy and postherpetic neuralgia: Differences in demographic data and sensory symptoms. *Pain* **146**, 34–40 (2009).
640. Norido, F., Canella, R., Zanoni, R. & Gorio, A. Development of diabetic neuropathy in the C57BL/Ks (db/db) mouse and its treatment with gangliosides. *Exp. Neurol.* **83**, 221–232 (1984).
641. Tesfaye, S. *et al.* Diabetic Neuropathies: Update on Definitions, Diagnostic Criteria, Estimation of Severity, and Treatments. *Diabetes Care* **33**, 2285 (2010).
642. Shi, T. J. S. *et al.* Coenzyme Q10 prevents peripheral neuropathy and attenuates neuron loss

- in the db/db- mouse, a type 2 diabetes model. *Proc. Natl. Acad. Sci. U. S. A.* **110**, 690–695 (2013).
643. Wright, D. E., Ryals, J. M., McCarson, K. E. & Christianson, J. A. Diabetes-induced expression of activating transcription factor 3 in mouse primary sensory neurons. *J. Peripher. Nerv. Syst.* **9**, 242–254 (2004).
644. Wiffen, P. J. *et al.* Gabapentin for chronic neuropathic pain in adults. *Cochrane Database of Systematic Reviews* vol. 2017 (2017).
645. Derry, S. *et al.* Pregabalin for neuropathic pain in adults. *Cochrane Database of Systematic Reviews* vol. 2019 (2019).
646. Lunn, M. P. T., Hughes, R. A. C. & Wiffen, P. J. Duloxetine for treating painful neuropathy, chronic pain or fibromyalgia. *Cochrane Database of Systematic Reviews* vol. 2014 (2014).
647. Moore, R. A., Derry, S., Aldington, D., Cole, P. & Wiffen, P. J. Amitriptyline for neuropathic pain in adults. *Cochrane Database of Systematic Reviews* vol. 2017 (2015).
648. Duehmke, R. M. *et al.* Tramadol for neuropathic pain in adults. *Cochrane Database of Systematic Reviews* vol. 2017 (2017).
649. Derry, S., Wiffen, P. J., Moore, R. A. & Quinlan, J. Topical lidocaine for neuropathic pain in adults. *Cochrane Database of Systematic Reviews* vol. 2017 (2014).
650. Agathos, E. *et al.* Effect of α -lipoic acid on symptoms and quality of life in patients with painful diabetic neuropathy. *J. Int. Med. Res.* **46**, 1779–1790 (2018).
651. McDonnell, A. *et al.* Efficacy of the Nav1.7 blocker PF-05089771 in a randomised, placebo-controlled, double-blind clinical study in subjects with painful diabetic peripheral neuropathy. *Pain* (2018) doi:10.1097/j.pain.0000000000001227.
652. Ito, A. *et al.* Anti-hyperalgesic effects of calcitonin on neuropathic pain interacting with its peripheral receptors. *Mol. Pain* **8**, 1744-8069-8–42 (2012).
653. Bramson, C. *et al.* Exploring the Role of Tanezumab as a Novel Treatment for the Relief of Neuropathic Pain. *Pain Med. (United States)* **16**, 1163–1176 (2015).
654. Liu, X., Treister, R., Lang, M. & Oaklander, A. L. IVIg for apparently autoimmune small-fiber polyneuropathy: First analysis of efficacy and safety. *Ther. Adv. Neurol. Disord.* **11**, (2018).
655. Lakhan, S. E., Velasco, D. N. & Tepper, D. Botulinum Toxin-A for Painful Diabetic Neuropathy: A Meta-Analysis. *Pain Med. (United States)* **16**, 1773–1780 (2015).
656. Salehi, H., Moussaei, M., Kamiab, Z. & Vakilian, A. The effects of botulinum toxin type A injection on pain symptoms, quality of life, and sleep quality of patients with diabetic neuropathy: A randomized double-blind clinical trial. *Iran. J. Neurol.* **18**, 99–107 (2019).
657. Park, J. H. & Park, H. J. Botulinum toxin for the treatment of neuropathic pain. *Toxins* vol. 9 (2017).
658. Tam, J., Rosenberg, L. & Maysinger, D. INGAP peptide improves nerve function and enhances regeneration in streptozotocin-induced diabetic C57BL/6 mice. *FASEB J.* **18**, 1767–1769 (2004).
659. Hamada, Y. & Nakamura, J. Clinical potential of aldose reductase inhibitors in diabetic neuropathy. *Treatments in Endocrinology* vol. 3 245–255 (2004).
660. Yagihashi, S. *et al.* Neuropathy in diabetic mice overexpressing human aldose reductase and effects of aldose reductase inhibitor. *Brain* **124**, 2448–2458 (2001).
661. Berti-Mattera, L. N., Kern, T. S., Siegel, R. E., Nemet, I. & Mitchell, R. Sulfasalazine blocks the development of tactile allodynia in diabetic rats. *Diabetes* **57**, 2801–2808 (2008).
662. Liedorp, M., Voskuyl, A. E. & van Oosten, B. W. Axonal neuropathy with prolonged

- sulphasalazine use. *Clin. Exp. Rheumatol.* **26**, 671–672 (2008).
663. Liu, X. S. *et al.* MicroRNA-146a mimics reduce the peripheral neuropathy in type 2 diabetic mice. *Diabetes* **66**, 3111–3121 (2017).
664. Kessler, J. A. *et al.* Double-blind, placebo-controlled study of HGF gene therapy in diabetic neuropathy. *Ann. Clin. Transl. Neurol.* **2**, 465–478 (2015).
665. Moore, S. A., Peterson, R. G., Felten, D. L., Cartwright, T. R. & O'Connor, B. L. Reduced sensory and motor conduction velocity in 25-week-old diabetic [C57BL/Ks (db/db)] mice. *Exp. Neurol.* **70**, 548–555 (1980).
666. Sima, A. A. F. & Robertson, D. M. Peripheral neuropathy in mutant diabetic mouse [C57BL/Ks (db/db)]. *Acta Neuropathol.* **41**, 85–89 (1978).
667. Sharma, A. K. *et al.* Peripheral Nerve Abnormalities in the Diabetic Mutant Mouse. *Diabetes* **32**, 1152–1161 (1983).
668. Bates, S. H., Kulkarni, R. N., Seifert, M. & Myers, M. G. Roles for leptin receptor/STAT3-dependent and -independent signals in the regulation of glucose homeostasis. *Cell Metab.* **1**, 169–178 (2005).
669. Veniant, M. & LeBel, C. Leptin: From Animals to Humans. *Curr. Pharm. Des.* **9**, 811–818 (2003).
670. Wang, B., Chandrasekera, P. & Pippin, J. Leptin- and Leptin Receptor-Deficient Rodent Models: Relevance for Human Type 2 Diabetes. *Curr. Diabetes Rev.* **10**, 131–145 (2014).
671. Li, M. *et al.* Neuronal nitric oxide synthase mediates statin-induced restoration of vasa nervorum and reversal of diabetic neuropathy. *Circulation* **112**, 93–102 (2005).
672. Tamura, Y., Murayama, T., Minami, M., Yokode, M. & Arai, H. Differential effect of statins on diabetic nephropathy in db/db mice. *Int. J. Mol. Med.* **28**, 683–687 (2011).
673. Tang, T. & Reed, M. J. Exercise adds to metformin and acarbose efficacy in db/db mice. *Metabolism.* **50**, 1049–1053 (2001).
674. Young, A. A. *et al.* Glucose-lowering and insulin-sensitizing actions of exendin-4: Studies in obese diabetic (ob/ob, db/db) mice, diabetic fatty Zucker rats, and diabetic rhesus monkeys (*Macaca mulatta*). *Diabetes* **48**, 1026–1034 (1999).
675. Do, O. H., Gunton, J. E., Gaisano, H. Y. & Thorn, P. Changes in beta cell function occur in prediabetes and early disease in the *Lepr* db mouse model of diabetes. *Diabetologia* **59**, 1222–1230 (2016).
676. Wattiez, A.-S. & Barrière, D. A. Rodent Models of Painful Diabetic Neuropathy: What Can We Learn from Them? *J. Diabetes Metab.* **01**, (2012).